

# **Hydrogeological characterisation of crystalline basement aquifers within the Limpopo Province, South Africa**

**by**

**Martin Holland**

Submitted in the fulfilment of the requirements for the degree Doctor of  
Philosophy in the Faculty Natural and Agricultural Sciences

University of Pretoria

Pretoria, South Africa



UNIVERSITEIT VAN PRETORIA  
UNIVERSITY OF PRETORIA  
YUNIBESITHI YA PRETORIA

**February 2011**

## *Acknowledgements*

The research was financially supported by the Water Research Commission (WRC) for the period 2007-2010. I would like to express my sincere gratitude to Dr. Shafick Adams from the WRC for his arrangements and support of the Limpopo basement aquifer project. The contribution of the members of the Steering Committee is also gratefully acknowledged. I also want convey my appreciation to the hundreds of rural communities I visited during this research and allowing me to go about my tasks without any objection.

I have received immense support during my research and would like to express my thanks to the following individuals:

- First and foremost, my supervisor, Prof. Kai Witthüser, for his continuous support, amicable mentorship and the main reason I pursued a career in Hydrogeology.
- To my co-supervisor, Prof. Louis Van Rooy, for his support in managing the arrangements of the WRC workshops and research deliverables. In this regard I also need to mention the help of Ms. Melinda de Swardt, the kingpin of the Department of Geology's administration.
- Special thanks to, Mr. Willem Du Toit and Mr. Robert Whitehead from the Limpopo (Department of Water Affairs) regional office, who supported this study fully and provided additional funding, in the form of drilling and geophysics. These individuals are the true 'groundwater hunters' of the Limpopo Province.
- The Limpopo (GRIP) consultants, who does a great job at maintaining and improving on one of the best groundwater datasets in the country, and especially to Mr. Reinhardt Weidemann, for sharing his expertise gained in this challenging hydrogeological environment.
- My colleagues at Water Geosciences Consulting, for the generous time allocations to complete my research, and to Mr. Jude Cobbing for improving on the English phrasing of my thesis.
- Most importantly, I would like to thank my loving wife and children for their belief in me and the sacrifices made during the time it took to complete this research (you are truly my inspiration).
- By far my biggest appreciation goes to my parents, who taught me the morals of life and molded me into the person I am today.
- Finally, I want to express my sincere gratitude to my sister, relatives and friends for your continuous support and encouragement.
- Comments on the manuscript from the external reviewers are greatly appreciated.

*"Some people dream of worthy accomplishments, while others stay awake and do them."*

*- Anon*

# **Hydrogeological characterisation of crystalline basement aquifers within the Limpopo Province, South Africa**

by

Martin Holland

Supervisor: Prof. K.T. Witthüser  
Co-supervisor: Prof. J.L. Van Rooy  
Department: Geology  
Degree: PhD Engineering and Environmental Geology

---

## ***Declaration***

I, Martin Holland declare that the thesis, which I hereby submit for the degree Doctor of Philosophy (Engineering and Environmental Geology) at the University of Pretoria, is my own work and has not previously been submitted by me for a degree at this or any other tertiary institution.

Signature: \_\_\_\_\_

Date: \_\_\_\_\_

## Abstract

Geologically complex crystalline aquifers are distributed extensively in Africa and also underlie large parts of the semi-arid Limpopo Province where some of the greatest groundwater needs in South Africa occur. The importance of these basement aquifers makes it vital to identify high yielding hydrogeological zones that can be targeted for water supply, to sustain areas of high population density with few or no alternative water sources. The biggest challenge is to understand the factors that determine the secondary permeability of these weathered-fractured rock aquifers. The focus of this study was therefore to systematically analyse regional factors that may influence borehole yields and aquifer transmissivities.

The study covered four distinct geological and morpho-structural domains within the Limpopo Province, covering about 23 500 km<sup>2</sup>. The borehole dataset compiled for the study consisted of over 8 000 boreholes contained in the Groundwater Resources Information Project (GRIP) Limpopo database of the South African Department of Water Affairs. Approximately 3 000 of these boreholes have been hydraulically tested and the lithology has been recorded in 1 200 cases. A commonly encountered problem of pumping tests analysis in crystalline aquifers is in choosing an appropriate model that best fits the observed drawdown response. In this thesis modern methods are proposed for the analysis of pumping test data in weathered-fractured rock aquifers and highlight the importance of diagnostic plots, especially derivatives, for the detection of flow regimes and the choice of the correct 'theoretical' model. Based on the classification no single analytical method can be universally applied to crystalline basement aquifers when considering the analysis of pumping test data.

The GRIP borehole dataset was analysed in conjunction with spatial information to identify the relationship of regional factors such as - geology, hydrology, weathering thickness, topography, geomorphology, neo-tectonic stresses, and structural lineaments - on groundwater occurrence. Geology has a clear influence, with boreholes exploiting alluvial aquifers composed of highly permeable material, and certain rock types such as pegmatite, showing generally higher borehole productivities. Favourable borehole locations from a topographical point of view are predictably along rivers and valleys. Other identified favourable groundwater targets are the metamorphic aureoles of younger granite intrusions. Despite the local importance of the regolith as a recharge and storage mechanism for the underlying fractured bedrock, no correlation between borehole yields and depth of weathering was found. The pattern of lineament and dyke orientations in the different morpho-structural domains led to a more complex conceptual model of groundwater occurrence. This model is inconsistent with the predicted regime based on regional stress field data and suggests that local variations have a strong influence on groundwater occurrence. Due to the complex geological history of the area, it is difficult to link open discontinuities to a distinct recent or past tectonic event. It can be concluded that regional stress field data, as in this case, may not account for local, possibly highly significant, stress field variations. The hydrogeological importance of several factors on groundwater occurrence presented in this study can be used as a working reference for future groundwater development programmes.





## *Table of contents*

<b>1. INTRODUCTION.....</b>	<b>15</b>
1.1. Problem statement .....	15
1.2. Investigation objectives .....	18
<b>2. CHARACTERISATION OF CRYSTALLINE BASEMENT AQUIFERS.....</b>	<b>20</b>
2.1. Conceptual framework.....	20
2.1.1. Classical weathered-fractured rock concept.....	20
2.1.2. General flow behaviour.....	22
2.2. Groundwater recharge .....	23
2.3. Groundwater quality .....	24
2.3.1. Geochemical studies.....	24
2.4. Groundwater hydraulics.....	25
2.4.1. Aquifer response evaluation.....	25
2.4.2. Aquifer models applicable to crystalline basement aquifers.....	27
2.4.3. Summary of conceptual models .....	28
2.5. ‘Sustainable’ yield concept.....	35
2.6. Development of groundwater .....	38
2.6.1. Exploration approaches .....	39
<b>3. HYDROGEOLOGICAL ASSESSMENT METHODS .....</b>	<b>41</b>
3.1. Investigation approach.....	41
3.1.1. Hydrogeological overview .....	42
3.2. Groundwater recharge estimation methods .....	43
3.2.1. Chloride Mass Balance (CMB) .....	43
3.2.2. Cumulative rainfall departure method.....	44
3.3. Geochemical investigation methods .....	45
3.3.1. Environmental and radiogenic isotopes .....	46
3.3.2. Chlorofluorocarbon (CFC) and sulphur hexafluoride (SF6).....	48
3.4. Hydraulic testing.....	51
3.4.1. Step drawdown test and well efficiency .....	51
3.4.2. Identification of characteristic flow regimes (constant discharge test).....	52
3.4.3. Pumping test interpretation .....	55
3.4.4. Recommending a long term yield for a single borehole.....	56
3.5. Assessment of factors controlling the occurrence of groundwater.....	56
3.5.1. GIS analysis.....	56
3.5.2. Lineament analysis .....	57
3.5.3. Geophysical methods .....	58
3.6. Development of a regional conceptual model .....	58
<b>4. DESCRIPTION OF STUDY AREA .....</b>	<b>59</b>
4.1. Physiography and climate.....	59
4.1.1. Geomorphology.....	63
4.2. Regional geology .....	64
4.2.1. Description of local geology .....	66



4.2.2.	Geological timeline of local occurrences .....	68
4.3.	Structural geology.....	68
4.4.	Hydrogeological description.....	72
4.4.1.	Aquifer systems.....	74
4.4.2.	Borehole data analysis.....	74
4.4.3.	Success rate and yields.....	78
4.4.4.	Transmissivity and recommended borehole yields .....	79
<b>5.</b>	<b>HYDROGEOLOGICAL CHARACTERISATION OF THE STUDY AREA.....</b>	<b>80</b>
5.1.	Characterisation of groundwater recharge.....	80
5.1.1.	Recharge estimates (Chloride Mass Balance).....	80
5.1.2.	Aquifer response to recharge.....	83
5.2.	Geochemical description .....	89
5.2.1.	Interpretation of results .....	89
5.2.2.	Discussion of stable isotope data.....	92
5.2.3.	Groundwater dating.....	93
5.2.4.	Groundwater quality hazards.....	103
5.3.	Pumping test analysis .....	104
5.3.1.	Aquifer response classification .....	104
5.3.2.	Hydraulic parameters .....	112
5.4.	Groundwater sustainability (source vs. resource).....	113
5.4.1.	Source yield.....	114
5.4.2.	Resource yield .....	115
5.4.3.	High yield test (potential well field).....	117
5.5.	Geological and geomorphologic influence on borehole productivity .....	125
5.5.1.	Geological setting.....	127
5.5.2.	Weathered layer (regolith) and erosion surfaces.....	129
5.5.3.	Topographic setting and drainages.....	130
5.5.4.	Relationship to dykes .....	132
5.5.5.	Relationship to lineaments .....	134
5.5.6.	Field observation (testing the results) .....	139
5.5.7.	Discussion of results.....	141
<b>6.</b>	<b>CONCLUSION .....</b>	<b>146</b>
6.1.	Synthesis.....	146
6.2.	Recommendations and suggestions for future investigations.....	147
6.2.1.	Groundwater management .....	148
<b>7.</b>	<b>REFERENCES.....</b>	<b>149</b>
<b>8.</b>	<b>APPENDIXES .....</b>	<b>158</b>
	Appendix A - Borehole hydrographs .....	158
	Appendix B - CRD simulations .....	159
	Appendix C - Surface topography vs. groundwater level correlation.....	161
	Appendix D - Hierarcial cluster analysis (dendrogram) .....	162
	Appendix E - Nitrate distribution map.....	162
	Appendix F - Details of pumping tests.....	163



## List of tables

Table 3.1. Methods of recognizing observed flow characteristics from hydraulic responses in crystalline basement aquifers.....	54
Table 4.1. Temperature (°C) variations of selected towns and climate stations.....	61
Table 4.2. Rainfall data for selected stations distributed throughout the study area.....	61
Table 4.3. Summary of borehole characteristics in the study area.....	74
Table 4.4. Statistical summary of transmissivities and recommended yields.....	79
Table 5.1. Summary of borehole characteristics in the study area.....	81
Table 5.2. Recharge estimates based on the CMB for selected localities in the study area.....	83
Table 5.3. Summary of short term monitoring groundwater level data for selected stations.....	83
Table 5.4. Recharge estimations based on the CRD method.....	88
Table 5.5. Mean values for the clusters distinguished by the hierarchical cluster analysis (EC in mS/m, all other in mg/l).....	90
Table 5.6. Chemical composition of rainfall within the study area (EC in mS/m, all other in mg/l).....	90
Table 5.7. Chemical composition of rainfall within the study area.....	95
Table 5.8. Potability classification of the area of investigation (EC in mS/m, all other in mg/l).....	103
Table 5.9. Microbiological analyses for all samples collected.....	104
Table 5.10. Most typical diagnostic plots encountered in the Basement aquifers under investigation.....	105
Table 5.11. Summary of selected hydrogeological parameters for the different drawdown behaviours.....	105
Table 5.12. Hydraulic test analysis results (test details is given in Appendix F).....	113
Table 5.13. Comparison of the results for the two constant rates.....	114
Table 5.14. Pumping test in the study area (GRIP dataset).....	115
Table 5.15. Simplified water balance for the Upper Brak River catchment.....	116
Table 5.16. Summary of pumping and observation boreholes of high yield test.....	117
Table 5.17. Results of geological, CCTV and geophysical logging of borehole H11-2593.....	120
Table 5.18. Summary of hydraulic parameters obtained from well field pumping test analysis.....	124
Table 5.19. Determined hydrogeological parameter based on the geology observed during drilling.....	127
Table 5.20. Determined hydrogeological parameter based on the geological setting of boreholes.....	128
Table 5.21. Determined hydrogeological parameter based on the topographic setting of boreholes.....	130
Table 5.22. Influence of proximity to rivers and streams on borehole productivity.....	132
Table 5.23. Transmissivity (m <sup>2</sup> /d) of boreholes according to distance to inferred dykes.....	133
Table 5.24. Productivity of boreholes according to distance to inferred lineaments.....	135
Table 5.25. Transmissivity (m <sup>2</sup> /d) of boreholes according to distance to inferred lineaments within the Limpopo Plateau.....	136
Table 5.26. Transmissivity (m <sup>2</sup> /d) of boreholes according to distance to inferred lineaments within the Letaba Lowveld.....	137
Table 5.27. A summary of drilling results in the Great Letaba Catchment.....	141
Table 5.28. Recommended drilling targets per structural domain.....	143

## List of figures

Figure 1.1. Study Area. ....	16
Figure 2.1. Permeability and porosity in basement aquifers (Chilton and Foster, 1995). ....	21
Figure 2.2. Simplified flow system for crystalline basement terrain (Adapted from Tóth, 1963; Chilton and Foster, 1995). ....	22
Figure 2.3. Recharge estimates for southern Africa (Xu and Beekman, 2003; Adams et al., 2004). ....	23
Figure 2.4. Most typical diagnostic plots encountered in hydrogeology (Renard et al., 2009). ....	26
Figure 2.5. Different modelling approaches for fractured rock aquifers (Kröhn, 1990). ....	28
Figure 2.6. Depending on the scale of interests a number of fracture flow models can be identified; matrix blocks (A), densely fractured rocks (B), fracture rocks with impermeable matrix (C), and combination of fracture network and matrix blocks (D). ....	29
Figure 2.7. Schematic illustration of an idealized confined aquifer. ....	29
Figure 2.8. Schematic illustration of an isotropic leaky confined aquifer. ....	30
Figure 2.9. Schematic illustration of an unconfined aquifer. ....	31
Figure 2.10. A fractured block illustrating the double porosity concept (Cinco-Ley, 1996 in Renard, 2005b). ....	31
Figure 2.11. Different flow phases observed in a single fracture (Van Tonder et al., 2002). ....	33
Figure 2.12. Flow dimension definition in well testing (Doe, 1991 in Van Tonder et al., 2002). ....	34
Figure 2.13. Concept of radial flow in 1, 2, 3, and generalization to n dimensions (Renard, 2005b). ....	35
Figure 2.14. The capture principle and the implications for sustainability and recharge. ....	36
Figure 2.15. Flow chart of recommended groundwater exploration of basement aquifers (Sami, 2009). ....	40
Figure 3.1. Overview of the applied hydrogeological assessment approach and methods. ....	41
Figure 3.2. Summary diagram of the stable isotope composition from precipitation to percolation. ....	46
Figure 3.3. Atmospheric mixing ratios of CFC-11, CFC-12, and SF <sub>6</sub> for the southern hemisphere. ....	48
Figure 3.4. Two cases of groundwater movement by piston-flow in confined aquifers and flow in an open aquifer where different fast flowing water is mixed in the well or spring. ....	50
Figure 3.5. Illustration of early, intermediate and late periods of pump tests responses (Gringarten 1982 in Leveinen, 2001). ....	52
Figure 3.6. Flow regime identification tool representing schematically the log-derivative of drawdown as a function of logarithmic time (Ehlig-Economides et al., 1994 in Renard et al., 2009). ....	53
Figure 3.7. Graphs of the first logarithmic derivative of the drawdown in a borehole for a few types of geometries and boundaries (Van Tonder et al., 2001). ....	53
Figure 3.8. The geological triangle method (MacDonald et al., 2005). ....	58
Figure 4.1. Regional surface drainage features, topography and study area. ....	60
Figure 4.2. Mean annual rainfall map together with selected monthly average charts for selected stations in mm/month. ....	62
Figure 4.3. The distribution of erosion surfaces in southern Africa (adapted from Partridge, 1998; Taylor and Howard, 1999). ....	63
Figure 4.4. Terrain morphological zones of the study area. ....	64
Figure 4.5. Generalised map of the Limpopo Mobile Belt showing the main features and subdivisions (adapted from Boshoff et al., 2006). ....	65
Figure 4.6. Regional geology of the study area (based on published 1:250 000 map sheets sourced from the Council for Geoscience). ....	67

Figure 4.7. Aeromagnetic map showing tectonic domains (Adapted from Stettler et al., 1989). Data Source: Council for Geoscience (SA). .....	69
Figure 4.8. Neo-tectonic stress map of southern Africa (Zoback, 1992). Long axes indicate the orientation of crustal shortening.....	69
Figure 4.9. Rose diagram derived from the strikes of all joint planes (left) and faults (right). .....	70
Figure 4.10. Identified structural domains based on the orientation of regional dykes (Aeromagnetic and published dykes). .....	71
Figure 4.11. Delineation of the Limpopo Plateau and Letaba Lowveld regions.....	73
Figure 4.12. Generalised section of the aquifer systems found in the area of investigation, including photo's of observed geological features.....	75
Figure 4.13. Distribution of borehole depths in the Limpopo Plateau and Letaba Lowveld.....	76
Figure 4.14. Distribution of groundwater levels in the Limpopo Plateau and Letaba Lowveld.....	76
Figure 4.15. Distribution of depth of first water strikes in the Limpopo Plateau and Letaba Lowveld. ....	77
Figure 4.16. Distribution of depths of weathering plus fracturing in the Limpopo Plateau and Letaba Lowveld. ....	77
Figure 4.17. Success rate for boreholes contained the GRIP dataset for the study area.....	78
Figure 4.18. Distribution of borehole airlift yield in the Limpopo Plateau and Letaba Lowveld. ....	78
Figure 4.19. Frequency histograms and cumulative distribution of transmissivities [ $m^2/day$ ] and recommended yield ( $l/s$ per day) for the Limpopo Plateau and the Letaba Lowveld.....	79
Figure 5.1. Regional recharge map for the Limpopo Province. ....	80
Figure 5.2. Annual recharge map based on the CMB-method. ....	82
Figure 5.3. Spatial distribution of monitoring boreholes and selected water level hydrographs for the period Jan-06 to Dec-09 (A3 map) (red lines represent daily water levels while black columns represent monthly rainfall).....	84
Figure 5.4. Hydrograph of monitoring station A6N0586 for the period (Jan-06 to Dec-09). ....	85
Figure 5.5. Hydrograph of monitoring station A9M008 for the period (Jan-06 to Dec-09). ....	86
Figure 5.6. Hydrograph of long term monitoring station A7N0524 near Mogwadi (1971 to 2009).....	86
Figure 5.7. Hydrograph of long term monitoring station A7N0549 near Polokwane (1971 to 2009). ....	87
Figure 5.8. Annual deviation from the average rainfall, together with the cumulative departure for the 104-year rainfall record of Polokwane. ....	88
Figure 5.9. Groundwater contour map of two selected areas and derived flow vectors.....	89
Figure 5.10. Spatial distribution of the hydrochemical groups identified by the HCA.....	91
Figure 5.11. Groundwater and precipitation isotopic compositions, depicted with the GMWL.....	92
Figure 5.12. Location isotope groundwater samples.....	93
Figure 5.13. Scatter-plot of $\delta^{13}C$ and against $^{14}C$ for all samples.....	94
Figure 5.14. Scatter-plot of $\delta^{13}C$ and against $^3H$ . Also shown are plots of expected exponential model values for $\delta^{13}C$ and $^3H$ showing mean residence time (MRT) (Adapted from, Verhagen, 2000). .....	94
Figure 5.15. Results of tritium. ....	95
Figure 5.16. Spatial distribution of CFC samples together with carbon 14 samples.....	97
Figure 5.17. Tracer plots comparing CFC-11 and CFC-12 concentrations for southern hemisphere air. The solid lines represent unmixed (piston) flow with selected apparent ages ( $\sim 1985^{\circ}$ ). The dashed line shows one example of binary mixing for the case of water recharged in 1985, 1995 and 2005 diluted with old, CFC-free water. ....	98
Figure 5.18. CFC-12 and SF6 groundwater data overlaid on the ideal mixing model curves. Samples categorised as upper or lower catchment (quaternary drainage A72A) (Figure 5.16). ....	99

Figure 5.19. CFC-12 and SF6 groundwater data overlaid on the ideal mixing model curves. Selected sites have been labelled.....	100
Figure 5.20. CFC-12 and SF6 groundwater data overlaid on the ideal mixing model curves. Selected sites have been labelled.....	101
Figure 5.21. Cross-section of the hypothetical hydrochemical model for the Merokome River catchment (B81F) (Section line illustrated in Figure 5.16). Based on the CFC and carbon 14 results. ....	102
Figure 5.22. Diagnostic plots (semi- log, log-log and derivative) of a 48 hour constant rate pumping test fitted with a Theis solution (borehole H16-0206).....	106
Figure 5.23. Diagnostic plots (semi-log) of the recovery data of borehole H16-0206 fitted with a conventional Theis-recovery solution (left) and a Theis solution for the Agarwal plot (right). 107	107
Figure 5.24. Diagnostic plots (semi- log, log-log and derivative) of a 24 hour constant rate pumping test with an unconfined solution (borehole H17-0774). ....	108
Figure 5.25. Diagnostic plots (semi- log, log-log and derivative) of borehole H17-0774 fitted with a fractured (double porosity) solution.....	108
Figure 5.26. Diagnostic plots (semi- log, log-log and derivative) of a 24 hour constant rate pumping test fitted with a fractured (double porosity) solution (borehole H04-2073).....	109
Figure 5.27. Diagnostic plots (semi-log) of the recovery data of borehole H04-2073 fitted with a conventional Theis-recovery solution (left) and a fractured (double porosity) solution for the Agarwal plot (right). ....	109
Figure 5.28. Diagnostic plots (semi- log, log-log and derivative) of a 24 hour constant rate pumping test fitted with a leaky aquifer solution (borehole H16-0131).....	110
Figure 5.29. Diagnostic plots (semi- log, log-log and derivative) of a 12 hour constant rate pumping test fitted with a single fracture (Gringarten et al., 1974) model (H03-3269). ....	111
Figure 5.30. Diagnostic plots (semi- log, log-log and derivative) of borehole H16-0084, indicating reservoir boundaries. ....	111
Figure 5.31. Location of pumping tests conducted in the study area. ....	112
Figure 5.32. Semi logarithmic plot of borehole H14-0279 with two different constant discharge rates.....	114
Figure 5.33. Distribution of drawdown percentage achieved from pumping tests in the study. ....	115
Figure 5.34. High groundwater potential area in the Upper Brak River catchment. ....	116
Figure 5.35. Borehole setting of pumping test conducted at the farm Brilliant (Drawdown achieved at the end of constant test is indicated on the map). ....	118
Figure 5.36. Diagnostic plot (semi- log and derivative) model and the CCTV footage of the inferred higher permeability zone.....	121
Figure 5.37. Diagnostic plot (semi- log and log-log ) fitted with a fracture (Barker, 1988) model of pumping borehole (H11-2593) and observation boreholes (H11-2596 and H11-1653). ....	121
Figure 5.38. Diagnostic plot (semi- log and log-log) fitted with a fracture (Barker, 1988) model of pumping borehole (H11-2593) and observation boreholes (H11-2596 and H11-1653). ....	122
Figure 5.39. Diagnostic plot (semi- log and log-log ) fitted with a fracture (Barker, 1988) model of pumping borehole (H11-2593) and observation boreholes (H11-2596 and H11-1653). ....	123
Figure 5.40. Diagnostic plot (semi- log and log-log) fitted with a fracture (Barker, 1988) model of pumping borehole (H11-2593) and observation boreholes (H11-2594 and H11-1652). ....	123
Figure 5.41. Diagnostic plot (semi- log, log-log and derivative) fitted with a fracture (Barker, 1988) model of pumping borehole (H11-2593) and observation borehole (H11-2595). ....	124
Figure 5.42. Cumulative frequency of transmissivity and recommended yields from boreholes based on the structural domains delineated in section 4.3. ....	125
Figure 5.43. Spatial distribution of transmissivity obtained from the GRIP dataset.....	126



Figure 5.44. Cumulative frequency distributions showing the influence of various rock types on borehole productivity (number of boreholes in brackets).....	127
Figure 5.45. Graphs showing the correlation between transmissivity and depth of weathering and between yield and depth of weathering.....	129
Figure 5.46. Cumulative frequency distributions showing the influence of erosion surfaces on borehole productivity (number of boreholes in brackets).....	130
Figure 5.47. Typical setting of boreholes in relation to rivers and topography.....	131
Figure 5.48. Frequency histograms and cumulative distribution showing the influence of dykes encountered on transmissivity estimates. ....	133
Figure 5.49. Box plot of transmissivity and dyke azimuth for both the Limpopo and Letaba regions. The box represents the 25 and 75 % quartiles, while the median is represented by the <i>horizontal line within the box</i> . Outliers are <i>marked by circles and by crosses</i> . The <i>vertical lines (whiskers)</i> connect the smallest and largest non-outliers.....	134
Figure 5.50. Distribution of shear zones, faults and lineaments in the Limpopo Plateau, with the lineament frequency rose diagram showing main structural trends.....	136
Figure 5.51. Box plot of borehole transmissivity in relation to the lineament azimuth in the Limpopo Plateau.....	137
Figure 5.52. Distribution of shear zones dykes, faults and lineaments in the Letaba Lowveld, with the lineament frequency rose diagram showing main structural trends (squares indicate field studies).....	138
Figure 5.53. Box plot of borehole transmissivity in relation to the lineament azimuth in the Letaba Lowveld. ....	138
Figure 5.54. Field study location and the 5 km geophysical profile near Dzumeri village.....	139
Figure 5.55. Field study location and the 800 m geophysical profile near Bolobedu.....	140
Figure 5.56. Stress orientations of southern Africa (Stacey and Wesseloo, 1998).....	142
Figure 5.57. Conceptualisation of transmissivity values obtained from various borehole settings in the Limpopo basement aquifers (rose diagram indicating mean transmissivities for selected lineament azimuths based on Table 5.25).....	144
Figure 5.58. Regional distribution of transmissivity to illustrate the potential productive groundwater areas. ....	145

### *List of abbreviations*

CRD	Cumulative Rainfall Departure
CFC	Chlorofluorocarbon
CMB	Chloride Mass Balance
CGS	Council for Geoscience
DWA	Department of Water Affairs
DWAF	Department of Water Affairs and Forestry
EC	Electrical Conductivity
SAWS	South African Weather Services
GIS	Geographical Information System
IAEA	International Atomic Energy Agency
GNIP	Global Network of Isotopes
SMOW	Standard Mean Ocean Water
GMWL	Global Meteoric Water Line
LMWL	Local Meteoric Water Line
TU	Tritium Unit
GRF	Generalised Radial Flow
GRIP	Groundwater Resources Information Project
K	Hydraulic Conductivity
MAP	Mean Annual Precipitation
MRT	Mean Residence Time
NGDB	National Groundwater Data Base
NWA	National Water Act (Act 36 of 1998)
S	Storativity
T	Transmissivity
WRC	Water Research Commission
WMA	Water Management Area



### *Units of measurements*

b	aquifer thickness [L]
d	depth to top of pumping well screen [L]
d'	depth to top of observation well screen [L]
l	depth to bottom of pumping well screen [L]
l'	depth to bottom of observation well screen [L]
Q	pumping rate [L <sup>3</sup> /T]
r	radial distance [L]
s	drawdown [L]
t	time (T)
$K_z/K_r$	vertical to horizontal hydraulic conductivity anisotropy
$H_0$	initial displacement (head)
a	annum
cm	centimetre
d	day
m/d	hydraulic conductivity
m <sup>2</sup> /d	transmissivity
mg/l	milligram per litre
ha	hectare
km <sup>2</sup>	square kilometre
ℓ/s	litre per second
N	Population
m	metre
m <sup>3</sup> /s	cubic metre per second
mamsl	metres above mean sea level
m.b.g.l	metres below ground level
Mm <sup>3</sup> /a	million cubic metres per annum
fmol/l	femtomol per litre
pptv	parts per trillion volume
pmol/l	picamol per litre
mmol/l	millimol per litre
mm	millimetre
Ωm	ohm metre
mS/m	milliSiemen per metre

## 1. INTRODUCTION

### 1.1. Problem statement

The development of crystalline basement aquifers as a reliable source of water supply is notoriously complex, and groundwater occurrence is spatially highly variable (Wright, 1992; Chilton and Foster, 1995; Banks and Robins, 2002). Crystalline basement rock is distributed extensively throughout Africa and underlies large parts of the semi-arid Limpopo Province in South Africa (Figure 1.1) Some of the greatest groundwater needs occur in the region and groundwater is the only dependable source of water for many users. Groundwater is available and widely used throughout the Province, but in varying quantities depending upon the hydrogeological characteristics of the underlying aquifer. Due to the low intrinsic primary permeability and porosity of the bedrock, crystalline aquifers differ in important ways from other aquifer types, and demand specific knowledge and techniques if groundwater is to be extracted and managed efficiently.

Of great importance is the concept of sustainable yield and whether it can be determined for a weathered-fractured aquifer that is known for 1) high failure rates of boreholes, 2) low storage capacity, 3) low recharge potential (Clark, 1985; Jones, 1985; McFarlane et al., 1992). However, from the onset it was realised that the evolving concept of sustainability in the groundwater field presents a challenge to any hydrogeologist. In many ways this can be attributed to the divergent opinions that exist as to whether natural recharge is important (i.e. Kalf and Woolley, 2005) or not (i.e. Bredehoeft, 2002) in assessing the sustainable development of groundwater. Sustainability is a broader concept than simple sustainable pumping, and it depends on the changes to the ecology, human welfare and water quality during groundwater development (“capture”). Today, there is an open debate regarding the concept of sustainable yield and whether it can be scientifically determined.

Although the debate regarding safe groundwater development continues, the basic physical principles are all that are available to hydrogeologists when it comes to predicting or anticipating the likely outcome of groundwater exploitation. Appropriate hydrogeological application is essential to optimise the use of Africa’s increasingly scarce water resources (Robins et al., 2006). One of the principal tools for these investigations is the groundwater model, but the reliability of such models depends partly on a sound conceptual model with an accurate knowledge of the geometry and the hydraulic properties of the aquifer. These aquifer properties are often determined by assessing the aquifers response to pumping and fitting the observed data to a known conceptual (theoretical) model. However, the choice of model is not easy as different models can have the same type of response.

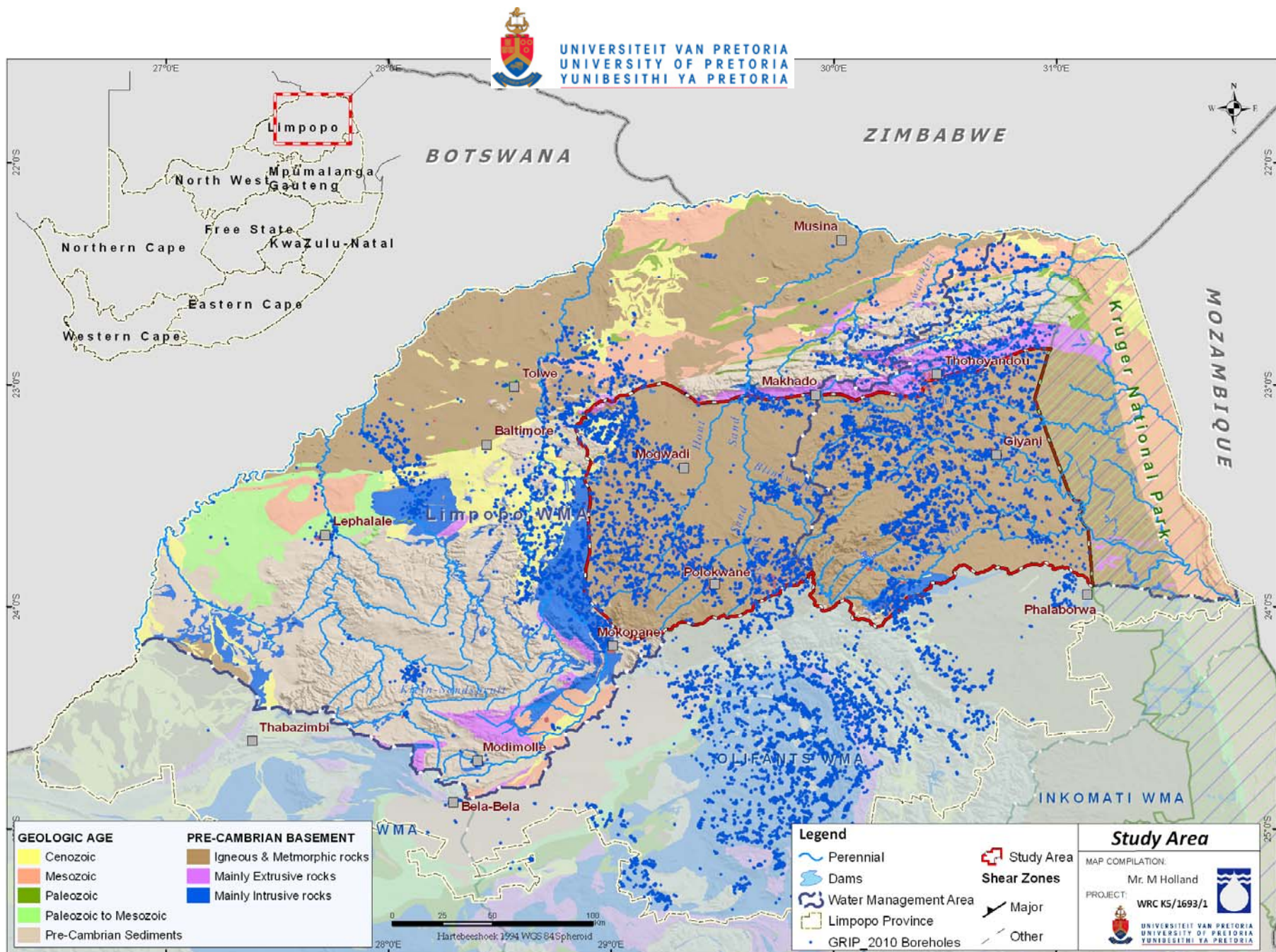


Figure 1.1. Study Area.



Across much of tropical Africa crystalline basement rocks have a thick cover of in situ, chemically-weathered overburden (Jones, 1985). Consequently, a large number of boreholes are completed in this shallow unconsolidated weathered zone (regolith). Since the regolith can be represented as a porous medium its hydrodynamic properties are easily measured with classical analytical models such as Theis (1935) and the Jacob's approximation (Cooper and Jacob, 1946). However, most crystalline basement aquifers respond as a dual aquifer system with a weathered zone overlying a fractured zone. The fractured bedrock may be more or less confined, depending on the hydraulic conductivity of the overlying material. The concept of an unconfined weathered zone overlying the fissure zone can be represented by 1) a leaky aquifer system comprising of an aquifer-water table aquitard model, or 2) a delayed gravity response assuming instantaneous drainage at the water table. Where the crystalline basement rocks are well exposed and essentially un-weathered, main groundwater occurrences are limited to fissure or fracture zones. In these regions characterisation of the flow dimension, location and connectivity of fractures is essential for interpreting the aquifer response to pumping (i.e. double porosity or single fracture models). Whilst several analytical models can be used to evaluate weathered-fractured aquifers, the difficulty is to identify the model that best represents reality. Kruseman and de Ridder (1990) accentuate that: "the choice of theoretical model is a crucial step in the interpretation of pumping tests. If the wrong model is chosen, the hydraulic characteristics calculated for the real aquifer will not be correct".

Determining hydraulic properties in basement rocks aquifers is clearly not straightforward and results are highly variable due to the intrinsic heterogeneity. Perhaps an even bigger challenge is to develop an understanding of the controls on groundwater occurrence (Clark, 1985; Jones, 1985; McFarlane et al., 1992; Henriksen, 1995; Neves and Morales, 2007). A lack of understanding of the occurrence, movement and recharge of groundwater in basement terrain has frequently contributed to the unsustainable use of this resource (Chilton and Foster, 1995). Independent or interrelated factors such as geomorphology (topography), lithology, brittle (neo-) tectonics, and surface water hydrology all play a significant role in the occurrence of groundwater in crystalline rocks, because together they control 1) the nature and depth of the regolith, 2) the development of fracture and fault zones and, 3) the presence of higher porosity material (or adjacent alluvium). Hence groundwater exploration in crystalline areas would normally pay close attention to locating weathered material, together with the geological and tectonic controls directly related to structural features which control deeper groundwater flow.

Despite some major hydrogeological investigations in the 1970s and the installation of numerous hand-pumped water supply boreholes for rural communities throughout south eastern Africa, the hydrogeology of crystalline aquifers are not yet fully understood. This can be largely be attributed to the lack of-, and poor accuracy of data. An assessment of factors influencing borehole yields is meaningless unless sufficient data are available to make statistically significant deductions. However, unless the same method of measurement (i.e. blow yield vs. tested yield) and recording is used it can be unrealistic to make any comparison between two crystalline regions as the lack of uniformity in the raw data give rise to different results rather than actual differences in

hydrogeology (Houston, 1992). In addition, it is difficult to prove that for example that a specific geological lineament orientation offers higher borehole productivity if there is a lack of derived hydrogeological data such as borehole yield and transmissivity. In the absence of sound hydrogeological data surrogate information such as specific capacity is often used as a measure of the water bearing capacity of the aquifer (Fernandes and Rudolph 2001; Neves and Morales 2007). It is commonly accepted that no single unique factor will guarantee high yielding boreholes and that the relative importance of specific factors influencing borehole yield vary according to the particular characteristics of the area or geological setting. Taking this into consideration, the study of influencing factors on groundwater occurrence is an attractive proposition in the crystalline bedrock of the Limpopo Province where the the siting of boreholes remains a challenge and is a random process in many cases.

## **1.2. Investigation objectives**

Approximately 35% of rural communities in the region are dependent on groundwater and 60% use surface- and groundwater conjunctively (DWAF, 2009). The importance of these basement aquifers makes it important to identify high yielding hydrogeological zones that can be targeted for water supply, to sustain areas of high population density with few or no alternative water sources. However, studies regarding the optimal locations for high yielding boreholes are rare. The Water Research Commission of South Africa initiated a study to determine sustainable yields of potential productive well fields in these basement aquifers, which formed the basis of this thesis. To stay clear of the conceptual ambiguities regarding the term sustainability, the focus was mainly on developing an understanding of groundwater -occurrence, -flow and -behaviour in these crystalline rocks.

The main objective was therefore to identify certain factors which may enhance borehole yields. The following factors were considered; 1) the geological and topographical setting, 2) dykes and linear anomalies (including their orientation), 3) regional tectonics (major horizontal principal stress), 4) weathering thickness, and 5) proximity to surface water drainages. The results will provide water resource planners with a number of regional groundwater exploration targets that may lead to improved borehole success rates and yields. While it is acknowledged that the basement aquifer covers the Limpopo Province extensively it is important to note that a specific study area was chosen based on the coverage of borehole data (Figure 1.1).

A secondary objective was the classification of aquifer systems (theoretical models) or “type curves” based on observed drawdown responses during hydraulic testing. Categorising these behaviours can greatly assist groundwater practitioners in choosing the correct conceptual (theoretical) model for pumping test interpretations, which will lead to more accurate parameter estimation and inevitably better decision making regarding abstraction rates.

More specific objectives of the research include:

- evaluation of sustainable yield (source vs. resource),
- identification of typical drawdown behaviours from the numerous pumping test data available from the Groundwater Resources Information Project (GRIP),
- proposed analytical methods for typical responses for basement aquifers, and
- an estimation of aquifer parameters.

These objectives can only be achieved with an adequate knowledge of the regional hydrogeology together with geology, geomorphology, and climate information. This includes an accurate description of:

- the structural geology,
- borehole success rates, yields, water strikes and depth of weathering, and fracturing,
- recharge -estimates and -processes (groundwater ages and flow mixing),
- chemical evolution of groundwater, and
- groundwater quality hazards affecting suitability (sustainability) of use.

It is foreseen that the content of this thesis will be of interest to all workers on groundwater in Precambrian bedrock, not only in the southern part of the African continent, but also elsewhere in the world.

## 2. CHARACTERISATION OF CRYSTALLINE BASEMENT AQUIFERS

### 2.1. Conceptual framework

Crystalline basement rocks (bedrock) are composed of hard, crystalline or re-crystallised rocks of igneous or metamorphic origin, such as granites, basalts, metaquartzites or gneisses with negligible primary porosity and permeability (Clark, 1985; Gustafson and Krásný, 1994). Crystalline bedrock is exposed (outcrops) in numerous locations throughout South Africa and covers approximately 15% of the total land area. However, almost the whole country is underlain by crystalline bedrock, albeit in places under a thick cover of more recent geological formations. They can be divided into three main suites in South Africa.

- I. Ancient rocks of the Archaean cratonic nuclei (i.e. Kaapvaal craton), including granites, gneisses and greenstones, such as the Halfway House Granite in Gauteng, South Africa.
- II. Metamorphic rocks of the mobile belts, showing strong deformation and often of Proterozoic age, such as the gneisses of the Limpopo Mobile Belt (i.e. Beit Bridge Complex).
- III. Anorogenic intrusions of various ages, such as the Bushveld Igneous Complex and Cape Granite Suite.

Potential composite aquifers are developed within the weathered overburden and fractured bedrock of these crystalline rocks, and are commonly referred to as basement-, hard rock-, bedrock- or weathered-fractured rock aquifers. In this study, the focus will be on the Archaean age crystalline lithologies.

#### 2.1.1. Classical weathered-fractured rock concept

Although more detailed weathering profiles for crystalline rock can be found from recent literature (i.e. Dewandel et al., 2003), the classical (traditional) weathering-fracturing concept proposed in the 1980s and 1990s (i.e. Jones, 1985; Acworth, 1987; Chilton and Foster 1995) still applies to most crystalline basement terrains. The “classical” model of a basement aquifer refers to the following layers which have specific hydraulic properties (illustrated in Figure 2.1):

- An overlying regolith (unconsolidated material derived from prolonged in-situ decomposition of bedrock.), with a thickness from negligible to a couple of tens of meters.
  - Weathering is more rapid in tropical parts of Africa, whilst in arid areas or higher-lying areas where the rate of weathering is low in comparison with that of erosion, the regolith may be thin or absent.
  - The regolith usually has a high porosity and a low permeability (due to clay-rich material) (Acworth, 1987). When saturated, this layer constitutes the reservoir of the aquifer.
- The porosity of the weathered profile generally decreases with depth, along with clay content, until fresh rock is reached.

- This fractured-weathered layer is generally characterized by a fracture density that decreases with depth, and which can be related to cooling stresses in the magma, subsequent tectonic activity (Houston and Lewis, 1988) or litho-static decompression processes (Wright, 1992)
- The horizon of fracturing between the fresh rock and the regolith frequently has a higher permeability, depending on a number of factors including the nature of the fracturing and the presence of clay in the fractures.
- This layer mainly assumes the transmissive function in the aquifer and is pumped by most of the wells drilled in hard-rock areas (Maréchal et al., 2007).
- Fresh basement (un-weathered) is permeable only locally where deep tectonic fractures are present.
  - The structural features are extremely variable in nature (with regard to frequency, spatial extent, interconnectedness, etc.) within the relatively impervious crystalline rock mass (Gustafson and Krásný, 1994).

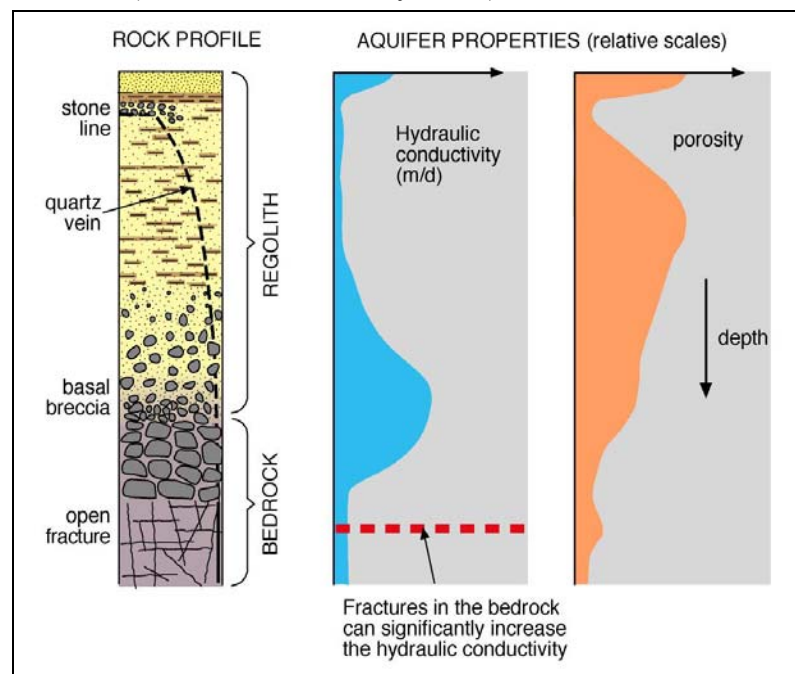


**Figure 2.1. Permeability and porosity in basement aquifers (Chilton and Foster, 1995).**

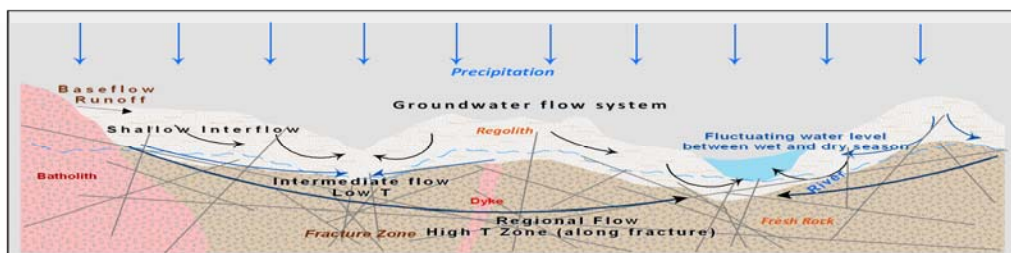
The main differences from one crystalline terrain to the next are in principal attributed to 1) the degree (thickness) of weathering and whether saturated or not, and 2) the extent of fracturing. However, these two complex components which largely influence the crystalline rocks potential as a groundwater supply depends on a number independent and interrelated factors on a regional and local scale. The common viewpoint (i.e. Wright and Burgess, 1992) of crystalline basement aquifers is that long-term borehole productivity relies on the presence of weathered material overlying the fractured rock or an alternative source of recharge such as a river or associated alluvium. Therefore, in more arid crystalline terrain with a lack of surface water resources and where a thinner weathered overburden is present, the interest of hydrogeologists in such aquifers is increased. In these cases focus is predominantly on the dominant fissure/fracture flow



developed in the underlying fractured bedrock (i.e. Dutta et al., 2006; Galanos and Rokos, 2006; Neves and Morales, 2007; Titus et al., 2009).

### 2.1.2. General flow behaviour

Flow in hard-rock aquifers is inherently very complex and is governed by the hydraulic potential gradient and the hydraulic conductivities in the regolith and underlying fractured bedrock. A classical model for the recharge processes and flow systems in the crystalline basement regions of sub-Saharan Africa can be found in Wright (1992). Theoretical studies of two-dimensional groundwater flow in vertical sections by Tóth (1963) indicated that local, intermediate, and regional flow systems could be superimposed on one another within a groundwater basin. This is somewhat in contrast to the general flow behaviour of crystalline aquifers which suggest that groundwater flow is essentially shallow, focused in the weathered and fractured zone, generally limited to 50 metre below ground level. However, regional flow occurs within the major interconnected fracture systems, while the main groundwater flow systems are relatively localised to the zones between recharge on watersheds to discharge by run-off or evaporation at valley bottoms (Figure 2.2). Fractures exposed to the surface can create preferential flow paths which short circuit the path to the water table. Due to its higher porosity the regolith zone acts as a reservoir that slowly feeds water downward into fractures in the bedrock. Where good hydraulic interconnection is present between the basement rock and regolith, it is likely that excessive exploitation of the basement rock aquifer would induce vertical leakage from the regolith, thereby effectively utilizing the regolith's resource (Howard and Karandu, 1992). However, the recharge to the bedrock from the overlying regolith is generally difficult to estimate as it is governed by the hydraulic conditions at the regolith–bedrock interface. Consequently only a few published studies address the issue of recharge from soil (regolith) to bedrock. One such investigation conducted in central Sweden by Rodhe and Bockgård (2006) showed that a granitic bedrock aquifer was recharged by vertical flow from the overlying 10 m thick till soil, based on the assumption that the bedrock can be represented as a continuous porous aquifer.



Mr. M Holland

**Figure 2.2. Simplified flow system for crystalline basement terrain (Adapted from Tóth, 1963; Chilton and Foster, 1995).**

## 2.2. Groundwater recharge

Groundwater recharge can be defined as the portion of total rainfall falling into a drainage basin that ultimately reaches the water table in the phreatic zone of an aquifer (Freeze and Cherry, 1979). Recharge to crystalline basement rocks is a function of the mode of chemical weathering of the surface and the rate of fracturing (Lerner et al., 1990). Harte and Winter (1996) indicated that four factors influence bedrock recharge patterns: (1) relief of land and bedrock surface above groundwater discharge areas; (2) lateral trends in bulk-rock horizontal conductivity; (3) local topographic features; and (4) local drift stratigraphy. Recharge is directly related to rainfall, although this relationship is not linear as shown in Figure 2.3.

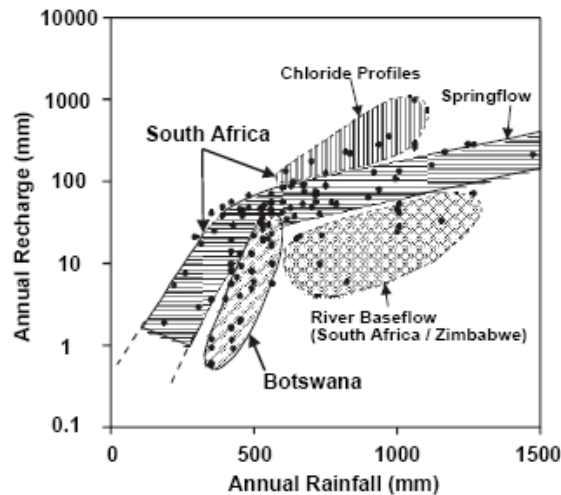


Figure 2.3. Recharge estimates for southern Africa (Xu and Beekman, 2003; Adams et al., 2004).

Across much of southern Africa potential evaporation is higher than average annual rainfall, and recharge is likely to be episodic and often via preferred pathways rather than uniformly distributed. Where mean annual rainfall is less than 400 mm, recharge from direct infiltration is likely to be small or negligible (Wright, 1992). Quantifying recharge is a common objective in many applications in groundwater hydrology in semi-arid areas such as the Limpopo Province and is especially relevant to discussions about groundwater sustainability. Methods of estimating recharge are subject to significant uncertainty in crystalline basement terrain, because of the heterogeneity and discontinuity of the aquifer and the resulting complexity of the groundwater flow system (Chilton and Foster, 1995). However, several of the conventional methods of recharge estimation can be used in semi-arid southern Africa if the underlying assumptions are taken into consideration (i.e. Xu and Beekman, 2003).

The Chloride Mass Balance (CMB) method has been suggested as the most reliable technique for determining recharge rates to fractured rock aquifers systems (Cook, 2003). However, the recharge rate determined from the CMB should be considered as a minimum rate because of the addition of other sources of chloride, which may occur, due to rock weathering (Banks et al., 2009). Therefore the CMB-method on its own might not give an accurate account of recharge estimations and should be used in conjunction with other recharge methods. Groundwater level fluctuations and rainfall correlation methods to estimate recharge have been applied in the

Namaqualand Basement aquifers (Adams et al., 2004). The analysis of water-level fluctuations can be useful for determining the magnitude of long-term changes in recharge caused, perhaps, by changes in climate or land use. Favourable aspects of the water fluctuation method include its simplicity and ease of use: it can be applied for any borehole that taps the water table, where an abundance of available water-level data exists (Healy and Cook, 2002).

### 2.3. Groundwater quality

Natural groundwater quality in most basement environments is generally good (Clark, 1985; Chilton and Foster, 1995), with low salinities and neutral to slightly acid pH values being common. However, salinities are elevated in areas of low recharge and/or prolonged residence times in the subsurface. Natural water quality in basement can occasionally be detrimental to human health through high levels of trace elements such as fluoride (Marais, 1999). Metals such as aluminium are also mobile in low pH groundwater. High iron concentrations associated with lateritic soils, whilst not harmful to human health, can stain appliances and clothes and make water unpalatable (Clark, 1985). Crystalline basement aquifers are very vulnerable to pollution of the groundwater, particularly where the regolith is thin, since groundwater movement through fractures is rapid and the fractured rock matrix provides little attenuation of contaminants. It is therefore necessary to test groundwater for natural quality, and groundwater development in a new area should always take water quality into account. Numerous village water supply boreholes in basement areas have been sited close to pit latrines, and microbial contamination has occurred, since both latrine and borehole penetrate to below the zone of lower permeability regolith. Poor water quality can be as great a constraint on the development of a resource, as low quantities.

#### 2.3.1. Geochemical studies

Advances in geochemical methods and approaches have aided our ability to interpret hydrochemical processes in groundwater systems, and improved understanding of how structural, geological, and hydrological features affect flow and chemistry (Glynn and Plummer, 2005). Multivariate statistical methods like cluster analysis classify and compare different chemical parameters of the water analysis and determines the relationship between them (Güler, et al., 2002; McNeil et al., 2005). The relationship of the statistically defined clusters of samples to geographic location illustrates an important message that geochemical survey datasets contain i.e. the variation in regional distribution.

Hydrochemical and isotope studies are frequently included in basement aquifer investigations and give valuable additional information on the structure of the aquifer system (i.e. McFarlane, 1992). In regional studies, hydrochemical and isotope data can be used to distinguish between shallow and deep aquifers (Nkotagu, 1996; Praamsa et al., 2009; Banks et al., 2009). They are also useful for identifying zones of interaction (mixing) and recharge processes (Sukhija et al., 2006; Jayasena et al., 2007; Horst et al., 2008). Radioisotopes such as tritium,  $^{13}\text{C}$  and  $^{14}\text{C}$  are used to determine the mean residence time (MRT) of groundwater. The accuracy of reliable dating of

water is however often limited by the uncertainty surrounding the initial radioisotope concentration (Verhagen et al., 1991). More innovative and integrative methods for recharge characterisation and MRT are currently available such as chlorofluorocarbon (CFC) sampling. CFCs have provided useful tools for tracing and dating post-1945 water and groundwater mixing properties (i.e. Busenberg and Plummer, 2000; Goody et al., 2006; Horst et al., 2008).

## 2.4. Groundwater hydraulics

Crystalline basement aquifers can be considered to fall on a continuum between porous media and conduit systems (Cook, 2003). The unconsolidated weathered mantle can be represented by a porous medium, while the consolidated fractured bedrock can be regarded as a fractured porous media with groundwater flows in the conduit network and water stored in the aquifer matrix between the conduits. The analysis of pumping test data studies the behaviour of an aquifer inversely and suffers from non-uniqueness, where the observed response of an aquifer can be fitted with two or more sets of aquifer parameters, boundary and initial conditions that differ completely from one another (Van Tonder et al., 2001). Usually this is solved by assuming a simple model based on a set of hydraulic parameters, boundary and initial conditions of a known conceptual model. However, the difficulty is to identify the model that best represents reality.

### 2.4.1. Aquifer response evaluation

To circumvent the difficulty in choosing an appropriate conceptual model, diagnostic plots are constructed. Diagnostic plots include log-log plots of the drawdown versus the time, semi-log plots of drawdown versus time or drawdown versus distance to the well. The drawdown curve of the observed dataset is then compared to the characteristic type-curve of a known conceptual ('theoretical') model. Theoretical models comprise of 1) the type of aquifer (i.e. confined, unconfined or leaky), 2) inner boundary conditions associated with the pumped well (i.e. fully or partially penetrating, small or large diameter, well losses), and outer boundary conditions (i.e. constant head, impermeable walls, leaky or open conditions, or to extend to infinity). The classical theoretical diagnostic plots of the time-drawdown relationships of unconsolidated and consolidated aquifers can be found in Kruseman and De Ridder (1990).

The analysis of the logarithmic derivative to facilitate the identification of an appropriate conceptual model best suited to interpret the data became standard in the petroleum industry after the work of Bourdet et al. (1983). However, despite the early introduction of the concept in hydrogeology by Chow in the early 1950s the use of derivative analysis remains both under-used and under-reported in the hydrogeological literature (Samani et al., 2006). In South Africa, the use of derivatives to characterise drawdown behaviour is mainly due to the development of the Flow Characteristic Excel-programmed code by Van Tonder et al., (2001). The program provides powerful tools for the detailed diagnostic and analysis of step, constant and recovery drawdown data.

The modern techniques of model identification include the use of logarithmic derivatives together with the drawdown as a function of time in logarithmic scale. The main advantages and limitations of the use of both drawdown and its logarithmic derivative versus time in the hydrogeological field are discussed in Renard et al. (2009). In applying traditional techniques, it is not always easy to visualize whether the interpretation is valid or not. The derivative is highly sensitive to subtle variations in the shape of the drawdown curve, which makes the problems more visible. It is expected that with the automatic fitting techniques through commercial software (which offer derivative plots), that the use of the derivative for model identification will become common practice in groundwater supply investigations. Renard, (2005b) and Renard et al. (2009) provides an excellent synthesis of theoretical diagnostic plots (drawdown and derivative) from which the aquifer type can be inferred from, based on the drawdown behaviours in response to constant pumping rate (Figure 2.4). The classification relating to Figure 2.4 is: a) Theis model infinite two-dimensional confined aquifer; b) double porosity or unconfined aquifer; c) infinite linear no-flow boundary; d) infinite linear constant head boundary; e) leaky aquifer; f) well-bore storage and skin effect; g) infinite conductivity vertical fracture.; h) general radial flow—non-integer flow dimension smaller than 2; i) general radial flow model—non-integer flow dimension larger than 2; j) combined effect of well bore storage and infinite linear constant head boundary.

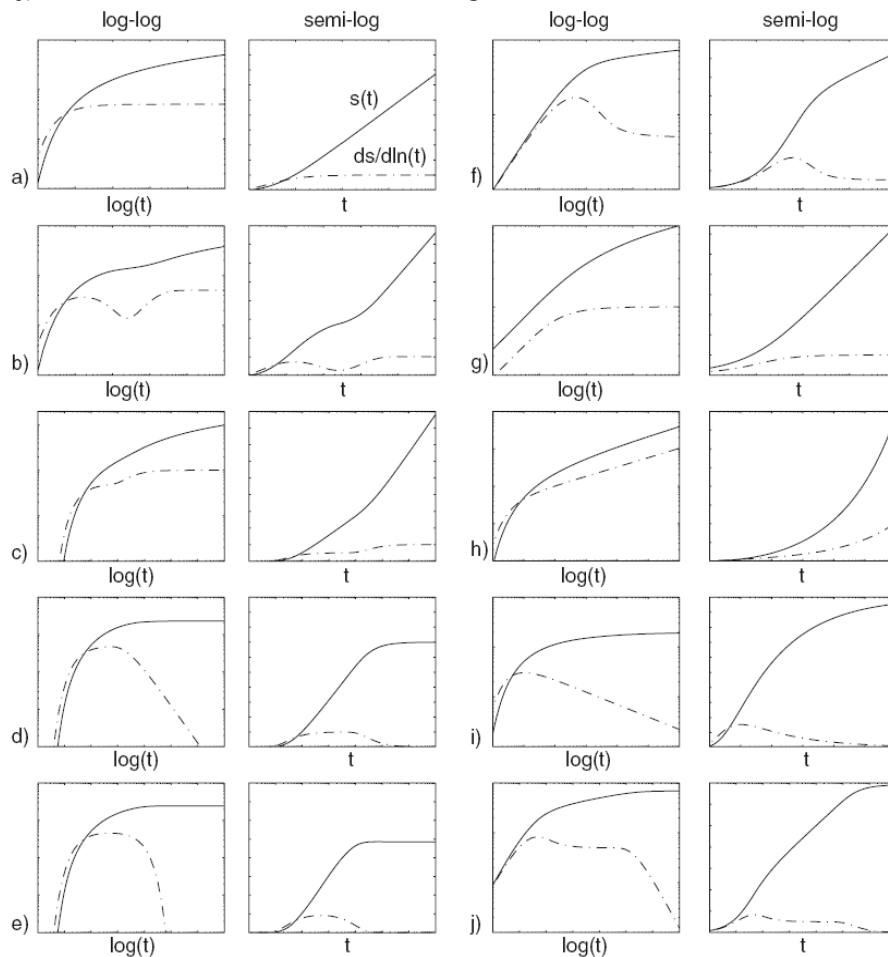


Figure 2.4. Most typical diagnostic plots encountered in hydrogeology (Renard et al., 2009).



#### 2.4.2. Aquifer models applicable to crystalline basement aquifers

The history of well hydraulics and well testing started in 1863 with Dupuit, who developed the first analytical solution to model radial flow to a well in steady state. In 1935, Theis published the most important analytical solution. The Theis solution assumes that the aquifer is confined, bidimensional, homogeneous, and isotropic. A good synthesis of the historical and current perspective including the future of hydraulic testing is presented in papers published by Renard (2005a) and Butler (2008). Both of these authors have pointed out the concerns over the significance of results obtained from applying homogenous solutions to clearly heterogeneous aquifers. This was more vividly put by Wu et al. (2005) as: “Are we comparing apples to oranges?” Despite the inconsistencies and shortcomings identified by authors such as Wu et al. (2005) and Yeh and Lee (2007), traditional methods are still widely applied because they are able to solve the inverse problem and yield results. In addition, inferring the degree of heterogeneity from a pumping test is extremely difficult and solutions considering more complex aquifer situations with strong heterogeneity remain to be seen. Renard (2005a) and Butler (2008) concluded that conventional pumping test analysis will continue to play an important role in providing practical information in water supply investigations.

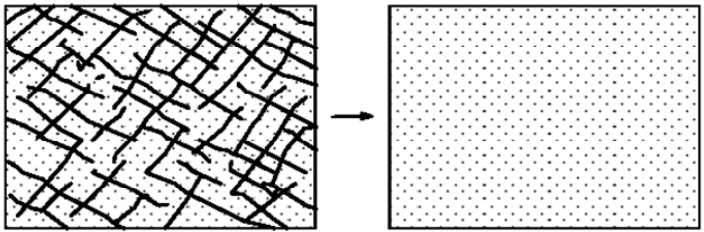
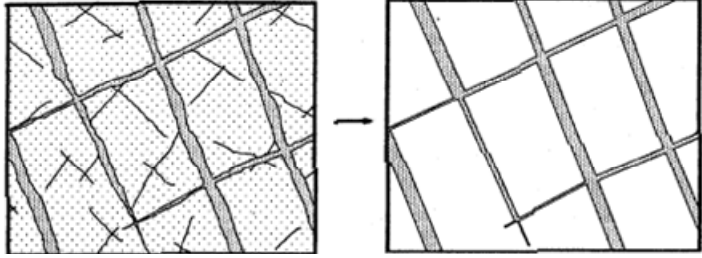
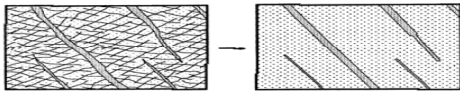
Since the early 1950s there has been a continuous and parallel development of analytical models and well-testing procedures that can be applied to weathered-fractured media such as: leakage from an adjacent aquifer (Hantush and Jacob 1955; Moench, 1985), partially penetrating well (Hantush, 1961), large diameter well (Papadopulos and Cooper, 1967), flow in an anisotropic unconfined aquifer with delayed gravity response (Neuman, 1974; Moench, 1997), dense network of fractures in a porous matrix (Moench, 1984; Barker, 1988), and single fracture intersecting the well (Gringarten et al., 1974; Gringarten and Ramey, 1974).

Many authors have indicated that crystalline basement rocks are usually semi-confined (fractured bedrock) with a water-table aquifer (the matrix - regolith) situated on top of it (Chilton and Smith-Carington, 1984; Rushton and Weller, 1985; Sekhar et al., 1994; Taylor and Howard, 2000; Van Tonder, 2002; Gonthier, 2009). These two components are hydraulically interconnected and cannot be treated separately. Consequently, many studies have applied a combination of pumping test solutions that govern vertical leakage such as the classical leaky-aquifer model or unconfined condition with delayed gravity response, while considering the double-porosity behaviour of the underlying bedrock (i.e. Taylor and Howard, 2000). To determine the existence of a vertical anisotropy of permeability in the fissured layer of a granitic hard-rock aquifer, Maréchal et al. (2004) interpreted the drawdown at the observation wells by means of the anisotropic unconfined Neuman (1972) method and at the pumping wells by using a horizontal fracture method developed by Gringarten and Ramey (1974). The study was further enhanced by applying the Barker (1988) theory, which takes into account the dimension of the flow, which results from the distribution and connectivity of the conductive fractures (Maréchal et al., 2007). Gernand and Heidtman (1997) conducted a 24-well 21 day pumping test to characterise a low-yielding fractured gneiss aquifer. Based on the drawdown curves, the authors used a single fracture model

for this aquifer test, and showed that in low-porosity crystalline bedrock a single fracture zone may yield most of the water to a well.

### 2.4.3. Summary of conceptual models

To describe the heterogeneity associated with fractured aquifers, three main approaches are commonly used to model groundwater flow and solute transport namely 1) the equivalent porous media approach, ii) the discrete fracture network approach, and iii) the dual porosity approach (Figure 2.5). A practical guide of the advantages and limitations of each approach and the principles that guide the choice of modelling approach can be found in Cook (2003).

	<p><b>Equivalent porous media (EPM)</b></p> <ul style="list-style-type: none"> <li>• Hydraulic properties can be described with a representative elementary volume (REV) concept.</li> <li>• Applicable for homogenous, densely fractured rocks or matrix blocks</li> </ul>
	<p><b>Discrete fracture network models</b></p> <ul style="list-style-type: none"> <li>• Applicable for fractured rocks with impermeable matrix</li> <li>• account for flow path geometry and fracture properties ( suited to smaller-scale modeling studies)</li> <li>• Matrix diffusion and storage must be negligible</li> </ul>
<p><b>Fracture matrix models</b></p> <ul style="list-style-type: none"> <li>■ Combination of discrete fracture network model and continua model for the matrix.</li> <li>■ Applicable for all types of fractured rocks, esp. sedimentary rocks or rocks with different fracture sets (D)</li> </ul>  <p>(Kröhn 1990)</p>	<p><b>Fracture matrix (dual porosity) models</b></p> <ul style="list-style-type: none"> <li>• Combination of discrete network model and continua for the matrix</li> <li>• Applicable to most types of fractured rocks, especially sedimentary rocks</li> <li>• Tendency to oversimplify geometry of the fracture network</li> </ul>

**Figure 2.5. Different modelling approaches for fractured rock aquifers (Kröhn, 1990).**

Modelling is important for improving our understanding of system behaviour. However, when constructing a conceptual model of a fractured rock aquifer, apart from identifying features that may be important in controlling the hydrogeology, it also depends on the scale of interest (Figure 2.6). A fractured rock aquifer may be connected on a large scale but may be dominated by a small number of larger fractures on a smaller scale.

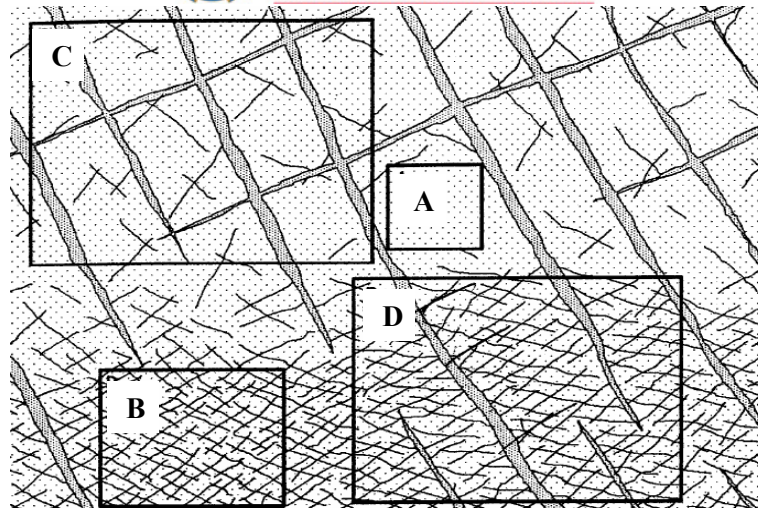


**Figure 2.6. Depending on the scale of interests a number of fracture flow models can be identified; matrix blocks (A), densely fractured rocks (B), fracture rocks with impermeable matrix (C), and combination of fracture network and matrix blocks (D) (Kröhn, 1990).**

It is clear that no single analytical method can be universally applied to crystalline basement aquifers when considering the analysis of pumping test data. Therefore, a summary of the concepts of the most applicable models is considered beneficial. Kruseman and de Ridder (1990) and Van Tonder et al. (2002) provide excellent well-illustrated handbooks to well-flow equations that cover a wider range of flow models and their application to field data.

*Homogeneously fractured, uniform aquifer (Ideal Confined)*

The aquifer is assumed to be infinite in lateral extent, fully confined (no recharge or leakage), two dimensional (large extension compared to its thickness), having a homogeneous transmissivity and storativity (Figure 2.7). In this approach, it is assumed that at the scale of interest the fractured aquifer behaves identically to an unconsolidated medium. A fractured aquifer will most likely fulfil this assumption if a dense network of uniform fractures intersects the rock. Theis (1935), and Cooper and Jacob (1946) described the unsteady-state radial convergent flow around the pumping well in a confined homogeneous and isotropic aquifer.

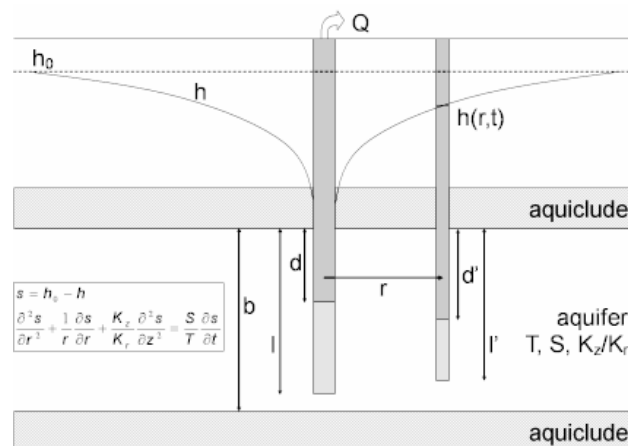


**Figure 2.7. Schematic illustration of an idealized confined aquifer.**



### *Leakage through the confining layer*

This model considers a confined aquifer overlain by an aquitard and another aquifer (Figure 2.8). It is assumed that the pumped aquifer is recharged from the un-pumped aquifer through the aquitard. The pumped aquifer is an ideal homogeneous isotropic and infinite two-dimensional aquifer. The flow is assumed to be vertical in the aquitard, there is no storage in the aquitard, the head remains constant in the unpumped aquifer, and the flow remains horizontal in the aquifer. Hantush and Jacob (1955) developed the first analytical solution for this situation. Moench (1985) has included wellbore storage and wellbore skin, including three configurations for simulating a leaky confined aquifer with aquitard storage. Case 1 assumes constant-head source aquifers supply leakage across overlying and underlying aquitards. Case 2 replaces both constant-head boundaries in Case 1 with no-flow boundaries. Case 3 replaces the underlying constant-head boundary in Case 1 with a no-flow boundary.

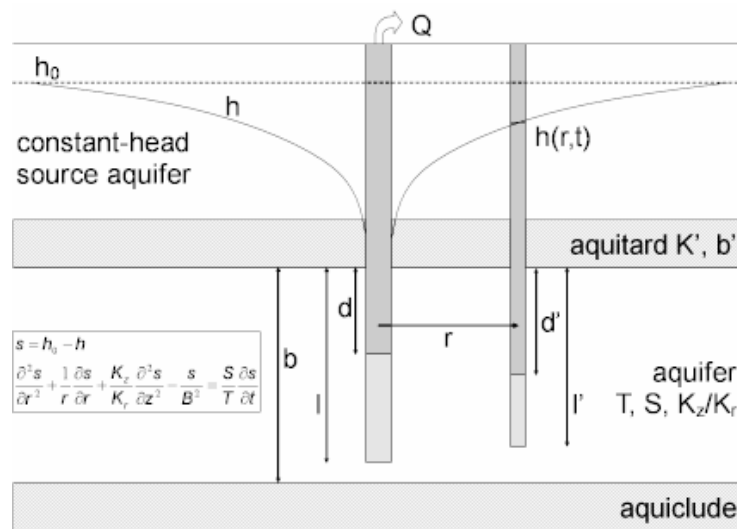


**Figure 2.8. Schematic illustration of an isotropic leaky confined aquifer.**

### *Unconfined aquifer*

Unconfined aquifers are commonly encountered in well-test analysis and are also known as water-table aquifers. The aquifer is bounded below by an aquiclude, but is not restricted by any confining layer above it. Therefore the water table is free to rise and fall as the saturated zone is in direct hydraulic relation with the unsaturated zone. The approach most often used is based on the concept of a delayed water-table response. It was initiated by Boulton (1954) and developed by Neuman (1972, 1974). Time-drawdown curves on a log-log plot show a typical sigmoidal shape, with three distinct stages (Renard, 2005b). In the early time, the drawdown follows a Theis type curve corresponding to the release of water from elastic storage. Then, there is a transition with a flattening of the curve. For late time, the drawdown follows a second Theis curve corresponding to the release of water from the drainage of the unsaturated zone.

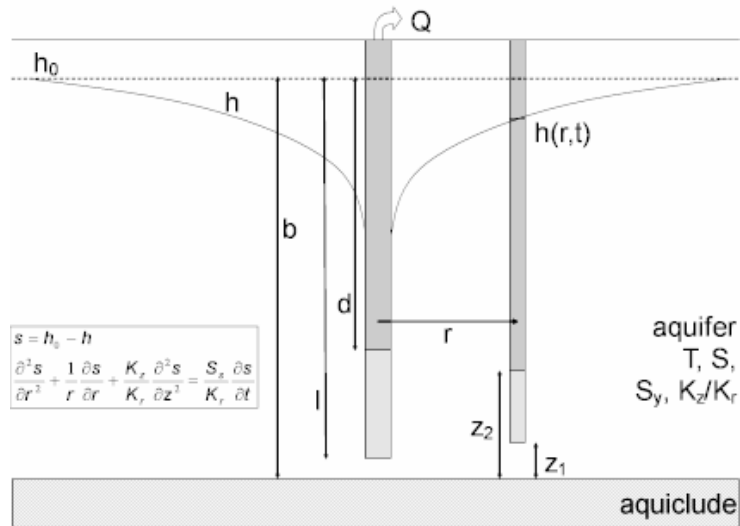


**Figure 2.9. Schematic illustration of an unconfined aquifer.**

*The double porosity model*

The concept of double porosity was introduced by Barenblatt et al. (1960), considering homogenous distributed conductive fractures embedded in a homogenous distributed matrix (blocks) (Figure 2.10). For both fracture and matrix, different conductivity and storage coefficients can be adopted (Van Tonder et al., 2002). The matrix blocks, however, are of low permeability but possess a high (primary) porosity and storage capacity. Only the fractures produce a flow directly to the well. The flow from the fracture into the well is radial. This implies a dense, homogeneous and continuous fracture network. The matrix blocks act as a source, which feeds water into the fractures.

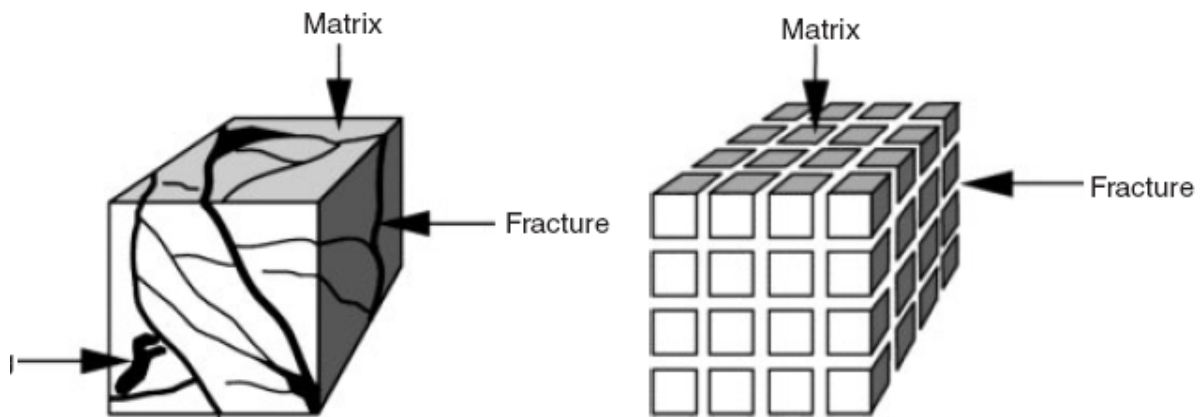


**Figure 2.10. A fractured block illustrating the double porosity concept (Cinco-Ley, 1996 in Renard, 2005b).**

Warren and Root (1963) introduced a pseudo-steady state block-to-fracture flow solution, but Kazemi (1969) using numerical models found that the flow is of transient block-to-fracture nature. Moench (1984) showed that the pseudo-steady flow case is, in fact, a special case of the transient flow restricted by a skin between fracture and matrix. Moench (1984) presented the most complete solution including pseudo-steady state and transient interporosity flow including

wellbore storage, well skin and fracture skin, and is therefore more advanced than the simple straight line approach proposed by Warren and Root (1963). However, Moench (1984) assumed an infinite extent of the matrix and fracture system under confined conditions, including an aquifer with uniform thickness and matrix blocks that are slab shaped or spherical.

The typical sigmoidal shape time-drawdown curve observed is similar to that from an unconfined aquifer. During early time, the water is pumped from storage in the fractured system and the matrix does not affect the flow. At intermediate times, water is released from the matrix while the drawdown in the matrix is small compared to drawdown in the fractures. During late time, the drawdown in the matrix approaches the drawdown in the fractures and the aquifer behaves like a single porosity aquifer with the combined property of the matrix and the fractures.

### *Individual fractures*

A more specific situation is the case of an individual fracture intersected by the well and acting as a drain in a larger porous aquifer. The concept assumes that a set of vertical fractures or a dyke can be idealised by a single vertical fracture which fully penetrates the confined and otherwise homogeneous aquifer (Bäumle, 2003). The unsteady-state flow towards the well follows distinct flow phases, which can be summarised as (Figure 2.11):

- Linear fracture flow (from fractures open to the borehole) is observed when the feature has a finite conductivity and is either embedded in an inert formation (matrix) or in a low conductive formation (Cinco and Samaniego, 1981).
- Bilinear flow occurs if the matrix is permeable enough; the linear flow in the fracture is superposed by a perpendicular linear flow from the formation to the fracture (where fractures are recharged via the pores).
- Linear flow from the formation to the fracture in the case of infinite conductive single features with negligible storage (Gringarten et al. 1974) (when all fractures have been dewatered and the rock mass determines the water supply to the borehole).
- Radial flow (also known as pseudo-radial flow or radial-acting flow) appears when the cone of depression is approximately circular. It is generally observed in a fully penetrating well (line source) located in homogeneous reservoirs, but also in a well in any fractured reservoir that can be considered as continuum. The start of the radial flow indicates the time at which the fractured reservoir behaves in a homogeneous manner.
- Spherical flow is observed in cases where the extraction source is a point in an isotropic medium, the cone of depression becomes a sphere (Gringarten and Ramey, 1973). In the real world, spherical flow will be observed only within small dimensions and over a short time period, because the spherical cone of depression will reach the bottom of the aquifer and the cone will become an ordinary radial flow.

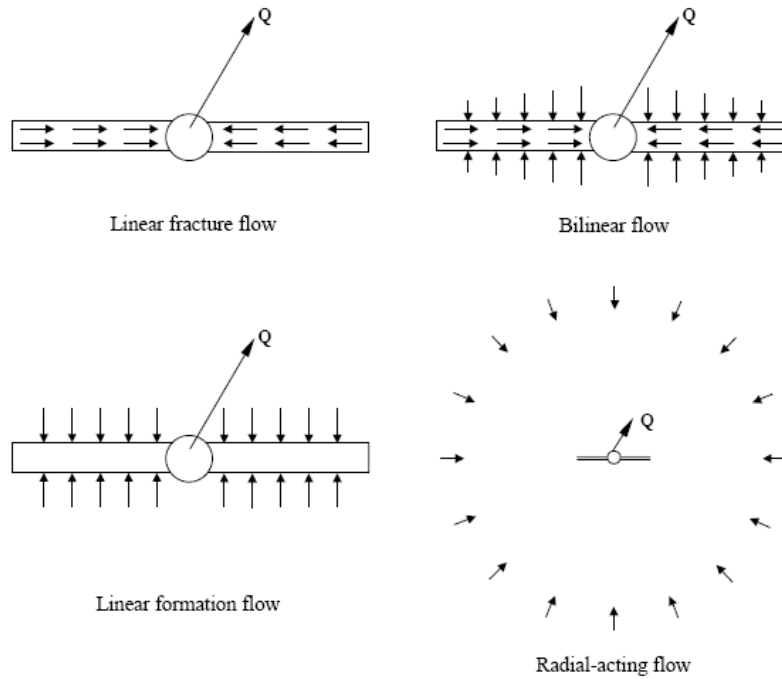


**Figure 2.11. Different flow phases observed in a single fracture (Van Tonder et al., 2002).**

Gringarten et al. (1974) developed an analytical solution to describe the unsteady-state linear flow from the rock formation into a well that fully penetrates a highly permeable vertical fracture zone. They considered a planar (zero-thickness) vertical fracture with negligible storage. It is assumed that the water is solely supplied by the host rock even at early times. They proposed two analytical solutions, which they referred to as the infinite conductivity, and the uniform flux solution. Their solutions are applicable if the fracture has very high or infinite conductivity. The advantage of the Gringarten type curve approach lies in the fact that only data of the transient phase from linear flow to radial-acting flow is needed (Van Tonder et al., 2002). In the case where the radial-acting flow starts data can be used for the estimation of the transmissivity, using common methods i.e. the Cooper-Jacob straight line method.

Gringarten and Ramey (1974) introduced an analytical model that describes the drawdown in a penny-shape bedding plane (horizontal) fracture with infinite conductivity and finite extension with uniform flux. The fracture is embedded in an infinite, homogeneous, horizontal matrix that has anisotropic radial and vertical conductivities and is limited by upper and lower impermeable boundaries. The model considers linear flow followed by radial-acting flow after a transition period.

#### *Generalised radial flow (GRF) model*

The spatial distribution of flow through the fractures towards the well depends entirely on the properties of the fracture network, such as fracture conductivity, fracture density and connectivity (i.e. Barker, 1988; Black, 1994). The characteristics of the fracture network determine the flow geometry, which is also known as the flow dimension. Addressing the concept of uncertain geometry of rock mass (i.e. porous or fractured dominance and preferred flow directions) requires

the use of fractal dimensions (Black, 1994). The symmetry of flow dimension as described by Barker (1988) indicates that the relationship between cross-sectional area of flow and distance from the source is given by:

$$A(r) = \alpha_n r^{(n-1)} \tag{2-1}$$

where:

$A(r)$  = cross-sectional area of flow ( $L^2$ )

$r$  = radial distance from the borehole ( $L$ )

$n$  = flow dimension (-)

The flow dimension  $n$  describes the geometry of the system by defining the rate that the cross-sectional flow area changes with respect to distance from the test borehole, i.e., the flow dimension is the power by which the flow area changes with respect to radial distance, plus one. Flow dimensions range between 1 and 3 (Barker, 1988; Black, 1994) and for a one dimensional flow geometry ( $n = 1$ ), the area through which flow occurs will remain constant, regardless of the distance  $r$  (Figure 2.12).

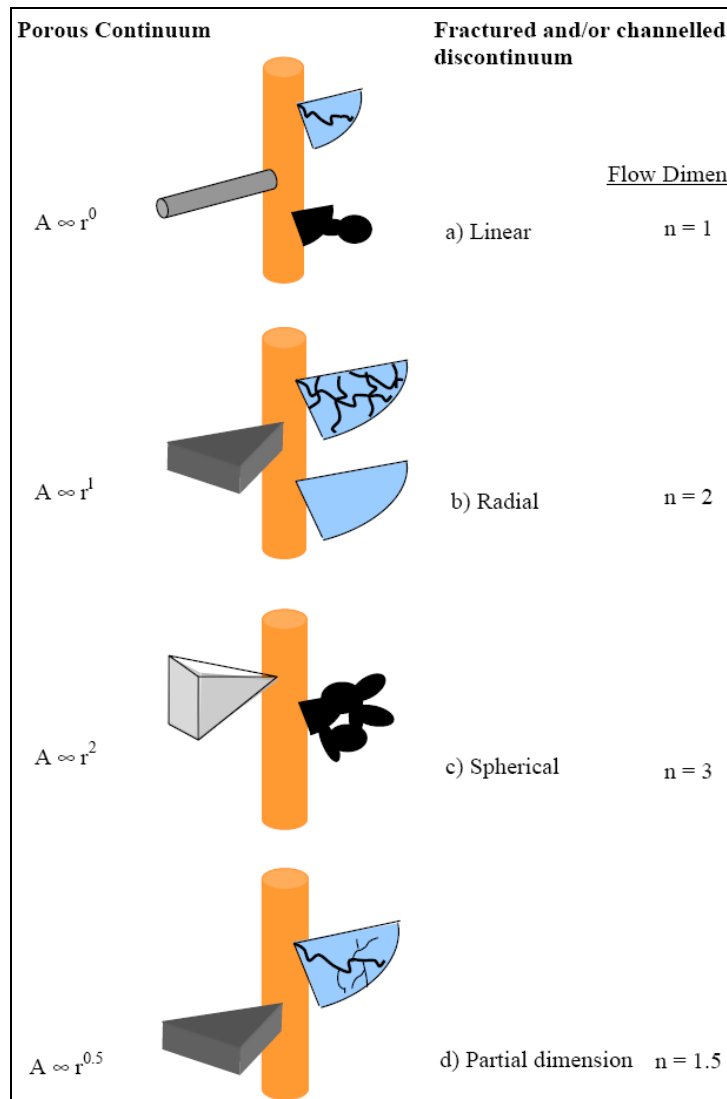


Figure 2.12. Flow dimension definition in well testing (Doe, 1991 in Van Tonder et al., 2002).

Flow towards a pumped well is usually concentrated along a certain fracture zone (one-dimensional) with large volumes of rock isolated from this zone of relatively high permeability activated by the pumping test. In contrast, the pattern of flow towards a fully penetrating well may be radial (two-dimensional) via a hard rock aquifer consisting of a well-connected fracture network isotropically distributed, or may be spherical (three-dimensional) if the well is only partially penetrating.

Barker (1988) introduced an analytical model that describes the drawdown in a fractured aquifer for various flow dimensions including linear, radial and spherical flows. These flow dimensions are seen as dependent on the fracture connectivity rather than as aquifer dimensions and are described by a factor  $n$ . Flow dimensions equal aquifer dimensions for integer values of  $n$ : for  $n = 1$  the flow is strictly linear, for  $n = 2$  the flow is radial (Theis model) and for  $n = 3$  the flow is spherical. The source dimensions with a finite storage capacity are defined by  $b^{n-3}$ , where  $n = 1$  implies a very thin cube source,  $n = 2$  a cylinder source and  $n = 3$  a sphere source, it extends as well to non-integer flow dimensions for intermediate cases (Figure 2.13). Matching of pumping test data with the GRF type curves (Barker, 1988) yields estimates of hydraulic diffusivity (i.e. the ratio of hydraulic conductivity and specific storage or transmissivity and storativity) and “generalized transmissivity”.

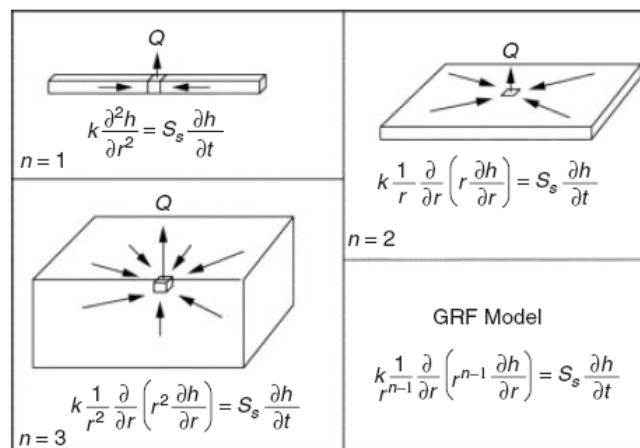


Figure 2.13. Concept of radial flow in 1, 2, 3, and generalization to  $n$  dimensions (Renard, 2005b).

## 2.5. ‘Sustainable’ yield concept

A misconception of the meaning of the word ‘sustainable’ in terms of groundwater use seems to exist, leading to degradation of wetland and riparian ecosystems due to stream dewatering and groundwater depletion. Sustainable yield is often confused with ‘safe yield’, which assumes the attainment of a long-term balance between groundwater abstractions and annual recharge and often calculated as a percentage of the natural recharge (Sophocleous, 1997; Zhou, 2009). The concept of ‘sustainable’ yield was introduced to overcome the shortcomings of the safe yield idea. In simple terms groundwater sustainability can be defined as development and use of groundwater in a manner that can be maintained for an indefinite time without causing unacceptable environmental, economic, or social consequences (Alley et al., 1999).

Despite Bredehoeft’s (2002) provocative theory, known as the “water budget myth”, that sustainable groundwater development has almost nothing to do with natural recharge, it is still widely accepted that natural recharge is a very important factor in the assessment of sustainability (Sophocleous, 2005; Alley and Leake, 2004; Kalf and Wooley, 2005, Zhou, 2009). However, Bredehoeft (2002) reminded hydrogeologists that aquifers are more complex than an oversimplified water balance can accommodate. According to Devlin and Sophocleous, (2005) distinction should be made between the concepts of sustainable pumping rate (source yield) and sustainability (resource yield) and that recharge rates cannot be ignored in spite of the fact that sustainable pumping rates can be estimated without them.

*Resource yield*

Aquifers are in a state of natural long-term equilibrium prior to pumping, and in order to maintain this equilibrium, groundwater abstractions must be balanced by increased recharge (increase in the amount of water entering the system) or reduced discharge (reducing the amount of water leaving the system) (Figure 2.14). The increase in recharge and decrease in discharge is termed ‘capture’ and equilibrium is achieved when it balances pumping. Thus, it is only after pumping that the change in recharge will contribute to the determination of a sustainable yield (Seward et al., 2006). When considering a groundwater basin as whole, all the individual abstraction points where ‘capture’ is possible, permissible and sustainable, will together define the basin yield (Seward et al., 2006).

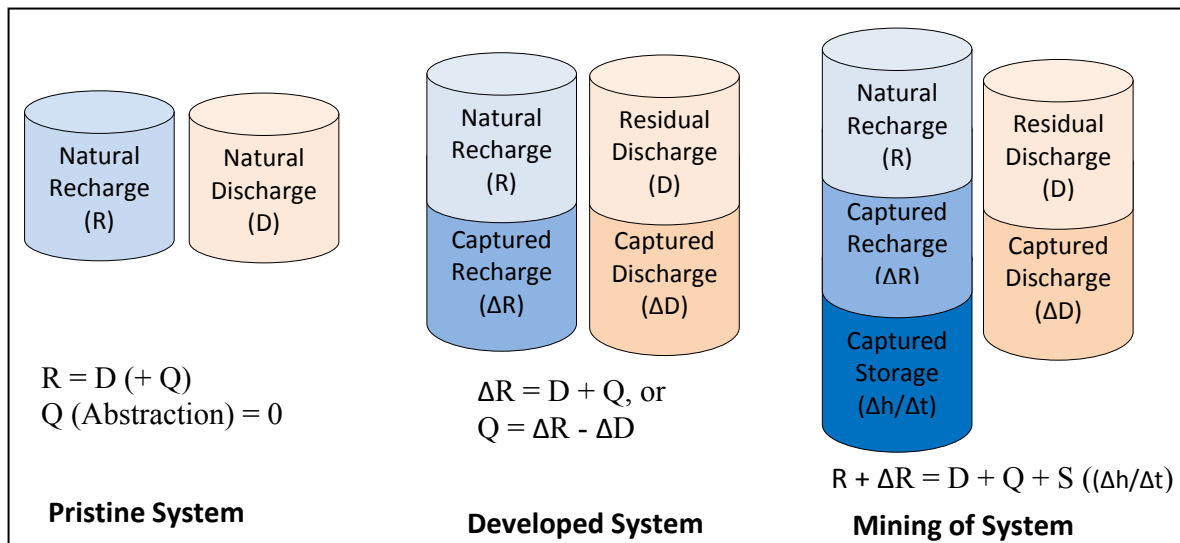


**Figure 2.14. The capture principle and the implications for sustainability and recharge.**

Abstractions from storage indicate on the other hand non-equilibrium conditions. Where the abstraction is greater than the difference between the maximum inflow ( $R + \Delta R$ ) and residual outflow ( $D$ ) then an additional mining yield (change in  $S$ ) is required to maintain the abstraction rate (Figure 2.14). It must be emphasized that the spatial distribution of these abstraction points strongly influences the total sustainable basin yield. Withdrawals from an aquifer might have a severe impact on individual ecosystems locally, but per square kilometre these withdrawals might



be minor in terms of total recharge and discharge. Hence, a sustainable yield should account for small-scale local impacts and simultaneously consider the ability of an aquifer as a whole to recover from pumping stress (Maimone, 2004).

Many may argue that the “capture recharge principal” does not generally apply to basement aquifers as the resource yield is rarely achieved due to poor boreholes yields and low distribution densities. However, despite the relatively low (often less than 1 ℓ/s) borehole yields in the Limpopo crystalline aquifers, deeply weathered and highly fractured regions boreholes can have yields in excess of 5 ℓ/s. A number of exceptionally high yielding areas not known anywhere else in Africa within the basement aquifer system occur in the Dendron (Mogwadi), Baltimore and Tolwe regions (Figure 1.1). These aquifers have sustained (supposedly sustainable) large scale irrigation for the last few decades, suggesting high storage potential, high permeabilities and an interconnected fracture network with a major source of recharge. Seeing that abstraction rates far exceed vertical recharge rates which amounts to a few millimetre of the 400 mm annual rainfall, it can be argued that these aquifers are potentially recharged through lateral saturated flow from adjacent aquifers, sometime called inter-aquifer recharge.

#### *Source yield (Sustainable pumping rate)*

If several hydrogeologists were asked how they arrive at their recommended borehole yield, the answers would be vague. Many of them would place the emphasis on experience in analysing the shape of the pumping test curve for multiple discharge tests (step test), constant discharge tests and recovery tests. In reality only through long term monitoring and groundwater flow models can a long term ‘sustainable’ pumping rate be determined. However, in many rural water supply projects it is simply not economical to study each aquifer in detail to ensure that the boreholes will not fail. In South Africa its common practice to try and maintain operational pumping levels above the level of the main yielding fracture. The sustainable pumping rate is in this context defined as the discharge rate that will not cause the water level in the well to drop below a prescribed limit, identified from the nature and thickness of the aquifer (especially water strikes) and the depth of the well. Van Tonder et al. (2001) compiled a user-friendly Excel spreadsheet known as the Flow Characteristic-method to recommend long term pumping rates for water supply boreholes in fractured rock. The FC-spreadsheet addresses the long-term assurance of water supply from a borehole based on available drawdown figures and estimates the influence that boundaries may have on the yield of a borehole. A complete explanation of the semi-analytical expressions and approximations can be found in a *Journal of Hydrology* publication by Van Tonder et al., 2001. The recommended ‘sustainable’ yield ( $Q_{sus}$ ) is determined as:

$$Q_{sus} = Q_{ob} \frac{S_p}{S_{ob}(t')} \quad (2-2)$$

where  $S_p$  is the drawdown of the well corresponding to the prescribed limit,  $S_{ob}(t')$  is the observed drawdown at the time  $t'$  during a test with a constant discharge rate  $Q_{ob}$  and  $t'$  represents the minimum operation time in which the drawdown shall not exceed the prescribed limit. In order to estimate the sustainable yield,  $S_{ob}(t')$  needs to be known over a long time period.  $S_{ob}(t')$  is



generally extrapolated using Theis's well equation or a Taylor series expansion based on the extrapolation of drawdown measurements at late time, including drawdown derivatives.

Although it is widely used in practice and has been adopted by Department of Water Affairs, the FC-spreadsheet is often misinterpreted and its limitations are not taken into account by the user, which include:

- The determined 'recommended' yield estimate is based on a probability of not exceeding the available drawdown. Such an approach does not follow the original sustainability concept (Alley et al., 1999), which takes environmental and social issues as well as the long-term protection of resource into account.
- The determined yield might be non-unique and dependent on the abstraction rate during the constant rate test and the extrapolation of the measured drawdown.
- If there are more than one abstraction boreholes in the aquifer system, the sum of the 'sustainable' yields must not be higher than the annual recharge for the area.

## 2.6. Development of groundwater

Studies on crystalline basement aquifers have predominantly focused on the development of groundwater resources in thick regolith (i.e. weathered overburden) with dominant intergranular flow in mainly tropical to sub-tropical regions (i.e. western and southern Africa and South America) (Wright and Burgess, 1992). Early workers focused mainly on establishing a correlation between the yield of a borehole and 1) its depth, 2) the geology, and 3) weathering thickness (i.e. Houston and Lewis, 1988; Barker et al., 1992; McFarlane et al. 1992; Chilton and Foster, 1995).

More recently, researchers have tried to identify the most important factor(s) in controlling borehole yields in crystalline terrain, in order to identify areas with higher groundwater potential (Mabee, 1999; Moore, 2002; Henriksen, 2003; Neves and Morales 2007). The influence of topography on borehole yield have been shown by many (i.e. McFarlane et al. 1992; Mabee, 1999; Henriksen, 1995) with the common result that wells located in valleys and flat areas show generally higher yields compared to wells located on slopes and hilltops. Although, specific rock types (i.e. granites, gneiss, schist) are in many cases the obvious factor in explaining the variation of borehole yields (Gustafsson and Krásný, 1994; Neves and Morales 2007), the influence is often supplanted by secondary features such as faults, fracture zones and dykes. As a result throughout the last decade the optimization of the location of wells in tectonically fractured areas throughout Africa, India and Brazil focused mainly on assessing the relationship between bedrock structure and groundwater production by analysing the position of wells in relation to lineaments (aeromagnetic data or Landsat images) (i.e. Greenbaum 1992; Fernandes and Rudolph, 2001; Owen et al., 2007; Solomon and Quiel, 2006; Henriksen and Braathen, 2006; Ranganai and Ebinger, 2008; Solomon and Ghebreab, 2008). These investigations are often based on tectonic models where the impact of original or present compressional stress on potential water bearing lineaments is assessed (Fernandes and Rudolph, 2001; Henriksen and Braathen, 2006; Neves and Morales, 2007; Owen et al., 2007). In some cases results showed that the majority of productive

water wells are associated with lineaments parallel to the regional maximum horizontal stress in the area (Fernandes and Rudolph, 2001). It is therefore expected that fractures perpendicular to the regional compressive stress are closed and dry (Owen et al. 2007). However, in many cases authors could not establish a firm relationship between well yields and lineaments (Greenbaum 1992; Gustafsson, 1994) and in most cases, there is no direct evidence that the structures responsible for the flow correlate with mapped lineaments (Mabee et al., 2002). According to Sander (2007) this may be attributed to local factors such as fracture infilling, fracture connectivity or the poor knowledge of current stress regimes. It is recognized that lineament mapping is often subjective (Mabee et al., 1994) and depends on factors such as data quality, extraction technique and interpretation method. But when correctly interpreted lineaments are used in conjunction with a good understanding of local geology, tectonics, geomorphology, hydrology and aquifer characteristics, the most promising setting and orientation of fractures for future groundwater exploration can be identified (i.e. Solomon and Quiel, 2006; Galanos and Rokos, 2006; Ranganai and Ebinger, 2008; Solomon and Ghebreab, 2008).

### 2.6.1. Exploration approaches

Due to the complexity of the geology, poor groundwater recharge and for many regions inadequate geological and geomorphology maps, the location of groundwater in crystalline bedrock will always be difficult. Although, groundwater is available for all rural communities as low yielding hand pump boreholes, it is only by detailed groundwater investigations and exploration that successful high yielding well fields may be developed. Sami (2009) placed special emphasis on a comprehensive geodynamic / strain analysis, highlighting the structural control of groundwater flow in the fractured aquifer (Figure 2.15). However, the approach overlooks the importance of geomorphologic processes on the nature and extent of weathering. In reality various groundwater exploration programmes may be followed. Some projects focus largely on lineament mapping (GIS & remote sensing), some projects have a strong focus on structural and tectonic history (i.e. Sami, 2009), while other projects follow a strong geophysical approach (Sander, 2007). In this regard the application of good base work in terms of aquifer characterisation before drilling commences is often overlooked.

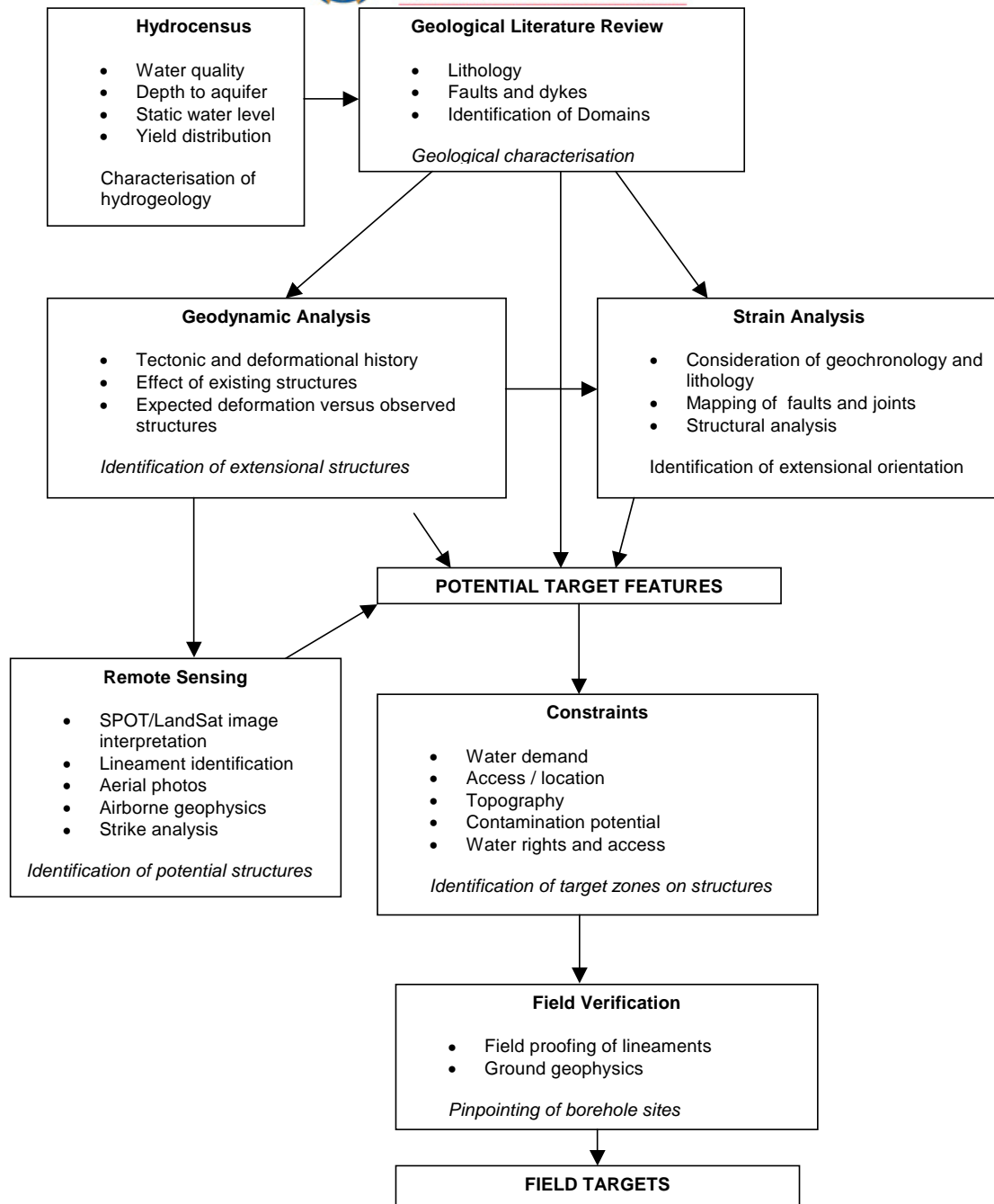


Figure 2.15. Flow chart of recommended groundwater exploration of basement aquifers (Sami, 2009).

### 3. HYDROGEOLOGICAL ASSESSMENT METHODS

#### 3.1. Investigation approach

The methods and approach to further the conceptual understanding of the hydrogeological functioning of the Limpopo crystalline basement aquifers can be summarised in Figure 3.1.

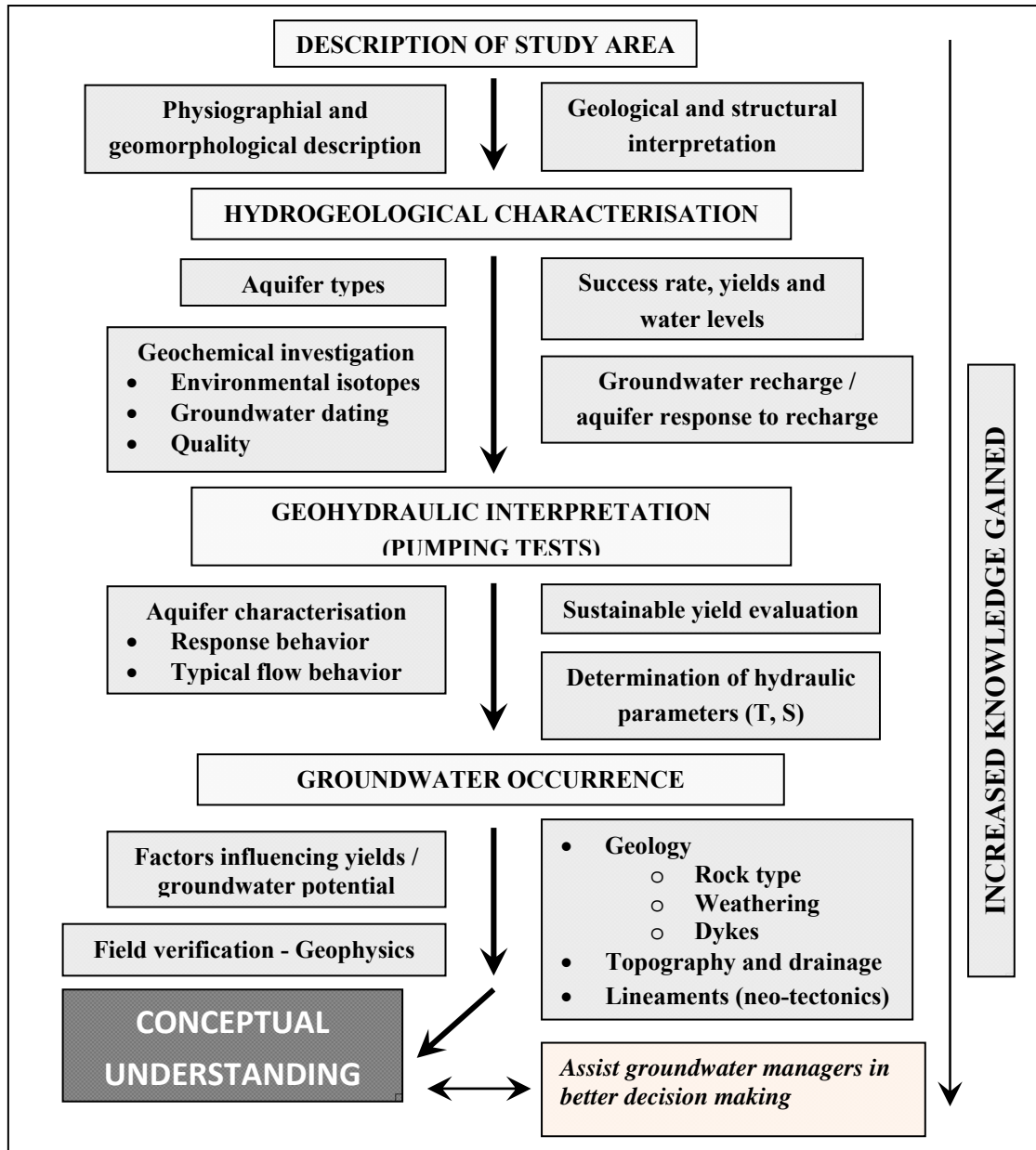


Figure 3.1. Overview of the applied hydrogeological assessment approach and methods.

### 3.1.1. Hydrogeological overview

The main objective of this phase to establish an understanding of the hydrogeological characteristics of a region based on existing information. In the context of groundwater occurrence (potential) it is important to characterise the physical feasibility of meeting water demands through groundwater. By overlaying the different information layers like geological and structural maps, borehole yields, dry boreholes (!), historic drilling success rates and depth to groundwater and groundwater chemistry using appropriate software (i.e. GIS) will give a first understanding of the aquifer characteristics, structural and geological influences of successful and unsuccessful boreholes as well as potential drilling targets, i.e. a basic conceptual model of the basement aquifer(s) in the area.

#### *Borehole data*

Water wells have been a source of water for people, animals and crops since the earliest civilizations in Africa and Asia (Misstear et al., 2006), while boreholes have been in supply since the advent of the drilling machine in the late nineteenth century. In the Limpopo Province alone some 30 boreholes are drilled per day to sustain the ever growing demand for water in the region. In view of the above the Limpopo Province Department of Water Affairs (DWA) initiated and implemented a Groundwater Resource Information Project (GRIP) in 2002 and thus became the first province in South Africa to do so (Botha, 2005). GRIP is a systematic approach to gather, verify, upload and use data to improve management and development of rural groundwater resources in South Africa. As the majority of these boreholes have been verified in the field, the spatial accuracy of borehole positions is within 10 m.

The dataset compiled for the study area consists of over 8 000 boreholes contained in the (GRIP) database. The lithology has been recorded and updated on 1 206 boreholes and approximately 3 000 boreholes have been tested. The majority of the pumping tests were single-well tests, primarily to recommend ‘sustainable’ abstraction rates for rural water supply schemes. It is important to note that these boreholes are not randomly distributed but were limited in many cases to the proximity of rural villages. In some cases the drilling target was chosen based on either geophysical field surveys or geological expertise, so a bias towards lineaments and other anomalies in the dataset may be apparent. Similarly, the pumping test results are biased towards larger transmissivity and yield values since low yielding or ‘dry’ boreholes were excluded from testing.

Although the determination of aquifer parameters was not a priority in the GRIP framework, pumping tests of over 2000 boreholes within the study area were analyzed using classical analytical models such as Theis (1935) and the Jacob’s approximation (Cooper and Jacob, 1946) method. These methods in additions to methods such as Barker (1988) are collated together with graphical plots (i.e. semi-log, log-log & derivatives) into the Flow Characteristic (FC) excel spreadsheet developed by the Institute for Groundwater studies in South Africa (Van Tonder et al. 2002). As a result, despite the fact that various consultants and contractors were used to conduct

and analyze the pumping tests over a number of years within the GRIP project framework, all analysis was conducted using the FC-spreadsheet. Transmissivity estimates are generally based on a late time fit of the time-drawdown curve using i.e. Cooper-Jacob or Theis methods. It should be noted that the pumping test data have been accumulated over a number of years under various conditions and may potentially be influenced by long-term climatic fluctuations, seasonal rainfall and changes in groundwater abstraction by farmers, communities and mines

### 3.2. Groundwater recharge estimation methods

The assessment on groundwater recharge is not intended to contribute to the literature on the importance of recharge to sustainability, but will provide some insight into recharge rates, process and behaviour that occur in the underlying crystalline basement aquifer.

#### 3.2.1. Chloride Mass Balance (CMB)

For a detailed description of the theory behind the CMB-method the reader is referred to the number of publications available on this subject (i.e. Wood, 1999; Kinzelbach et al., 2002; Adams et al., 2004). The CMB-method can be applied to the saturated zone to estimate a ‘true’ total recharge originating from both diffuse and preferential flow components through the unsaturated zone. The CMB-method in the saturated zone has been used in basement aquifers throughout southern Africa to estimate recharge (Xu and Beekman, 2003; Adams et al., 2004). This method entails determining the recharge over an entire drainage area by integrating the ratio of average chloride content in rainfall (wet and dry deposition) to that of groundwater over the whole area. The CMB-method can be represented by the equation (Kinzelbach et al., 2002):

$$R_t = \frac{P * Cl_p + D}{Cl_{gw}} \quad (3-1)$$

where:

P = precipitation (mm per time)

R<sub>t</sub> = total recharge (mm per time)

D = dry deposition (in mg per m<sup>2</sup> and time)

Cl<sub>p</sub> = concentration in precipitation (mg/l)

Cl<sub>gw</sub> = concentration in recharging groundwater (i.e. average over profile) (mg/l)

The Cl<sub>gw</sub> originates from various flow components in the unsaturated zone. For a regional R<sub>t</sub>, Cl<sub>gw</sub> represents the harmonic mean of chloride concentrations in groundwater:

$$Cl_{gw} = \frac{N}{\sum_{i=1}^N \frac{1}{Cl_{gw-i}}} \quad (3-2)$$



### 3.2.2. Cumulative rainfall departure method

The Cumulative Rainfall Departure (CRD) method is a water balance approach and is based on the premise that equilibrium conditions develop in an aquifer over time, i.e. average rate of losses equating to average rate of recharge of the system. In other words groundwater level fluctuations are caused by rainfall events. The method requires monthly rainfall and groundwater level data, as well as information pertaining to aquifer properties (storativity), abstraction and the size of the recharge area. The CRD-method allows aquifer characteristics and components such as i) recharge or storativity, and ii) the impact of abstraction or iii) the natural response of rainfall to be determined. The CRD series is represented by the mathematical relationship (Bredenkamp, et al., 1995):

$${}_{av}^1CRD_i = \sum_{n=1}^i R_n - k \sum_{n=1}^i R_{av} \quad (i = 0,1,2,3,\dots,N) \quad (3-3)$$

where:

$R$  is rainfall values with subscript “ $i$ ” indicating  $i$ -th month and “ $av$ ” the average.

$$k = 1 + (Q_p + Q_{out}) / (AR_{av}).$$

If, according to the regression  $k > 1$ , which indicates that pumping or an external impact has affected the water level, the natural water levels could be simulated from equation (3-3) by setting  $k = 1$ .

Xu and Van Tonder (2001) derived a new formula for the CRD-method. The  $k$  parameter applied in the Bredenkamp et al., (1995) is important to mimic groundwater flow. Recharge is calculated as (Xu and Beekman, 2003):

$$CRD_i = \sum_{i=1}^N R_i - \left( 2 - \frac{1}{R_{av,i}} \sum_{i=1}^N R_i \right) i R_i \quad (3-4)$$

where:

$R_t$  often range from 0 to  $R_{av}$ , 0 = aquifer being closed and  $R_{av}$  = open aquifer system.

The cumulative rainfall average would conform to  $R_{av}$  if  $R_i$  does not show a trend ( $R_t = k R_{av}$ ). It is assumed that the CRD is the driving force behind the monthly water level changes if the other stress is relatively constant. The groundwater level will rise if the cumulative departure is positive and will decline if it is negative. Since:

$$rCRD_i = S_y [\Delta h_i + (Q_{pi} + Q_{out}) / (AS)] \quad (3-5)$$

where:

$r$  is that fraction of a CRD which contributes to recharge,  $S_y$  is specific yield,  $\Delta h_i$  is water level change during month  $i$  (L),  $Q_{pi}$  is groundwater abstraction ( $L^3/T$ ),  $Q_{out}$  is natural outflow,  $A$  is recharge area ( $L^2$ ).

### 3.3. Geochemical investigation methods

The regional geochemical description is based on approximately 2 500 borehole analyses sampled over the last decade as part of the GRIP programme. The analyses included mainly major ions pH and electrical conductivity. Further chemistry data was obtained from the following sources 1) Rossouw (2010), which included 52 groundwater samples for major ions, trace elements, tritium ( $^3\text{H}$ ), stable isotopes ( $^2\text{H}$  and  $^{18}\text{O}$ ) and bacterial analysis. A further 7 CFC, radiocarbon and stable isotopes ( $^2\text{H}$  and  $^{18}\text{O}$ ) groundwater samples were captured from Talma and Weaver (2003) in addition to radiocarbon data captured from the comprehensive multi-tracer study conducted in by Verhagen et al. (2009). As part of this investigation, 11 samples analysed for Chlorofluorocarbons (CFCs), sulphur hexafluoride ( $\text{SF}_6$ ), stable isotopes ( $^2\text{H}$  and  $^{18}\text{O}$ ) and major ions, and 5 samples analysed for radiocarbon. The water quality sampling was performed according to SABS/ISO 5667 standards and the samples were analysed in a SANAS accredited laboratory.

#### *Database preparation*

A high percentage of trace elements values were below the analytical detection limit (censored data) and therefore not used in the multivariate analysis. Furthermore data with unacceptable errors in the charge balance ( $> 5\%$ ) were excluded from further analysis:

$$\text{E.N.}[\%] = 100\% \cdot \left| \frac{(\text{Cations} - \text{Anions})}{(\text{cations} + \text{Anions})} \right| < 5\% \quad (3-6)$$

The distribution characteristics of each variable in the database were evaluated by histograms and their measures of location and dispersion. Since most of the applied statistical analysis assumes normally distributed data (Güler et al., 2002), a studentized range test ( $n > 1\,000$  valid samples) for normality with a level of significance of 0.01 was performed. The studentized range test compares the ratio of the sample range and standard deviation to tabulated critical values (Pearson and Hartley, 1970). While  $\text{NO}_3$ , Si and  $\text{HCO}_3$  follow a normal distribution, the following variables were log-transformed so they more closely correspond to a normal distribution: Na, Ca, Mg, K, Cl,  $\text{Ca}$ ,  $\text{SO}_4$  and EC. These variables were used in the multivariate statistical analysis.

#### *Multivariate statistical analysis*

Hierarchical cluster analysis (HCA) has been proven to be an extremely powerful grouping mechanism (Güler et al., 2002 Lambrakis et al., 2004). Groundwater is classified into groups, which is a different grouping from conventional geochemical graphical techniques (e.g. Piper, Schoeller and Stiff diagrams). This different grouping is mainly due to the use of a much greater combination of chemical and physical parameters (e.g. temperature) to classify water samples.

Ward's linkage rule was used to analyse the distances among linkages for the entire group of observations and the squared Euclidean distances were used to determine the distance between observations. An HCA results in a graphical representation of the hierarchical grouping along with the corresponding rescaled distance to achieve the linkage (dendrogram). The clusters with the greatest increase in the rescaled distance are usually chosen as the final number of clusters. Cluster membership is then saved for each observation and group averages compared to the sample population average. Mapping of cluster membership is used to spatially interpret the identified structures in the geochemical dataset (chemical signatures).

### 3.3.1. Environmental and radiogenic isotopes

The use of environmental isotope techniques may, in addition to conventional investigation methods, provide further insight into the storage properties of the natural hydrological system and has become a routine in most hydrogeological studies in the last few decades. Isotopes act as natural occurring tracers in groundwater (commonly referred to as environmental tracers) which can provide valuable information on aquifer characteristics and groundwater flow paths to the hydrogeologist that would otherwise be difficult, if not impossible, to establish (Verhagen et al, 1991). A detailed discussion on the application of environmental isotopes in hydrogeology is available in Clark and Fritz (1997) and more recently in a special issue of *Environmental Geology* (Thomas and Rose, 2003).

#### *Stable isotopes (deuterium ( $^2H$ ), oxygen-18 ( $^{18}O$ ))*

During phase changes of water between liquid and gas, the heavier water molecules tend to concentrate in the liquid phase, which fractionates the hydrogen and oxygen isotopes. Water that evaporates from the ocean is isotopically lighter than the water remaining behind and precipitation is isotopically heavier; that it contains more  $^2H$  and  $^{18}O$  than the vapour left behind in the atmosphere. These isotopic ratios from an environmental sample can be compared with the isotopic ratio of standard mean ocean water (SMOW) (Hiscock, 2005). When  $\delta^2H$  is plotted as a function of  $\delta^{18}O$  for water found in continental precipitation, an experimental linear relationship is found that can be described by the equation (Craig, 1961):

$$\delta^2H = 8\delta^{18}O + 10 \quad (3-7)$$

This is known as the global meteoric water line (GMWL). The position of any pair of  $\delta^2H$  and  $\delta^{18}O$  values on this line for rainwater worldwide will depend on local climatological conditions (temperature, latitude, altitude, and rainfall amount effects) (Figure 3.2). After the infiltration of precipitation only physical processes such as diffusion, dispersion, mixing and evaporation alter the groundwater isotopic condition. Oxygen-18 ( $^{18}O$ ) stable isotope is utilised to identify the recharge process and mixing of groundwater from different sources. Surface waters contain a distinct composition of stable isotopes due to enrichment caused by evaporation.

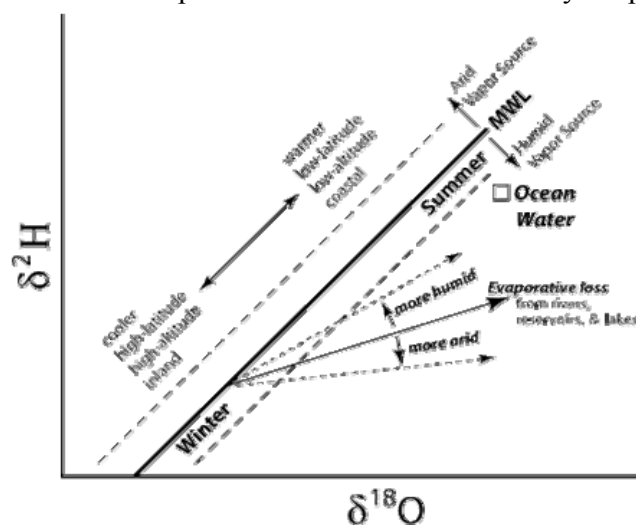


Figure 3.2. Summary diagram of the stable isotope composition from precipitation to percolation.

*Radioactive Isotopes (tritium ( $^3\text{H}$ ), radiocarbon ( $^{14}\text{C}$ ) and carbon  $\delta^{13}\text{C}$ )*

Tritium ( $^3\text{H}$ ) occurs as a result of man-made (thermonuclear devices) processes is a radioactive isotope of hydrogen having mass 3 and half-life of 12.38 years (Hiscock, 2005). The unit of measurement is the tritium unit (TU) defined as 1 atom of tritium occurring in  $10^{18}$  atoms of H and equal to  $3.19 \text{ pCi L}^{-1}$ . Tritium in the atmosphere is typically in the form of the molecule  $\text{H}^1\text{H}^3\text{O}$  and enters the groundwater as recharging precipitation. When rainwater is isolated from the atmospheric source, i.e. during groundwater recharge, no new tritium is added and the tritium concentration will decrease with this characteristic half-life. The changes in atmospheric  $^3\text{H}$  are monitored by the International Atomic Energy Agency (IAEA) through a global monitoring network. In Southern Africa, tritium levels in rainfall rose from initial (natural) values of about 5 TU to 60 – 80 TU as a result of fall-out of nuclear weapon testing in the early 1960's. Due to this tritium is an ideal isotope to be used for age dating of groundwater that recharged after 1952 (Pannatier *et al.*, 2000). According to Weaver *et al.*, (1999) tritium studies can provide semi-quantitative age determinations of groundwater:

- Water with zero tritium ( $< 0.5 \text{ TU}$ ) has a pre-1952 age.
- Water with significant tritium concentrations ( $> 5 \text{ TU}$  in the southern hemisphere) is of post-1952 age.
- Water with little, but measurable, tritium (between 0.5 and 5 TU) seems to be a mixture of pre- and post-1952 water.

However, with half-life of 12.32 years and a decay rate of 5.626% per year have been reduced by a factor of 8 in the period from (1963 to 2000) (Mook and de Vries, 2001). With no further atmospheric nuclear weapons testing, tritium will continue to drop to near natural background levels. Therefore, usage of tritium for age dating groundwater recharge is reaching its limit and alternative tools, such as chlorofluorocarbons (CFCs) (discussion to follow) were devised over the last decade or so for quantifying modern groundwater recharge.

Radiocarbon occurs in the environment as a result of natural (cosmic radiation) and as with tritium; thermonuclear tests increased the atmospheric level of radiocarbon to peak in the early 1960's. Carbon dioxide  $\text{CO}_2$  from the air is trapped in rain and snow and labelled with environmental  $^{14}\text{C}$ . As this water infiltrates into the subsurface recharging groundwater it becomes isolated from the atmosphere. Radioactive decay causes the  $^{14}\text{C}$  content in the dissolved inorganic carbon to gradually decline. Radiocarbon has a half-life of 8 270 years, making it a useful tool for “dating” groundwater up to an age of 50 000 years. In contrast to  $^3\text{H}$ ,  $^{14}\text{C}$  is not strictly a conservative tracer of water, as numerous chemical processes can alter the  $^{14}\text{C} / ^{12}\text{C}$  ratio (i.e. the dissolution of carbonate minerals). Based on the hydrochemistry and  $\delta^{13}\text{C}$  values these unrealistic old radiocarbon ages can be corrected (Verhagen *et al.*, 1991; Plummer and Sprinkle, 2001). The unadjusted age of groundwater can be determined by:

$$t = -8270 \ln \left( \frac{A}{A_0} \right) \quad (3-8)$$

where:

$t$  = the decay of the carbon isotope (years)

$A$  = the activity per unit mass of sample

$A_0$  = the specific capacity (disintegration per unit time per unit mass of sample) of  $^{14}\text{C}$

Vogel (1970) suggested a rule of thumb initial  $^{14}\text{C}$  recharge value of about 85% for many aquifers. In principle however, this initial value may be as low as 50% in carbonate aquifers, approach 100% in purely crystalline terrain and has to be assessed for each area. During the early sixties, atmospheric  $^{14}\text{C}$  concentrations rose due to thermonuclear fallout and declined since. In qualitative terms, groundwater radiocarbon values of  $> 100$  pMC can be interpreted as falling in the thermonuclear era, i.e. recharged over the past four decades. Mean residence times (MRT) can then be estimated on the assumption of the exponential model weighting function by considering observed  $^3\text{H}$  or  $^{14}\text{C}$  concentrations (Verhagen, 2000).

### 3.3.2. Chlorofluorocarbon (CFC) and sulphur hexafluoride ( $\text{SF}_6$ )

Groundwater dating with chlorofluorocarbons (CFCs) and sulphur hexafluoride ( $\text{SF}_6$ ) is based on historical data for the atmospheric mixing ratios of these compounds over the past 50 years, their Henry's Law solubility in water, and measurement of CFC and  $\text{SF}_6$  concentration in water samples (IAEA, 2006). The apparent age of a groundwater is then dependent on the Henry's Law constant calculated at the recharge temperature, which is generally taken to be equivalent to the annual average air temperature. Figure 3.3 shows concentrations of CFC-11, CFC-12 and  $\text{SF}_6$  in pptV, respectively, expected in southern hemisphere (USGS, 2009).

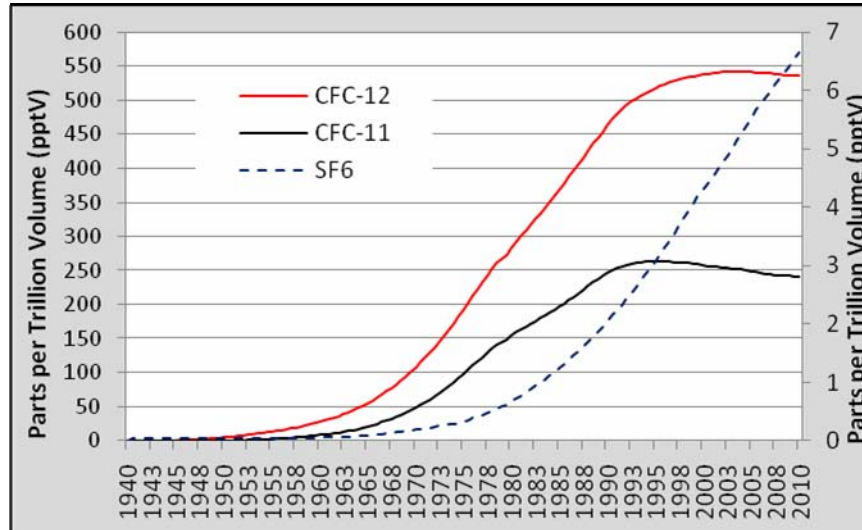


**Figure 3.3. Atmospheric mixing ratios of CFC-11, CFC-12, and  $\text{SF}_6$  for the southern hemisphere.**

The International Atomic Energy Agency (IAEA) provides a detailed guidebook on the use of chlorofluorocarbons in hydrology (IAEA, 2006). The ratios of any two CFCs can provide useful information on the date of recharge of groundwater because the three CFCs of interest were introduced at different times and have different atmospheric growth rates. However, several assumptions are necessary in assigning an apparent groundwater age and are described in detail in

the IAEA guidebook (IAEA, 2006). Contamination of groundwater with chlorofluorocarbons appears to be the greatest limitation on CFC dating (Gooddy et al., 2006). Some commonly recognized sources of CFC contamination include seepage from septic tanks, landfills infiltration or disposal of industrial wastes, and recharge from rivers contaminated with CFCs. One criterion for rejection of apparent CFC ages is that calculated CFC concentrations in air (in pptv) are greater than that possible for water in solubility equilibrium with air at the time of the peak in atmospheric concentration (IAEA, 2006).

Another important factor when considering the dating of groundwater with CFCs is to collect and analyse a water sample for CFCs that is representative of the aquifer at a given location. It is then assumed that the water sample was in solubility equilibrium with the unsaturated zone air at the time of recharge. Groundwater temperature may not be a reliable indicator of the recharge temperature and recharge temperatures are more precisely estimated from measurements of other dissolved gases, such as nitrogen and argon (Gooddy et al., 2006). However, nearly all groundwater samples have concentrations of noble gases in excess of Henry's Law solubility at the recharge temperature. The source of this excess has been attributed to 'excess air' and is probably a result of the forcible solution of air bubbles trapped in soil or rock as water infiltrates (Gooddy et al., 2006). Typically, the amount of excess air is determined by analysis of the concentrations of different noble gases or from the nitrogen/argon ratio in the sample (IAEA, 2006). When such measurements are available, it is possible to correct CFC ages for the presence of excess air. The content of "excess air" is often less than 2 cm<sup>3</sup>/kg of water, but can be substantially higher in samples recharged along floodplains of rivers, or arroyos, or where recharge occurs through fractured rocks (Böhlke, 2006). As a result an excess air of between 1 and 5 cm<sup>3</sup>/kg was assumed for samples collected.

#### *Groundwater mixtures*

CFC ages are generally based on absolute concentrations. As a result, when waters of different ages mix, the CFC concentration changes and so does the apparent age. When used together, CFCs and SF<sub>6</sub> can help to resolve the extent to which groundwater mixing occurs, and therefore provide indications of the likely groundwater flow mechanisms (Gooddy et al., 2006). Plots of one tracer against another can be useful in distinguishing hypothetical mixing processes. According to Cook and Böhlke (2000) four hypothetical mixing models can be typically used to describe some of the variation seen in groundwater mixtures: piston flow (PFM), exponential piston flow (EPM), exponential mixing (EMM) and binary mixing (BMM). Binary mixing of young water with old (pre-tracer) water is one of the simplest models to consider. The two principal geohydraulic conditions of groundwater flow are schematically shown in Figure 3.4.

In some cases, water reaching the open interval of a borehole or discharging from a spring is nearly uniform and can be approximated with a piston-flow model, analogous to water flowing through a pipe from the point of recharge to the point of discharge without mixing during transit. Exponential mixing can be used to describe discharge from an unconfined aquifer receiving uniform areal recharge. According to Gooddy et al. (2006) the exponential- piston model



corresponds to a situation in which an aquifer receives distributed recharge in an up-gradient unconfined area, and then continues beneath a down-gradient confined area.

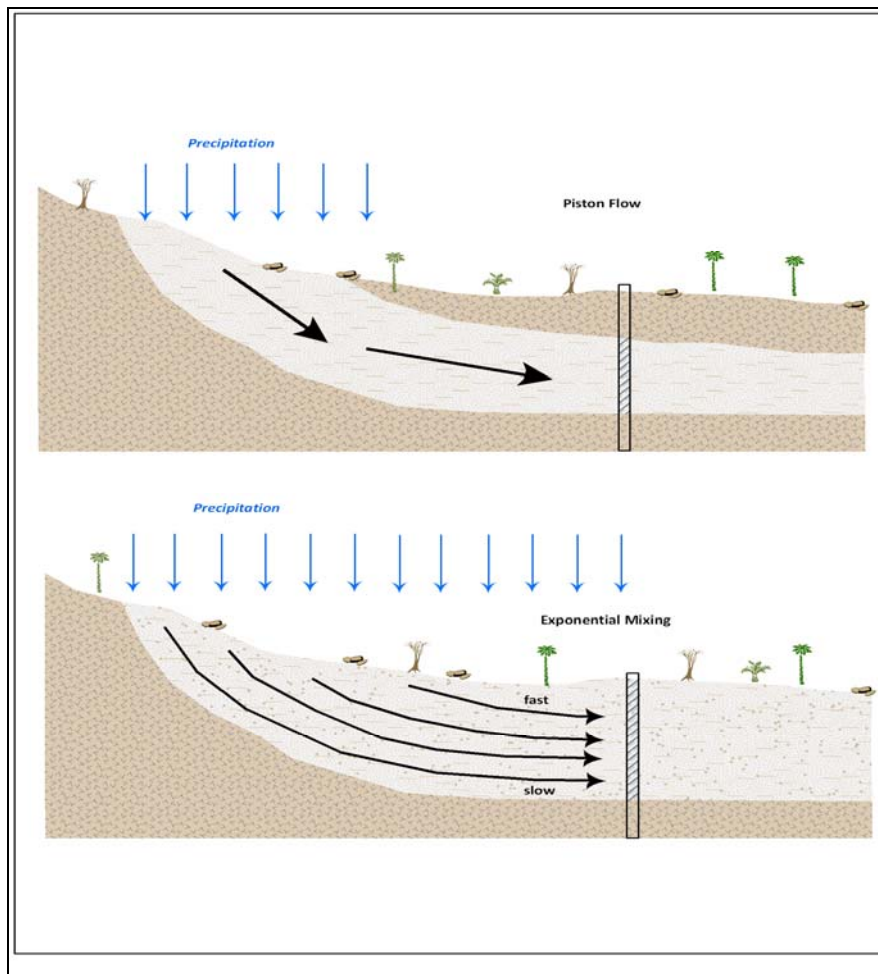


**Figure 3.4. Two cases of groundwater movement by piston-flow in confined aquifers and flow in an open aquifer where different fast flowing water is mixed in the well or spring.**

### *CFC sampling*

The sampling procedure for CFCs is complicated and requires special sampling equipment to avoid atmospheric contact. CFC and SF<sub>6</sub> samples were collected unfiltered and without atmospheric contact in glass bottles contained within metal cans. The apparatus used ensured the sample is protected from possible atmospheric contamination by a jacket of the same water. Groundwater samples were collected from 11 boreholes in January 2004 using a submersible pump, with each purged for roughly 3 to 5 well volumes prior to the sample being taken (Photo 1). Samples were shipped to the British Geological Survey groundwater laboratory (Wallingford, UK) for CFC and SF<sub>6</sub> analysis.



**Photo 1. Photograph of discharge hose, canisters and glass bottles used for the CFC sampling.**

### 3.4. Hydraulic testing

By means of the pumping test, the hydraulic response to pumping is measured and analyzed with the objective to 1) characterise an aquifer, 2) quantify its hydraulic properties, and 3) determine the efficiency and sustainable yield. The type and duration of a pumping test depends on the planned usage of the borehole, but typical tests include a multiple discharge test (step-drawdown test), a constant discharge test and a recovery test. In crystalline aquifers short-term pumping tests (i.e. 24 hrs) may be adequate to predict the sustainability of an abstraction if the abstraction rate is small and the aquifer relatively uniform. However, the sustainability at higher abstraction rates can generally not be reliably assessed using short-term tests. The heterogeneous and discontinuous nature of crystalline basement aquifers requires generally long term testing (i.e. 1 to 10 days) preferably with a comprehensive monitoring network to determine whether groundwater levels will stabilize during abstraction.

#### 3.4.1. Step drawdown test and well efficiency

Step-drawdown tests are basically made with the purpose to establish a relation between the yield and the corresponding drawdown in a well. In this regard the test is conducted to estimate the greatest flow rate that may be sustained by the pump well for the duration of the constant discharge. More importantly the efficiency and the realistic yield of a borehole can be assessed using a step-drawdown test in which the discharge rate  $Q$  is increased in a series of steps each lasting one to two hours; the drawdown in the well  $S_w$  at the end of each step is recorded. If there are no well losses, the drawdown increases linearly with discharge rate, but in most practical situations the drawdowns for higher discharge rates are greater than predicted by a linear relationship. Jacob (1947) proposed the non-linear relationship:

$$S_w = BQ + CQ^2 \quad (3-9)$$

where:

$B$  is the formation loss and  $C$  is the well loss coefficient. The values of  $B$  and  $C$  can be found directly from the diagnostic plot of  $S_w/Q$  versus  $Q$  itself; it will yield a straight line whose slope is equal to  $C$ ; the value of  $B$  can be found by extending the straight line until it intercepts the  $Q = 0$  axis. Under best conditions, an efficiency of about 80 % is the maximum that is normally achievable in most cased boreholes, while under less than ideal conditions, an efficiency of 60 % is probably more realistic (Heath, 1983).

### 3.4.2. Identification of characteristic flow regimes (constant discharge test)

In pumping test analyses, the effects of different factors in the well, its immediate vicinity, in the aquifer and at the aquifer boundaries on the responses should be distinguished (Figure 3.5).

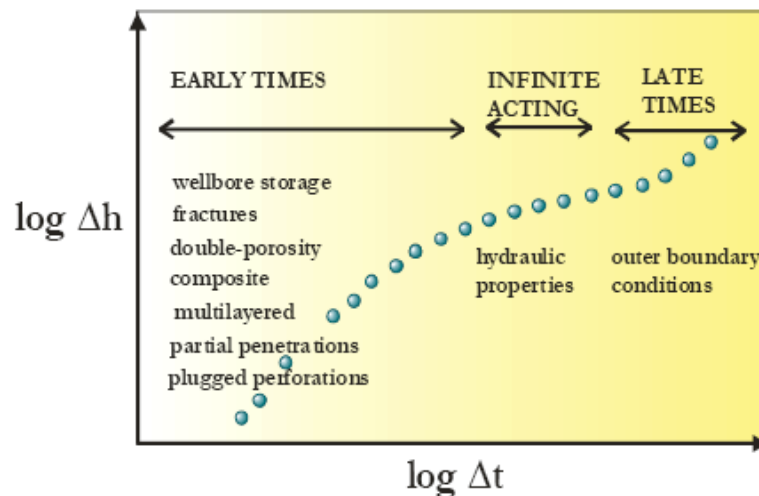


**Figure 3.5. Illustration of early, intermediate and late periods of pump tests responses (Gringarten 1982 in Leveinen, 2001).**

The distinction can be attempted made by applying a number of diagnostic plots. Diagnostic plots include:

- the drawdown  $s$  versus time  $t$  in a log-log plot ( $\log s$  vs.  $\log t$ ),
- the drawdown versus the logarithm of time (semi-log plot:  $s$  vs.  $\log t$ ),
- the drawdown versus the square root of time ( $s$  vs.  $t^{1/2}$ ),
- the drawdown versus the fourth root of time ( $s$  vs.  $t^{1/4}$ ), and
- the time derivative of the drawdown versus the time in a log-log.

Plotting the observed drawdown from the dataset simultaneously with the log derivative can greatly enhance the identification of certain flow regimes and facilitates the selection of an appropriate model (Renard et al., 2009). The type of flow regime is not an intrinsic property of a fractured hard rock aquifer because it usually changes in time during a pumping test, which is reflected in the time drawdown behaviour at the pumped well and observation wells. A useful diagram presented by Ehlig-Economides et al. (1994) developed primarily for well tests in the petroleum shows in a synthetic way the behaviour of the derivative as a function of the main type

of flow behaviour within a log-log plot (Figure 3.6). The diagram can be superposed to the data and shifted to identify visually and rapidly the type of flow that occurs during a certain period of the test.

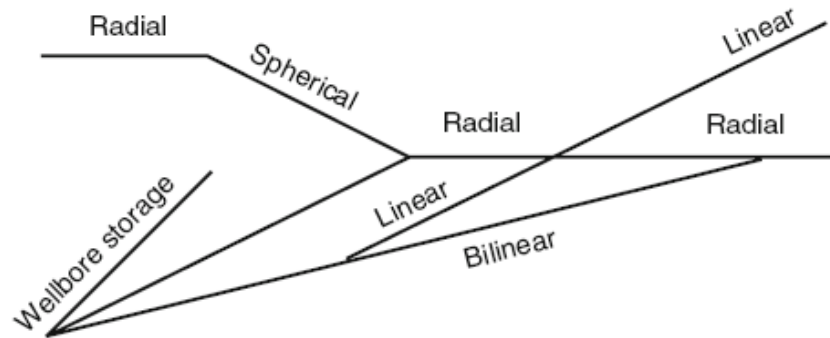


**Figure 3.6. Flow regime identification tool representing schematically the log-derivative of drawdown as a function of logarithmic time (Ehlig-Economides et al., 1994 in Renard et al., 2009).**

Another useful illustration to identify the characteristics that can be obtained from the derivative graph was developed by Van Tonder et al. (2001) (Figure 3.7).

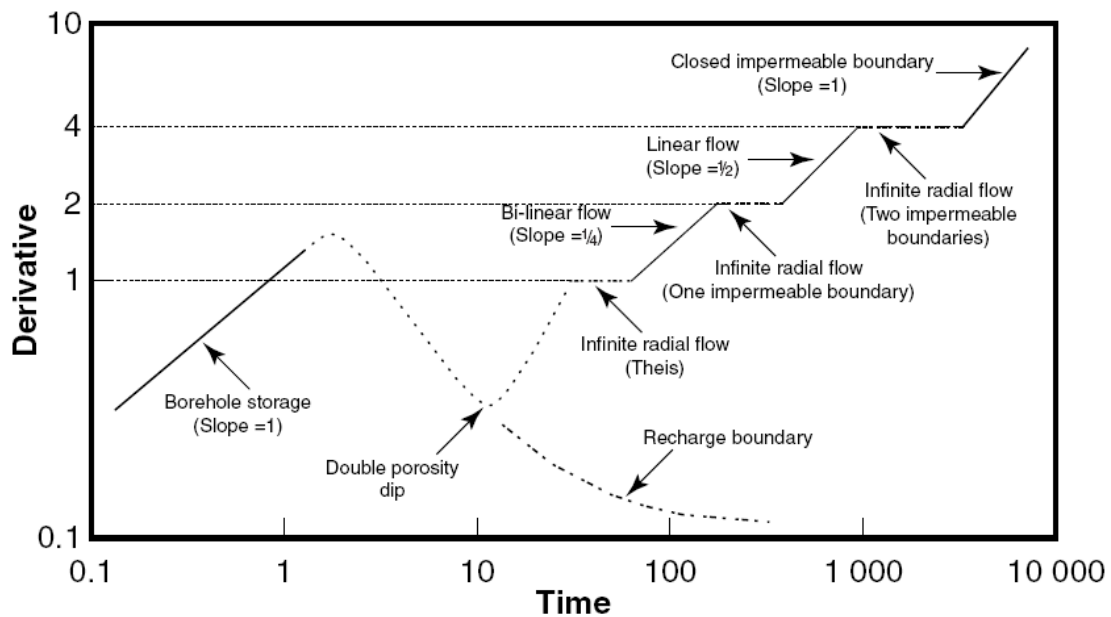


**Figure 3.7. Graphs of the first logarithmic derivative of the drawdown in a borehole for a few types of geometries and boundaries (Van Tonder et al., 2001).**

All characteristics of the log-log time-drawdown straight line slopes remain the same, and provide the following information. A summary of the theoretical methods applicable to weathered-fractured rock systems is presented in Table 3.1.



**Table 3.1. Methods of recognizing observed flow character in crystalline basement aquifers.**

Aquifer Type/Characteristic	Flow regime	Diagnostic plots			Typical theoretical model (see section 2.4.3)
		Semi-log	Log-log	Derivative {special }	
Homogenous, isotropic	radial	straight	(Theis-type)	stabilises	Theis (1935) / Cooper and Jacob (1946)
Leaky		*	*	decrease	Hantush and Jacob (1955) Moench (1985)
Unconfined		*	typical S-shape	slight dip (early times) stabilises	Neuman (1972, 1974).
Double porosity	linear or Bi-linear (early times) radial	two parallel straight-line sections	typical S-shape	characteristic dip stabilises	Warren & Root (1963) Moench (1984)
Single vertical fracture or dyke	linear flow (fracture)	reverse C-shape	straight line, slope 0.5	straight line, slope 0.5	Cinco-Ley and Samaniego (1981) Boonstra & Boehmer (1986)
	bilinear		straight line, slope 0.25	straight line, slope 0.25 {s vs t <sup>1/4</sup> : straight}	
	linear (formation)		straight line, slope 0.5	straight line, slope 0.5 {s vs t <sup>1/2</sup> : straight}	Gringarten et al. (1974)
	pseudo-radial		straight line		stabilises
Single horizontal fracture	storage	*	straight line with 1 slope	*	Gringarten and Ramey (1974)
	linear		straight line with 0.5 slope	straight line with 0.5 slope	
	pseudo-radial	straight line	*	stabilises	
General radial flow	n < 2 (linear)	*	*	positive slope	Barker (1988)
	n > 2 (spherical)			negative slope	
Fracture dewatering	-	flattening at fracture position		characteristic hump(s) (intermediate to late)	
Closed no flow boundary		tripling of slope	-		Kruseman and de Ridder (1990)
Recharge boundary		Decrease in slope		strong downward trend	

\* - Refer to Figure 2.4 in section 2.4.1 for the typical drawdown behaviour observed for these models.

### 3.4.3. Pumping test interpretation

To advance the conceptual understanding of basement aquifers behaviour in response to pumping, over 2 359 semi-log, log-log and derivative plots from the GRIP dataset were visually interpreted with the aim of establishing the various conceptual aquifer models observed in the region. The data were analyzed with the software package AQTESOLV Pro version 4.5 using automatic curve fitting or manual fitting of late time data with the appropriate analytical solution/conceptual model (i.e. confined, unconfined, leaky and fractured aquifers). The aquifer and well parameters were obtained from the inverse curve-fitting procedure. The following procedure for the analysis of pumping test data is proposed for the Limpopo crystalline aquifers (modified after Bäumlé, 2003):

- Ensure proper planning and execution of a pumping test (i.e. ensure constant pumping rates, insufficient drawdown, poor monitoring) to obtain representative results
- Develop a conceptual understanding of the geological setting (use geological map etc. if no field visit is done) of the test
- Create the diagnostic plots from pumping test data and define the flow regime according to 1) the summary provided in Table 3.1, 2) the type-curves in Figure 2.4 (see section 2.4.1), and 3) the graphical illustrations in Figure 3.6 and Figure 3.7).
- Choose the appropriate analysis method(s) and determine the aquifer and well parameters from the curve fitting of the drawdown and the recovery data. In principle, the best match of the measured time-drawdown data to an analytical solution has to be found by either a graphical or computer-operated method.
- If different flow regimes can be identified during a test, each section can be evaluated using the corresponding analysis method (i.e. stabilising of the derivative can indicate the state of infinite acting radial flow (IRF) and the late time data can be evaluated with traditional methods such as Theis (1935).
- The analytical solutions for fractured aquifer systems contain two fitting parameters 1) representing the aquifer matrix, and 2) the fracture (conduit).
  - The geometric properties of the fracture such as the fracture half-length can be obtained or verified from geological or geophysical investigations.
  - The hydraulic parameters of the aquifer matrix can be evaluated from hydraulic tests which are not influenced by the lineament (i.e. IRF phase).
  - By inserting these values, the equation describing the fracture type flow regime can be solved for the remaining parameters.
- Drawdown influenced by fluctuating pumping rates should rely on an accurate description of the recovery data. The recovery of a pumped aquifer can be interpreted in the same way as the drawdown by using diagnostic plots. Through a simple transformation of the time variable, Agarwal (1980) devised a procedure that uses solutions developed for drawdown analysis (i.e. the Theis type-curve) to analyze recovery data.



#### 3.4.4. Recommending a long term yield for a single borehole

Although Van Tonder et al., (2001) recommend a very conservative approach for the estimation of recommended yields (i.e. assuming no recharge), the use and application of the FC-spreadsheet is often not understood. The inspection of the diagnostic plots to assess the drawdown behaviour and to identify the theoretical model needed in the analyses, should supplement the recommended borehole yield estimate. All of these conventional time drawdown analysis is accessible in the FC-spreadsheet. As discussed in the beginning of this chapter (see section 3.1.1) the GRIP dataset is an existing dataset and no attempt was made to re-analyse the over 2000 pumping test analysis. Another major shortcoming identified in the GRIP dataset is the lack of observation monitoring conducted during pumping tests. Single borehole tests generally will not identify impermeable boundaries, recharge boundaries, or interconnection between other groundwater and surface water unless these conditions exist in very close proximity to the well being tested.

### 3.5. Assessment of factors controlling the occurrence of groundwater

Statistical evaluations are commonly used to identify correlations between borehole yields and physical features which can be observed. These features (or factors) can be divided into the following components:

- Geological or lithological (comparison of yields obtained from various rock types and geological settings).
  - Regolith thickness (correlation of borehole yields with thickness of weathering).
- Terrain, geomorphological or hydrological features (includes correlations of borehole yields with respect to relief, erosion surfaces and surface water drainages).
- Structural correlations (asses the relationship between yields and proximity to lineament in addition to the lineament azimuth).

Cumulative frequency plots of borehole yield and transmissivity (or specific capacity) are able to characterise the regional occurrence of groundwater. With the advances of Geographical Information Systems (GIS) techniques, an integrated and conjunctive analysis of large datasets (spatial and non-spatial) over vast areas is possible.

#### 3.5.1. GIS analysis

Analysis of large datasets in regional studies requires the application of Geographical Information Systems (GIS). The visual representation of the associated geographic phenomena together with their spatial dimensions and their associated attributes provides a rapid, integrated and cost effective tool in any groundwater investigation. To study the influence of different factors like the topographical setting on transmissivities and borehole yields, a hydrogeological database was created in ArcGIS using the 1:250 000 geological and 1:50 000 topographic vector files as well as borehole coordinates. With this approach it is possible to extract spatial information based on the location of a borehole (i.e. geology, proximity to a lineament, dyke or river course etc.) (Holland and Witthüser, 2009). Boreholes were then grouped according to their location and the

corresponding arithmetic mean values of transmissivity and yield calculated. The level of confidence (significance) that a mean of a sub-group deviates from the total population mean is based on a one-sample Student t-test. In testing the null hypothesis that the population mean is equal to a specified value  $\mu_0$ , one uses the statistic

$$t = \frac{\bar{x} - \mu_0}{s / \sqrt{n}} \quad (3-10)$$

where  $s$  is the sample standard deviation of the sample and  $n$  is the sample size.

Boreholes within a 100 m buffer zone along major river courses were regarded as representing alluvial aquifers. Similarly a 500 m buffer (in- and outside of the mapped features) was used to present the metamorphic aureole that developed during the granite intrusion of the batholiths. The topographic setting of a borehole (along river, valley, flat surface, slope and mountain) was based on drillers' reports and the depth of weathering was derived from almost 600 boreholes with detailed geological logs. These logs are based on the drill chips captured at 1 m intervals during drilling. The logs were also used to indicate whether diabase or dolerite was encountered during drilling, representing the intersection of a dyke. Dykes were furthermore inferred from the interpretation of aeromagnetic data from the South African Council for Geoscience (CGS). The magnetic nature of the dykes makes aeromagnetic data ideal for mapping these features and most magnetic lineaments identified on aeromagnetic maps are therefore associated with dyke swarms (Stettler et al., 1989).

### 3.5.2. Lineament analysis

The use of lineament mapping, especially in crystalline lithologies with poor primary porosity, is of major importance for groundwater exploration and was incorporated into the GRIP framework by the Department of Water Affairs (DWA) for the Limpopo Province. The mapping and interpretation of lineaments is conducted by geological remote sensing consultants on behalf the DWA Limpopo regional office. The satellite imagery used for the capturing of lineaments is from the medium resolution ASTER (Advanced Spaceborne Thermal Emission and Reflectance) missions. ASTER data is a good choice for groundwater development projects, due to their large spectral resolution, reasonably high spatial resolution, ability to derive DEMs and low cost of acquiring the imagery (Sander, 2007). The mapping of lineaments in the Limpopo Province takes place in a digital environment using GIS and is mapped at a scale of 1:50 000. These interpreted lineaments may reflect a number of features such as faults, fracture zones, joints, foliations, dykes (not interpreted as dykes), lithological contacts and linear branches of the drainage systems. According to Braathen and Gabrielson (1998) a large lineament can enhance fracturing up to 300 m away while Clark (1985) suggested that the area of influence might be less than 150 m and Fernandes and Rudolph (2001) reduced it further to 70 m in their studies. Considering the spatial margin, all boreholes within 150 m of a lineament were considered to be targeting a lineament in this study.

It is recognized that lineament mapping is often subjective (Mabee et al., 1994, Sander, 2007) and that a two-dimensional lineament of geological origin, mapped on remote-sensing imagery, provides little direct information on the type of feature, its depth, dip or potential infilling (Sander 2007). However, the extent to which these lineaments influence or relate to borehole productivity in the Limpopo Province has not yet been assessed. In this regard this investigation can be regarded as an initial regional assessment of the potential relationship between mapped lineaments and borehole productivities from which future studies could improve on.

### 3.5.3. Geophysical methods

Individual boreholes will still need to be sited carefully, and this is usually done by means of geophysical techniques. Three basic principle surface geophysical methods were used to confirm regional lineaments and to pinpoint drilling targets, which include electrical resistivity, electromagnetic and magnetic methods. One way to improve a geophysical interpretation and the confidence in borehole siting is to combine the use of maps, field observations and geophysics in a method known as geological triangulation (MacDonald et al., 2005) (Figure 3.8).

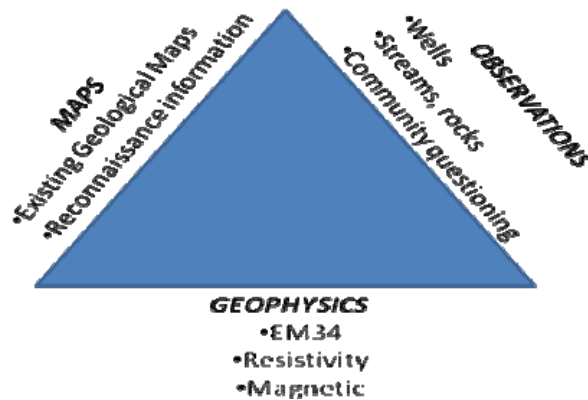


Figure 3.8. The geological triangle method (MacDonald et al., 2005).

### 3.6. Development of a regional conceptual model

The development of a conceptual hydrogeological model is the single most important step in managing an aquifer. The knowledge obtained from the hydrogeological assessments described in this chapter provides us with a conceptual understanding of the occurrence of groundwater and the typical behaviour of the aquifer to pumping in the crystalline aquifers in the Limpopo Province. In return this could assist groundwater managers with better decision making on groundwater exploration targets, improved aquifer parameter estimation and higher confidence in borehole yield recommendations. The development of a conceptual understanding should be an iterative process, being updated as new data become available or as the understanding of the system is improved.

## 4. DESCRIPTION OF STUDY AREA

### 4.1. Physiography and climate

The Limpopo Province is in the north-eastern corner of South Africa, bordering on Zimbabwe in the north and Mozambique in the east. The study area covers an area of approximately 23 500 km<sup>2</sup> and straddles the eastern and western parts of the Limpopo and, Luvuvhu/Letaba Water Management Areas respectively (Figure 4.1). In the Limpopo WMA portion of the study area the main surface drainages are the Sand-, Hout- and Brak Rivers. The gentle relief results in relatively slow flowing rivers which accumulate extensive alluvial deposits on their floodplains particularly along the Sand River. All of these rivers flow towards the Limpopo River in the north and eventually reach the Indian Ocean in Mozambique.

In both WMA's the runoff is highly seasonal and variable, with intermittent flow in many of the tributaries. Only a small number of river courses are perennial and most rivers sustain flow only during the wet season (December to April) or following intense rainfall events. The two main perennial rivers in the Luvuvhu/Letaba WMA portion of the study area are the Great Letaba- and Little Letaba rivers. The mountainous zone or Great Escarpment in the WMA includes the northern portion of the Drakensberg mountain range, which lies on a north-south axis (Figure 4.1). This zone is deeply incised by the major tributaries draining towards the east. The topography of the area varies from a zone of high mountains in the west through low mountains and foothills in the central parts to plains in the east. The average elevation in the central part of the study area is 400 to 800 metres above sea level, and is 1200 to 1600 metres above sea level in the Blouberg and Soutpansberg (north of Makhado) regions (Figure 4.1).

#### *Climate*

The climate varies from sub-tropical to semi-arid. The western parts have a dry, hot steppe semi-arid climate, becoming cool along the escarpment. The Luvuvhu/Letaba WMA is characterised by subtropical temperatures with a fairly high humidity. Large variations are observed for seasonal temperatures, while the eastern parts of the study area (i.e. Polokwane) experience cooler generally temperatures compared to the north-eastern parts (i.e. Giyani). Maximum temperatures are experienced in January and minimum temperatures occur on average in July (Table 4.1).



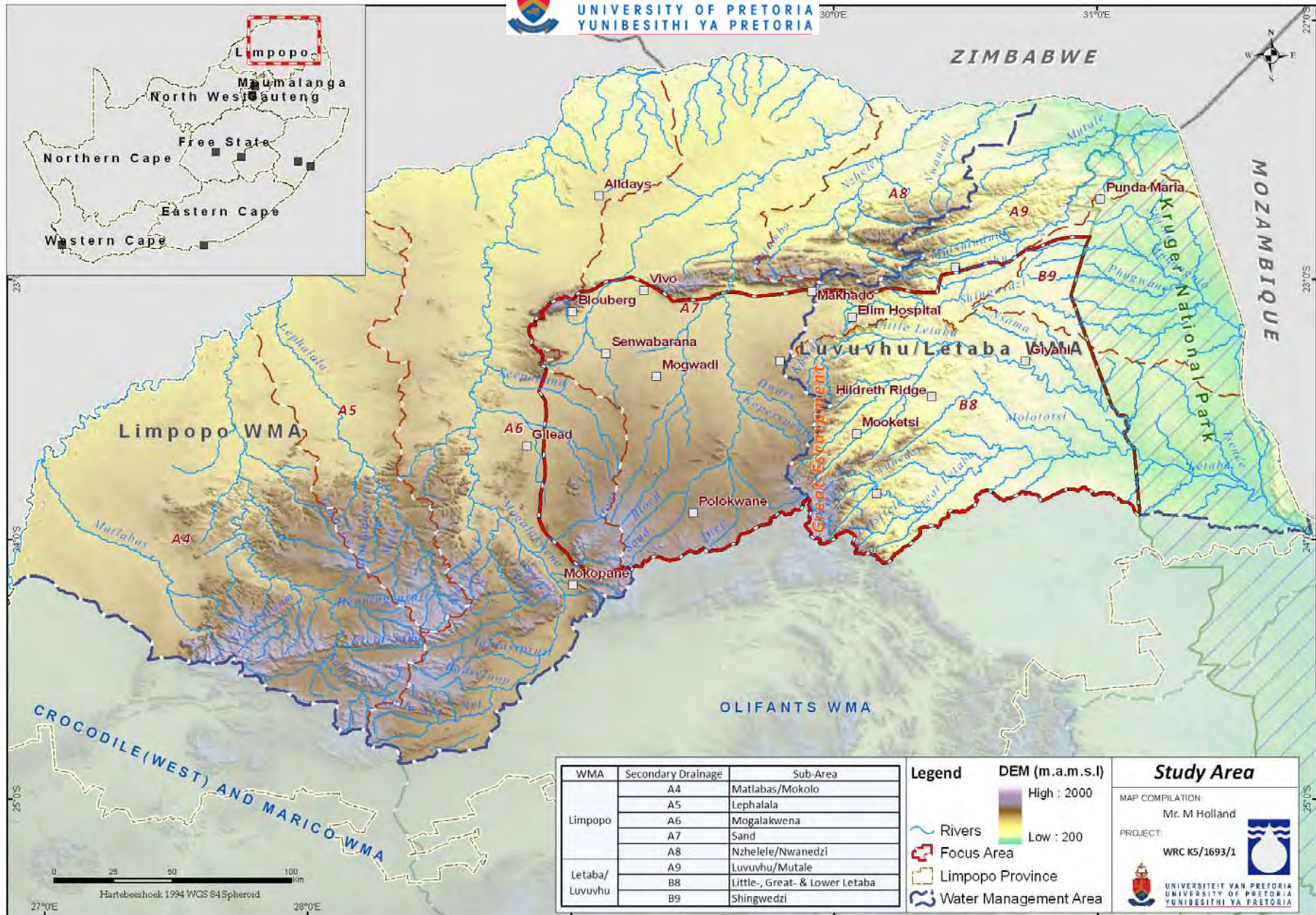


Figure 4.1. Regional surface drainage features, topography and study area.

**Table 4.1. Temperature (°C) variations of selected towns and climate stations.**

Station*	Summer		Winter		Annual	
	Min	Max	Min	Max	Min	Max
Polokwane	16	27	8	22	25	12
Mara	17	29	8	25	27	12
Tzaneen	18	27	14	24	25	16
Modjadji	14	26	11	23	25	13
Levubu	18	28	12	25	27	15
Thoyandou	18	29	12	26	27	15
Giyani	19	31	11	27	29	15

\*- South African Weather Services (SAWS).

Long term rainfall records exist for several South African Weather Services (SAWS) meteorological stations distributed throughout the area. The spatial distribution of climate stations in the study area together with the average monthly rainfall for selected stations is illustrated in Figure 4.2. and presented in Table 4.2.

**Table 4.2. Rainfall data for selected stations distributed throughout the study area.**

Nr*	Station*	Start Date	Status	Annual Rainfall (mm)		Elevation (mamsl)
				Mean	Median	
677099	Chloe-Sisal	1965	Active	365	342	1139
721562	Dendron	1971	Active	403	400	1040
679227	Hans Merensky School	1960	Active	950	911	727
721665	Mara Police	1947	Active	454	442	1051
766779	Palmaryville	1907	Active	916	887	581
677834	Pietersburg Hospital	1904	Active	455	450	1318
723073	Rosbach	1974	Active	912	867	994
724790	Shangoni	1972	Closed (2003)	446	397	431
722779	Soekmeaar	1965	Active	648	585	1135

\*- South African Weathers Services.

Orographic rains occur frequently along the Great Escarpment and the mean annual rainfall varies accordingly from 1 000 mm in the central parts to only 300 mm in the west and 400 mm in the east respectively. As a result of the low rainfall over most of the study area, relatively little surface runoff is generated. The runoff is highly seasonal and variable, with intermittent flow in many of the tributaries. Only a number of major river courses are perennial and most rivers sustain flow only during the wet season (November to March) or during intense rainfall events. The spatial rainfall variability is clearly illustrated in Figure 4.2. The average potential mean annual gross evaporation (as measured by A-pan) ranges from 1 600 mm in the central mountainous region to over 2 000 mm in the western and eastern areas.



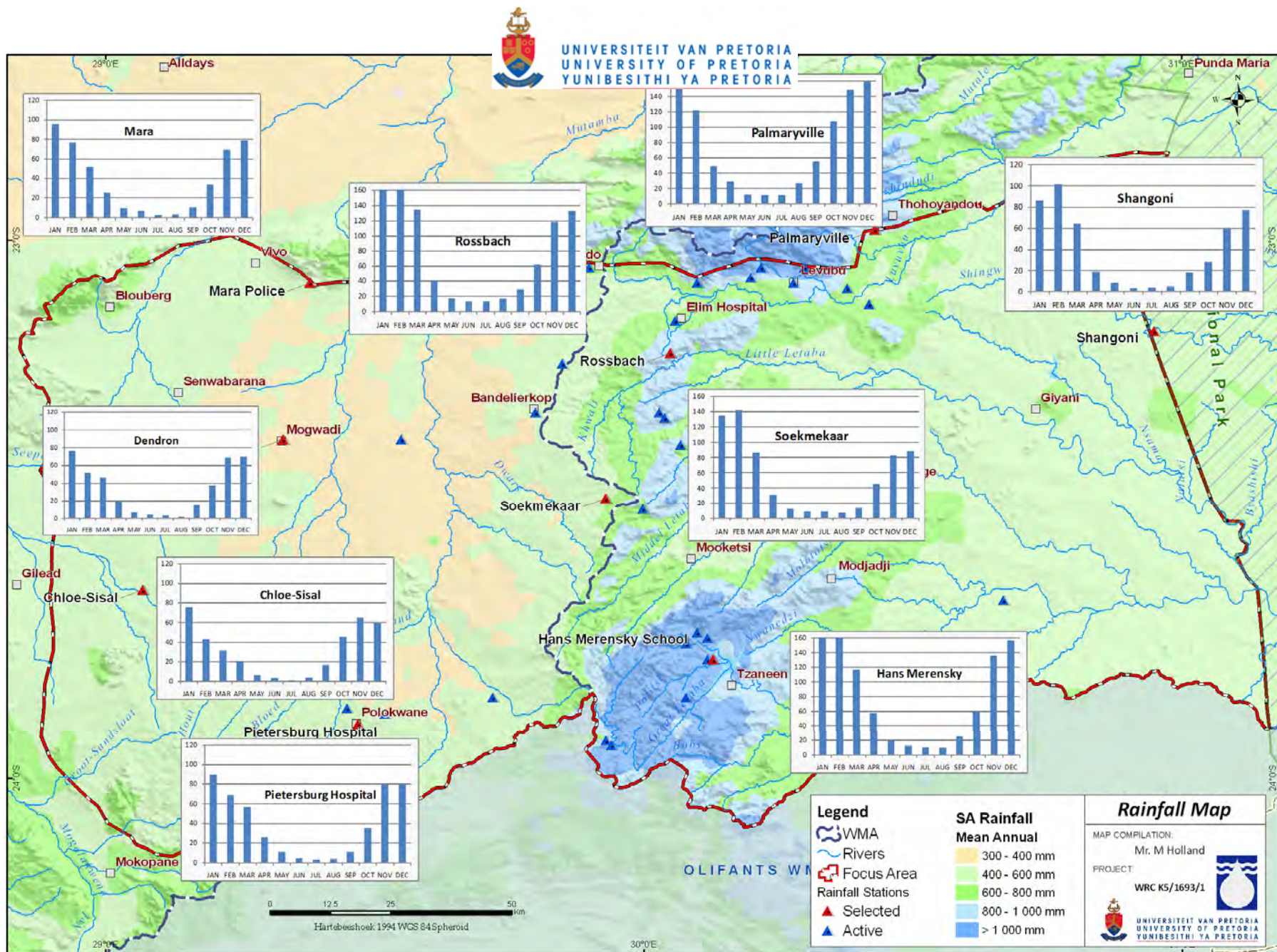
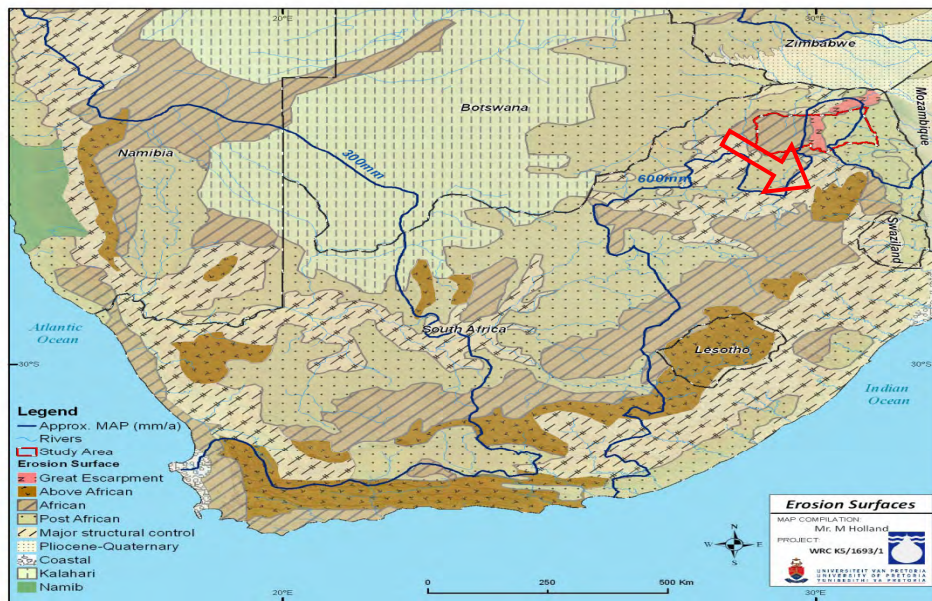


Figure 4.2. Mean annual rainfall map together with selected monthly average charts for selected stations in mm/month.



#### 4.1.1. Geomorphology

Although the age of a land surface by itself is not an indication of the water bearing properties of the weathered zone, the factors controlling the nature and thickness of the weathered zone is partly covered by its geomorphological history. The subcontinent has been subdivided into a number of denudational land surfaces of differing age. Tectonic movements and sea level changes initiated the onset of each erosion cycle due to a new set of base levels (Partridge and Maud, 1987). King (1975) recognised the following geomorphic cycles with their approximate inception age: Gondwana (190 Ma), Post-Gondwana (135 Ma), African (100 Ma), Post-African (20 Ma), Pliocene and Quaternary (2 Ma). The erosion surfaces of southern Africa investigated by Partridge (1998) are presented in (Figure 4.3).



**Figure 4.3. The distribution of erosion surfaces in southern Africa (adapted from Partridge, 1998; Taylor and Howard, 1999).**

The geomorphic development of the subcontinent resulted in the Karoo cover being stripped and the subsequent superimposing of drainage systems onto the underlying geological formations. The study area is largely situated on the African surface in the east and the Post African surface in the west (Figure 4.3). These surfaces represent long periods of weathering and erosion. The weathering fronts associated with the different erosion surfaces would have influenced the regional groundwater levels as well as the creation of groundwater flow paths. Groundwater investigations undertaken in the 1980s and 1990s suggested that the regolith was likely to be

better developed beneath the older erosion surfaces than the younger ones resulting in higher borehole yields (Jones, 1985; McFarlane et al., 1992).

Geomorphic features observed in the study area are plains, hills, inselbergs, low mountains, lowlands, foothills and valleys. The area can be divided into a number of terrain morphology units (Kruger, 1983). These geomorphic zones together with a W-E topographic profile are shown in Figure 4.4.

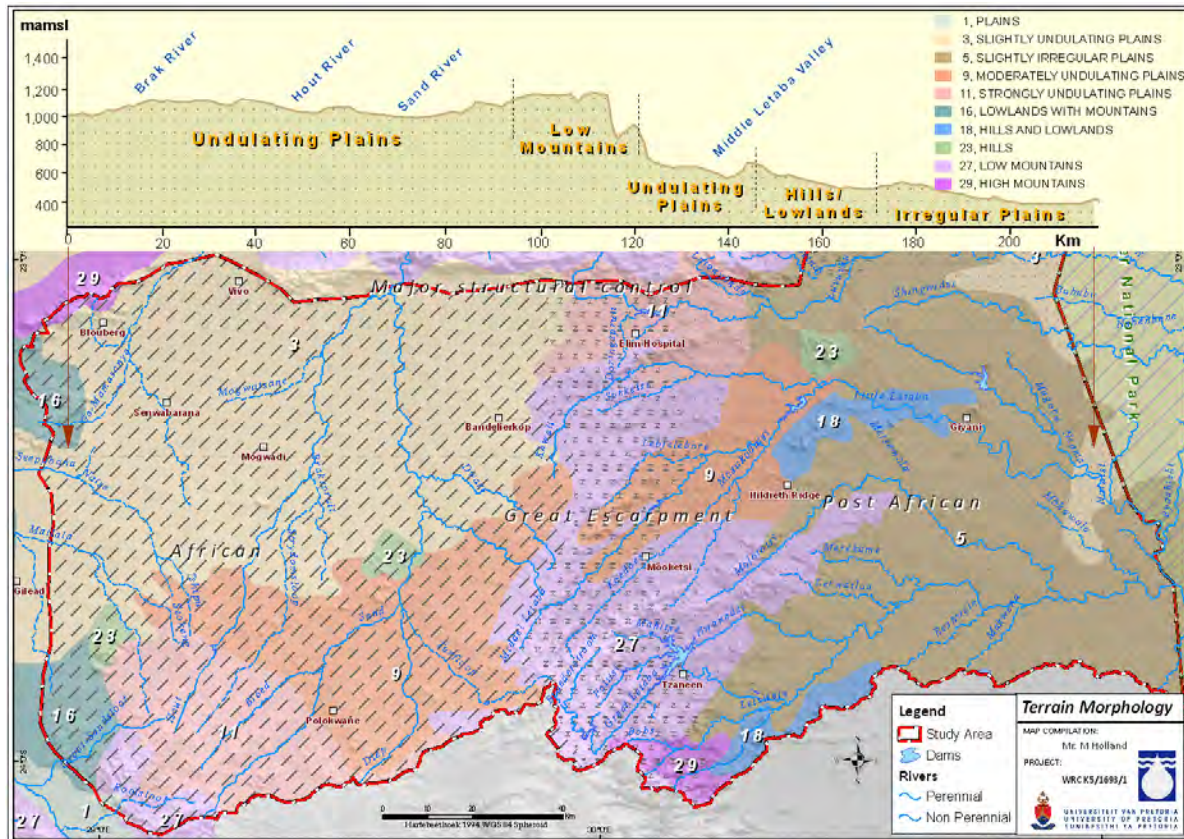


**Figure 4.4. Terrain morphological zones of the study area.**

The plateau to the west of the escarpment can be described as an extremely old erosion surface underlain by primitive basement rocks into which several mature rivers have incised themselves. The escarpment contains a series of northeasterly trending mountain spurs, containing the upper reaches of rivers such as the Middle Letaba. Towards the east of the escarpment the ground surface drops eastwards to form a plain known as the Lowveld region.

## 4.2. Regional geology

Geologically, the study area covers part of the junction between the granite-greenstone terrain of the north-eastern part of the Kaapvaal Craton and the highly metamorphic rocks of the Southern Marginal zone of the Limpopo Mobile Belt (Figure 4.5). Some authors (i.e. Roering et al. 1992) have suggested that the Limpopo Mobile Belt in the northern part of South Africa is the world's earliest example of a Himalayan-type continent-continent collisional orogeny between two large



cratons (Kaapvaal- and Zimbabwe Cratons). However, according to Kramers et al., (2006) no consensus regarding the geological process, setting or timing of the Limpopo Mobile Belt have been reached. The resulting Limpopo Mobile Belt consists of three main crustal zones, namely the Northern Marginal Zone, the Central Zone and the Southern Marginal Zone, which lie parallel to one another in an ENE direction (Figure 4.5).

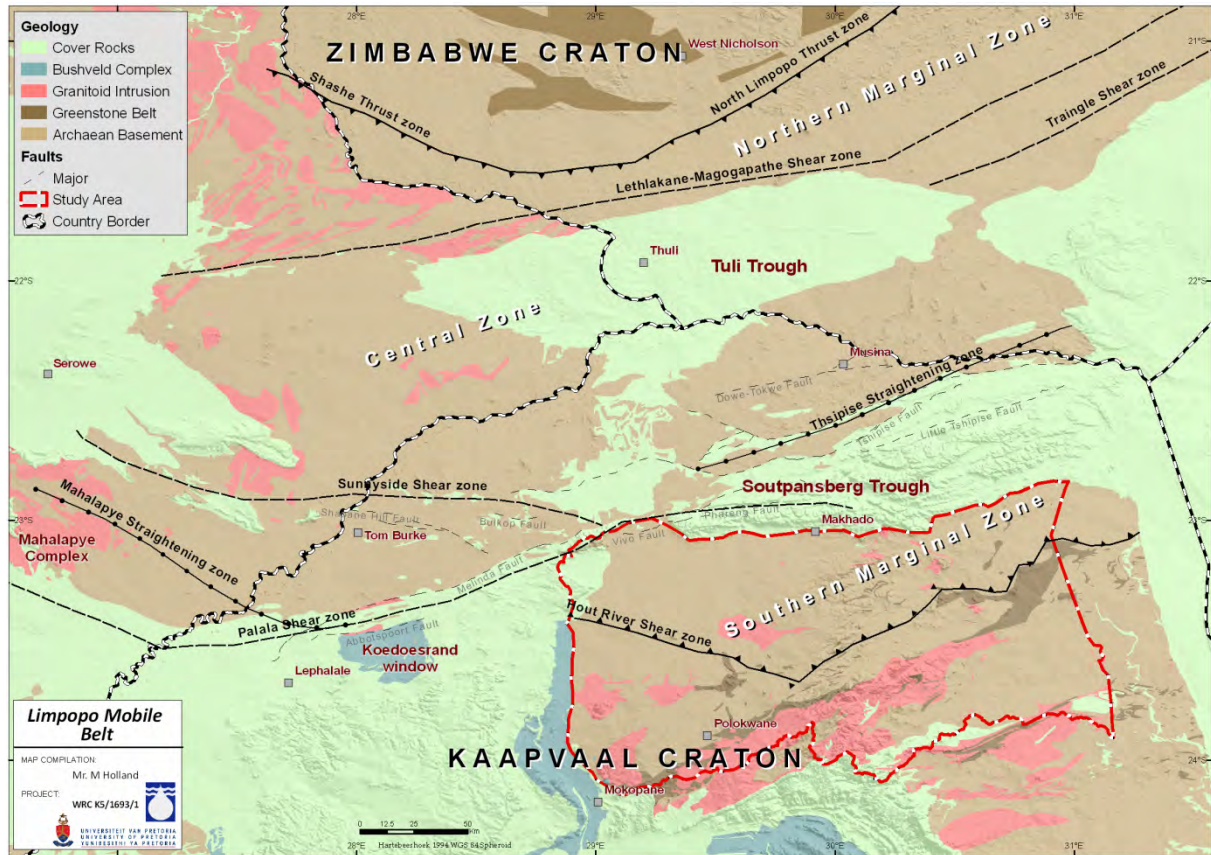


**Figure 4.5. Generalised map of the Limpopo Mobile Belt showing the main features and subdivisions (adapted from Boshoff et al., 2006).**

The northward dipping Hout River Shear Zone forms the boundary between the low-grade metamorphism granitoid-greenstone terrane of the Kaapvaal Craton to the south and the higher grade metamorphism rocks zones of the Southern Marginal Zone to the north (Figure 4.5). In general the HRSZ comprises EW striking, steeply northward-dipping thrusts and reverse faults, as well as several NE-SW striking strike-slip faults (Smit et al., 1992). The Hout River Shear Zone can be traced for over 250 km from west to east across the southern margin of the Limpopo Mobile Belt and acts as a complex thrust system developed over a width of up to 4 km in places (Anhaeusser, 1992).

#### 4.2.1. Description of local geology

The geology of project area is dominated by Archaean basement rocks (granite, gneiss and greenstone) which outcrop in an approximately rectangular area bordered (Figure 4.6);

- to the south by younger overlying sedimentary strata and the major surface water divide,
- to the north by the Soutpansberg Group (Volcanic rocks),
- to the west by the Northern limb of the Bushveld Complex, and
- to the east by the Drakensberg basalts of the Lebombo mountains.

##### *Archaean Gneisses*

The geology of the study area is dominated by two lithostratigraphical units in the crystalline complex, namely the Goudplaats-Hout River Gneiss and Groot-Letaba Gneiss. These Palaeoarchaean (3,600-3,200 million years) gneissic bodies range from homogenous to strongly layered, leucocratic felsic to mafic minerals (Anhaeusser, 1992). According to Robb et al. (2006) the previous subdivision of the strongly migmatized Hout River Gneiss and less well-migmatized Goudplaats Gneiss is no longer regarded as tenable. However, granitoid gneisses occurring between the Murchison (Gavelotte Group) and the Pietersburg-Giyani greenstone belts have been grouped together under the term Groot-Letaba Gneiss (Brandl and Kröner, 1993). These rocks are bounded in the southeast by the Letaba Shear Zone (Figure 4.6).

##### *Archaean Greenstone Belts*

The Rhenosterkoppies (Zandrivierspoort Formation), Pietersburg (Pietersburg Group), Giyani (Giyani Group) and northern part of the Murchison (Gravelotte Group) Greenstone Belts occur in the study area. They are composed largely of extrusive mafic and, to lesser extents, ultramafic and felsic rock. These Greenstone Belts are infolded mainly into grey granitic gneisses which dominate the early Archaean terranes (Brandl et al., 2006). The NE-trending Pietersburg and Giyani Greenstone Belts extend parallel up to the southern part of the SMZ of the Limpopo Belt. The Murchison Greenstone Belts exists along a major ENE-WSW crustal lineament known as the “Thabazimbi-Murchison Lineament” (TML). Because of the orientation of the TML, the Greenstone Belts and the LMB, many of the geological structures recorded in the study area are parallel with this NE-SW trend.

##### *Neoarchaean Intrusions*

A number of massive, unfoliated granite intrusions occur as batholiths, plutons and stocks in the study area. These granitic intrusions form prominent topographical features that can be seen north of Polokwane. The most distinct of these plutons are Matlala Granite, Moletsi Granite, Mashashane Suite (Granites) and Matok Granite. The Matok Granite was emplaced just north of the HRSZ. The Duivelskloof leucogranite and the Turfloop Granite, which forms elongated northeast-trending batholiths, are the most voluminous granite bodies in the study area. However, the contacts with the surrounding granitoid gneisses of these large batholiths are not well defined. Various other granite intrusives occur throughout the study area including the Schiel Complex located immediately north of the northeast-orientated Kudus River Lineament (Figure 4.6).



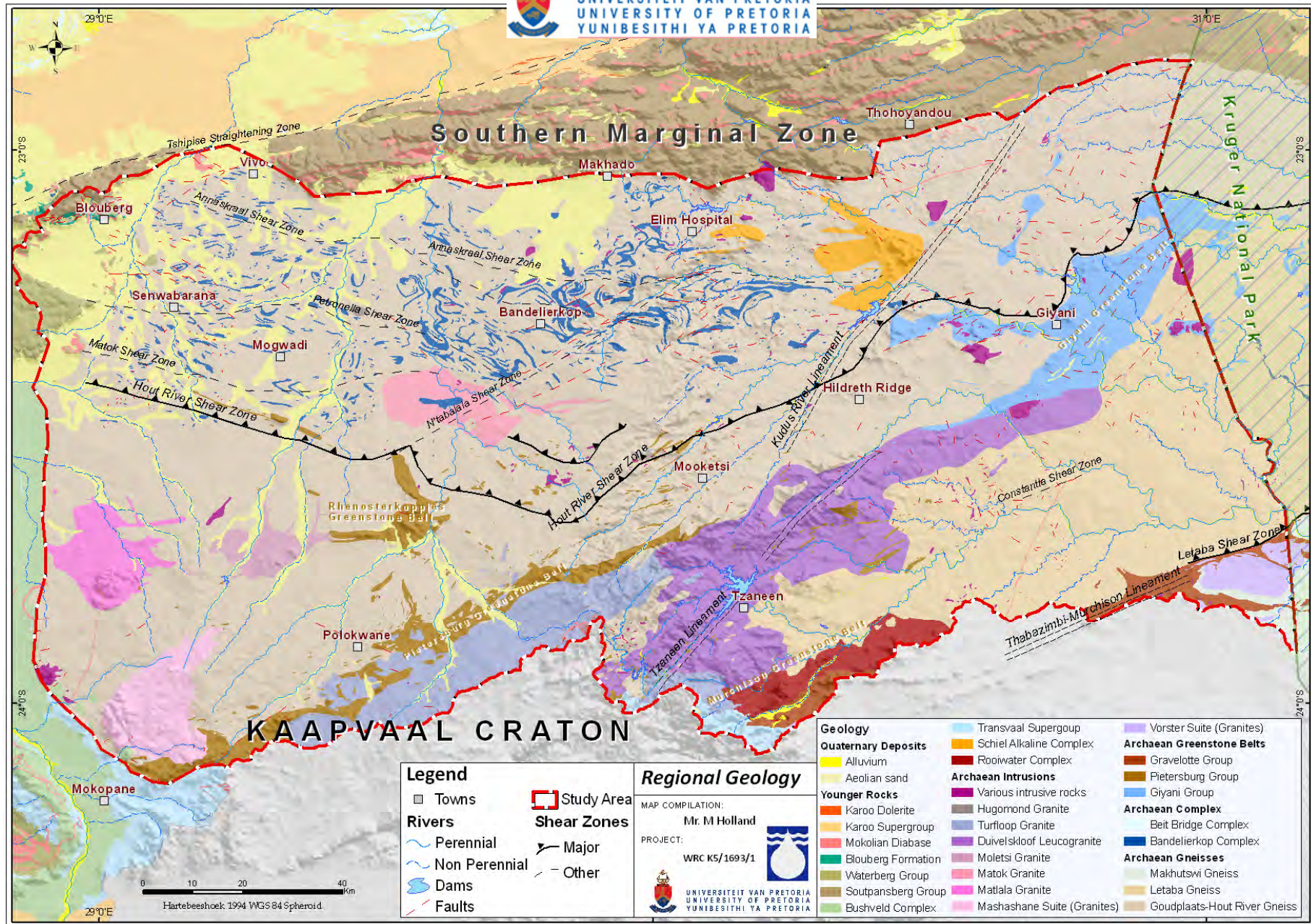


Figure 4.6. Regional geology of the study area (based on published 1:250 000 map sheets sourced from the Council for Geoscience).



### *Younger rocks of significance*

The Soutpansberg Group emerges as a large east west trending mountain range (escarpment) from the Kruger National Park in the east to Vivo in the west, and forms the northern border of the present study area. Outliers of the volcano-sedimentary Soutpansberg rocks also outcrop further to the west (Figure 4.6). The Waterberg Group (arenites and rudites) similarly outcrops along the north-western margin of the study area and rests unconformably on the rocks of the Bushveld Complex and the Archaean gneisses. The western edge of the study area is bound by the northern limb of the Bushveld Complex. This is a large economically important layered intrusive complex, comprising the lower Rustenburg Layered Suite and Lebowa Granites Suite above, which intruded into the Archaean basement. The eastern margin of the study area is marked by the eastern edge of the Kaapvaal craton. This area is underlain by rocks of the Drakensberg Group (Karoo Supergroup) which comprise flood basalts and pyroclastic deposits. The presence of quaternary cover of soil, calcrete and ferricrete is common. These covers are generally not very thick but widespread towards the northeast of the area. Water bearing alluvial deposits is found mostly along the lower reaches of the major tributaries, but is limited in extent. Alluvial deposits are indicated on the 1:250 000 geological map sheets and are presented in Figure 4.6.

#### 4.2.2. Geological timeline of local occurrences

The summary of crystallisation/emplacement age for granitoid intrusions and other younger rocks pertaining to the study area is based on Robb et al., (2006) and Kramers et al., (2006):

- 3 600 – 3 200 Ma Palaeoarchaean intrusions (Goudplaats-Hout River Gneiss)
- ± 3 200 Ma Greenstone Belts (Giyani, Pietersburg, Murchison)
- 3 200 – 2 800 Ma Mesoarchaean intrusions (Groot Letaba Gneiss; Voster Suite)
- 2 800 – 2 500 Ma Neoaarchaean intrusions (i.e. Matok- Matlala granites)
- 3 100 Ma Central Kaapvaal Craton is stable
- 2 700 Ma Limpopo Belt (First event)
- 2 700 Ma Ventersdorp-related mafic dykes.
- 2 060 Ma Intrusion of the Bushveld Complex
- 2 000 Ma Palala Shear Zone Reactivation (Second Limpopo event)
- > 1 850 Ma Deposition of Waterberg Group
- 1 850 Deposition of Soutpansberg Group
- 180 Ma Extrusion of Drakensberg Flood Basalts

### 4.3. Structural geology

One of the most differentiating structural features of the study area is the frequency and orientation of dyke swarms. Dyke swarms may be useful paleo-stress indicators as they record fractures that result from regional stress field operative at the time. Stettler et al. (1989) subdivided parts of the Kaapvaal Craton and the Limpopo Belt according to the prevailing aeromagnetic lineament pattern into five domains (Figure 4.7).

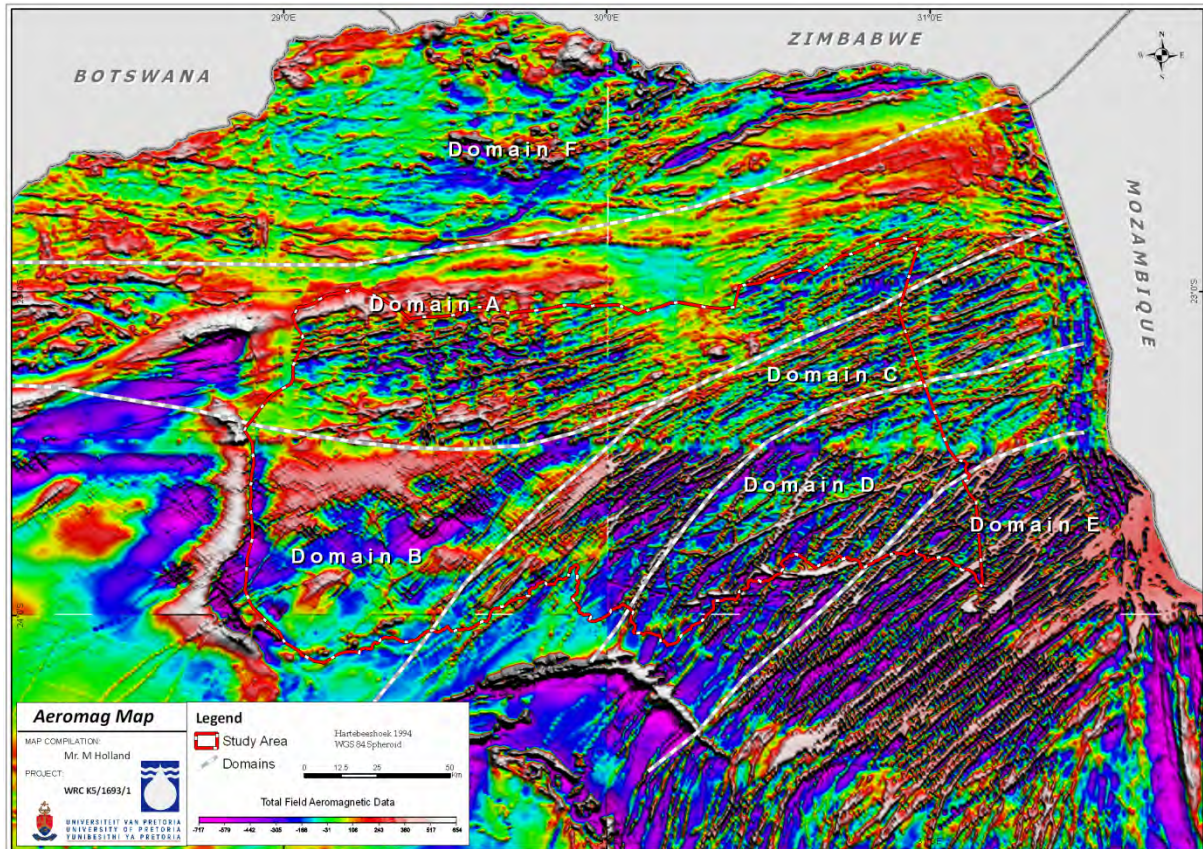


Figure 4.7. Aeromagnetic map showing tectonic domains (Adapted from Stettler et al., 1989). Data Source: Council for Geoscience (SA).

The age and orientation of the predominantly ENE to NE trending dyke swarms and associated aeromagnetic lineaments coincide with the 2 700 million years Ventersdorp rift structures, but also include similar NE trending Karoo-age dolerite dykes (Uken and Watkeys, 1997). During this period the northeastern Kaapvaal Craton underwent NW-SE extension, in contrast to the current NE-SW extensional regime (Figure 4.8). On the basis of data compiled into the World Stress Map database there is a suggestion of a horizontal principal stress direction oriented NW to NNW (Heidbach et al., 2008).

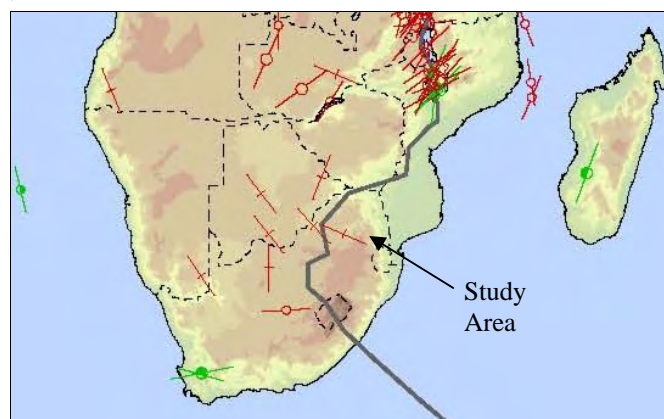
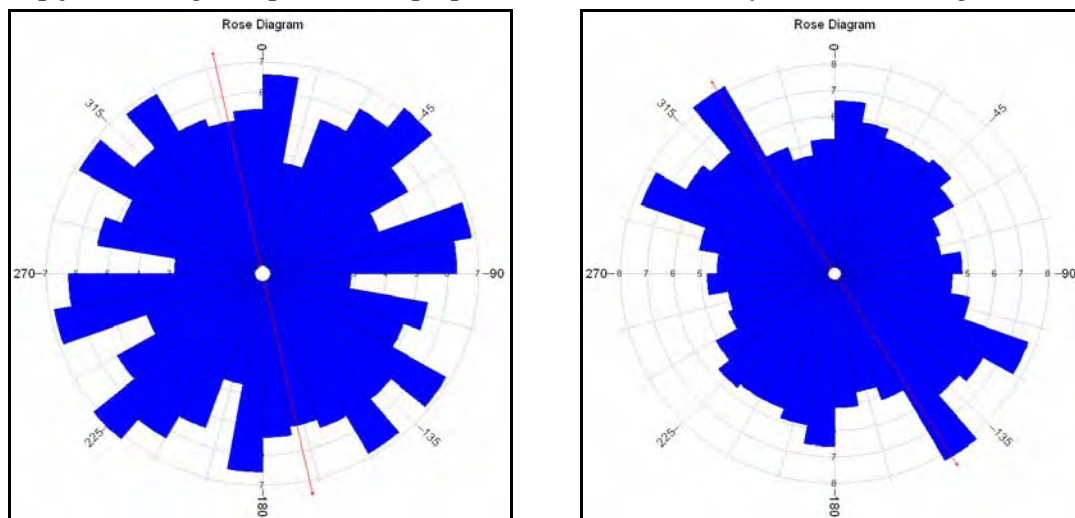


Figure 4.8. Neo-tectonic stress map of southern Africa (Zoback, 1992). Long axes indicate the orientation of crustal shortening.

According to Bird et al. (2006) southern Africa is not in a state of horizontal compression. Instead, it is generally in a state of horizontal extension which may be a result of the unbroken lithosphere's resistance to relative rotation between the Somalia Plate and the Africa Plate. More specific to the study area, Bird et al. (2006) highlighted that the ENE-WSW trending Tshipise-Bosbokpoort fault system described by Brandl (1995), is inconsistent with the strain rate field model because it is almost orthogonal to computed horizontal principal stress direction. It is evident that in regions with multiple deformation events and structural inheritance, all, none or some of the geological structures may be related to the current stress regime. This is clearly evident from field observations obtained by Petzer (2009) where normal faults and open joints were also formed in the NW-SE direction (Figure 4.9). Therefore structures inherited from the Precambrian are presumably open under the current neo-tectonic stress regime. These joints show a very poor correlation with the predominant NE trending dyke pattern; the main azimuths of the outcrop joints being oblique or even perpendicular to the main dyke azimuths (Figure 4.10).



**Figure 4.9. Rose diagram derived from the strikes of all joint planes (left) and faults (right).**

Whereas some of these joints could have formed due to dilatation (i.e. pressure release as a result of erosion or plutonism), it is believed that many of these joints are actually tectonically induced, suggesting that the study area was at one stage subjected to compression. Such a regime would favor the formation of open joints in the NE-SW direction, but at the same time closing many brittle structures that might have been favourable groundwater conduits in the geological past. Joints striking NE-SW were probably reactivated during successive tectonic events (for example the NNE-SSW extension during later Karoo times) and lie parallel to one of two preferred lineament orientations (NE-SW and NNE-SSW), as identified by the dolerite dykes in the study area. The study area shown in Figure 4.10 can clearly be subdivided into four structural domains on the basis of aeromagnetic lineament strike direction and frequency. Most of the magnetic anomalies in the studied area are caused by linear features, inferred as dykes.



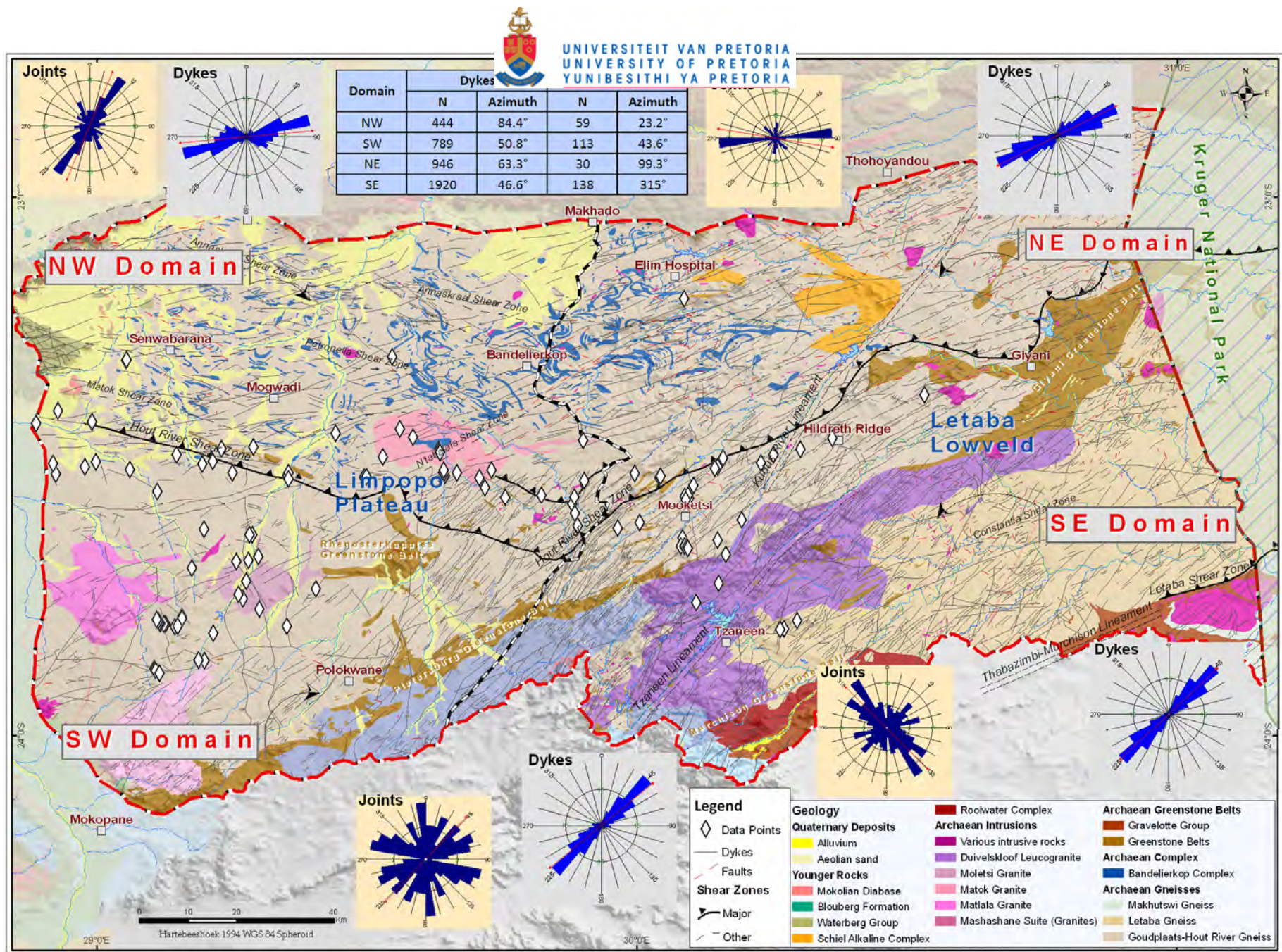


Figure 4.10. Identified structural domains based on the orientation of regional dykes (Aeromagnetic and published dykes).



Interpretation of magnetic lineaments was conducted by the Council for Geoscience (South Africa) based on regional airborne magnetic data with a 1 km line spacing. The predominant ENE dyke swarm trend appear to be cut by NW trending dykes, suggesting that the latter intruded last. These trends cut across earlier ENE trending crustal features such as the Greenstone belts, suggesting that the crust became mechanically homogenous at the time of the dyke events (Stettler et al., 1998). The Limpopo north-western and south-western domains are predominantly characterized by the gneissic rocks of the Goudplaats-Hout River Group with a much lower frequency of dykes and lineaments compared to the Letaba northeastern and south-eastern domains (Figure 4.10). Dykes in the NW and SW domain have a mean strike direction of  $85^\circ$  and  $51^\circ$  respectively. The two eastern structural domains show a high degree of preferred orientation and are characterized by the highest dyke intensity. Dyke trends in the NE domain are predominantly ENE ( $63^\circ$ ) and cut obliquely across the greenstone belts. Dykes in the SE domain have a strike direction of  $47^\circ$  and are almost parallel to the large elongated leucogranite batholith. The Hout River Shear Zone can be regarded as the margin between the northern and southern domains. These regions correspond closely to the domains identified by Stettler et al. (1989) and provide a tectonic and morphostructural framework to describe hydrogeologic parameters on a regional scale.

#### **4.4. Hydrogeological description**

To determine the variability of basement aquifers in the Limpopo Province, it was deemed necessary to split the area based on the topography, surface drainages and geological domains as set out in previous sections. The western portion of the area is referred to as the Limpopo Plateau and the eastern portion as the Letaba Lowveld (Figure 4.11).

##### *Limpopo Plateau*

The region is characterized by a number of batholiths, forming distinct inselbergs interpreted as residual hills that became exhumed in successive stages of stripping of weathering cover of the African erosion surface. The thickness of the regolith in the Limpopo Plateau generally extends to between 15 and 50 metres below surface. Below the weathered zone is a zone of fracturing, which according to geohydrological studies done by Dziembowski (1976) and Jolly (1986) in the Dendron/Mogwadi area may extend to depths greater than 120 m. This area is known for its high yielding boreholes which far exceed the typical expectations of crystalline aquifers with blow yields of more than 40  $\ell/s$  often recorded. As a result the area supports a number of large scale irrigation schemes. Towards the south west of Makhado, electrical resistivity depth soundings collected by Timmerman et al. (1983) indicate weathering depths of between 20 and 40 m. Borehole siting, drilling and pumping tests around Polokwane by Du Toit (1986) showed weathering depths of between 9 and 36 m. Du Toit (1986) concluded that although there is some correlation between yield and weathering depth, higher yields ( $> 3 \ell/s$ ) are more often associated with the fractured fissure layer irrespective of the thickness of the overlying weathered layer. The only substantial deposits of alluvium occur along the major surface drainage courses (i.e. Sand- and Hout Rivers). Orpen (1986) estimated the thickness of alluvium deposits along the Sand River

to be not more than 8 to 15 m. Nel (2000) suggested that in the absence of a continuous impermeable clay (colmation) layer, the alluvial and weather-fractured aquifers are in hydraulic continuity. The alluvial deposits typically consist of red or sandy clay (calcified in places) which overlies sand, gravel and pebbles. A survey conducted by Vegter (2003a) on the Polokwane/Pietersburg Plateau groundwater region found that 52% of boreholes drilled were successful (yield > 0.1 l/s).

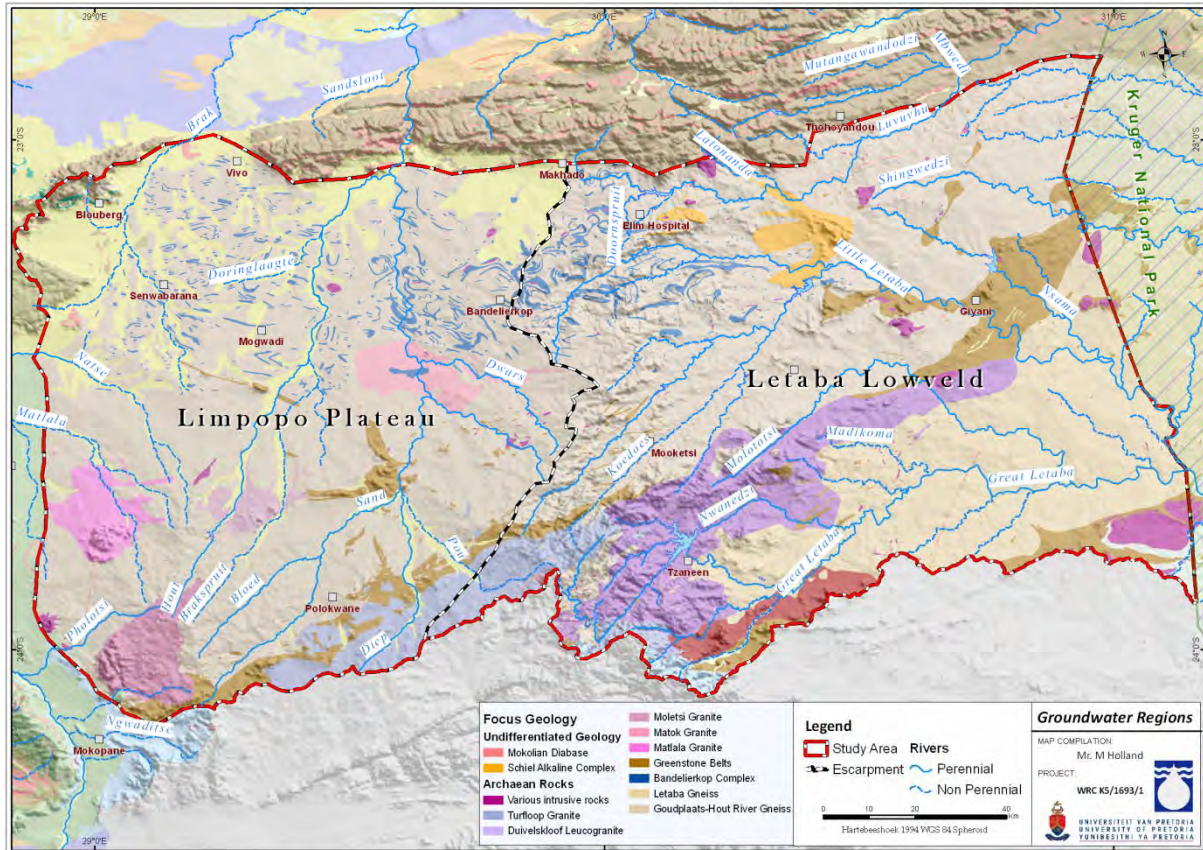


**Figure 4.11. Delineation of the Limpopo Plateau and Letaba Lowveld regions.**

### *Letaba Lowveld*

Along the great escarpment the Letaba Lowveld is characterised by mountainous terrain, incised valleys, high rainfall and dense vegetation. A number of perennial springs occur in this area. The gneisses in the Mooketsi area are well weathered but regolith thickness rarely exceeds 30 m. The leucogranites underlying the higher lying areas including the footwalls east of the escarpment have a thin or absent weathered layer (i.e. the Tzaneen and Mooketsti areas) (Figure 4.11). According to Bush (1988) weathering depths rarely exceed 30 m. These elongated intrusive granitoids occur as bouldery hills with little soil cover, and are considered to be least prone to chemical weathering due to the exposure of the bare rock surface. It is expected that the weathering depth in the younger leucogranites is less than in the surrounding gneisses. Alluvial deposits occur along the major drainage courses (i.e. Molototsi-, Groot Letaba- and Klein Letaba Rivers). A survey conducted by Vegter (2003b) on the Lowveld groundwater region found that the success rate of boreholes is slightly lower compared to the Polokwane/Pietersburg Plateau groundwater region, with 49% of boreholes yielding more than 0.1 l/.



#### 4.4.1. Aquifer systems

A conceptual illustration of the aquifer systems typically found in the study area is provided in Figure 4.12. The aquifers systems developed in the Limpopo Plateau and Letaba Lowveld are:

- 1) Composite aquifers; comprising of a variable thickness of regolith overlying bedrock, the upper part of which is frequently fractured.
- 2) Deeper fractured aquifers; composed mainly of crystalline material (i.e. igneous and metamorphic rocks) characterised by an intact and relatively unweathered matrix with a complex arrangement of interconnected fracture systems.
- 3) Alluvial aquifers; alluvial material overlies or replaces the weathered overburden and creates a distinct intergranular aquifer type. These elongated aquifers follow rivers (so-called valley trains), sand rivers or drainage lines with limited width and depth, which typically vary according to the topography and climate.

#### 4.4.2. Borehole data analysis

Compared with the Letaba Lowveld, the Limpopo Plateau is generally characterized by deeper boreholes due to deeper water strikes, water levels and weathering depths (Table 4.3). The depth of weathering is based on the driller's description of the formation where rock type is weathered and represents the in-situ weathered material only. The relatively thin weathering depth (generally less than 20 m) along with water strikes below the weathered zone suggest that yields are mainly derived from water bearing fractures struck at depth.

**Table 4.3. Summary of borehole characteristics in the study area.**

m.b.g.l*	Limpopo Plateau				Letaba Lowveld			
	<i>N</i>	<i>Min</i>	<i>Mean</i>	<i>Max</i>	<i>N</i>	<i>Min</i>	<i>Mean</i>	<i>Max</i>
<b>BH Depth</b>	<u>2 066</u>	7	70	250	<u>2 813</u>	8	63	182
<b>Water Level</b>	<u>1 563</u>	0.6	17	83	<u>2 177</u>	0.5	14.8	73
<b>Water Strike</b>	<u>202</u>	1	36	87	<u>646</u>	1	28	80
<b>Weathering</b>	<u>481</u>	1	22	63	<u>750</u>	3	18	82

\*- meters below ground level.

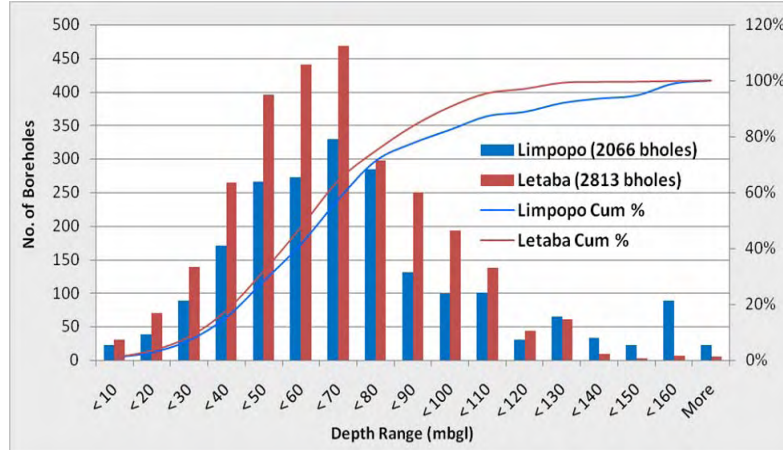
The Limpopo Plateau with elevations generally higher than 1 000 mamsl is largely situated on the African erosion surface while the lower lying plains of the Letaba Lowveld with elevations below 800 mamsl are associated with the post-African surface as described by Partridge and Maud (1987). Studies conducted by the British Geological Survey in the early 1990s on crystalline aquifers throughout Africa revealed that the regolith was generally thicker beneath the oldest and uppermost erosion surface, the African surface, compared with the post-African erosion surface so offering greater storage and possibly a more productive resource potential (McFarlane et al. 1992).



Figure 4.12. Generalised section of the aquifer systems found in the area of investigation, including photo's of observed geological features.



The borehole depths follow a normal distribution (Figure 4.13) for both regions with 60% of boreholes drilled to depths between 50 and 80 m, indicating the tendency to drill to fixed depths regardless of the hydrogeological conditions encountered. However, boreholes drilled in the Limpopo Plateau are generally deeper than in the Letaba Lowveld (Table 4.3.), with 42% of boreholes exceeding 60 m depth in the Limpopo Lowveld in comparison to 34% in the Letaba Lowveld.



**Figure 4.13. Distribution of borehole depths in the Limpopo Plateau and Letaba Lowveld.**

Recorded groundwater depths follow approximately a log-normal distribution (Figure 4.14), with modes (highest frequency) between 5 and 10 m.b.g.l for both study areas and 90% of groundwater levels below 30 m.b.g.l The arithmetic mean depth to groundwater (Table 4.3) is slightly higher for the Limpopo Plateau (17 m.b.g.l) in comparison to the Letaba Lowveld (15 m.b.g.l).

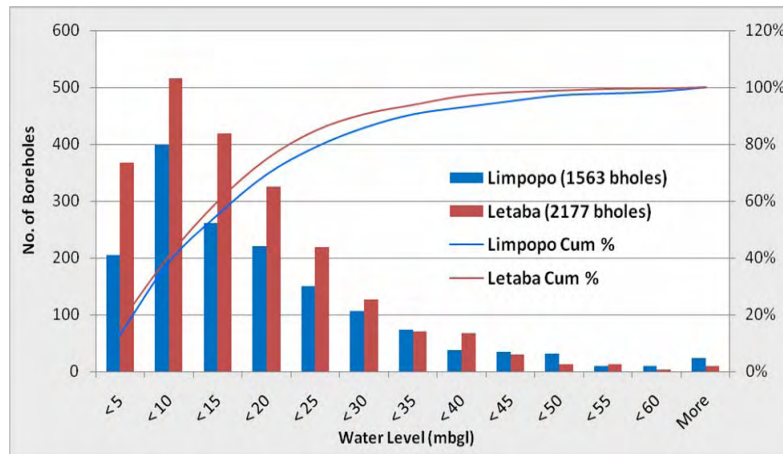


**Figure 4.14. Distribution of groundwater levels in the Limpopo Plateau and Letaba Lowveld.**

Fewer than 1 000 borehole database entries for both study areas contain information on water strike depths, but their frequency distribution (Figure 4.15) is markedly similar to the borehole depth distribution (Figure 4.13), suggesting that drilling is stopped once a sufficient water strike is encountered. 60% of boreholes encountered water before a depth of 40 m in the Limpopo Plateau and before 30 m in the Letaba Lowveld. This might explain the generally shallower drilling depths in the Letaba Lowveld, with a potentially higher risk of borehole failure during droughts.

202 boreholes (25 %) in the Limpopo Plateau encountered water beyond a depth of 50 m, compared to a mere 8% in the Letaba Lowveld region, suggesting a deeper base of weathering and fracturing in the Limpopo Plateau.

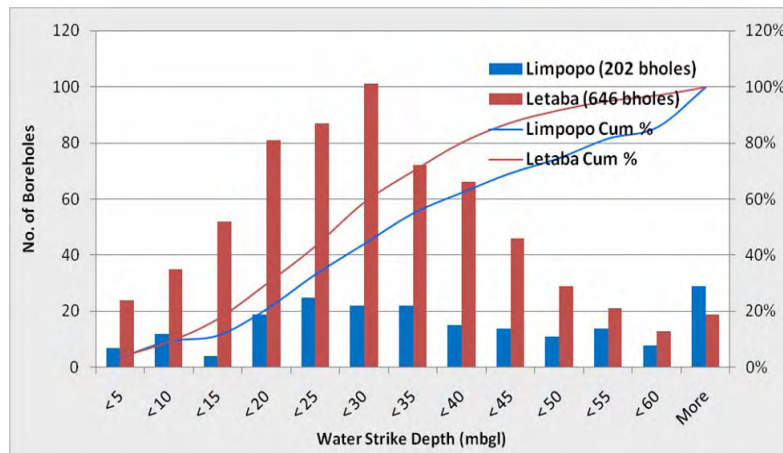


**Figure 4.15. Distribution of depth of first water strikes in the Limpopo Plateau and Letaba Lowveld.**

Figure 4.16 depicts the depth of weathering and/or fracturing based on over 1 200 geological logs for the regions. In most cases it is difficult to distinguish the depths of weathering from fracturing from the geological logs. A combined dataset was therefore produced and can be regarded as a proxy for the depth to fresh bedrock. The average depth of weathering / fracturing is 45 m in the Limpopo Plateau compared to the shallower 36 m in the Letaba Lowveld (see Table 4.3). The depth of weathering / fracturing exceeds 60 m for 23% of boreholes in the Limpopo Plateau and only for approximately 10% of boreholes in the Letaba Lowveld. In summary, boreholes drilled in the Limpopo Plateau are generally deeper, show deeper- water strikes, water levels and depths of weathering compared to the Letaba Lowveld.

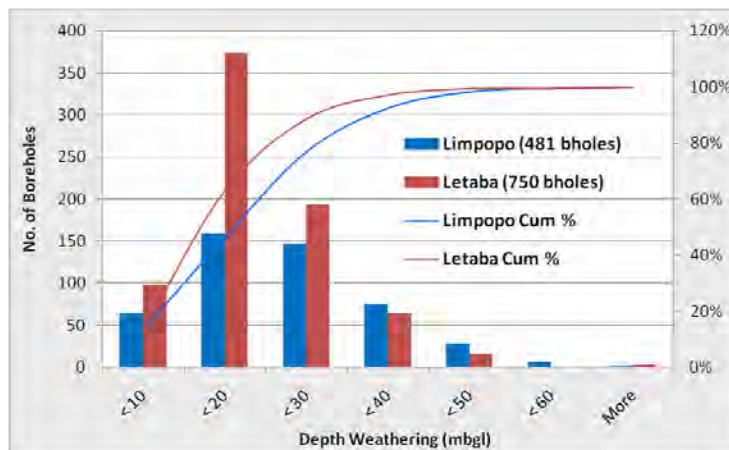


**Figure 4.16. Distribution of depths of weathering plus fracturing in the Limpopo Plateau and Letaba Lowveld.**

#### 4.4.3. Success rate and yields

The yield data obtained from the GRIP dataset were examined in terms of the drilling success rate achieved (Figure 4.17). Any borehole equipped with a pump even if no yield data were recorded was regarded as successful. In 30% of the cases no yield or equipment status were recorded and in 9% of the cases dry drills (boreholes) were noted. 61% of boreholes can be regarded as successful with yields greater than 0.1  $\ell/s$ . This value is considerably higher than Vegter's (2003a; 2003b) success rate of 49 and 52% for the Letaba and Limpopo groundwater regions respectively, which was based on data from the National Groundwater Database prior to the Limpopo GRIP programme. The increased drilling success rate may be attributed to the success of the programme in terms of groundwater development for rural communities.

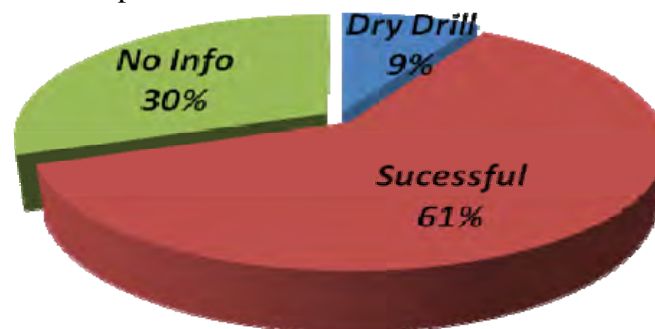


**Figure 4.17. Success rate for boreholes contained the GRIP dataset for the study area.**

The frequency distribution of airlift yields (for boreholes with airlift yield data) shows distinct differences between the two regions (Figure 4.18). While the total number of dry boreholes is higher in the Letaba Lowveld than in the Limpopo Plateau, they constitute only 25% of all boreholes in comparison to 35% in the Limpopo Plateau. 30% of boreholes in the Limpopo Plateau and 39% of boreholes in the Letaba Lowveld had an airlift yield between 0.1 and 3  $\ell/s$ , while 35% of boreholes drilled in the Limpopo Plateau and 36% in the Letaba Lowveld yielded more than 3  $\ell/s$ . Clark (1985) suggested that yields above 1  $\ell/s$  are considered good yields from basement aquifers. Therefore the borehole yields obtained from the Limpopo basement rocks are generally good considering the high percentage of borehole exceeding 1  $\ell/s$  (Figure 4.18).

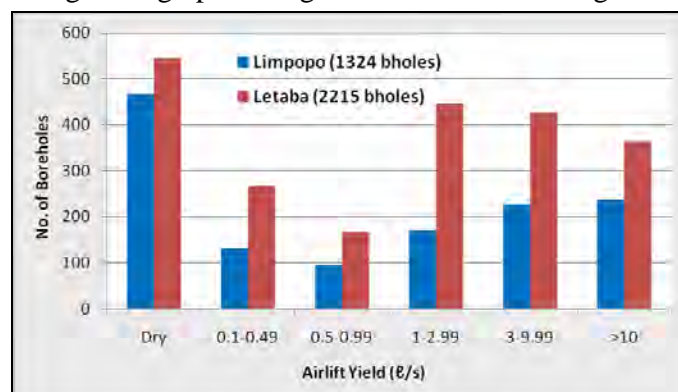


**Figure 4.18. Distribution of borehole airlift yield in the Limpopo Plateau and Letaba Lowveld.**

#### 4.4.4. Transmissivity and recommended borehole yields

Transmissivity estimates obtained from the GRIP dataset analysed with the (FC method) was generally based on a late time fit of the time-drawdown curve using i.e. Cooper-Jacob or Theis methods, or by estimating the effective transmissivity values from the average maximum derivatives (representing T-late). Borehole yields are based on the recommended abstraction rates for a 24 hrs pumping cycle. The distributions of transmissivities and borehole yields for the Limpopo Plateau and the Letaba Lowveld are positively skewed and follow lognormal distributions (Figure 4.19).

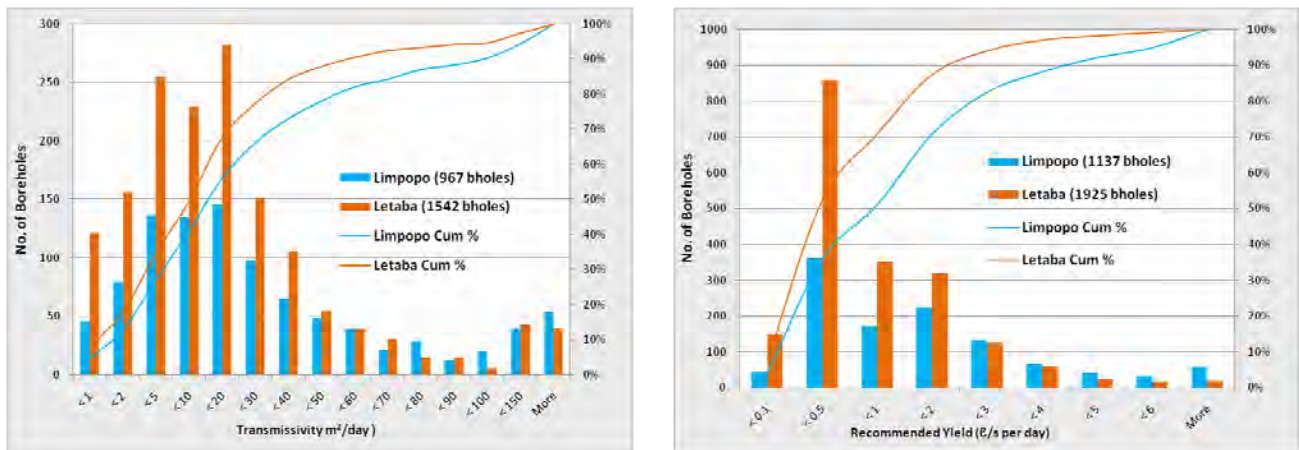


**Figure 4.19. Frequency histograms and cumulative distribution of transmissivities [ $m^2/day$ ] and recommended yield ( $\ell/s$  per day) for the Limpopo Plateau and the Letaba Lowveld.**

Lognormal distributions are frequently reported in regional studies of fractured rock aquifers (i.e. Hoeksema and Kitanidis, 1985; Razack and Lasm, 2006). Seventy percent of derived transmissivities lie between  $4 m^2/d$  and  $40 m^2/d$ ; however, several boreholes with significantly high yields, especially in the Limpopo Plateau, “push” the arithmetic mean for this area to  $38 m^2/d$  (Table 4.4). A significant correlation between transmissivity and the recommended yield with a determination coefficient ( $R^2$ ) of 73 % was found.

**Table 4.4. Statistical summary of transmissivities and recommended yields.**

Parameter	Transmissivity $m^2/d$			Rec. Yield $\ell/s$ per day		
	Study area	Limpopo Plateau	Letaba Lowveld	Study area	Limpopo Plateau	Letaba Lowveld
Nr. Of BH's	2 509	967	1 542	3 062	1 137	1 925
Arithmic Mean	29.6	38	24.5	1.0	1.4	0.8
Median	11	15	10	0.5	0.8	0.4
Harmonic Mean	3	2.9	3.1	0.1	0.17	0.20
Standard Error	1.1	2.2	1.2	0.02	0.05	0.02
Standard Deviation	56.4	67.9	47.1	1.38	1.76	1.06



## 5. HYDROGEOLOGICAL CHARACTERISATION OF THE STUDY AREA

### 5.1. Characterisation of groundwater recharge

No systematic recharge studies have been conducted in the area of investigation. National datasets such as the Groundwater Assessment Projected II (GRA II) (DWAf, 2006) or Vegter's (1995) recharge map can be used to obtain a first estimate of regional recharge. The distribution of recharge based on the GRA II dataset is presented in Figure 5.1. The GRA II dataset is based on the chloride method and adjusted to account for factors such as depth to groundwater, landcover, variation of MAP and slope. Groundwater recharge in the Limpopo WMA is approximately 702 million m<sup>3</sup>/a (assuming recharge being 2% of mean annual precipitation (MAP) and 376 million m<sup>3</sup>/a in the Luvuvhu/Letaba WMA (2% to 3% of MAP).

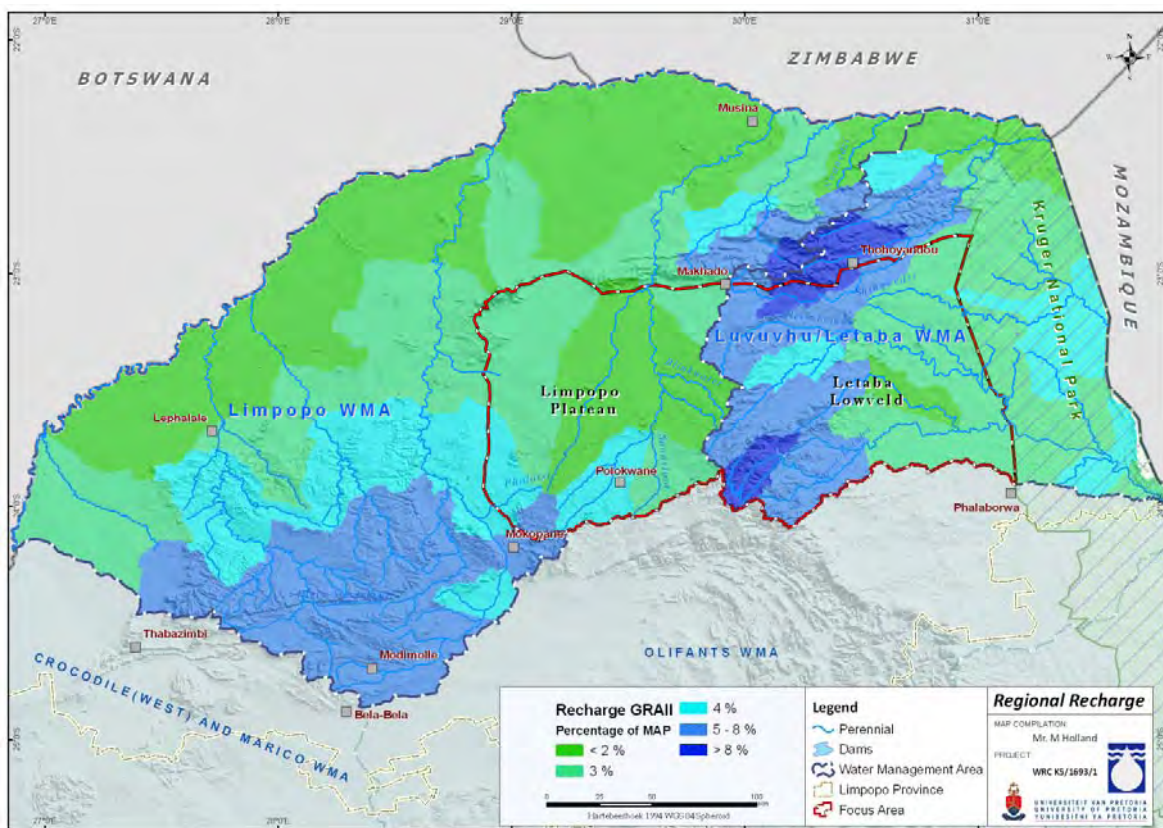


Figure 5.1. Regional recharge map for the Limpopo Province.

#### 5.1.1. Recharge estimates (Chloride Mass Balance)

Regional and local estimates of recharge were obtained using chloride concentrations in rainwater and groundwater, together with annual rainfall. Three bulk rainfall stations were installed in the area for the application of the CMB and isotope characterization. Unusually high chloride values for rainfall obtained at the start of the study suggest that these samples were influenced by aerosol deposits and dry depositions indicating that the bulk rainfall collectors overestimated the total

chloride deposition. Therefore, a couple of manual rainfall samples were collected during the study. Further chloride concentrations were obtained from the Department of Water Affairs<sup>1</sup> as part of the National Rainwater Monitoring Programme which operates five rainfall sampling collectors in the Blouberg and Taaiboshgroet area. Table 5.1 lists the chloride values obtained from the sampled rainwater of the individual rainfall event as well as the bulk rainfall samples from the DWA. Based on the results chloride concentrations range from 0.39 to 7.3 mg/l. However, according to Bean (2003) chloride values above 5 mg/l represent site-specific enrichment within the given sampling period and would result in an over-estimation of recharge.

**Table 5.1. Summary of borehole characteristics in the study area.**

Site	Sample ID	Date	Cl (mg/l)	Comment
Mufeba (UP1)	MERS 1	08-Mar-08	6.3	Bulk sample (Could be polluted)
Bochum (UP2)	BORS 1	09-Mar-08	7.3	
Rawesi (UP3)	CORS 1	09-Mar-08	6.3	
Mufeba (UP1)	RA 1	03-Mar-09	0.61	Event based
Rawesi (UP3)	RAW 2	15-Mar-09	0.39	Event based
Rawesi 2 (UP3)	RAS 3	15-Mar-09	0.77	Event based
Bochum (UP2)	BC1	15-Mar-09	0.69	Event based
Polokwane (UP4)	Rain2	01-Feb-10	0.34	Event based
DWA (1 to 5) Taaiboschgroet Area*	Blouberg Eldorado Greenfields Langjan Rosyth	2002/2003 late summer	0.68	Bulk Rainfall Collectors
		2003/2004 early summer	1.34	
		2003/2004 Mid summer	0.91	
		2003/2004 late summer	0.44	
		2003/2004 winter	1.96	
		2004/2005 Early Summer	0.80	
		2004/2005 Late Summer	1.43	
		2005/2006 Mid summer	0.63	
		2005/2006 Late summer	0.57	

\*- Based on the harmonic mean chloride values of five stations within the Taaiboshgroet area.

Excluding erroneous values an average concentration of 0.69 mg/l is obtained. The spatial location of the sampling rainfall collector sites are shown in Figure 5.2, together with the distribution of chloride content in groundwater from over 4 000 boreholes.

<sup>1</sup> E-mail correspondence (2009) – Eddie van Wyk (Hydrological Services - Department of Water Affairs)



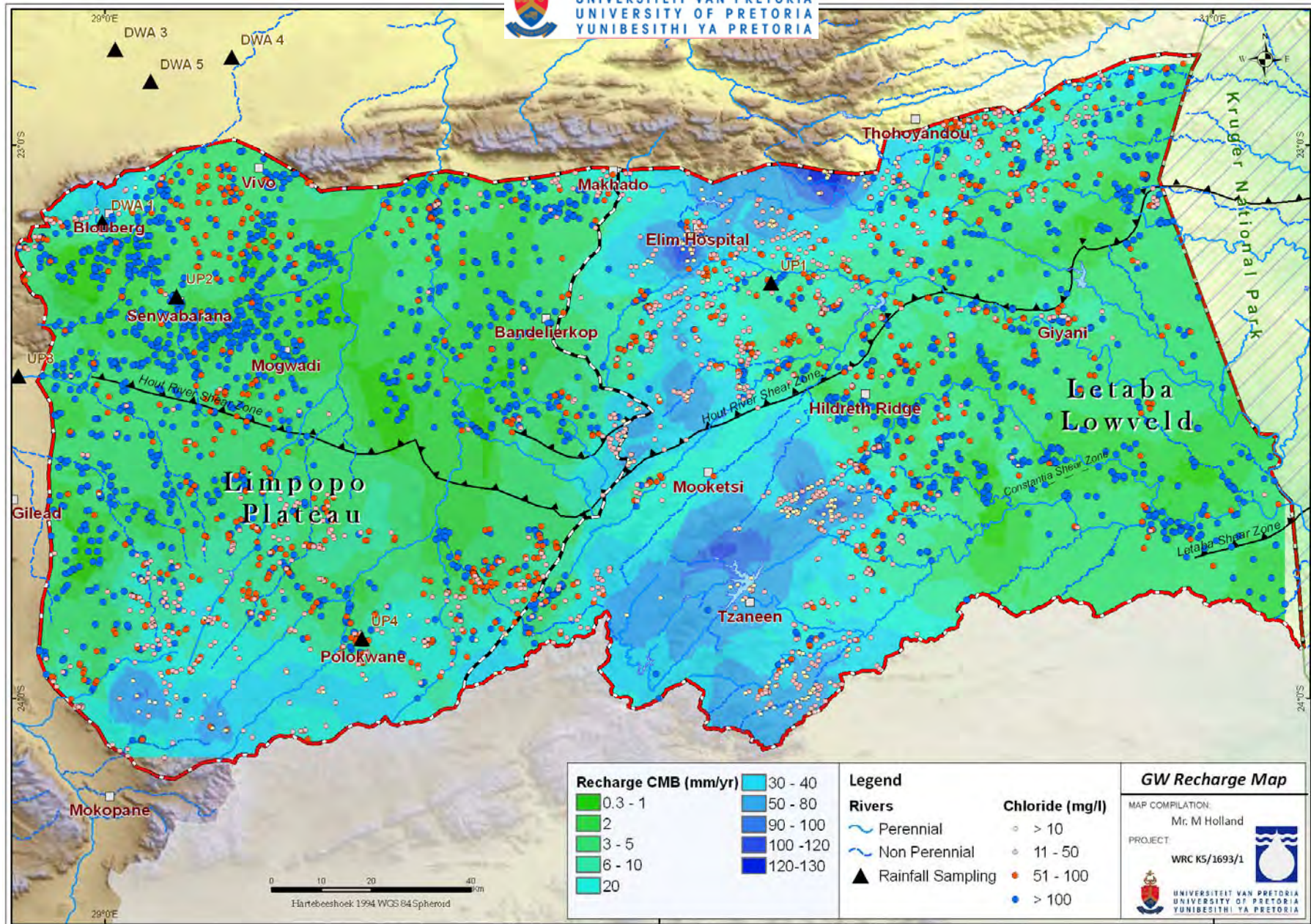


Figure 5.2. Annual recharge map based on the CMB-method.

Interpolations from the CMB results were based on the Kriging techniques, while site specific results are shown in Table 5.2. The average concentrations of groundwater in boreholes surrounding the localities (10 km radius) were used to determine the average rate of recharge per year. Recharge rates vary from 0.4 to 4.6 % of MAP. Active recharge zones are related to the higher lying areas associated with the main surface water drainage divides (i.e. along the Great Escarpment and to the south of Polokwane).

**Table 5.2. Recharge estimates based on the CMB for selected localities in the study area.**

Locality	Annual Rainfall (mm)*	Chloride (mg/l)		Average Recharge	
		$Cl_{rf}$	$Cl_{gw}$	Mm/year	% of MAP
Chloe	365	0.6	147.3	1.5	0.4
Mogwadi	392	0.7	153.7	1.8	0.5
Tzaneen	950	0.75	10.2	70.0	7.4
Mara	454	0.6	77.2	3.5	0.8
Palmaryville	916	0.75	26.1	26.4	2.9
Polokwane	455	0.6	40.1	6.8	1.5
Rosbach	912	0.75	10.8	63.4	7.0
Shangoni	446	0.7	76.1	4.1	0.9
Soekmeaar	648	0.7	15.2	29.8	4.6

\*- South African Weathers Services.

### 5.1.2. Aquifer response to recharge

Over 50 boreholes are currently installed with continuous groundwater level loggers within the study area as part of the Limpopo (DWA) regional office monitoring network. The available groundwater levels from these stations extend back to between 2005 and 2006. A summary of the short term water level data obtained from selected monitoring boreholes is presented in Table 5.3 and illustrated spatially in Figure 5.3.

**Table 5.3. Summary of short term monitoring groundwater level data for selected stations.**

Station	Start		Downloaded		WL Fluctuation <sup>#</sup>		
	Date	WL*	Date	WL*	Min*	Max*	Dh (m)
A6N0586	Mar-06	4.2	Aug-09	4.4	5.2	3.5	1.7
A7N0019	Jan-06	12.6	Aug-09	13.3	14.9	8.2	6.7
A7N0041	Jul-06	6.8	Aug-09	7.1	8.6	8.2	0.4
A7N0524	Oct-05	31.2	May-09	31.7	32.1	31.0	1.2
A7N0637	Jul-05	9.6	Aug-09	9.4	12.3	6.5	5.8
A9N0008	Sep-05	6.1	Aug-09	6.6	14.9	8.2	6.7
B8N0504	Sep-06	25.6	Aug-09	26.9	28.0	25.4	2.5
B8N0510	Sep-06	19.7	Aug-09	18.8	19.8	16.8	3.0
B8N0514	Mar-06	22.1	Aug-09	19.0	22.1	18.9	3.2
B8N0517	Mar-06	19.3	Aug-09	18.7	20.4	17.3	3.1
B8N0518	Mar-05	11.9	Aug-09	12.9	12.9	10.4	2.5
B8N0521	Oct-05	8.3	Aug-09	8.2	8.4	6.9	1.5

\*- meters below ground level.

<sup>#</sup> - The largest amplitude of the groundwater level over the measurement period and the difference between them.



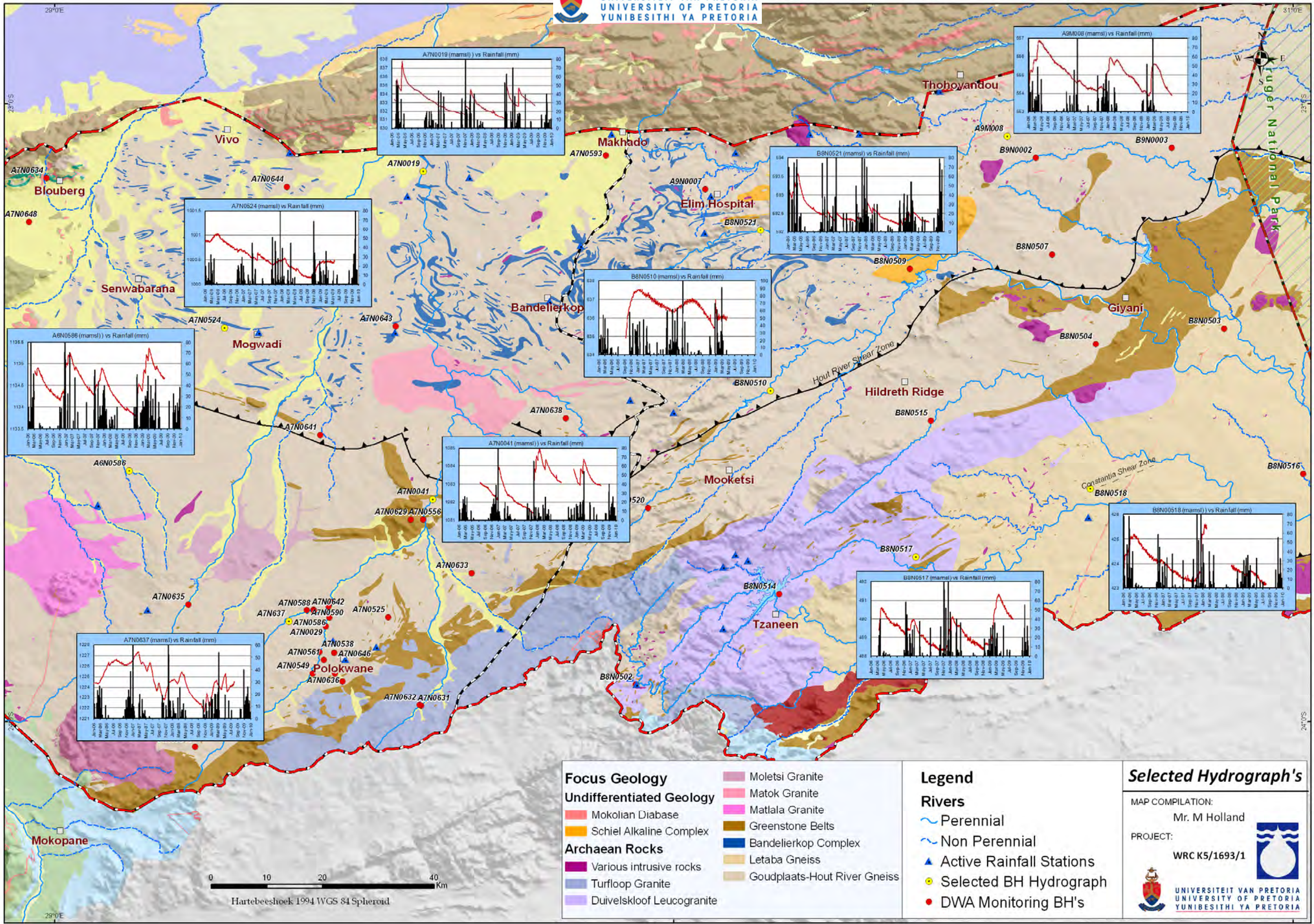
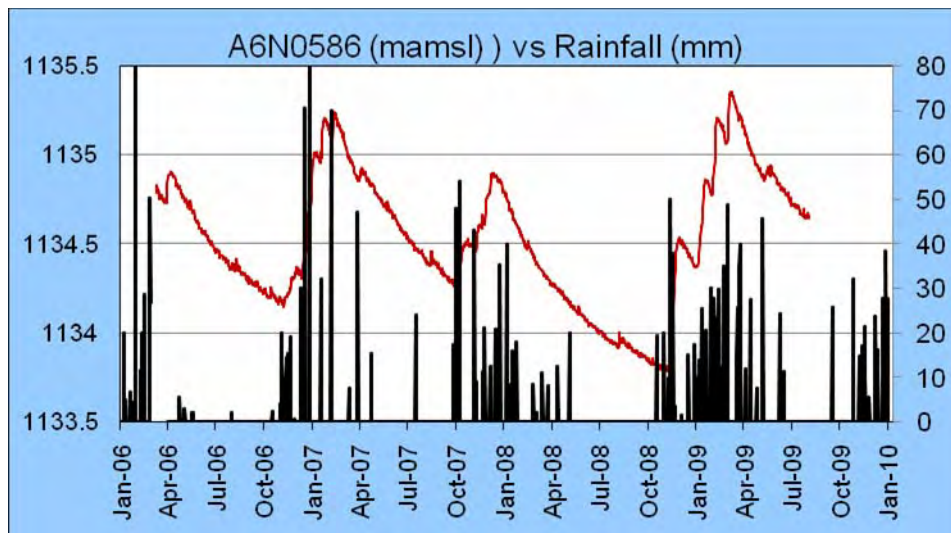


Figure 5.3. Spatial distribution of monitoring boreholes and selected water level hydrographs for the period Jan-06 to Dec-09 (A3 map) (red lines represent daily water levels while black columns represent monthly rainfall).



Generally, groundwater levels fluctuate according to the characteristics of precipitation events (i.e. amount, duration, and intensity) and various hydrogeological variables (i.e. topography, thickness of the unsaturated zone, and matrix composition of saturated and unsaturated materials) (Moon et al., 2004). Groundwater level fluctuations from the observed hydrographs vary between 0.4 and 6.7 m with a mean hydrostatic fluctuation of 3.2 m. Extreme fluctuations of more than 5 m may relate to anthropogenic influences on groundwater levels (i.e. A7N0524 is located near the Mogwadi (Dendron) irrigation groundwater control area).

An indication of the hydrostatic response trends were based on daily water level measurements together with daily rainfall data (Figure 5.3). For comparative purposes all hydrographs were based on a four year period (January 2006 to December 2009). The response of the aquifer to recharge displays well-identified seasonal water-level fluctuations. Therefore, it is expected that during the four year monitoring period, data permitting four distinct recharge periods should be observed. A typical natural hydrograph response for the study area is illustrated in Figure 5.4.



**Figure 5.4. Hydrograph of monitoring station A6N0586 for the period (Jan-06 to Dec-09).**

The Hydrological Year in South Africa is the period from 1 October to 30 September, as the lowest river and spring discharge (base flow) is typically observed at this time. The recession of the groundwater levels generally occurred during the second half of the Hydrological Year, i.e. from Apr/May to October. The following general observations are made:

- Maximum groundwater levels are mostly encountered during February or March.
- The period of groundwater recharge depends on the duration of the rainfall season.
- A three to four month lag is seen between the onset of the rainy season and peak water levels.
- Rapid increases in water levels are associated with extreme single rainfall events, while progressive increases are related to long periods of low intensity rainfall events.
  - During these significant rainfall periods (i.e. 2006/2007 season) groundwater levels increase to above the preceding year's level and the recession period is often reduced considerably.



- A typical exponential water level decline is observed after the rainy season.
- In contrast during below average rainfall periods the succeeding recession period may continue throughout the season with little or no recharge at all (i.e. Figure 5.5).
  - This is also evident in monitoring boreholes A7N0019, B80509 and B80518 (Figure 5.3) for the periods between Jan and March 2007.
- Where a strong relationship between rainfall and water level (aquifer) response exist active recharge occurs.

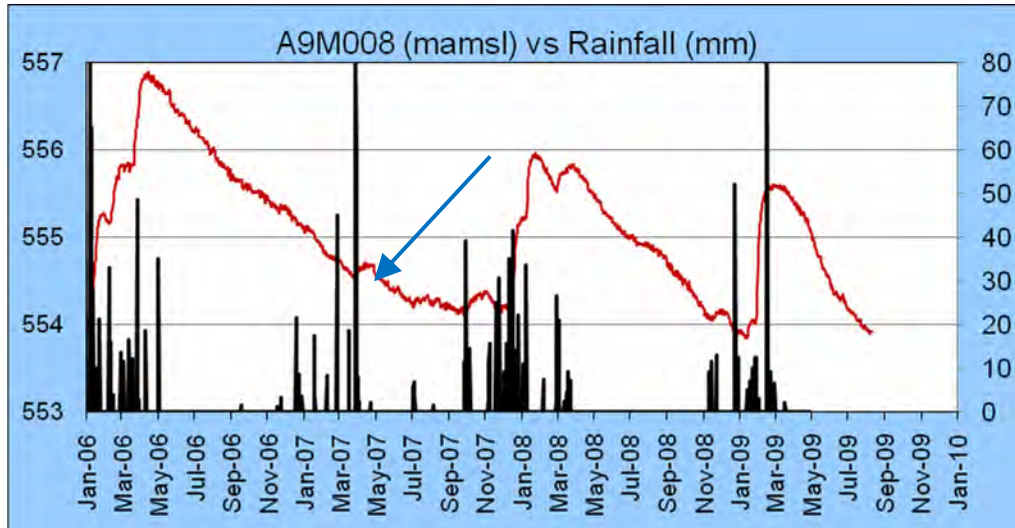


**Figure 5.5. Hydrograph of monitoring station A9M008 for the period (Jan-06 to Dec-09).**

*Impact of rainfall variability on groundwater levels*

The monthly groundwater level fluctuations for selected stations are presented together with the monthly rainfall data from the closest rainfall station in Appendix A. Only 12 monitoring stations cover periods of at least 20 years. Figure 5.6 illustrates monthly groundwater level data versus the annual rainfall departure from the MAP.

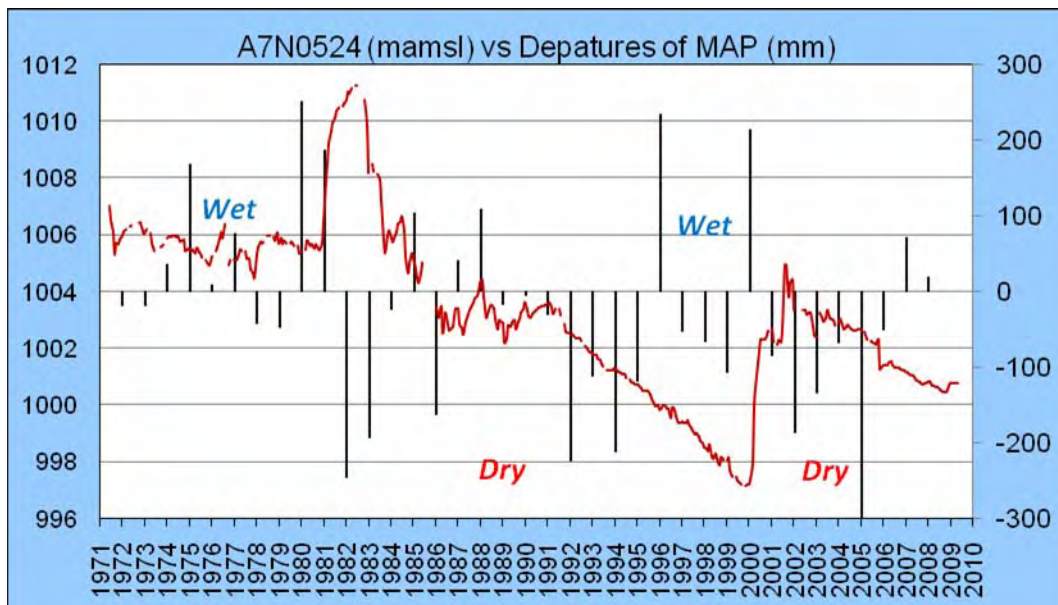


**Figure 5.6. Hydrograph of long term monitoring station A7N0524 near Mogwadi (1971 to 2009).**

According to Meyer (2005) major wet periods was experienced during 1971/72 to 1980/81 and again from 1993/94 to 2002/03, while a major dry period was experienced during 1982/1983 to 1992/1993. The wet and dry cycles have a major impact on groundwater recharge which can be easily distinguished from Figure 5.6.

The monitoring borehole is located approximately 3 km from the Mogwadi (Dendron) irrigation scheme. Jolly (1986) indicated an increase in groundwater abstraction for irrigation from 9 million m<sup>3</sup>/a in 1968 to 21 million m<sup>3</sup>/a in 1986 (no recent estimates are available). Although evidence of over-abstraction is aggravated by below average rainfall, the groundwater level declined by 6 m since the early 1970s. Groundwater levels declined steadily for a decade from 1990 to 2000, despite this being regarded as a wet period. According to Masiyandima (2009) certain management interventions were implemented in the 1990s which together with an above average rainfall for 2000 lead to a recovery of groundwater levels in 2001/2002. Continued decline of the groundwater level suggest that management interventions were not effective in controlling over abstraction. The groundwater level declines are also enhanced by a number of consecutive below average rainfall years and are also evident in monitoring station A7N0549 near Polokwane (Figure 5.7).

Figure 5.8 shows the large variability in rainfall over the last 100 years from the Polokwane rainfall station. There is a good relationship with major wet and dry cycles (11 and 18 years) identified by Meyer (2005) for southern Africa. The last decade can be regarded as the most years with below average rainfall for the entire 104 year record, which will definitely have an influence on groundwater recharge.

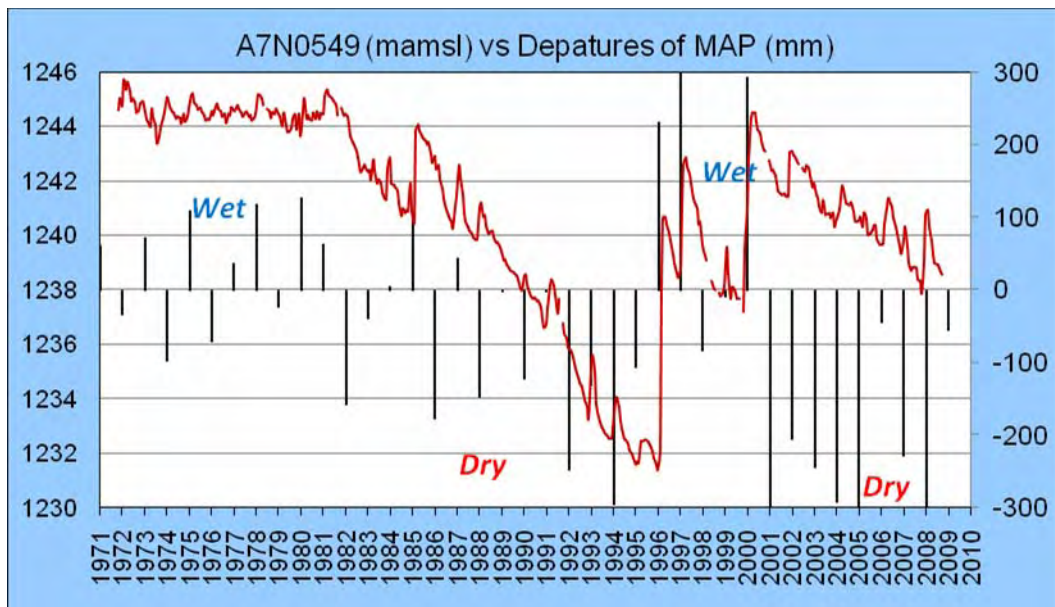
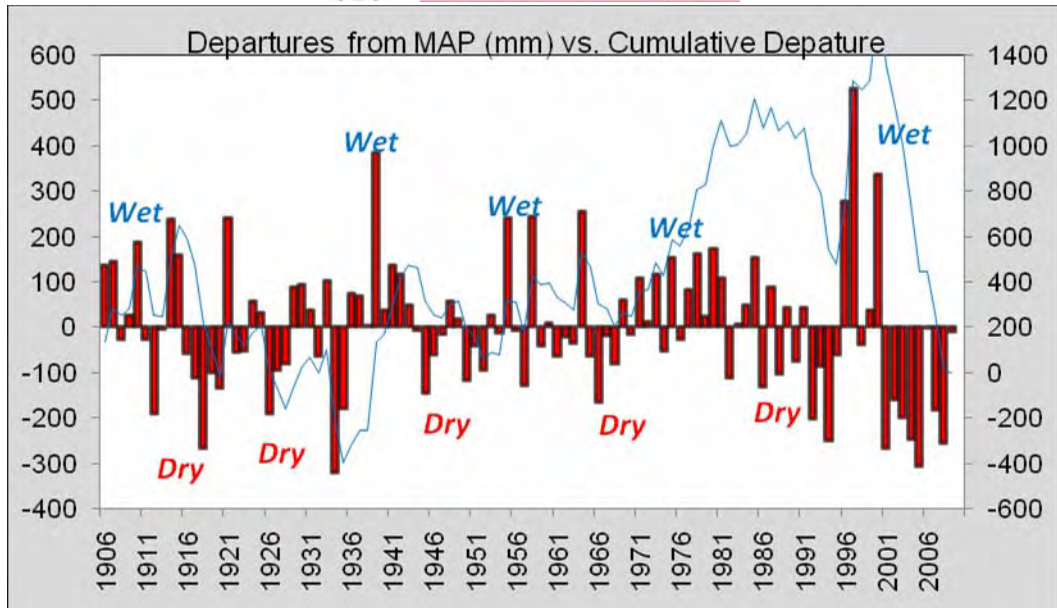


Figure 5.7. Hydrograph of long term monitoring station A7N0549 near Polokwane (1971 to 2009).



**Figure 5.8.** Annual deviation from the average rainfall, together with the cumulative departure for the 104-year rainfall record of Polokwane.

*Cumulative rainfall departure (CRD)*

The recharge excel spreadsheet (developed by Xu and Van Tonder, 2000) is used to simulate recharge for the selected monitoring stations within the study area. The results of the CRD simulations are shown in Appendix B and the recharge estimates obtained based on the results are shown in Table 5.4. Due to the limited period of monitoring the CRD recharge values differ in some cases considerably from the CMB estimates. The CMB method estimates recharge over an extensive period as opposed to the shorter term CRD simulation.

**Table 5.4. Recharge estimations based on the CRD method.**

Site	Station	Date		CRD Recharge	Area Km <sup>2</sup>	CMB Recharge
		Start	End			
Polokwane	A7N0549	Dec-92	Oct-08	1.8 %	20	1.5 %
Thohoyandou	A9M009	Jan-06	Aug-09	2.3 %	12	1.9 %
Nwamitwa	B8N0517	Mar-06	Oct-09	1.7 %	25	2.5 %
Chloe	A6N0586	Mar-06	Aug-09	1.4 %	15	0.4 %
Mara	A7N0019	Mar-06	Aug-09	1.5 %	35	0.9 %
Rosbach	B8N0521	Jan-06	Aug-09	2.5 %	20	7 %

*Groundwater Flow*

Groundwater levels from approximately 360 boreholes were used to construct a groundwater contour map for two areas within the Limpopo Plateau and Letaba Lowveld (Figure 5.9). The potential correlation between the measured head (static water level) and topography (surface elevation) was investigated by cross-plotting the data for each dataset (Appendix C). A very good correlation between the measured head and topography is obvious ( $R^2 = 0.99$ .) The observed correlation is used to improve the interpolation of water levels in data-scarce environments (Bayesian interpolation). In general, the water table is a subdued reflection of the topography.



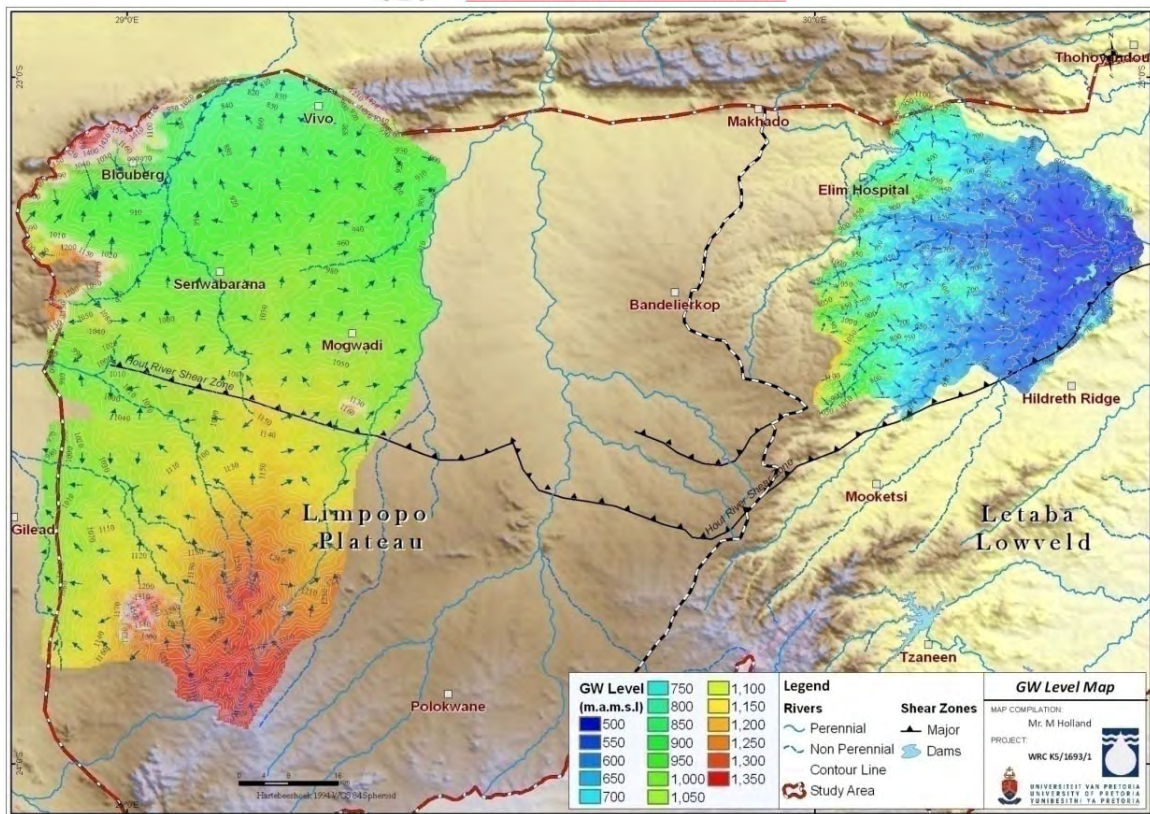


Figure 5.9. Groundwater contour map of two selected areas and derived flow vectors.

## 5.2. Geochemical description

To determine the spatial variation in the groundwater chemistry, a hierarchical cluster analysis (HCA) was applied to classify the large number of analysis into groups that are similar to each other but distinct from other groups (see section 3.3). The relationship of the statistically defined clusters of samples was then related to its geographic location.

### 5.2.1. Interpretation of results

Based on the visual assessment of the rescaled distance in the dendrogram, three distinct hydrochemical clusters were identified for each of the sub-areas (Limpopo Plateau and Letaba Lowveld) (Appendix D). A summary of the chemical data is presented in Table 5.5. The three groups of each sub-area represent trends between the main water types observed in the study area. In gross chemical terms, Group I and V samples are characterised by low mineralisation as indicated by the low electrical conductivity (EC) and a relative enrichment in bicarbonate, attributed to a fresh, recently recharged groundwater. Group II and IV samples show a general increase in mineralisation which is rich in bicarbonate with increasing sodium, potassium and EC concentrations, suggesting groundwater that is actively being mixed. Group III and VI are distinguished by significantly higher chloride, sodium and nitrate content and can be considered as relatively old groundwater at the end of chemical development.



**Table 5.5. Mean values for the clusters distinguished by the hierarchical cluster analysis (EC in mS/m, all other in mg/l).**

Parameter	Limpopo Plateau				Letaba Lowveld			
	Group I	Group II	Group III	TOTAL	Group IV	Group V	Group VI	TOTAL
Nr. of BH's	235	364	208	807	333	196	364	893
pH	8.1	8.2	8.2	8.2	8.1	8.0	8.1	8.1
EC	67.7	119.0	283.4*	146.4	73.8	41.4	196.8*	116.8
Na	75.3	119.6	301.0*	153.5	53.3	26.7	209.5*	111.1
Ca	33.2	54.2	119.5	64.9	42.6	28.9	83.7	56.4
Mg	25.5	50.5	108.8	58.2	41.1	17.6	80.8	52.1
K	5.0	12.5	14.6	10.8	3.9	1.6	5.5	4.0
HCO <sub>3</sub>	309.0	399.4	469.5	391.2	346.3	195.7	519.0	383.7
SO <sub>4</sub>	15.2	29.8	99.8	43.6	14.6	6.3	47.8	26.3
Cl	46.4	155.0	614.3*	241.7*	52.2	22.3	326.7*	157.5
NO <sub>3</sub>	19.7	37.1	64.4*	39.1	20.0	6.9	58.4*	32.8
F	0.7	0.4	0.7	0.6	0.4	0.4	0.7	0.5
TDS	535.6	866.1	1802.3*	1011.2*	580.6	309.2	1342.5*	831.5
Dominant Facies	Na-HCO <sub>3</sub>	Na-Mg-HCO <sub>3</sub>	Na-Cl	-	Mg-HCO <sub>3</sub>	Ca-Mg-HCO <sub>3</sub>	Na-Cl, Na-Mg-HCO <sub>3</sub>	-

\*- Within maximum allowable limits for drinking water in South Africa (SANS 2006).

As a result the dominant water types in Limpopo Plateau vary from a Na-HCO<sub>3</sub> to a Na-Mg-HCO<sub>3</sub> and Na-Cl groundwater facies and are explained as follows:

- The direct infiltration of Ca-HCO<sub>3</sub> dominated rainwater (Table 5.6) which evolved to a Na-HCO<sub>3</sub> facies due to the replacement of calcium by sodium through cation exchange in the aquifer matrix or alternatively due to the weathering of albite to kaolinite in the crystalline rocks, releasing sodium and bicarbonate.
- The Na-Cl facies is a result of prolonged residence and fluid-rock interaction times in the subsurface in areas of discharge (i.e. alluvium along rivers) or low recharge and also towards the foothills of the Blouberg Mountains (Figure 5.10).

**Table 5.6. Chemical composition of rainfall within the study area (EC in mS/m, all other in mg/l).**

Site	Mufeba (UP1)	Rawesi 2 (UP3)	Rawesi (UP3)	Rawesi 2 (UP3)	Bochum (UP2)
Date	03-Mar-09	09-Mar-09	15-Mar-09	15-Mar-09	15-Mar-09
pH	5.9	6.4	5.8	7.26	7.08
EC	0.84	4.18	0.45	5	3
Na	0.8	0.5	0.4	0.3	0.05
Ca	0.5	2.3	0.5	1.55	0.7
Mg	0.1	0.3	0.2	0.25	0.08
K	0.4	0.6	<0.1	0.81	0.2
HCO <sub>3</sub>	6	24	6	19.2	12.12
SO <sub>4</sub>	1.1	3.7	1.4	2.74	1.13
Cl	1	2.1	1	1.77	0.69
NO <sub>3</sub>	0.3	0.9	1.2		
Facies	Na-Ca-HCO3	Ca-HCO3-SO4*	Ca-HCO3-SO4-Cl*	Ca-HCO3-SO4*	Ca-HCO3
EN %	-22	-52	-41	-52	-66

\*- Bulk rainfall sample may be polluted.

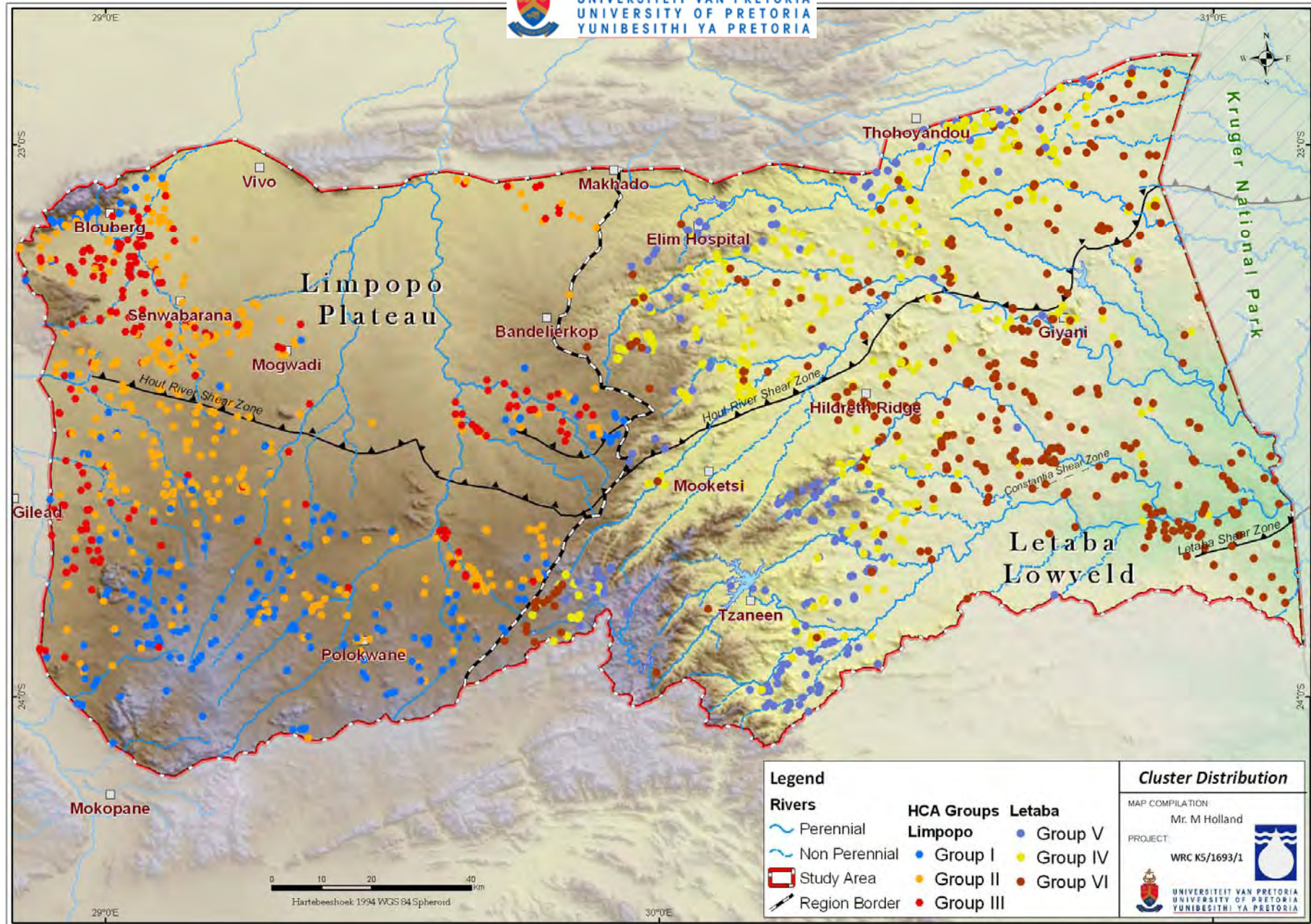


Figure 5.10. Spatial distribution of the hydrochemical groups identified by the HCA.



Groundwater in the Letaba Lowveld is generally a fresher Mg-HCO<sub>3</sub> facies (in comparison with the Limpopo Plateau), with a recognizable pattern of elevated mineralization with reduced precipitation/recharge. The dominant Mg-HCO<sub>3</sub> may be explained by the abundance of ferromagnesian minerals present within the rocks of the area, by ion exchange processes or the precipitation of calcite ( $SI_{\text{calcite}} = 0.8$ ). The water chemistry appears to evolve from a Ca-Mg-HCO<sub>3</sub> towards a Na-Cl predominance. The direction of this trend is consistent with increasing specific conductance and groundwater flow, (see Figure 5.9) which is generally related to the relative age and the length of the groundwater flow paths. The high degree of spatial and statistical coherence (Figure 5.10) supports the regional hydrochemical model, where changes in water chemistry are a result of increasing rock-water interactions along hydrological flow paths.

### 5.2.2. Discussion of stable isotope data

The isotopic ratios ( $\delta D$  and  $\delta^{18}O$ ) of groundwater samples for each region within the study area are plotted in Figure 5.11, relative to the global meteoric water line (GMWL). A number of boreholes plot between the GMWL and a hypothetical local meteoric water line (LMWL) (including the single rainfall sample collected), suggesting that recharge seems to take place rapidly, possibly via preferred pathways in higher lying areas preventing any significant evaporation. Although not very distinct some samples are enriched in their heavy isotopic content due to significant kinetic (non-equilibrium) evaporation, suggesting evaporative losses of rainwater before infiltration. Thus, the recharge of partially evaporated water takes place in this area. There is also a distinct difference between groundwater samples observed between regions, clearly indicating the influence of more local rainfall regimes. Unfortunately not enough isotope rainfall data is available to reflect the particular rainfall selectivity between the four regions. The spatial setting of boreholes sampled for isotopes is presented in Figure 5.12.

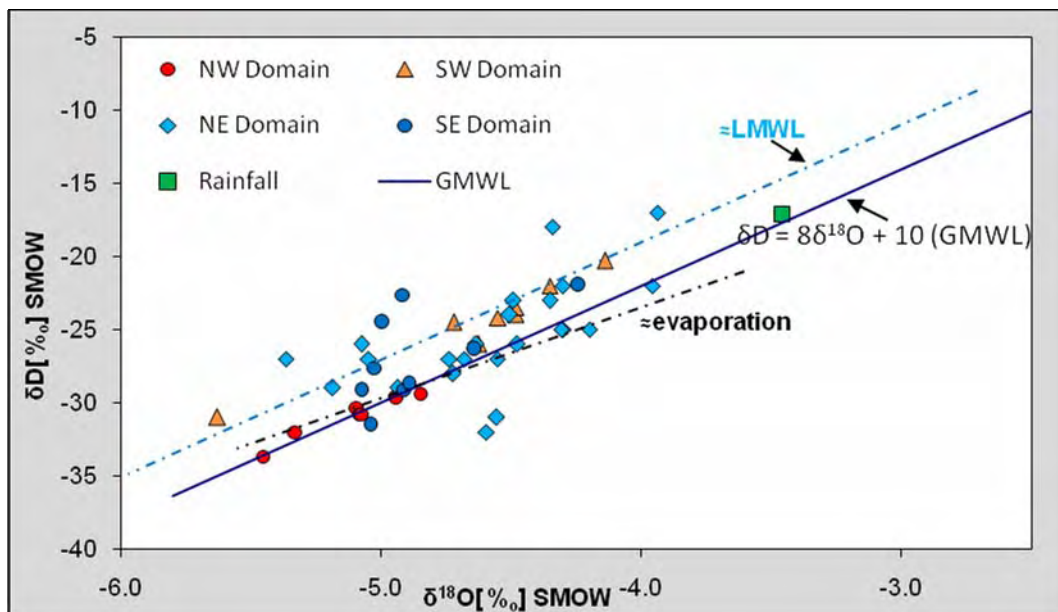


Figure 5.11. Groundwater and precipitation isotopic compositions, depicted with the GMWL.

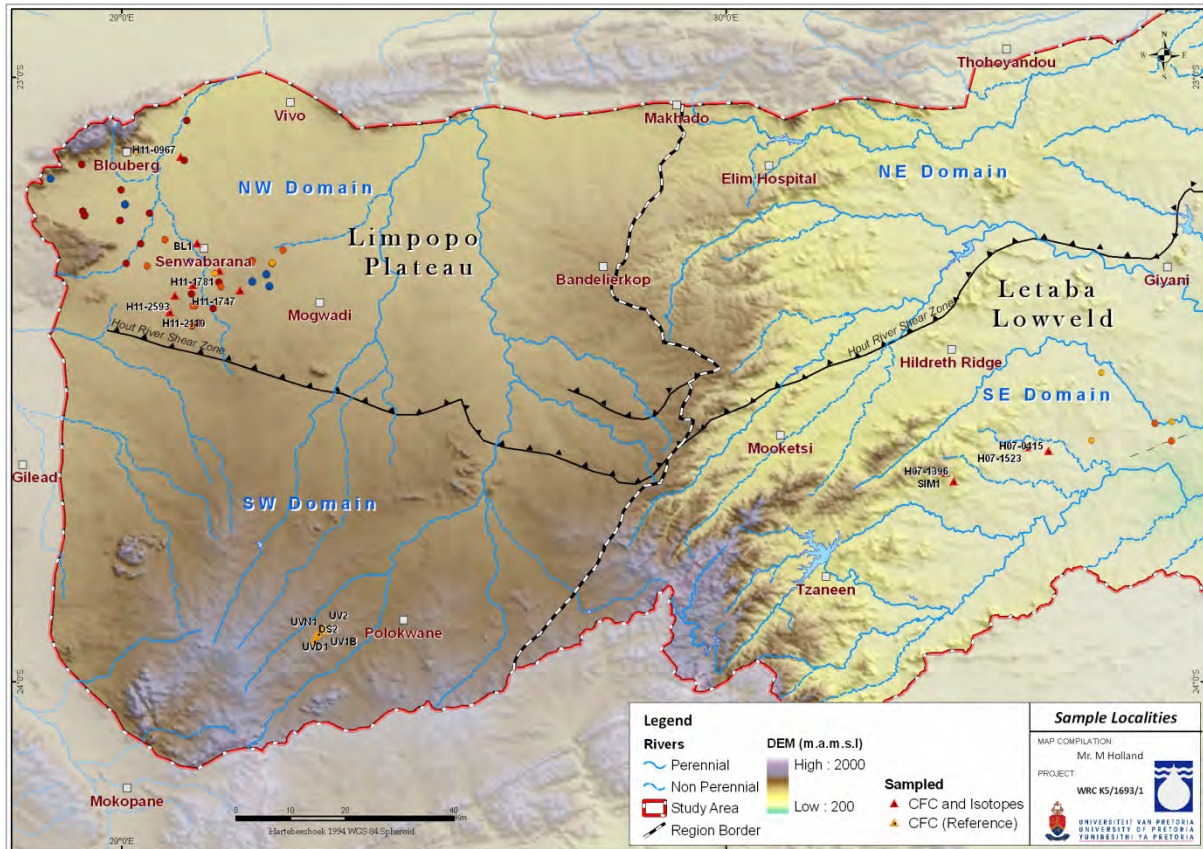


Figure 5.12. Location isotope groundwater samples.

### 5.2.3. Groundwater dating

#### *Radiocarbon and tritium*

The majority of  $^{14}\text{C}$  samples plot between 85 and 95 pMC and the  $\delta^{13}\text{C}$  between -5 and -7‰ (Figure 5.13). The  $^{14}\text{C}$  content does not vary significantly and is consistent with that of very recent water that has only been slightly diluted with dissolved carbonate. Initial  $^{14}\text{C}$  concentrations of 80 and 90% was suggested by Verhagen et al., 2009 for the Bochum (Senwabarwana) area and Talma and Weaver (2003) used an initial  $^{14}\text{C}$  of 85-100% for the Leeukuil area 10 km west of Polokwane. One sample from Region D shows an increase in  $\delta^{13}\text{C}$ , evidence of ongoing isotope exchange or dilution processes with aquifer material, but the bulk of the samples Region B and D are within -9 and -12‰, which may be a reflection of the grassland vegetation in the area. Generally, these samples have  $^{14}\text{C}$  values that have similar trends to the bulk of the samples, suggesting that there has been no major dilution of  $^{14}\text{C}$  which affects relative ages or residence times.



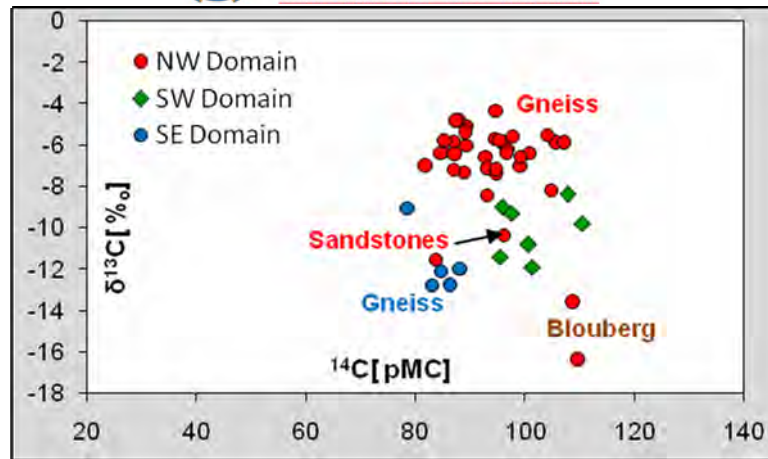


**Figure 5.13.** Scatter-plot of  $\delta^{13}\text{C}$  and against  $^{14}\text{C}$  for all samples.

A plot of  $^{14}\text{C}$  against  $^3\text{H}$  together with the inferred MRT values calculated by the exponential mixing model by Verhagen (2000) is shown on Figure 5.14. The  $^{14}\text{C}$  values can be interpreted as ground water mean residence times ranging from a few decades up to about 1 000 years, implying fairly rapidly turned-over ground water.

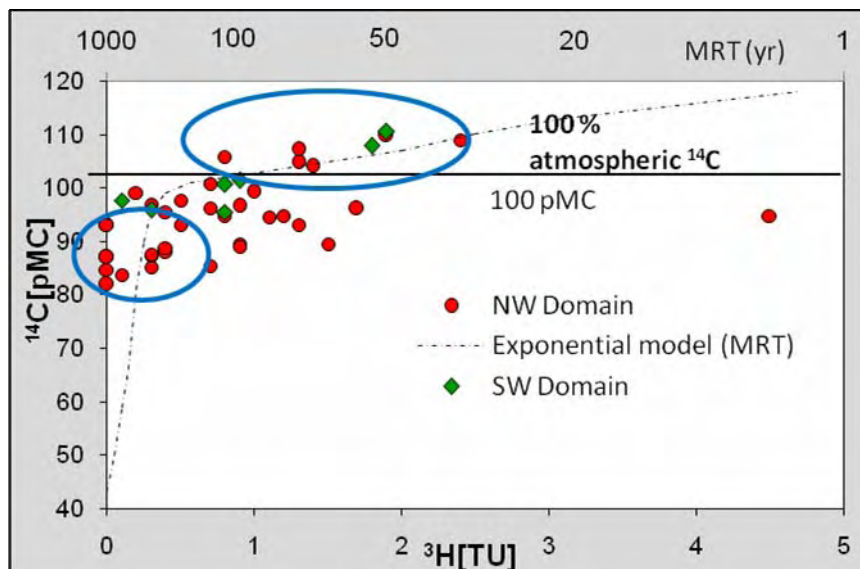


**Figure 5.14.** Scatter-plot of  $\delta^{13}\text{C}$  and against  $^3\text{H}$ . Also shown are plots of expected exponential model values for  $\delta^{13}\text{C}$  and  $^3\text{H}$  showing mean residence time (MRT) (Adapted from, Verhagen, 2000).

Groundwater radiocarbon values of  $> 100$  pMC can be interpreted as falling in the thermonuclear era, i.e. recharged over the past three and a half decades. In this time-span, interpretations can be constrained further by tritium. Many radiocarbon values of  $> 100$  pMC accompanied by tritium  $> 1$  TU may be ascribed to post-1963 (thermonuclear) recharge. Another group of samples with values of  $^{14}\text{C} < 90$  pMC and  $^3\text{H} < 1$  TU represent older water with an approximate mean residence time of between 500 and 1000 years. Tritium samples with no radiocarbon analysis proved futile

in determining ages of groundwater, since tritium values did not exceed 3 TU representing a mixture of old and recent water (pre- and post bomb testing) (Figure 5.15).

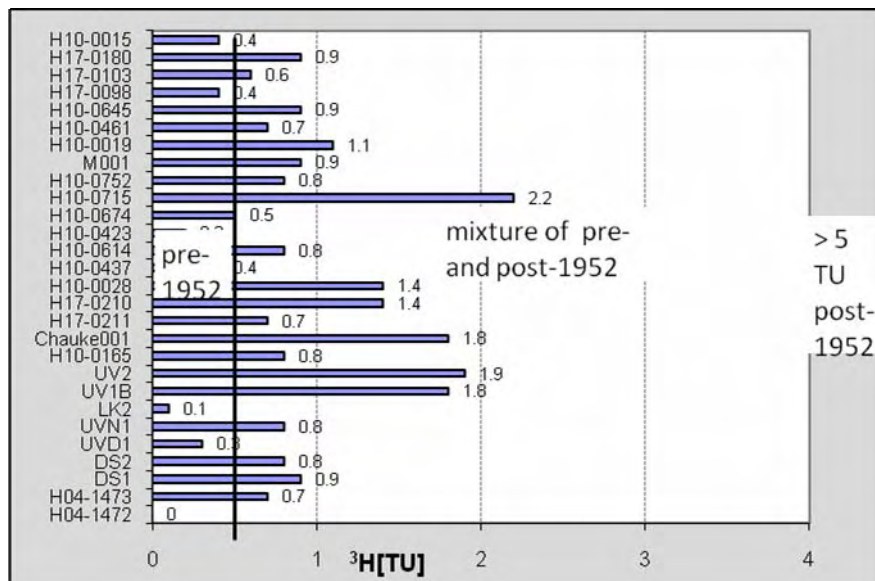


Figure 5.15. Results of tritium.

### Chlorofluorocarbons

It is important to note that only a limited number of CFC samples could be taken and results should be seen as the basis for future CFC applications in the Limpopo basement aquifers. Table 5.7 shows the concentrations of CFCs, SF<sub>6</sub> and selected chemical parameters found in each of the boreholes. Samples for this investigation were collected from boreholes in the NW and SE domain within quaternary catchment A72A and B81F respectively (Figure 5.16).

Table 5.7. Chemical composition of rainfall within the study area.

Region	Site	CFC-12 (pmol/l)	CFC-11 (pmol/l)	SF <sub>6</sub> (fmol/l)	Cl (mg/l)	NO <sub>3</sub> (mg/l)	Elevation (mamsl)	Air Temp*
NW Domain	H11-0967	0.93	1.33	0.69	140	51.6	893	19.5
	BL1	0.51	1.23	0.98	239	43	975	19.5
	H11-1781	0	0.06	3.57	243	12.9	1018	19.5
	H11-1535	1.43	0.26	0.82	188	47.3	1023	19.5
	H11-2593	0.39	0.56	1.02	242	26.2	1045	19.5
	H11-1747	0.13	0.09	0.1	185	18.1	1060	19.5
	H11-2110	0.2	0.14	0.29	224	21.9	1060	19.5
SW Domain	UV2 <sup>#</sup>	0.3	0.15	-	67	28.4	1320	18.5
	UVN1 <sup>#</sup>	0.07	0.03	-	28	16.8	1321	18.5
	UVD1 <sup>#</sup>	0.07	0.01	-	28	3.9	1325	18.5
	UV1B <sup>#</sup>	0.62	0.3	-	50	18.1	1331	18.5
	DS2 <sup>#</sup>	0.3	0.1	-	26	10.8	1338	18.5
	LK2 <sup>#</sup>	0.26	0.13	-	62	21.9	1340	18.5
	DS1 <sup>#</sup>	0.27	0.14	-	23	52.5	1386	18.5
SE Domain	H07-0415	0.14	0.3	0.1	228	43	492	20.5
	H07-1523	0.01	0.45	0.25	169	275.2	521	20.5
	H07-1396	0.64	0.21	0.1	33	0.9	700	20.5



	SIM1	1.18	1.59	1.28	12	6.9	840	20.5
--	------	------	------	------	----	-----	-----	------

# - Samples captured from Talma and Weaver (2003).

\*- Mean annual temperature of recharge location.



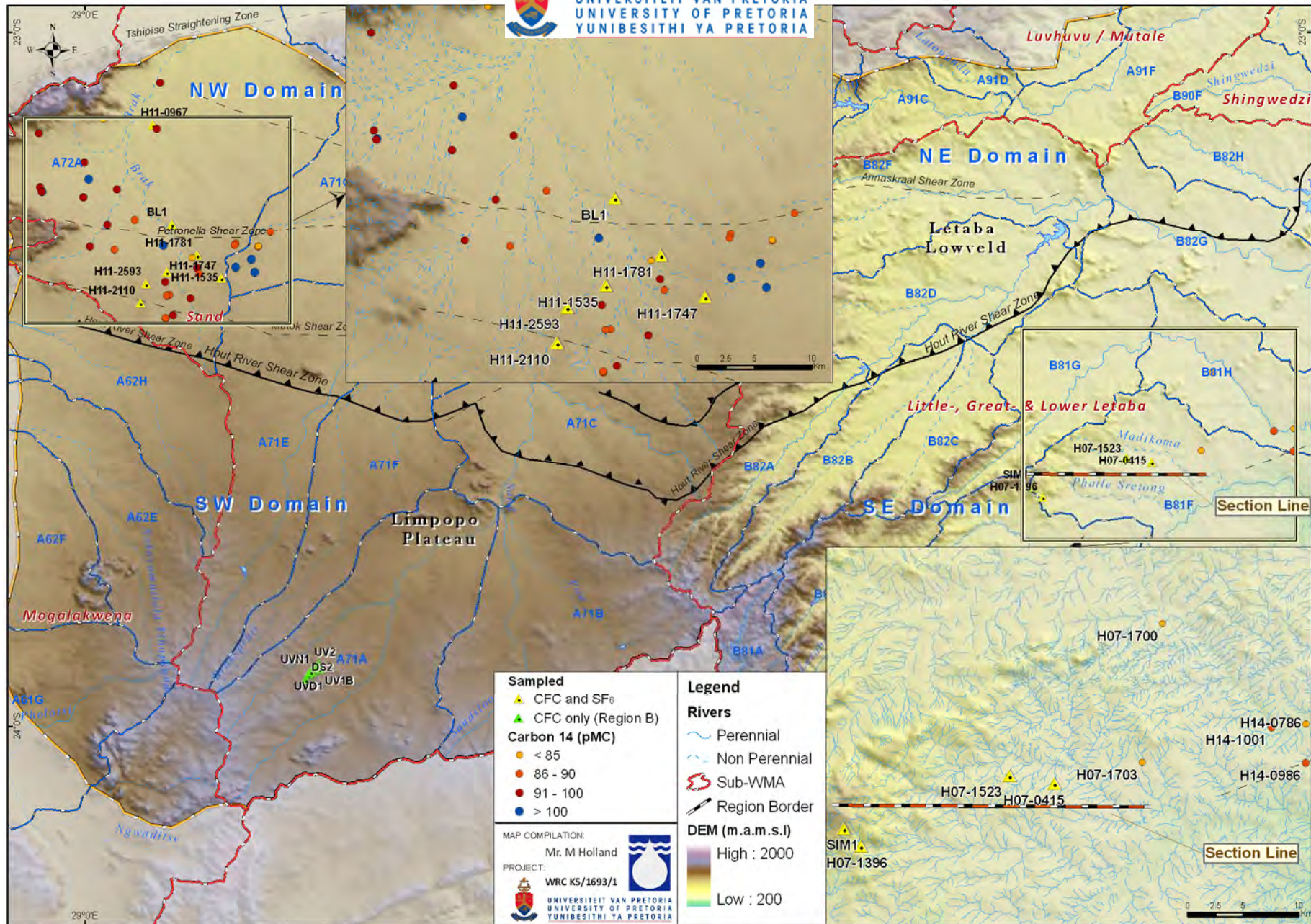


Figure 5.16. Spatial distribution of CFC samples together with carbon 14 samples.



Modern air saturated water at 10°C is calculated to have a concentration of 2.97 pmol/L for CFC-12, 5.40 pmol/L for CFC-11 and 2.3 fmol/L for SF<sub>6</sub> (IAEA, 2006). All groundwater samples fit within these guidelines except sample H11-1781 with a SF<sub>6</sub> concentration above modern atmospheric concentrations, suggesting a sampling or analysis error, or some natural or anthropogenic addition of SF<sub>6</sub>. Theoretical variations in the concentrations of CFC-11 and CFC-12 were constructed using cases of piston flow and binary mixing (Figure 5.17).

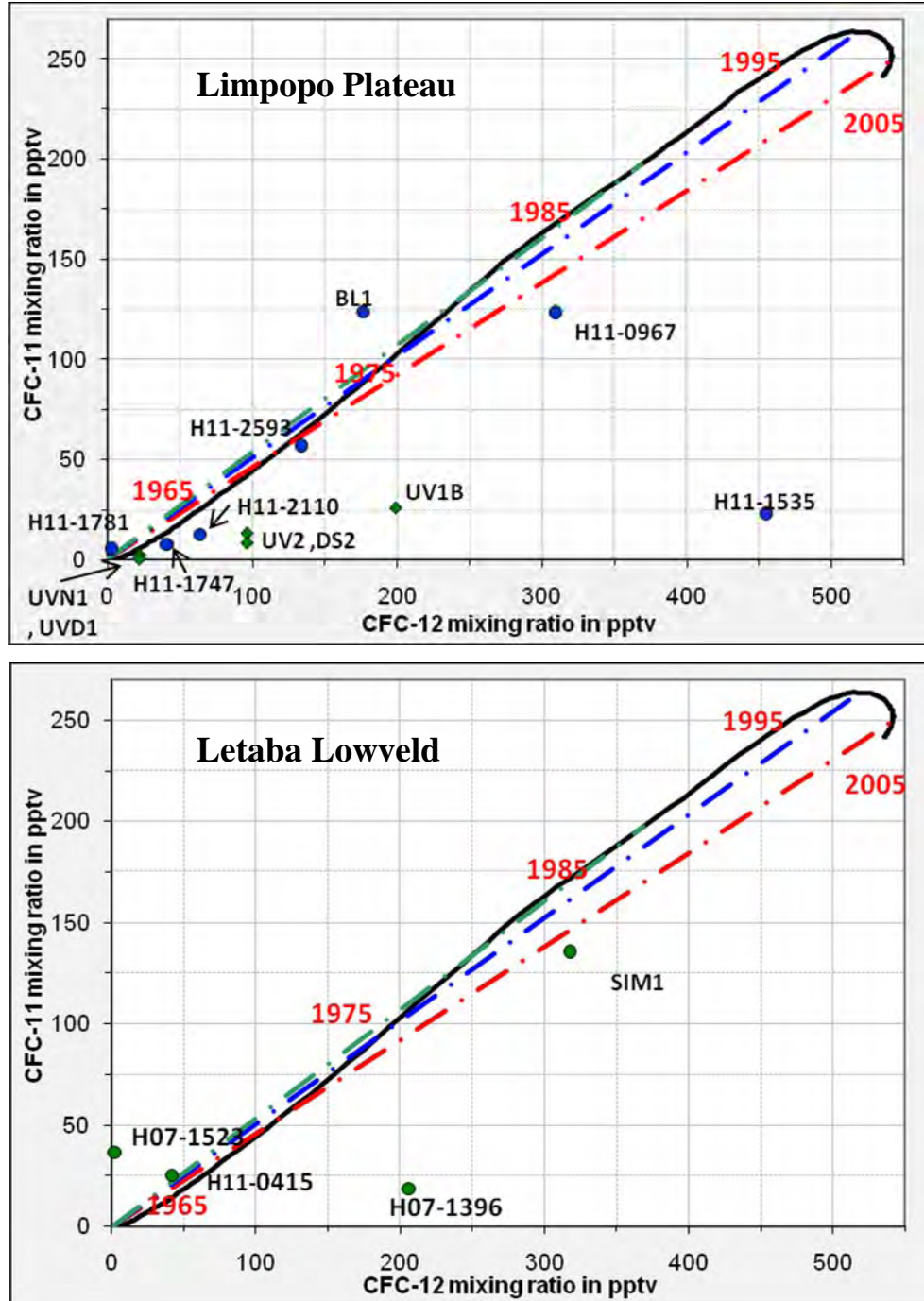
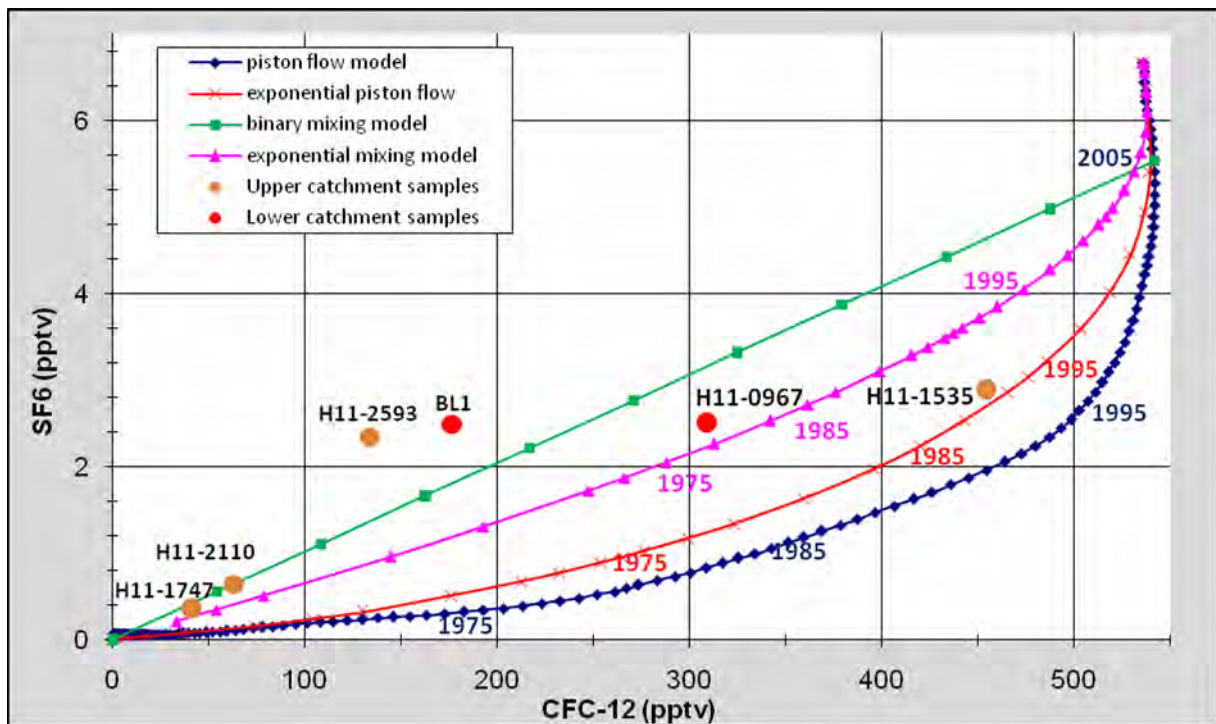


Figure 5.17. Tracer plots comparing CFC-11 and CFC-12 concentrations for southern hemisphere air. The solid lines represent unmixed (piston) flow with selected apparent ages ('1985'). The dashed line shows one example of binary mixing for the case of water recharged in 1985, 1995 and 2005 diluted with old, CFC-free water.

The region bounded by the CFC input function (solid line) and the mixing line represents the range of CFC-11 and CFC-12 concentrations that can be expected in waters if air–water equilibrium and mixing with old, CFC-free water account for the observed variations in CFC concentrations. Samples plotting outside the region bounded by piston flow and binary mixing (see, for example, H07-1396, H11-1535 and UVB1) have been affected by other processes such as contamination, degradation or an introduction of excess air that have altered the CFC concentrations from air–water equilibrium values. These lower CFC-11/CFC-12 ratios are most likely due to degradation of CFC-11 and have been observed in some studies (i.e. Bockgård et al., 2004). CFC-11 and CFC-12 have similar input data curves which doesn't allow for differentiation between exponential binary and piston flow. In contrast, Figure 5.18 shows SF<sub>6</sub> versus CFC-12 plot for the Limpopo Plateau samples.



**Figure 5.18.** CFC-12 and SF<sub>6</sub> groundwater data overlaid on the ideal mixing model curves. Samples categorised as upper or lower catchment (quaternary drainage A72A) (Figure 5.16).

A number of samples plot outside the region bounded by piston flow and binary mixing (2002 to pre-CFC) (see, for example, H11-2593, BL1) and may have been affected by SF<sub>6</sub> contamination. All other samples plot within the region bounded by the binary mixing model and piston flow model. The boreholes that were sampled are essentially in the upper Brak River catchment (A72A) with two samples in the middle and lower parts of the catchment (BL1 and H11-0967). The youngest sample H11-1535 (apparent age of 20 years, 1990) is located up gradient of these samples. It is expected that the upper catchment represent younger water related to more recent recharge events. From previous discussions it seems that this sample may have been contaminated by CFC-12 (see, Figure 5.17). However, a number of samples (H11-2110 and H11-1747) in the upper catchment consist of apparent ages of 45 to 50 years and plot between the BMM and EMM curve. Despite the high SF<sub>6</sub>/CFC-12 ratio in samples H11-2593 and BL1, these boreholes are

down gradient from each other and have an apparent age of 35 and 40 years. The sample (H11-0967) in the lower catchment plot close to the EMM curve and have an apparent age of 30 years (1980).

Based on the results the direction of inferred flow lines based on the groundwater gradient (see section, 5.1.2) does not coincide with the direction of increasing water age. Samples from quaternary drainage A72A present a complex chemical model with highly mineralised water, with no clear flow regime suggesting a highly heterogeneous system with a number of likely flow paths (i.e. recent recharge from fractures exposed to the surface or high lying areas; old groundwater from river losses or diffuse flow). This is clearly illustrated in a correlation plot of apparent age vs. elevation in Figure 5.19 where high lying areas does not necessarily relate to younger age. In contrast CFC samples from the south-eastern domain (quaternary drainage B81F) indicate that younger waters are related to higher lying areas while older sample are related to lower lying areas (Figure 5.19). It must be highlighted that these samples do not relate to an identified flow path but rather indicate the variations observed between the higher and lower lying samples.

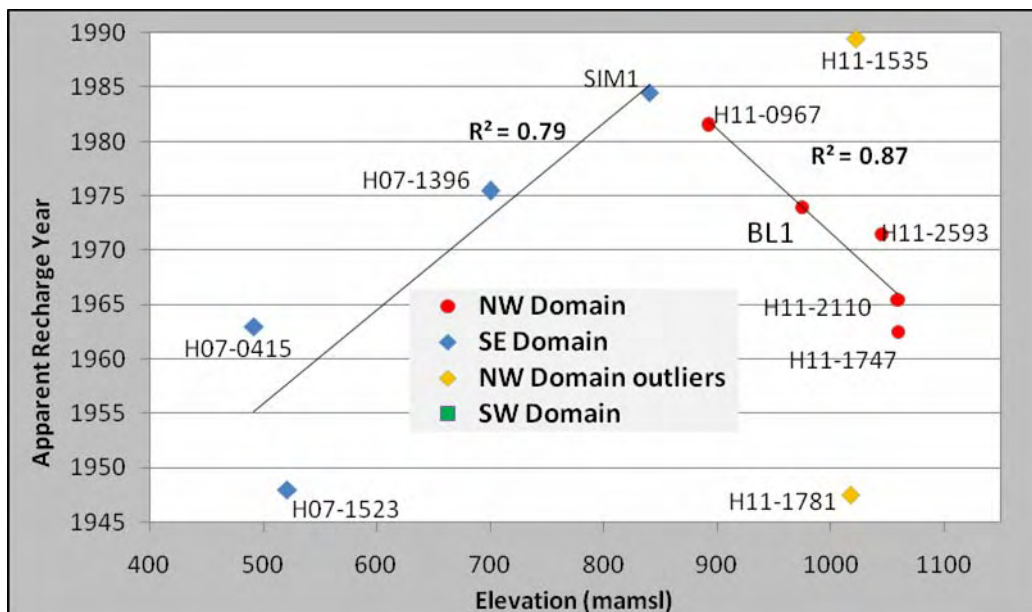


**Figure 5.19. CFC-12 and SF6 groundwater data overlaid on the ideal mixing model curves. Selected sites have been labelled**

Generally samples representing the upper catchment (SIM1 and H07-1396) lie close to the exponential piston- and piston flow models (Figure 5.20). These samples are located on the Tzaneen escarpment with an apparent age of 25 years (1985) and 35 years (1975) respectively. In the low reaches of the catchment sample H07-0415 is much older with an apparent age of 45 years (1965), while sample H11-1523 has a CFC-12 concentration below detection limit and is therefore pre-CFC age. These samples may indicate exponential mixing suggesting mixing between the old groundwater and modern water from recent recharge.



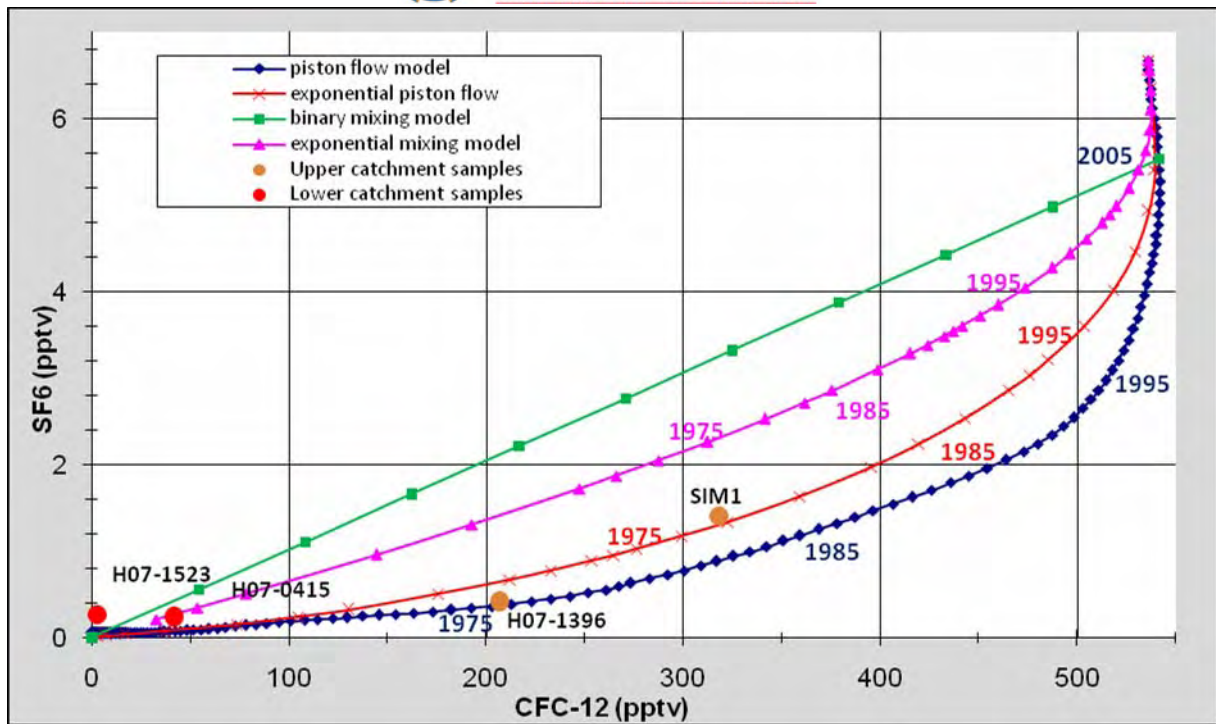


**Figure 5.20. CFC-12 and SF6 groundwater data overlaid on the ideal mixing model curves. Selected sites have been labelled.**

Ideally flow paths should have been identified and sampled; however, in this case the sparse distribution of samples allows us only to infer a regional concept of groundwater flow regimes from the higher to lower lying areas (Figure 5.21). The model suggest that deeper groundwater, recharged from higher lying unconfined conditions (i.e. Tzaneen escarpment) moves down gradient from under (semi-)confined conditions towards low lying discharge areas. Loosing ephemeral rivers may lose evaporative younger water to the older groundwater system in the area, especially along drainages incised into the basement rock with a thin or absent alluvium and/or regolith layer.

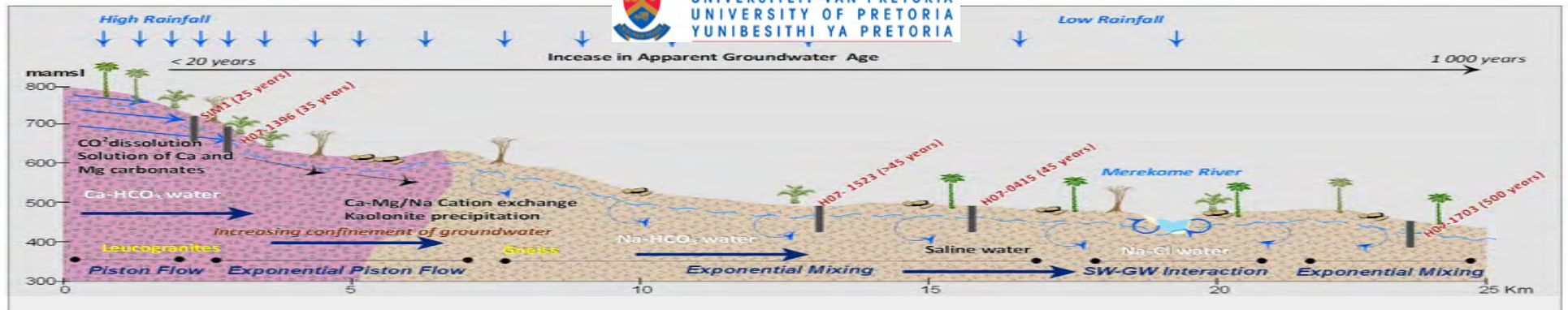


Figure 5.21. Cross-section of the hypothetical hydrochemical model for the Merokome River catchment (B81F) (Section line illustrated in Figure 5.16). Based on the CFC and carbon 14 results.

#### 5.2.4. Groundwater quality hazards

Table 5.8 presents the overall drinking guideline classification of the major ion chemistry of the Limpopo Plateau and Letaba Lowveld basement aquifer region under investigation. Results show that many rural groundwater supplies exceed the acceptable limits for drinking water.

**Table 5.8. Potability classification of the area of investigation (EC in mS/m, all other in mg/l).**

SANS 241:2006	EC	Ca	Mg	Na	K	SO <sub>4</sub>	Cl	NO <sub>3</sub> as N	F	
Class I Rec. operational Limit	< 150	< 150	< 70	< 200	< 50	< 400	< 200	< 10	< 1	
Class II Max. allowable limited	150- 370	150- 300	70- 100	200- 400	50- 100	400- 600	200- 600	10-20	1-1.5	
Exceeding Class II (Consumption period)	7 years									1 year
<b>Limpopo Plateau</b>										
	EC	Ca	Mg	Na	K	SO <sub>4</sub>	Cl	NO <sub>3</sub> as N	F	TDS
Class I	70%	94%	75%	85%	99%	99%	73%	54%	87%	96%
Class II	26%	4%	15%	11%	1%	0%	20%	27%	5%	0%
> Class II	4%	2%	9%	4%	0%	1%	6%	19%	8%	4%
<b>Letaba Lowveld</b>										
	EC	Ca	Mg	Na	K	SO <sub>4</sub>	Cl	NO <sub>3</sub> as N	F	TDS
Class I	75%	95%	72%	87%	100%	99%	78%	53%	88%	95%
Class II	19%	3%	12%	8%	0%	0%	14%	14%	4%	0%
> Class II	6%	2%	16%	6%	0%	1%	8%	33%	8%	5%

The most noticeable elements of concern for water consumption are nitrate (measured as nitrogen (N)) and fluoride. In addition, several samples show major ion concentrations (i.e. Mg, Na, Cl) and subsequently electric conductivities beyond acceptable limits. This can mostly be related to evaporative concentration of elements in discharge areas or due to low recharge values as well as long residence times for selected samples. According to Marais (1999), the single most important reason for groundwater sources in South Africa being declared unfit for drinking is nitrate levels exceeding 10 mg/l (as N). The main inputs of nitrate to groundwater in rural environments are derived from anthropogenic activities such as inappropriate on-site sanitation and wastewater treatment, improper sewage sludge, drying and disposal, and livestock concentration at watering points near boreholes. The extensive occurrence of nitrate in groundwater in uninhabited regions (see Appendix E) suggest non-anthropogenic sources possibly related to evaporative enrichment of dry and wet deposition, biogenic point sources through N-fixing organisms, or to a geogenic origin (Tredoux and Talma, 2006). In contrast to nitrate, the occurrence of fluoride is primarily



controlled by geology and climate. Therefore, there are no preventative measures under the given spatial limits of water supply to avoid contamination.

Heterotrophic bacterial counts are used to indicate the general microbiological quality of water, i.e. the amount of bacteria present in the water. The total coliform bacteria count, which includes bacteria from the faecal group, is an indicator of the general sanitary quality of the groundwater, with many of these bacterial colonies originating potentially from an aquatic environment. The total faecal coliform bacteria count, which is related to human or animal faecal pollution, refers to probable faecal pollution of water. The presence of coliform bacteria implies the potential presence of waterborne pathogens (DWAF, 1996). According to the Department of Water Affairs' water quality guidelines (DWAF, 1996) for domestic use, the total heterotrophic bacterial plate count of all groundwater samples from both areas indicates a slight or increased risk of bacterial infection and infectious disease transmission. Fourteen groundwater samples show a significantly increased risk for infectious disease transmission according to the total coliform bacterial range and two samples indicates a significant risk for faecal coliform and e.coli (Table 5.9).

**Table 5.9. Microbiological analyses for all samples collected.**

Allowable compliance contribution (DWAF, 1996)*				
95% min.	100	Not detected	Not detected	Not detected
4% min.	1 000	10	1	Not detected
1% min.	10 000	100	10	1
Sample	Heterotrophic count/ml	Total Coliform count/100ml	Faecal Coliforms count/100ml	E.Coli count/100ml
Nr of Samples	51	19	10	10
Compliance 4% min.	45	4	5	5
Compliance 1% min.	11	14	2	2

\* The allowable compliance contribution shall be at least 95% to the limits indicated with a maximum of 4% and 1% respectively.

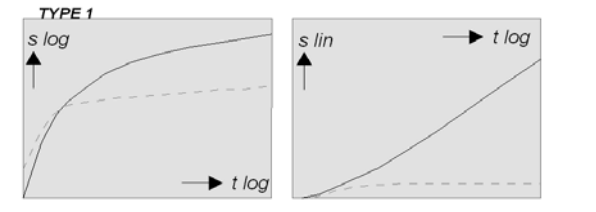
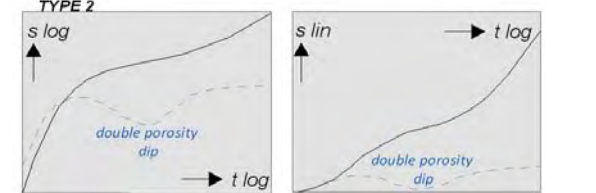
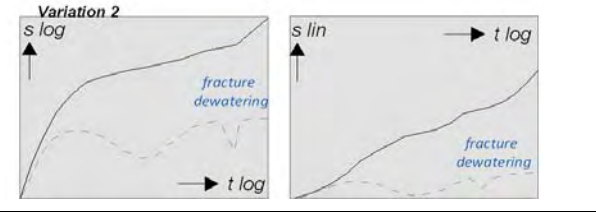
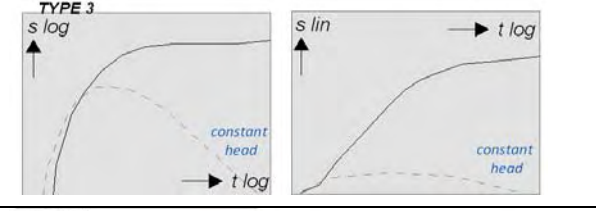
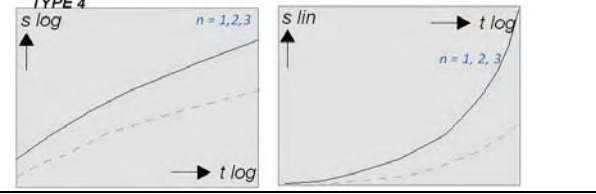

### 5.3. Pumping test analysis

#### 5.3.1. Aquifer response classification

Due to the intrinsic difficulty in identifying an appropriate theoretical model that fits the observed pumping test data, a classification scheme based on the typical drawdown behaviours encountered in the study area was identified. The observed datasets (2 359 boreholes) were visually compared to a set of typical diagnostic plots as discussed in section 3.4.2 in order to identify which model can be used to best interpret the data. The schematic diagnostic plots of the typical drawdown behaviours identified for the study area basement lithologies are conceptualised in Table 5.10.



**Table 5.10. Most typical diagnostic plots encountered in the Basement aquifers under investigation.**

<p>TYPE 1: Theis model (infinite two-dimensional confined aquifer) – Approximate straight line type</p> <p><b>387</b> boreholes (16 % of all BH's)</p>	
<p>TYPE 2: Double porosity or unconfined porous aquifer – approximate S-type</p> <p><b>568</b> boreholes (24 % of all BH's) (80 % have distinct double porosity dip)</p>	
<p>Variation 2: Fracture dewatering - Stepwise drawdown</p> <p><b>514</b> boreholes (22 % of all BH's) (87 % have distinct double porosity dip) (54 % suggest dewatering of fractures)</p>	
<p>TYPE 3: Constant-head or leaky aquifer – Drawdown stabilizes</p> <p>May also represent too low pumping rates or too short duration to stress the aquifer</p> <p><b>569</b> boreholes (24 % of all BH's)</p>	
<p>TYPE 4: Single fracture or general radial flow (GRF) model – Steepening of drawdown response</p> <p><b>106</b> boreholes (4% of all BH's)</p>	
<p>TYPE 5: Porous aquifer with limited extent (closed reservoir)</p> <p>Boundary conditions is distinct in this group but may be observed in all of the above</p> <p><b>215</b> boreholes (9% of all BH's)</p>	

Type 1, Variation 2 and Type 3 drawdown curve categories have typically above average transmissivity and recommended yields, type curves provide the most Type 5 have below average recommended yields in line with increased drawdowns observed during testing (Table 5.11). These low yielding boreholes have low transmissivities and the lowest potential in terms of bulk water supply. The relatively high average drawdown achieved for Type 3 curves in comparison with the population average indicates that near steady state conditions were reached in most cases. Accordingly, the low drawdown averages of Type 1 curves may indicate that in most cases unsteady state conditions prevailed (typical Theis type-curve) at the end of the test. Variation 2 which represent distinct fracture dewatering curves has the highest constant rate averages and be regarded as the most productive aquifer types.

**Table 5.11. Summary of selected hydrogeological parameters for the different drawdown behaviours.**



Class	Nr. of BH's	Rec. Yield $\ell/s$ per day	Transmissivity $m^2/d$	Constant Rate $\ell/s$ per day	Drawdown during test
TYPE 1	387	1.2	34.7	4.8	17.6
TYPE 2	568	0.9	24.1	3.4	21.7
Variation 2	514	1.4	35.1	5.5	18.8
TYPE 3	569	1.2	31.2	4.4	23.8
TYPE 4	106	1.0	36.8	4.8	18.9
TYPE 5	215	0.4	12.5	2.1	30.2
<b>All</b>	<b>2359</b>	<b>1.1</b>	<b>29.4</b>	<b>4.3</b>	<b>20.4</b>

### TYPE 1 (Theis)

These refer to an ideal confined, unconsolidated, homogeneous and isotropic aquifer. These assumptions are hardly applicable to basement (fractured) rock aquifers unless a dense network of interconnected fractures intersects the rock and builds a continuum comparable to a porous aquifer. A series of borehole drawdown behaviours can be matched with a typical Theis-curve (unsteady-state) equation (Figure 5.22). Early time behaviour is characterised by linear flow with a slope of 0.5 and may be indicative of fracture flow. Late times the derivative stabilises indicating infinite acting radial flow. The start of radial flow indicates the time at which the fractured reservoir behaves as homogenous.

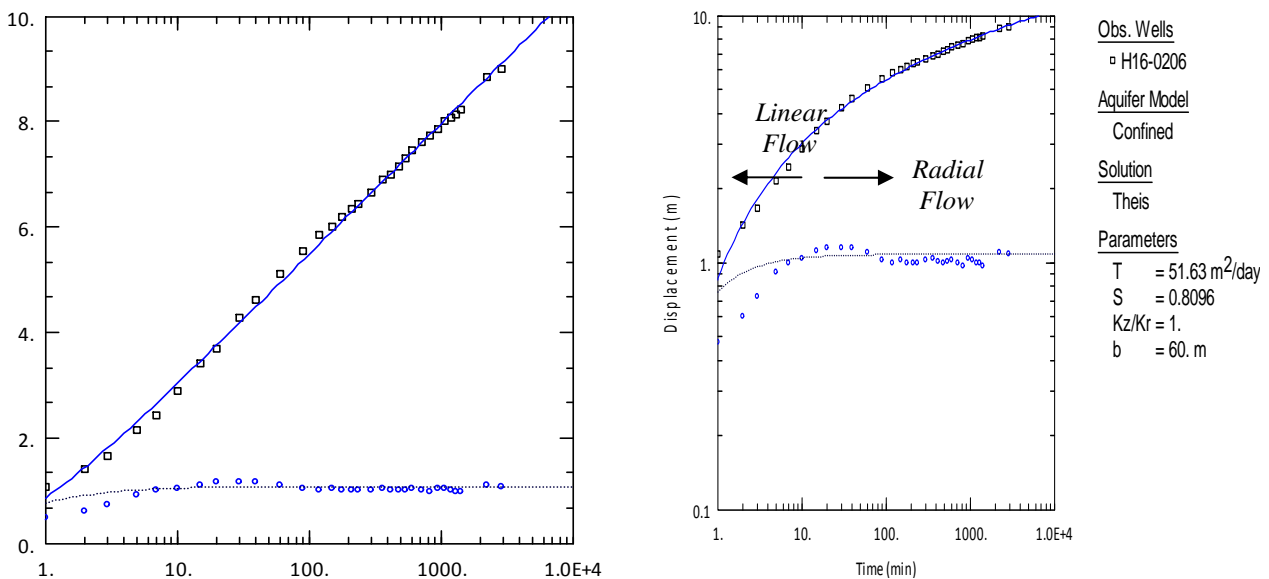


**Figure 5.22. Diagnostic plots (semi-log, log-log and derivative) of a 48 hour constant rate pumping test fitted with a Theis solution (borehole H16-0206).**

The shape of the recovery-curve may provide valuable additional information in cases where the drawdown-curve was disturbed due to variations in the pumping rate. In this example the recovery data fitted with a Theis recovery method (in addition to the Agarwal plot) confirms the homogenous behaviour identified in the drawdown-curve (Figure 5.23). In the absence of no flow boundary conditions both (drawdown and recovery) curves must show the same behaviour due to superposition (Van Tonder et al., 2002).



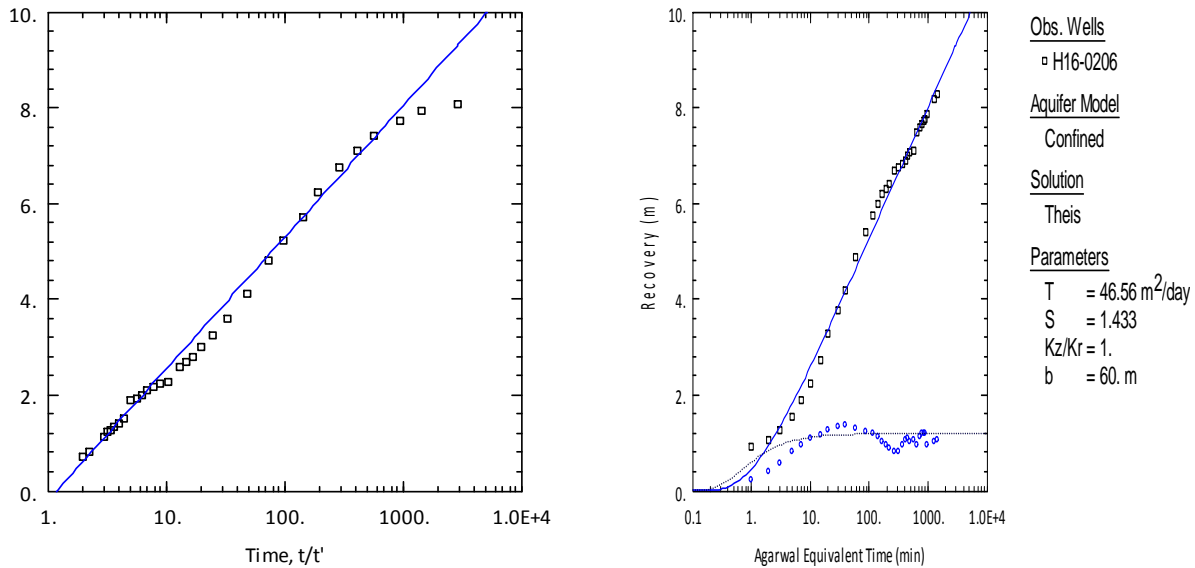


**Figure 5.23. Diagnostic plots (semi-log) of the recovery data of borehole H16-0206 fitted with a conventional Theis-recovery solution (left) and a Theis solution for the Agarwal plot (right).**

#### *TYPE 2 (Unconfined or double porosity)*

The most common behaviour of all boreholes tested in the study area is an inflection of the drawdown at intermediate times, reflected by a pronounced double porosity dip in the derivative. Early pumping times indicate the depletion of a first reservoir that is well connected to the pumping well (i.e. fractures or the saturated zone of an unconfined aquifer). At intermediate pumping times the drawdown is stabilised by a delayed flux provided by a second compartment of the aquifer, which can be either 1) the vertical delayed recharge from the overlying, less permeable part in an unconfined aquifer (Neuman 1974; Moench, 1997) or 2) the drainage of matrix blocks in fractured aquifers (Moench, 1984; Barker, 1988). At late time, the system either tends toward a typical infinite acting radial flow asymptote or boundary conditions may be encountered. In the first instance the semi-log plot shows the characteristic parallel straight line segment at early and late pumping times, while a no-flow boundary is characterised by a doubling of the value of the derivative (Ehlig-Economides et al. 1994; Van Tonder et al., 2002). Borehole H17-0774 were fitted with both an unconfined Neuman (1974) and double porosity Moench (1984) solution (Figure 5.24 and Figure 6.6). In both cases a good curve fit was achieved highlighting the difficulty in choosing an appropriate model. A detailed description of the geology and conceptual model will greatly assist in choosing the correct analytical model.

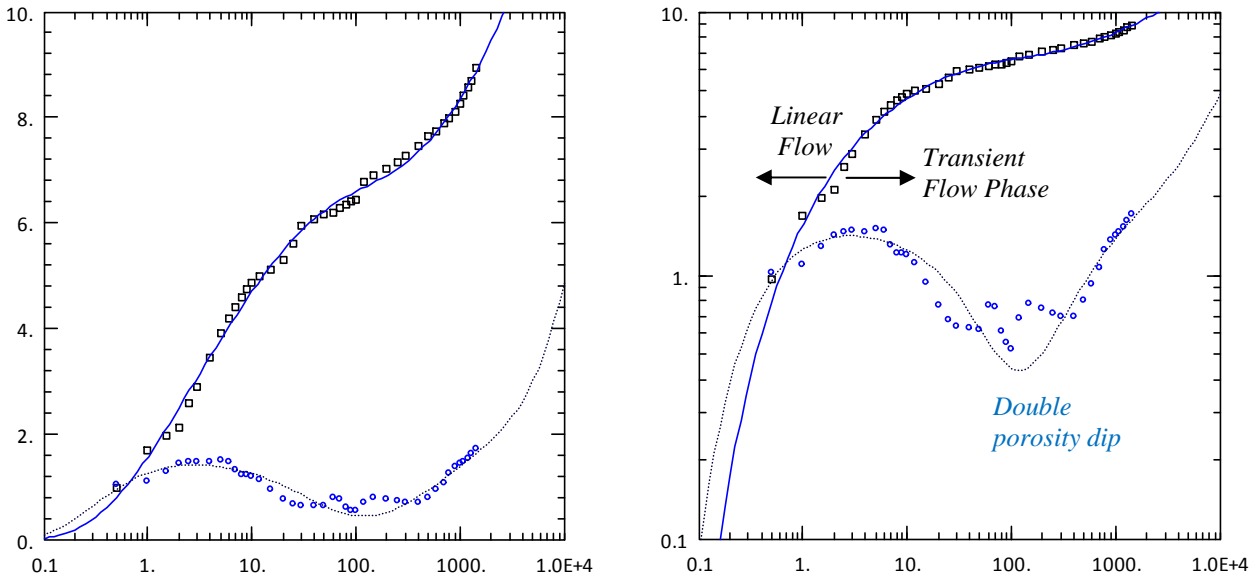


Figure 5.24. Diagnostic plots (semi- log, log-log and derivative) of a 24 hour constant rate pumping test with an unconfined solution (borehole H17-0774).

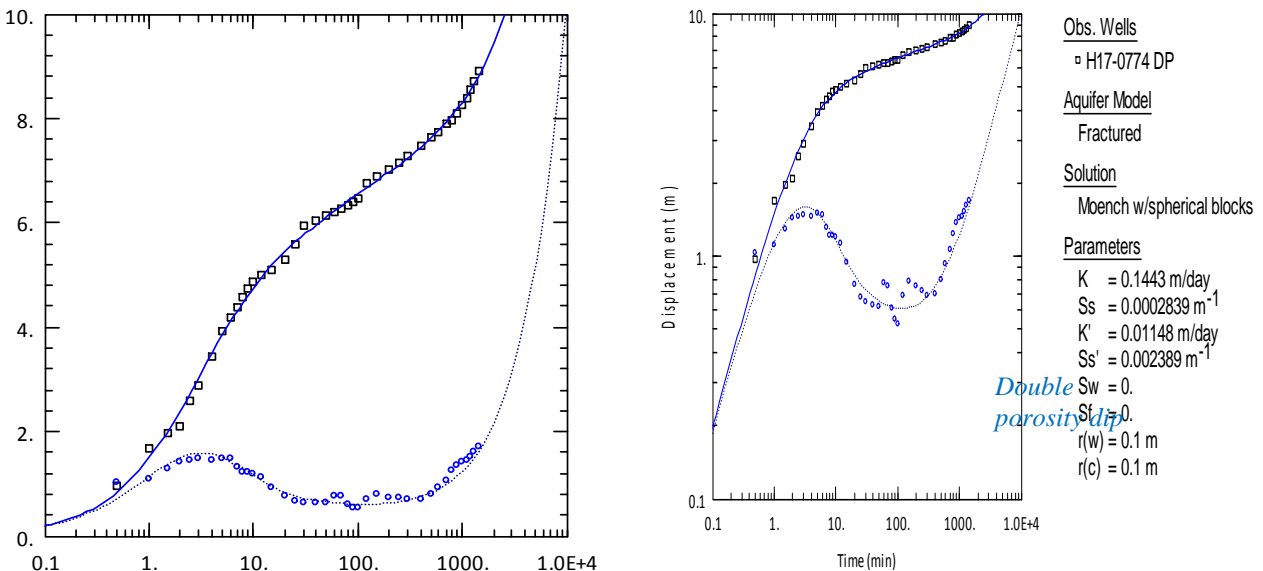
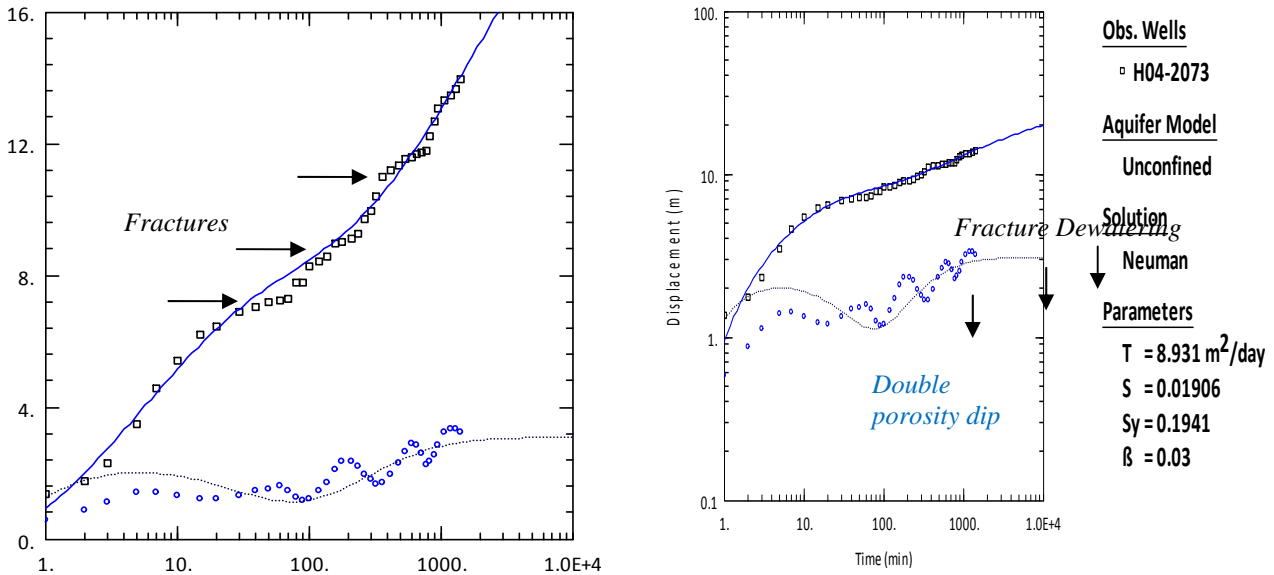


Figure 5.25. Diagnostic plots (semi- log, log-log and derivative) of borehole H17-0774 fitted with a fractured (double porosity) solution.

### Variation 2

The drawdown behaviour is characterised by distinct dips (fracture dewatering) during late times of the associated derivative data (Figure 5.26). In this conceptual model the early flow towards the well is from fracture storage, supported at intermediate times by drainage of the rock matrix before water is derived from both systems at late times with frequent dewatering of discrete fracture systems. Once these fractures are dewatered, a marked increase in drawdown and decrease in transmissivity becomes apparent.



**Figure 5.26. Diagnostic plots (semi- log, log-log and derivative) of a 24 hour constant rate pumping test fitted with a fractured (double porosity) solution (borehole H04-2073).**

In the example illustrated in Figure 5.26 a number of discrete fractures (water strikes) were evidently dewatered. Although a conventional fracture solution was used, more disturbed drawdown curves (due to the dewatering of fractures) make the evaluation complicated and often only parts of the curve can be modelled. The recovery-curve methods provide an alternative approach for fitting of the pumping test where the drawdown curve have been affected by fracture dewatering (Figure 5.27).

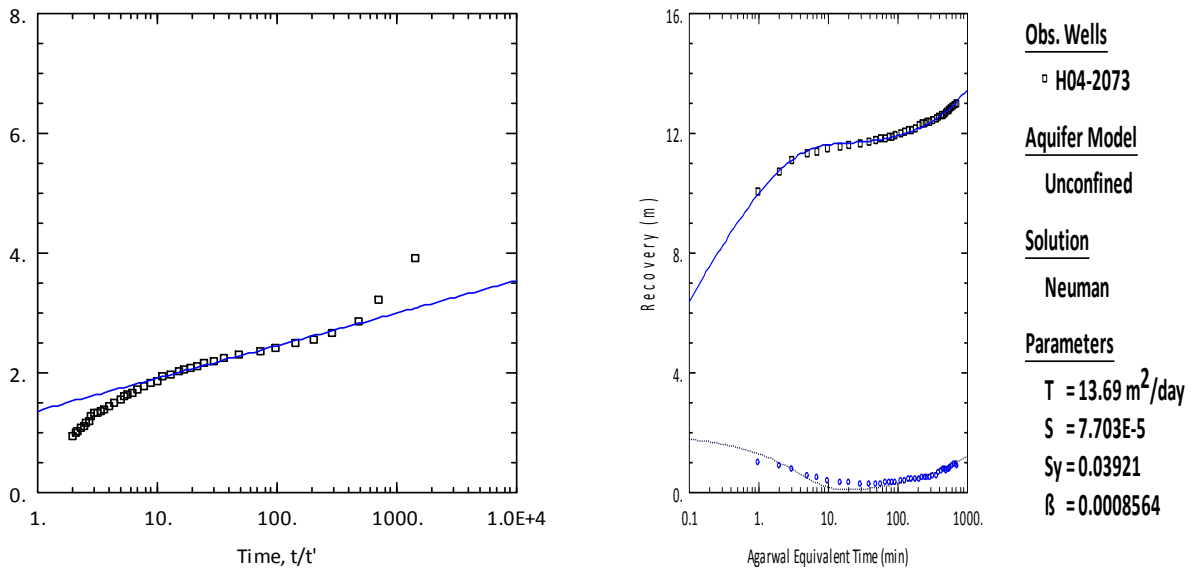


**Figure 5.27. Diagnostic plots (semi-log) of the recovery data of borehole H04-2073 fitted with a conventional Theis-recovery solution (left) and a fractured (double porosity) solution for the Agarwal plot (right).**



### TYPE 3 (Leaky or Constant Head)

At early pumping times, a Theis-type curve is observed (0 to 100 minutes), at intermediate times, water from the aquitard leaking into the aquifer. Eventually, at late times all the leakage through the aquitard becomes constant and the flow towards the well reaches steady state (Figure 5.28).

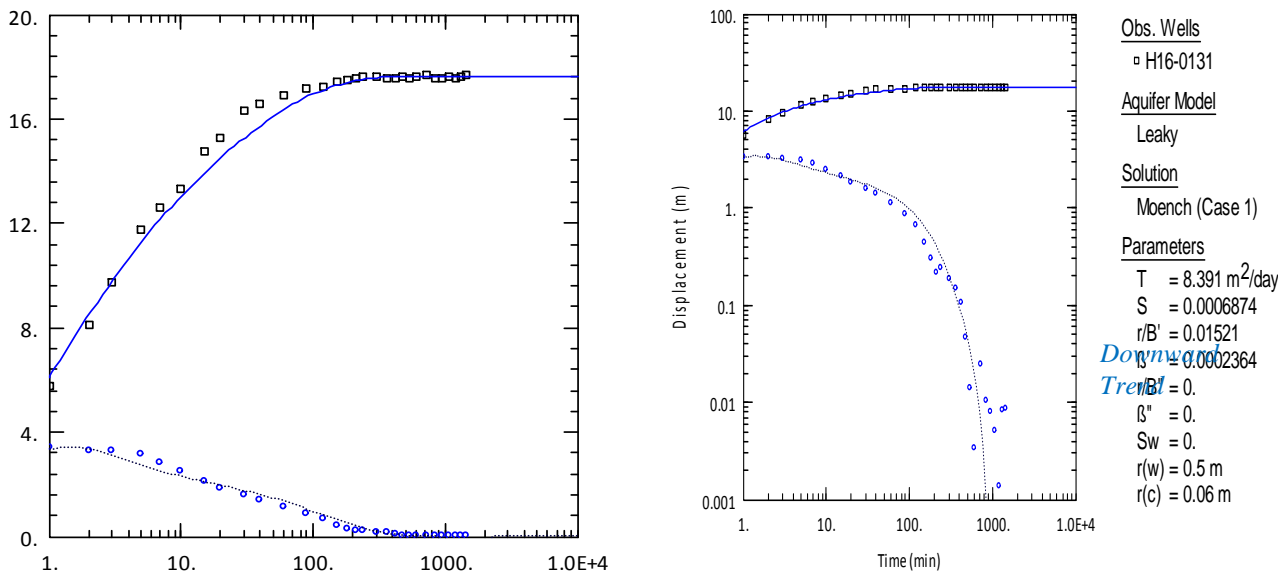


**Figure 5.28. Diagnostic plots (semi-log, log-log and derivative) of a 24 hour constant rate pumping test fitted with a leaky aquifer solution (borehole H16-0131).**

A similar behaviour (leakage) is observed when the cone of depression reaches a recharge boundary (constant-head). Renard et al. (2009) noted that in theory a leaky aquifer case can be distinguished from a constant head case by looking at the shape of the derivative). The derivative tends towards zero earlier in the case of a leaky aquifer much faster than in the constant head case (see Figure 2.4, section 2.4.2).

### TYPE 4 (Single Fracture – General radial flow)

Type 4 can be regarded as a fractured aquifer system characterised by an early period in which the effect of the fracture dominates and very little water is contributed by the aquifer (matrix). The flow towards the well takes place in the fracture only and is parallel (i.e. linear in the fault). At intermediate times water is supplied by the fracture and matrix. The extensive occurrence of near vertical dykes, lineaments and shear zones (see section 4.3) in the crystalline rock, in addition to the fact that most boreholes are completed once a single moderate- or high-yielding fracture is encountered, it is to be expected that a number of drawdown behaviours can be fitted with a single fracture model. An example is borehole H03-3269 (Figure 5.29), which seemingly targeted the Matok shear zone. In this case it was assumed that the fracture zone (set of vertical fractures) acted as a conduit and based on the drawdown behaviour the curve was idealised with a single vertical fracture model (Gringarten et al., 1974). A fracture half-length of 100 m was assumed (although fracture half-lengths of several hundreds of meters, up to above 1000 m are encountered in study area).



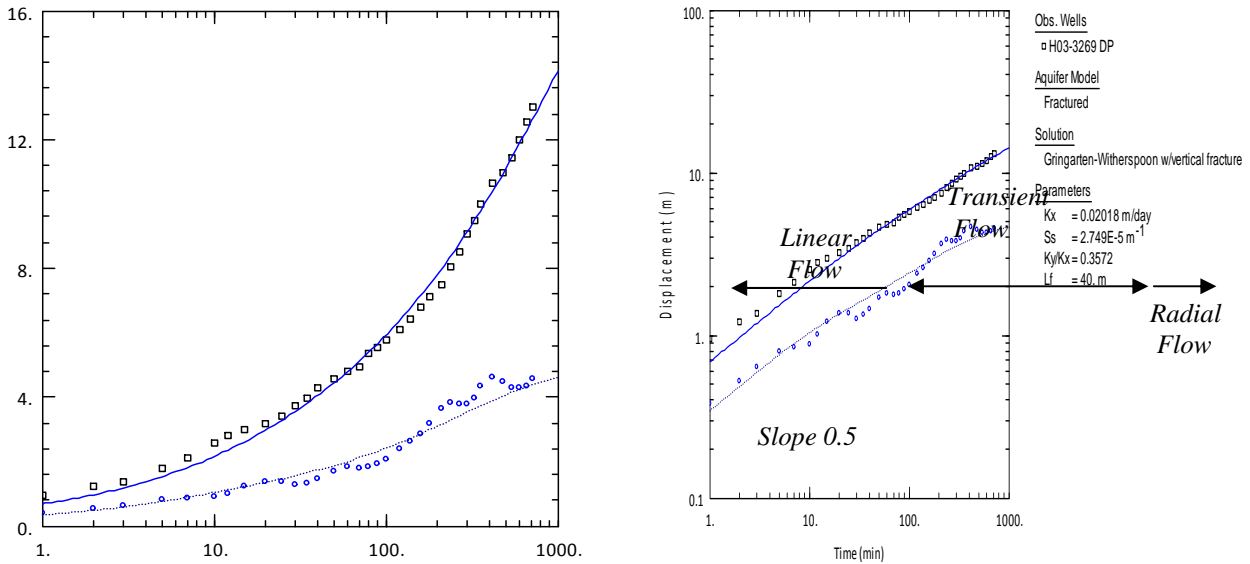


Figure 5.29. Diagnostic plots (semi- log, log-log and derivative) of a 12 hour constant rate pumping test fitted with a single fracture (Gringarten et al., 1974) model (H03-3269).

*TYPE 5 (Closed reservoir)*

A feature of these type-curves is the obvious influence of barrier boundaries which increases the rate of drawdown as the limits of the fissure systems are reached by the pumping effects (Figure 5.30). The shape of the drawdown has a characteristic steepening in the semi-log, log-log and derivative plots. Interestingly 50 % of Type 5 tests were pumped for 8 hours or less and achieved the highest drawdown (Table 5.11).

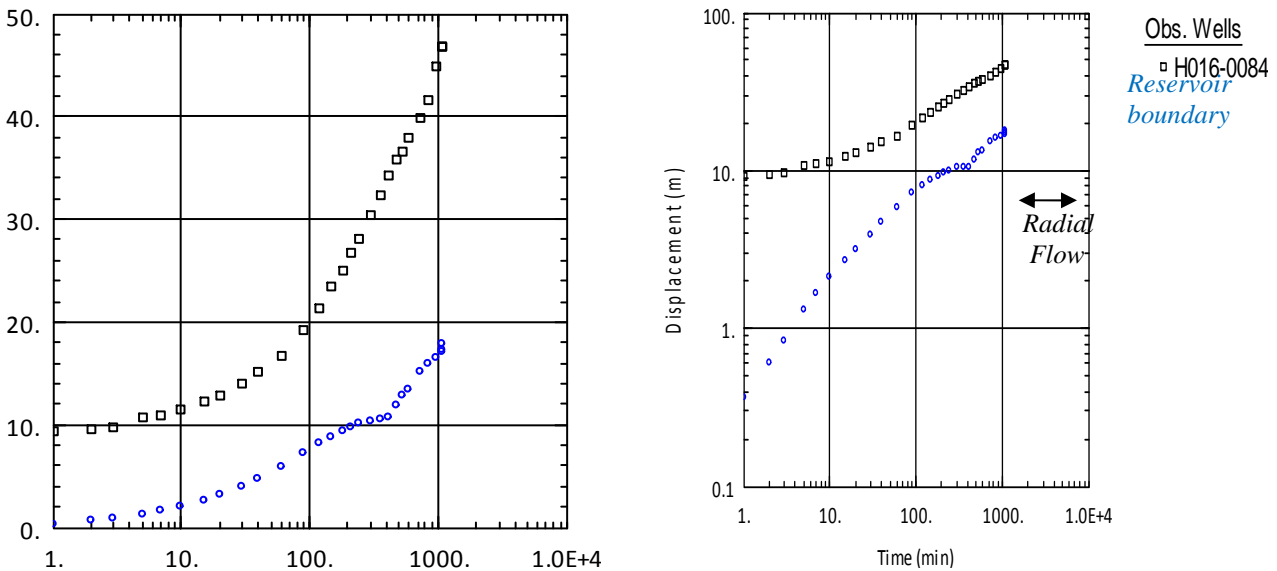


Figure 5.30. Diagnostic plots (semi- log, log-log and derivative) of borehole H16-0084, indicating reservoir boundaries.

This may be a clear indication of an excessive pumping rate, where the aquifer could simply not supply efficient water to the borehole to sustain the discharge rate chosen. In these cases, parameter estimation is extremely difficult and the test should be repeated with a lower pumping rate.

### Summary of aquifer characterisation

The exact shape of the diagnostic plot (drawdown behaviour) depends on the values of the hydraulic (and physical) parameters that control them. These typical behaviours can occur over shorter or longer periods, which is in some cases extremely clear and in others more difficult to identify. Therefore the curves shown in the preceding section are indicative of a certain category of response and not strictly identical with a single response that one should expect in field situations. Analyses of pumping tests in crystalline basement aquifers do not satisfy the underlying assumptions for porous media. In particular:

- basement rock aquifers are neither homogenous nor isotropic,
- the aquifer often represents semi-confined to unconfined conditions,
- flow from fractures will neither be two-dimensional radial, nor will it be constrained to a single one-dimensional channel. The characteristic of the fracture network determine the flow geometry, and
- well bore storage and skin is not negligible, and can overlie other effects, which are important for the parameter estimation (Van Tonder et al., 2002; Misstear et al., 2006).

### 5.3.2. Hydraulic parameters

The locations of all pumping tests conducted within the project framework are illustrated in Figure 5.31.

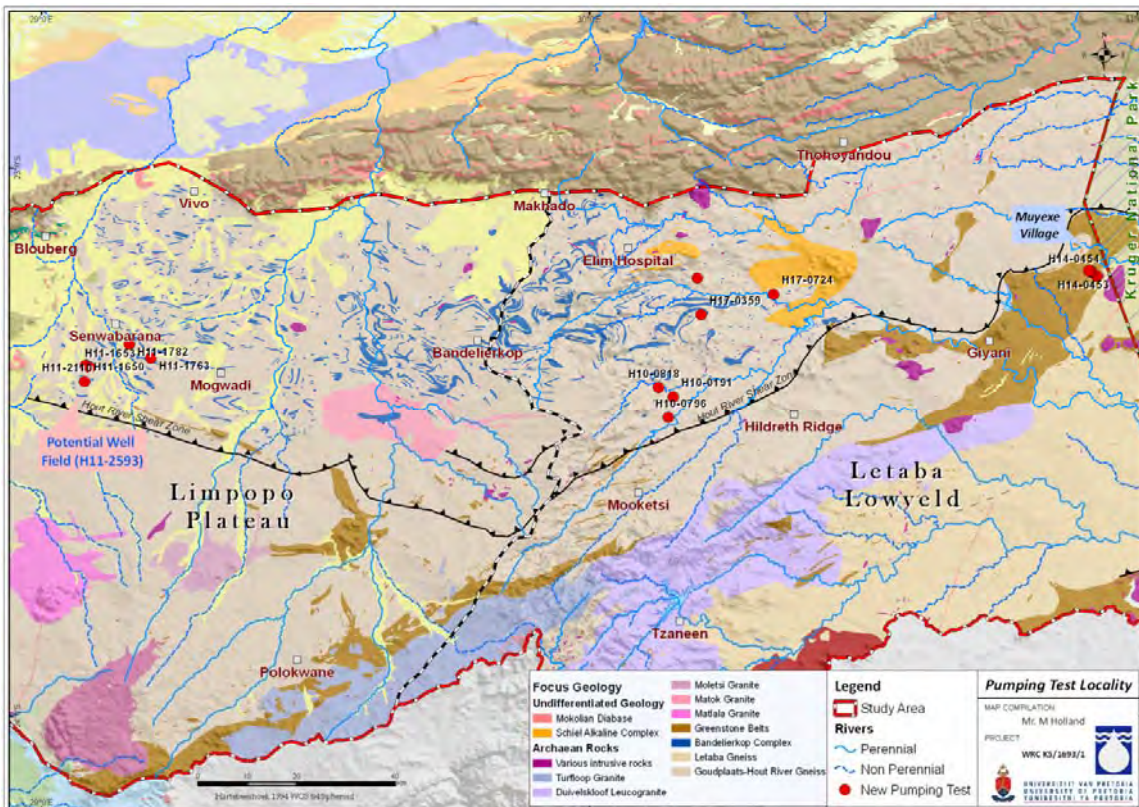


Figure 5.31. Location of pumping tests conducted in the study area.

The hydraulic parameters obtained from the pumping test analysis and the analytical solutions applied for the curve matching procedure are summarised in Table 5.12. The representative values for T and S were obtained from the aquifer test analysis using the pumped and observation boreholes (if available). Although well loss and well efficiency was not a priority for this assessment it was analysed for some boreholes. In most cases well losses exceeded  $3\ 800\ \text{ec}^2/\text{m}^5$ , which can be regarded as severe losses according to Walton (1962) (Appendix F). The confidence level of the determined hydraulic parameters (T and S) generally increases if observation boreholes are present. The arithmetic average storativity value determined is  $5.E-02$  and  $7.E-03$  for the Limpopo Plateau and Letaba Lowveld respectively, coinciding closely with the chosen constant storativity value of  $1.E-03$  used in the analysis (FC-method) of the GRIP dataset.

**Table 5.12. Hydraulic test analysis results (test details is given in Appendix F).**

Area	BH Nr.	Applied solution	Aquifer Type	T m <sup>2</sup> /d	S	Observation BH's	Theis Recovery-method
Limpopo Plateau	H11-1650 <sup>#</sup>	Barker	Fractured	330	2.E-01	H11-1651 (301m), H11-1652 (255m)	470
	H11-1653 <sup>#</sup>	Moench	Fractured	220	2.E-03	H11-1651 (398m), H11-1652 (441m), H11-1654 (451m)	344
	H11-2110*	Neuman-Witherspoon	Leaky	180	6.E-05	H11-2109 (211m)	310
	H11-1782*	Hantush-Jacob	Leaky	50	2.E-04	H11-1781 (48m)	30
	11-1763	Neuman-Witherspoon	Leaky	4	-	H11-1764 (120m)	9
Letaba Lowveld	H10-0818*	Hantush-Jacob	Leaky	47	9.E-04	H10-0823 (40m)	30
	H10-0796 <sup>#</sup>	Neuman	Unconfined	7	1.E-03	H10-0100 (40m)	17
	H10-0191 <sup>#</sup>	Hantush	Leaky	1	3.E-03	H10-0816 (180m)	20
	H14-0277*	Neuman	Unconfined	95	2.E-03	H14-0279 (220m)	137
	H14-0279*	Barker	Fractured	51	3.E-04	H14-1288 (50m), H14-1301 (250m)	130
	H14-0453*	Neuman	Unconfined	77	4.E-04	H14-0277 (130m), H14-0454 (290m)	170
	H17-0359	Neuman	Unconfined	4	-	-	10
	H17-0724	Neuman	Unconfined	1	-	-	15
	H17-0774	Neuman	Unconfined / Fractured	4	-	-	11
	H14-0454	Neuman	Unconfined	16	-	-	20
	H14-0275	Gringarten-Ramey	Fractured	43	-	-	45

\* - Observation hole monitored with drawdown.

# - Observation borehole monitored with no-influence.

#### 5.4. Groundwater sustainability (source vs. resource)

The following discussion will show that the recommended 'sustainable' yield is non-unique and can be influenced by factors such as the constant rate during testing. It will also be highlighted that long term borehole yields are recommended without consideration of the combined (aquifer) yield.

### 5.4.1. Source yield

The most common factor influencing a proper analysis of a pumping test is insufficient drawdown achieved due to, a too low pumping rate or too short duration. If the aquifer is not stressed sufficiently it's impossible to identify the main fracture zone or possible boundary conditions. Two constant rate tests were performed on borehole H14-0279; in 2005 the test was conducted at a rate of 3.7 ℓ/s for 24 hrs and in 2009 the test was conducted at a rate of 6.2 ℓ/s for 48 hrs (Figure 5.32).

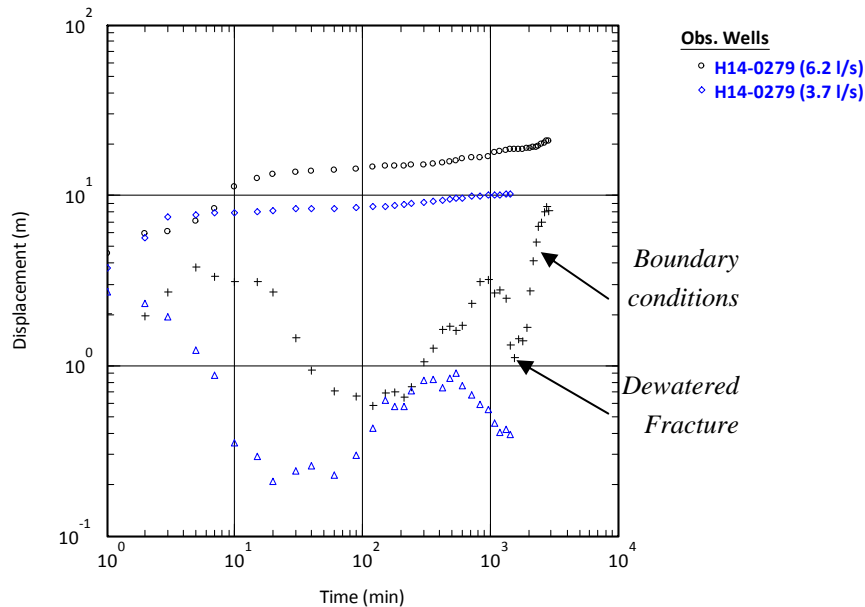


**Figure 5.32. Semi logarithmic plot of borehole H14-0279 with two different constant discharge rates.**

The pumping test data produced different drawdown curves. Although the position of the fracture is seen in both derivative plots, the dewatering of the fracture (or no-flow boundary) is only seen after 1 440 minutes (i.e. in the second test). By comparing the recommended yield results obtained from the FC spreadsheet it is evident that the higher constant rate estimated the lower 'sustainable' yield (Table 5.13).

**Table 5.13. Comparison of the results for the two constant rates.**

Constant Rate	3.7 (ℓ/s)		6.2 (ℓ/s)	
Date	2005		2009	
Rest Water level (m.b.g.l)	7.7		7.6	
Drawdown (Available) (m)	53		55	
Final Drawdown (24 hr) (m)	10.2			
Final Drawdown (48 hr) (m)	-		20.9	
Available drawdown	Drawdown	Yield*	Drawdown	Yield*
Main water strike <sup>@</sup>	19	2.7	19	1.4
Final Drawdown	10.2	1.9	20.9	1.3
Transmissivity (Late T m <sup>2</sup> /day)	30		7	

<sup>@</sup> - Distance from rest WL to main water strike (m) – BH Log

# - Estimated from the geometric mean of the end drawdown and main water strike

\* - Recommended abstraction (ℓ/s per day).



Using the position of the main water strike as the available drawdown, the estimated yields are 2.7 and 1.4  $\ell/s$  respectively for the low and high rate tests. The 2.7  $\ell/s$  obtained from the lower rate test may therefore, be an over estimate of the ‘sustainable’ yield of borehole H14-0279. This clearly illustrates the problem encountered when using the main water strike as available drawdown when the achieved drawdown is far above the position of the main water strike. This is a common pitfall of the pumping tests conducted in the Limpopo Province, where the constant rate is often decided before hand without site specific considerations. Only a third of all boreholes tested in the study area, achieved a final drawdown of 80-90 % of the available drawdown (water level to the pump intake) (Figure 5.33).

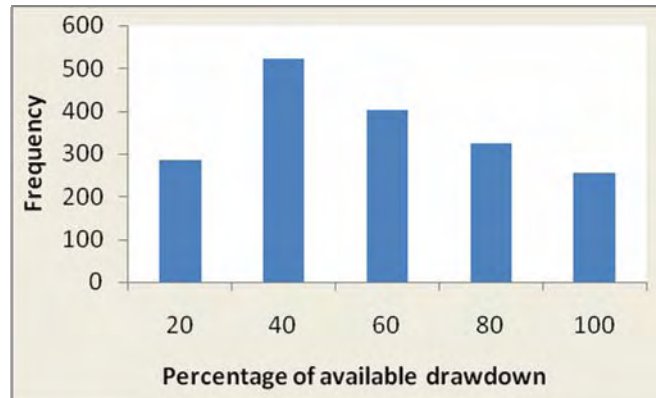


**Figure 5.33. Distribution of drawdown percentage achieved from pumping tests in the study.**

Another common shortfall of pumping tests conducted in the study area is pre-determined duration for the tests. Because boundary conditions were not encountered during the 24 hr pumping test it wasn’t considered during the yield estimate and a recommended yield of 1.9  $\ell/s$  was determined (using the final drawdown as available drawdown). Considering the boundary conditions evident from the 48 hr test, 1.3  $\ell/s$  is recommended (Table 5.13). Almost 85% of boreholes tested in the study area were pumped for 24 hrs or less (Table 5.14). However, using the final drawdown during a test as available drawdown can be regarded as the minimum ‘sustainable’ yield of the borehole if the water strike has not been reached.

**Table 5.14. Pumping test in the study area (GRIP dataset).**

Hours	<12	12	24	48	72	96	Total
Nr. of Tests	335	547	1054	213	63	1	2213
Percentage	15%	25%	48%	10%	3%	0.1%	100%

These common shortfalls may be directly related to the poor emphasis on step-drawdown rates to accurately determine a constant rate that will ensure interpretable drawdown curves are obtained at the pumping well and observation points.

#### 5.4.2. Resource yield

Pumping tests are probably the most important aquifer investigations techniques, however, as seen from the preceding discussion long term assured water supplies (30 years+) to a community

or village with substantial infrastructure investments are often based on a mere 12 or 24 hr pumping test. This can in theory lead to a sustainable source yield but an unsustainable resource yield. An example of such a case is the Upper Brak River catchment where numerous pumping tests were conducted for rural water supply purposes. The catchment lies to the west of the Dendron-Vivo groundwater control area where large scale irrigation has sustained (though not necessarily sustainably) agricultural activities in the region for the last 40 years. As illustrated in Figure 5.6 (section 5.1.2) and Figure 5.34 (insert) groundwater levels have declined by 6 m since the early 1970s. Considering that the impacts of groundwater consumption on the ecological environment are largely unknown the aquifer can be considered as being partially mined.

To evaluate the situation in the Upper Brak River catchment all recommended borehole yields were accumulated and compared to the rate of natural recharge (Table 5.15). Based on the results the area has a combined recommended yield of 10.4 Mm<sup>3</sup>/a, which is almost twice the annual vertical recharge of 6 Mm<sup>3</sup>/a (2% of MAP). Although not all of these boreholes are in operation and in most cases infrastructure (i.e. electricity) is required, the example does show that recommended source yields may exceed the resource yield (in this case recharge).

**Table 5.15. Simplified water balance for the Upper Brak River catchment.**

Area	Boreholes	Recharge	Rainfall	Recharge	Yield*
763 km <sup>2</sup>	149 (mean yield of 2.2 l/s)	2%	392 mm/a	6 Mm <sup>3</sup> /a	10.4 Mm <sup>3</sup> /a

\* - As determined by the FC-method for a 24 hr duty cycle.

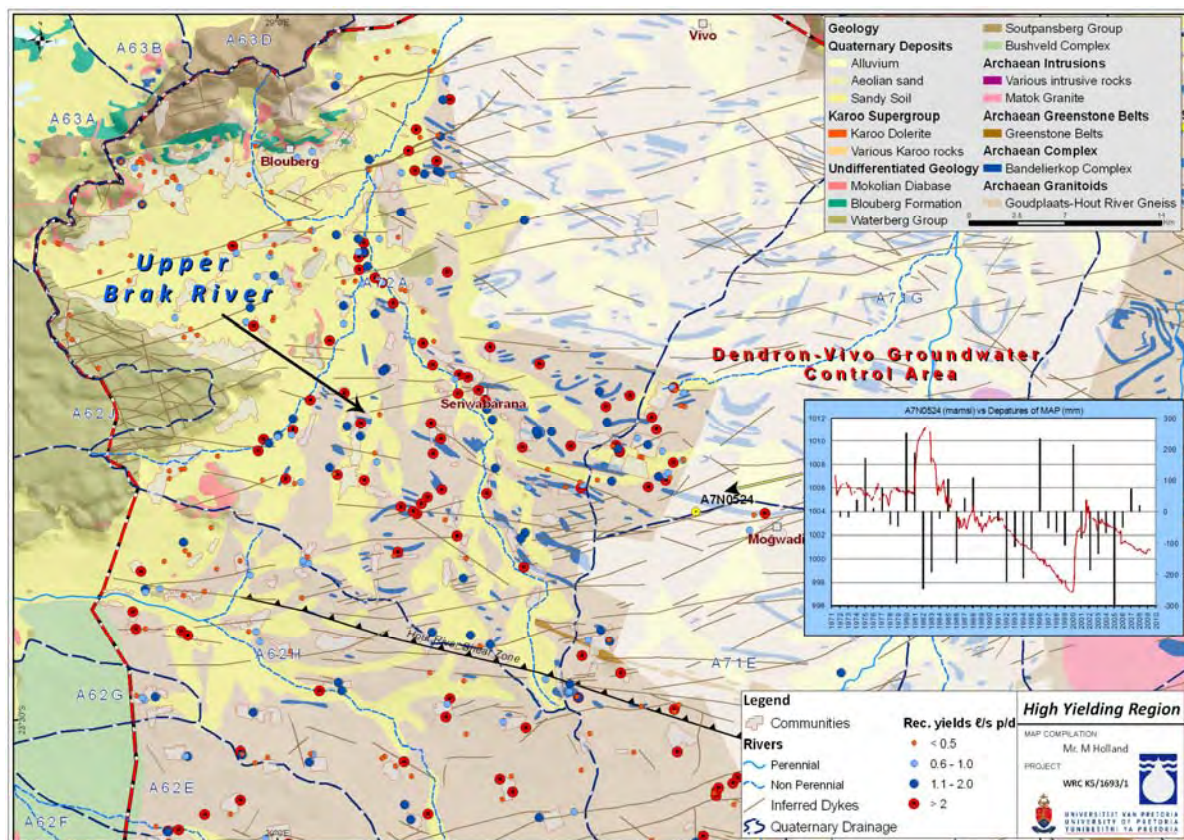


**Figure 5.34. High groundwater potential area in the Upper Brak River catchment.**



### 5.4.3. High yield test (potential well field)

Due to increasing water demand from the Blouberg local municipality this site (Brilliant Farm) has been earmarked as a potential well field. To further the understanding of aquifer behaviour in response to pumping especially in high yielding fractured bedrock, a constant discharge test was conducted on borehole (H11-2593) with at a rate of 55 ℓ/s for a period of just over 60 hours. The exceptional yield of 55 ℓ/s is arguably the highest constant rate test conducted to date on the Limpopo basement aquifers. Photo 2 shows the drilling and hydraulic testing of borehole H11-2593. Three observation boreholes were drilled at right angles to the large diameter pumping test hole (Figure 5.35) (Table 5.16).



**Photo 2. Drilling and testing of borehole H11-2593.**

**Table 5.16. Summary of pumping and observation boreholes of high yield test.**

BH ID	Area	Distance from abstraction hole (m)	BH Depth (m)	Start WL (m.b.g.l)	Drawdown (m)	End WL (m.b.g.l)
H11-2593	-	Pump Well	84	24.04	7.49	31.53
H11-2596	South	38	52	23.85	4.64	28.49
H11-1653		233	78	23.23	2.41	25.64
H11-2594	West	58	120	24.09	3.67	27.76
H11-1652		215	90	22.86	2.34	25.2
H11-2595	North	65	72	23.86	2.73	26.59

To identify inflow horizons and fractures, down-hole geophysics was conducted prior to the completion of the borehole (casing). Logging operations included a CCTV inspection, and the use of a natural gamma, electrical resistivity and neutron probe (Photo 3). An electrical conductivity and temperature log was completed after the completion of the borehole. Table 5.17 shows geophysical and fluid measurements and, the identification of the particular transmissive fractures in borehole H11-2593.

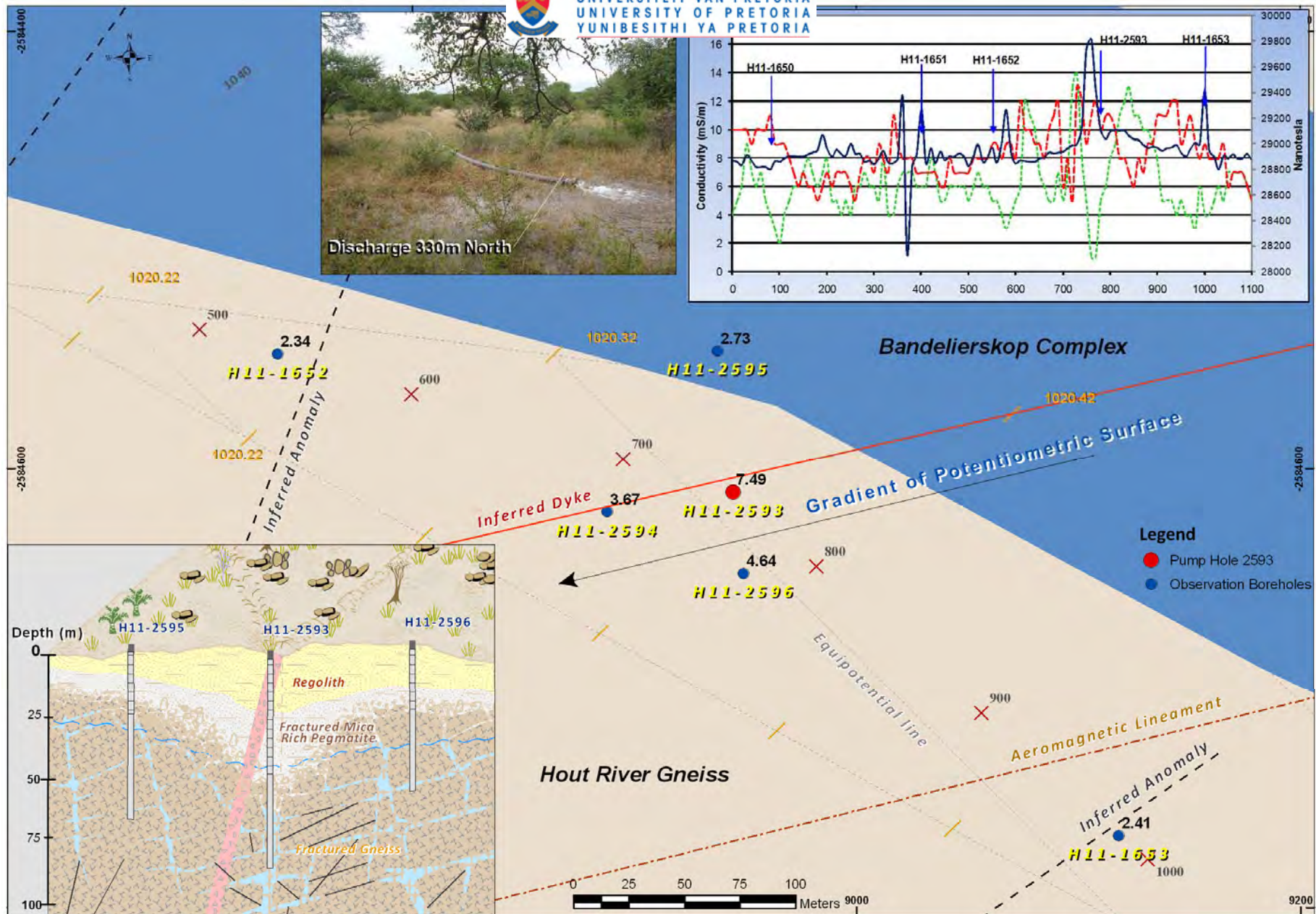
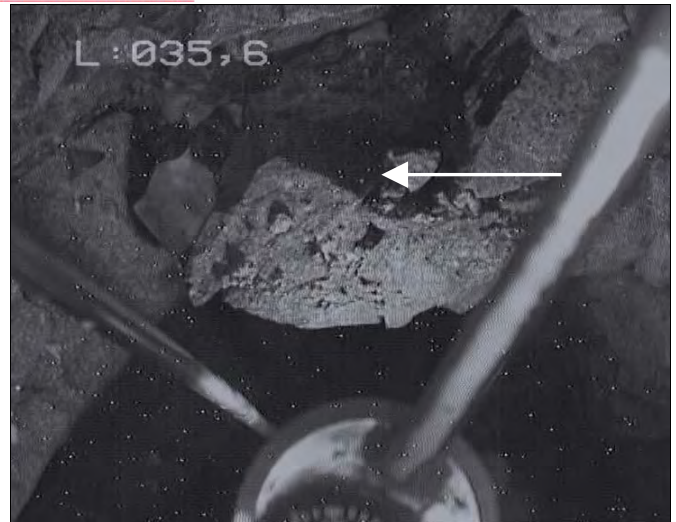


Figure 5.35. Borehole setting of pumping test conducted at the farm Brilliant (Drawdown achieved at the end of constant test is indicated on the map).





**Photo 3. Geophysical and CCTV logging of borehole H11-2593, footage showing water strike at 36 m.b.g.l.**

Based on the results the following interpretations are made:

- The *natural gamma* log clearly indicates an increase in radiation in the quartzitic zone (39 to 49 m.b.g.l). A high content of quartz, K-feldspar and plagioclase was clearly observed in the drill chips which are high in  $^{40}\text{K}$ .
- Two distinct zones can be identified from the *resistivity* log. Low conductivity observed from 35 to 52 m.b.g.l. may indicate a porous fractured zone while an increase in conductivity from 52 m.b.g.l representing a zone of more solid (intact) rock. The base of weathering is inferred at 30 m.b.g.l.
- Decrease in the *neutron* signal between 35 and 38 m.b.g.l suggests the increased capture of neutrons due to higher hydrogen content. This indicates an increase in the amount of water due to higher water filled porosity, and although not clear, could be interpreted as locations of major flowing fractures.
- A sharp increase in electrical conductivity at 36 m.b.g.l and again at 42 m.b.g.l confirm this as the main water bearing zone with groundwater entering as discrete horizons or fissures with a slightly different conductivity. In addition, two distinct flow systems (highlighted on EC graph) are observed which represents limited vertical mixing between these two zones. A distinct drop in temperature at  $\approx 35$  m.b.g.l supports the notion of inflows from fractures.



Table 5.17. Results of geological, CCTV and geophysical logging of borehole

Geology (log)	Water Strike*	Natural Gamma (cps)	Electrical Resistivity ( $\Omega$ m)	Neutron-N (cps)	Fluid Conductivity (mS/m) / Temp (C°)	CCTV (Images)
		0 6 12 18	70 170 270	0 1000	132 137 142	
Coarse Calcareous weathered material, dominated by quartz		0	0	0	0	
Fine weathered material, particles coated with cement but are quartz dominated		5	5	5	5	
Weathered diabase, mainly fine grained black material with quartzofeldspathic gneiss	RWL 24 m	10	10	10	10	
Fractured diabase, with some quartzofeldspathic gneiss	EWL#	15	15	15	15	
Coarse grained quartzofeldspathic gneiss (almost entirely quartzitic)	36 m	20	20	20	20	
Medium to coarse grained quartzofeldspathic gneiss	44 m	25	25	25	25	
	56 m	30	30	30	30	
	66 m	35	35	35	35	
		40	40	40	40	
		45	45	45	45	
		50	50	50	50	
		55	55	55	55	
		60	60	60	60	
		65	65	65	65	
		70	70	70	70	
		75	75	75	75	
<b>Base of borehole 84 m</b>	BH Diameter: 300 mm Casing: 250 mm solid to 17 m Perforated to 41 m		Rest Water Level: 24 m Pump installation: 39 m			

\* - Drillers log.

# - End water level (7.53 m drawdown).

During the constant discharge test, a drawdown of 7.53 m was achieved. From the drawdown curve a higher permeable zone were reached at 1 560 minutes, and lasted approximately 220 minutes, before it was dewatered. It's clearly visible as a distinct decrease followed by an increase of the derivative curve (Figure 5.36). This zone can be interpreted as the dewatering of a fracture or it can be related to the dewatering of a highly transmissive zone From the geophysical (geological) logging and the CCTV footage (Figure 5.36), this zone (30.5 m.b.g.l) can be regarded as a higher permeability basal breccia which represents the horizon of fracturing between the fresh rock and the regolith.

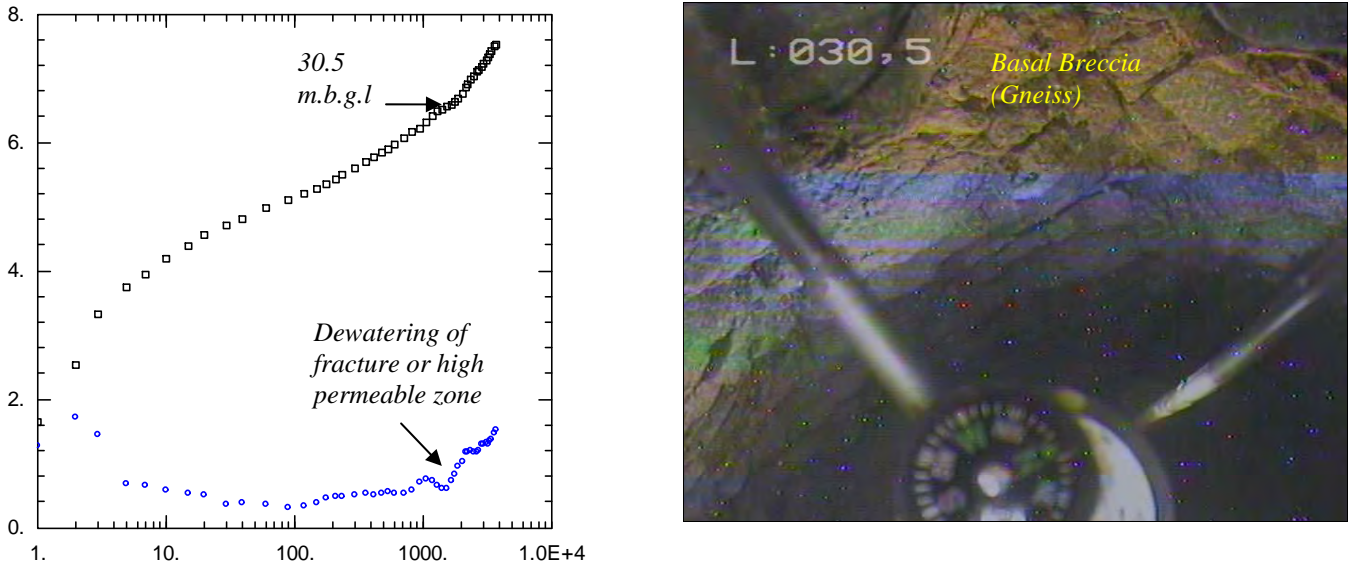


**Figure 5.36. Diagnostic plot (semi- log and derivative) model and the CCTV footage of the inferred higher permeability zone.**

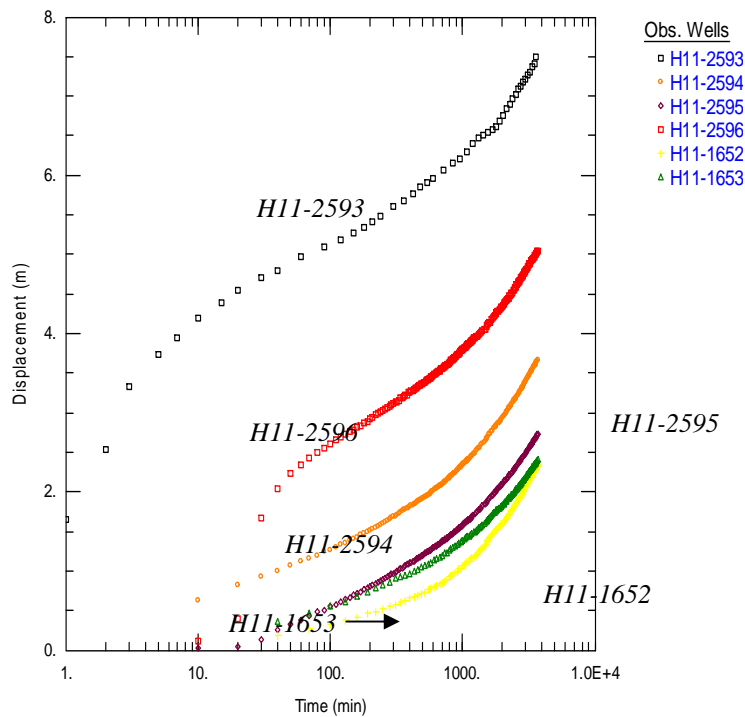


**Figure 5.37. Diagnostic plot (semi- log and log-log ) fitted with a fracture (Barker, 1988) model of pumping borehole (H11-2593) and observation boreholes (H11-2596 and H11-1653).**

The distinct double porosity dip of the derivatives and the typical sigmoidal type drawdown behaviour of the pumping borehole suggest that a fractured aquifer model can be justified for the dataset. Figure 5.38 illustrates the curve fit of borehole H11-2593 with the general radial flow model by Barker (1988) and its extension to dual porosity.

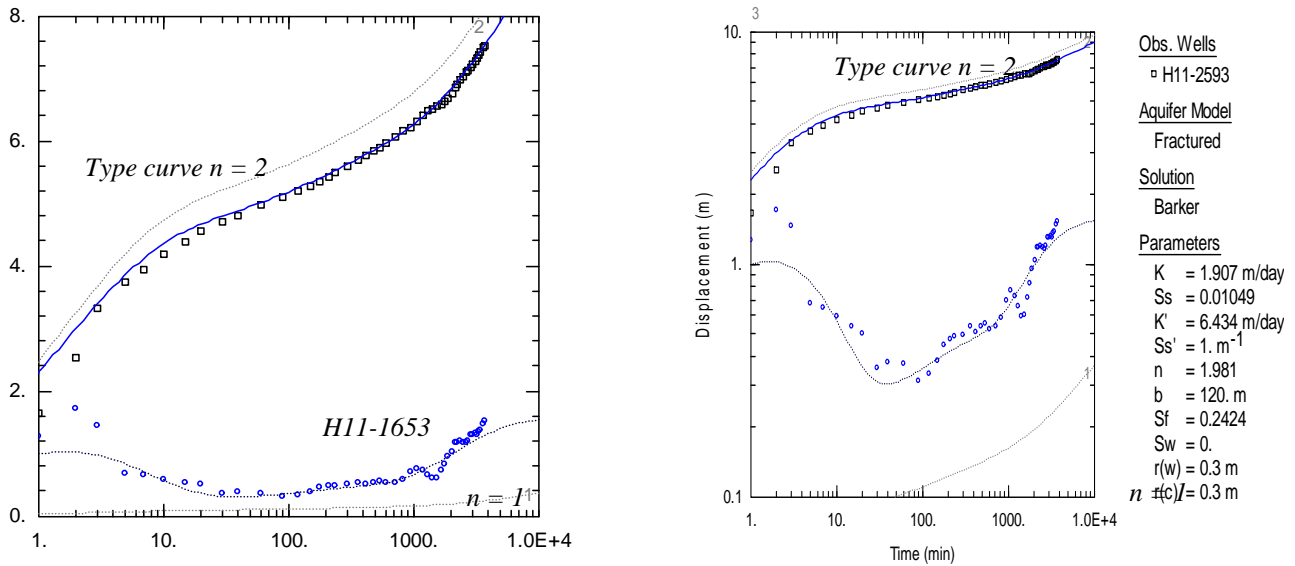


**Figure 5.38. Diagnostic plot (semi- log and log-log) fitted with a fracture (Barker, 1988) model of pumping borehole (H11-2593) and observation boreholes (H11-2596 and H11-1653).**

The diagnostic plot also indicate the family type curves of flow dimensions of  $n=1$  and  $n=2$  respectively (see section 2.4.3). Early pumping times are characterised by well bore storage effects and flow through fractures, followed by a transient flow phase (contribution of the matrix flow) at intermediate times and finally a characteristic bilinear flow regime indicative of flow in fractures and the matrix (Figure 5.38). An increase in the value of the derivative and an upward trend in the time drawdown data at later pumping times are often interpreted as no-flow boundaries, which can be incorrect (Van Tonder, 2002). It may be related to the end of the hydraulic active fracture zone which was increasingly being stressed at later times. Van Tonder and Steyl (2010) have shown that the representative transmissivity in fractured aquifers decrease with time of a pumping test, except if the borehole was situated close to a river.

A slightly better hydraulic connection based on drawdown versus distance is observed between the observation boreholes to the south (H11-2596; H11-1653) and west (H11-2594; H11-1652) of the pumping borehole, compared to the observation borehole (H11-2595) to the north (see Table 5.16 and Figure 5.37). For this reason the observation boreholes were grouped and analysed accordingly to their observed behaviour with respect to the abstraction borehole. Observation borehole (H11-2596) to the south responded in a similar way to the pumping borehole indicating well bore storage at early times followed by bilinear flow at late pumping times (Figure 5.39). The furthest observation borehole to the south (east) (H11-1653) has a predominant linear flow regime at late pumping times, characterised by a linear derivative.



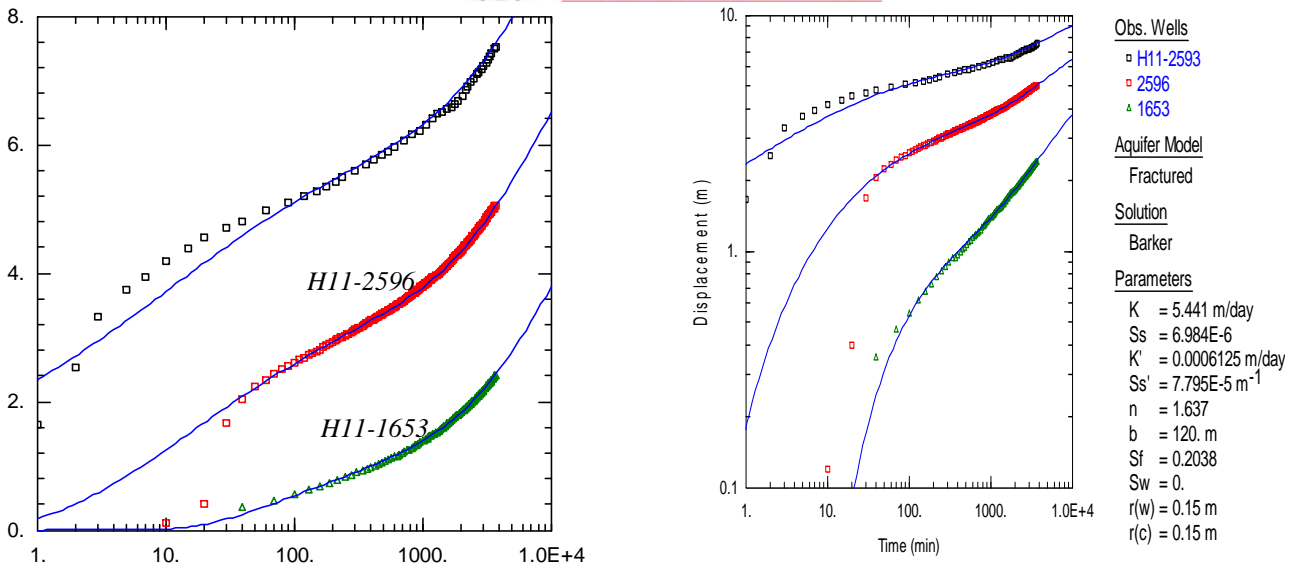


Figure 5.39. Diagnostic plot (semi- log and log-log ) fitted with a fracture (Barker, 1988) model of pumping borehole (H11-2593) and observation boreholes (H11-2596 and H11-1653).

Similarly the furthest observation borehole to the west (H11-1652) shows linear flow followed by a transient flow phase (Figure 5.40). Observation borehole H11-2594 has predominantly a bilinear flow regime, which corresponds to the partial flow dimension of  $n = 1.5$ .

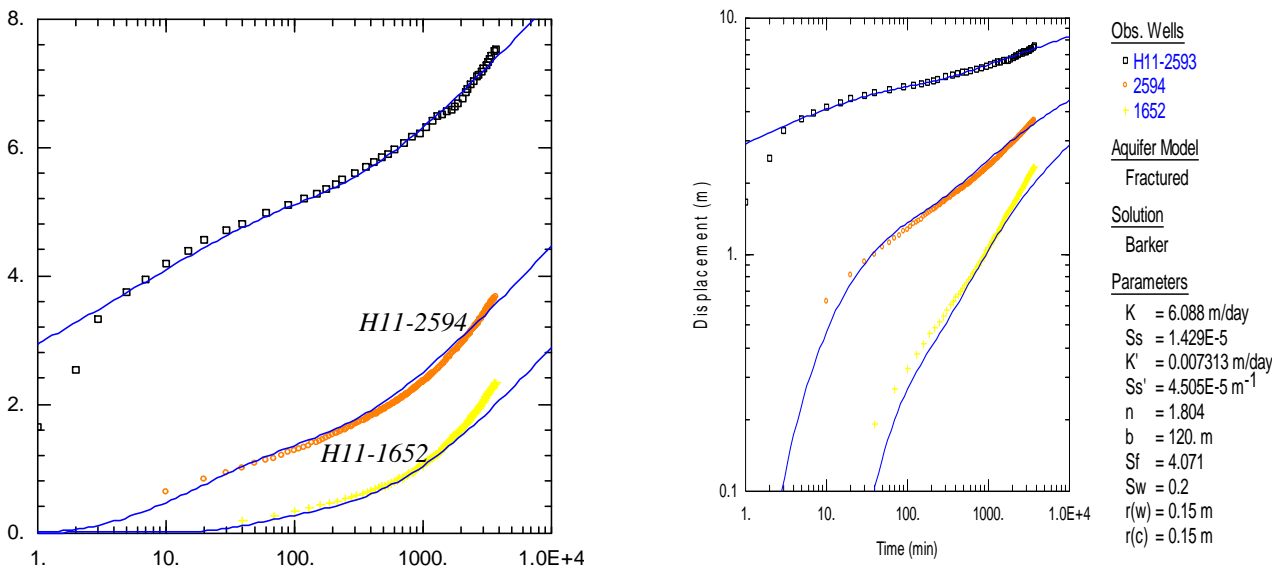
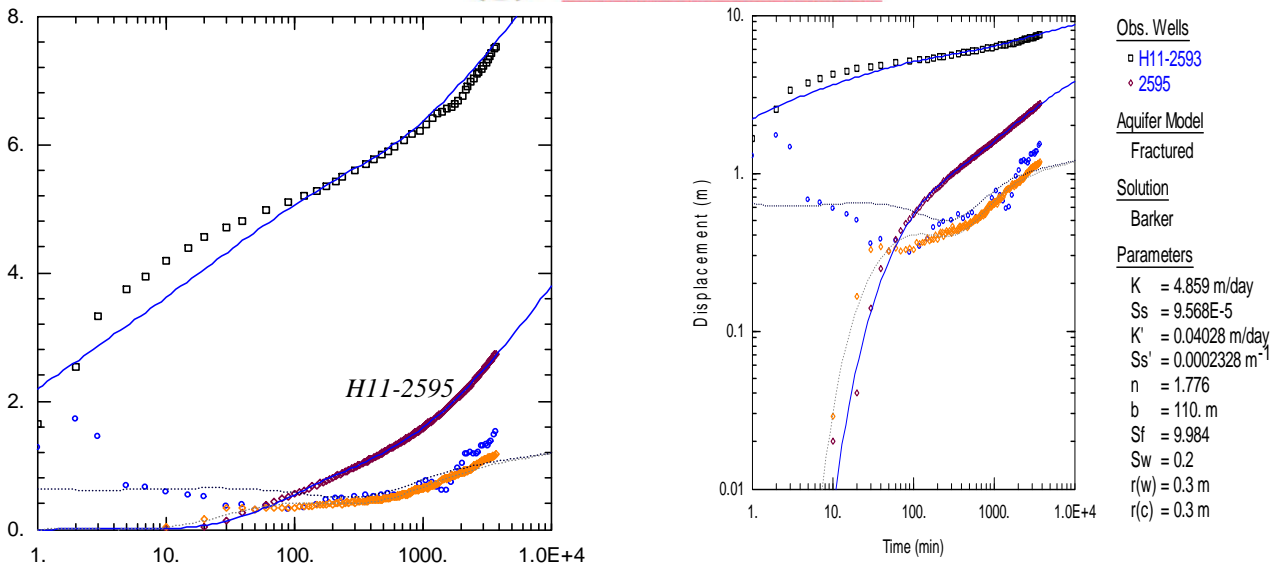


Figure 5.40. Diagnostic plot (semi- log and log-log) fitted with a fracture (Barker, 1988) model of pumping borehole (H11-2593) and observation boreholes (H11-2594 and H11-1652).

The drawdown behaviour of the observation borehole (H11-2595) to the north of the pumping borehole (H11-2593) is illustrated in Figure 5.41. The borehole is characterised by well bore storage followed by a linear flow regime ( $n=1$ ).



**Figure 5.41. Diagnostic plot (semi- log, log-log and derivative) fitted with a fracture (Barker, 1988) model of pumping borehole (H11-2593) and observation borehole (H11-2595).**

A summary of the hydraulic parameters obtained from the curve fitting results are illustrated in Table 5.18. Observed responses in all of the boreholes can be matched with type curves based on the Barker (1988) fracture model. Fitting of the model was biased towards the observation boreholes by placing more weight to these observation boreholes. The obvious good fit of the model (both drawdown and derivative) to the data suggests a sound conceptual model and increased confidence in the estimated parameters.

**Table 5.18. Summary of hydraulic parameters obtained from well field pumping test analysis.**

Observation Boreholes	Distance from abstraction hole (m)	Simultaneous curve fit		
		Hydraulic conductivity (m/day)	Specific storage (S <sub>s</sub> )(m <sup>-1</sup> )	Flow dimension
H11-2593	Pump Well	1.9	0.01	n = 1.9
H11-2596 and -1653	38 and 233	5.9	2.1E-06	n = 1.7
H11-2594 and -1652	58 and 215	6.1	1.5E-05	n = 1.8
H11-2595	65	4.9	9.5E-05	n = 1.8

The studied pumping test setting can be regarded as an unconfined aquifer in the weathered zone underlain (and virtually de-connected by a semi-pervious layer) from a deeper (semi-)confined aquifer. The obtained flow dimensions at the scale of the pumping test are around 1.5 to < 2, suggesting an intermediate flow between bilinear (partial flow dimension) and cylindrical flow (like Theis), implying fairly good connectivity of the fracture network. The flow in this anisotropic fractured rock seems to be generated by a sub-horizontal fracture network (suggested by geophysical logging), connected to a second probably sub-vertical to vertical fracture network. The average hydraulic conductivity from the studied pumping test relates to an effective transmissivity of 677 m<sup>2</sup>/day and, the average specific storage (4.5E-05 m<sup>-1</sup>) relates to a storativity

of 0.004 respectively, considering an aquifer thickness of 120 m. The specific storage of  $4.5E-05 \text{ m}^{-1}$  falls in the upper range of characteristic values ( $3.3E-06$  to  $6.9E-05 \text{ m}^{-1}$ ) for fissured rock (Batu, 1998).

### 5.5. Geological and geomorphologic influence on borehole productivity

This section outlines the identified relationship between the factors that potentially influence groundwater productivity in the crystalline rocks of the study area. The following factors were considered; 1) the geological and topographic setting, 2) dykes and linear anomalies (including their orientation), 3) regional tectonics (maximum horizontal stress), 4) weathering thickness (erosion surface), and 5) proximity to surface water drainages. In order to identify these factors, the dataset was spatially sub-divided using available GIS layers and related to borehole yield (recommended abstraction rate) and transmissivity. Selection criteria ranged from lithology, weathering thickness, rivers, topography, dykes and lineaments. It must be noted that the assessed boreholes were not drilled randomly, but after preliminary site-investigations. The dataset is in this regard biased towards anomalies and higher yields in comparison to random sampling of basement aquifers. However, the large number of successful as well as unsuccessful boreholes compensates partially for this statistical bias.

The four structural domains identified play a major role in the variability of borehole productivity in the larger study area. The cumulative distribution function in Figure 5.42 indicates that the NW domain is more productive followed by the SW domain, the NE domain and then the SE domain. It should be pointed out that major part of south-eastern comprises the Tzaneen escarpment underlain by the poorly weathered and poorly fractured Duivelskloof leucogranite, which have a low groundwater potential as discussed earlier. This is also confirmed by a visual inspection of the spatial transmissivity distribution map (Figure 5.43). The observed variations in transmissivities are not solely related to the dominant dyke orientation or dyke density that formed the basis of the structural regions, but rather factors such as geology, topography and thickness of weathering.

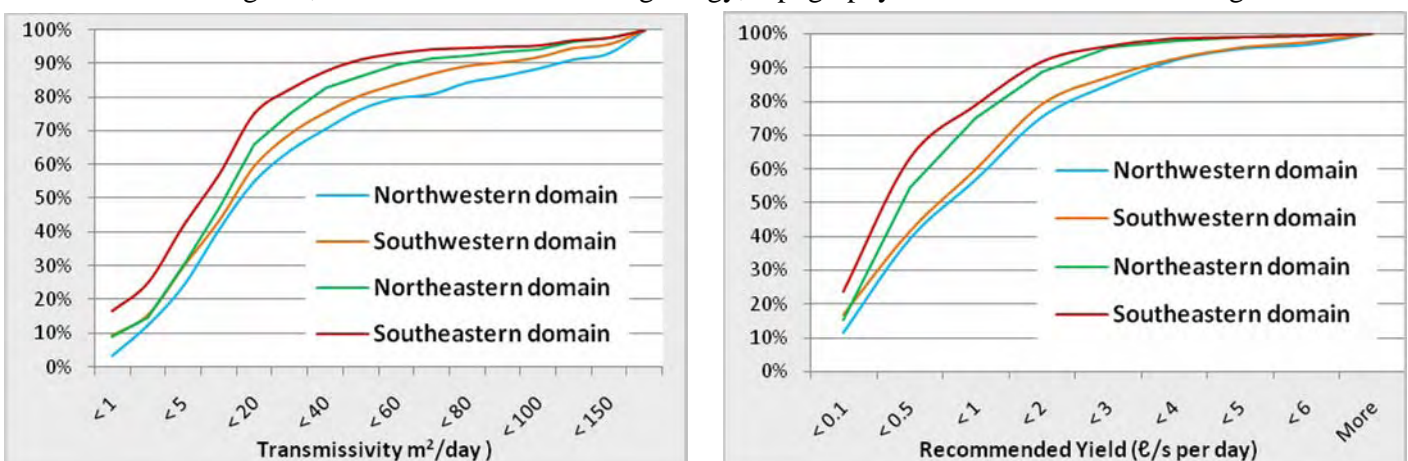


**Figure 5.42. Cumulative frequency of transmissivity and recommended yields from boreholes based on the structural domains delineated in section 4.3**Error! Reference source not found..



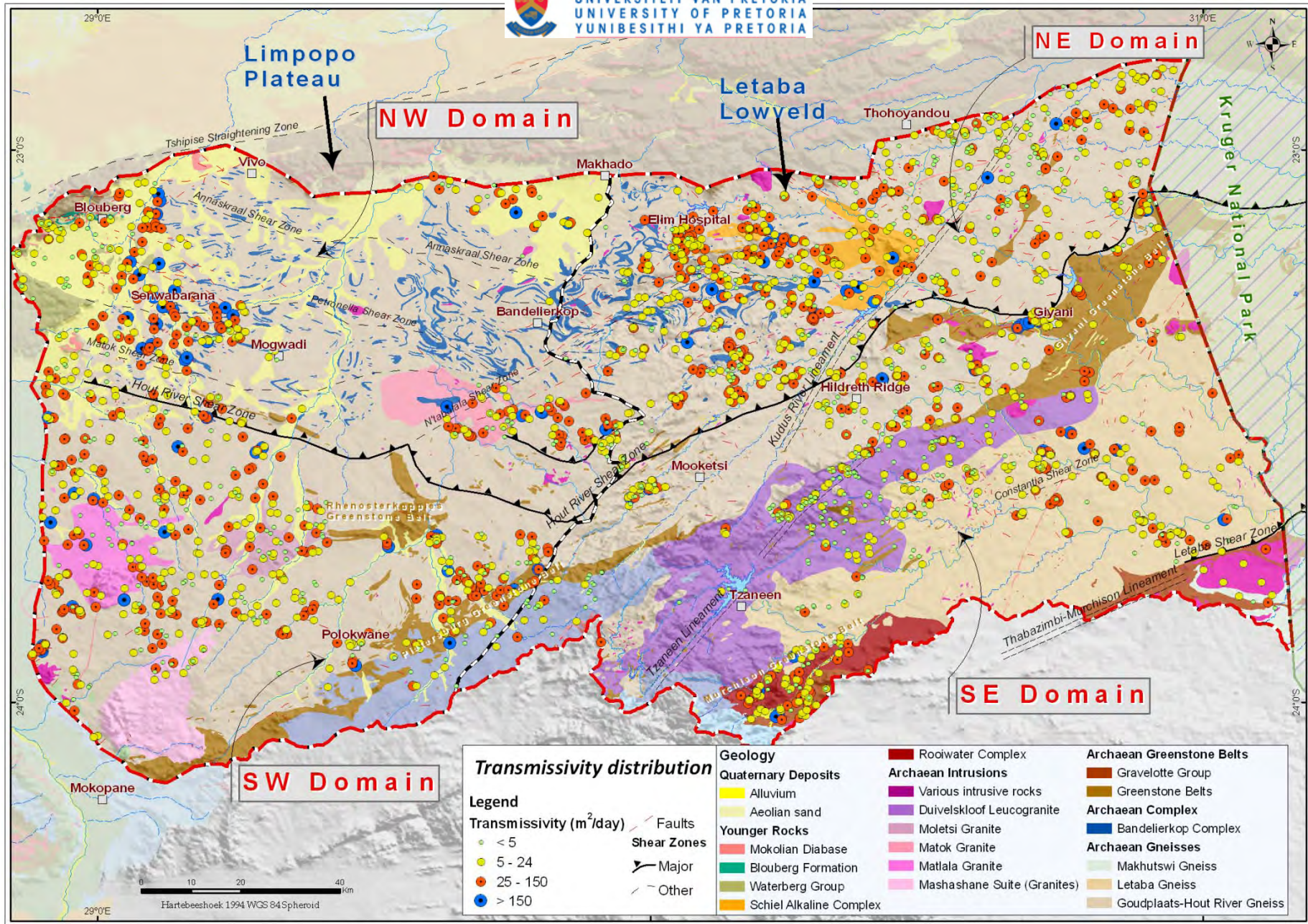
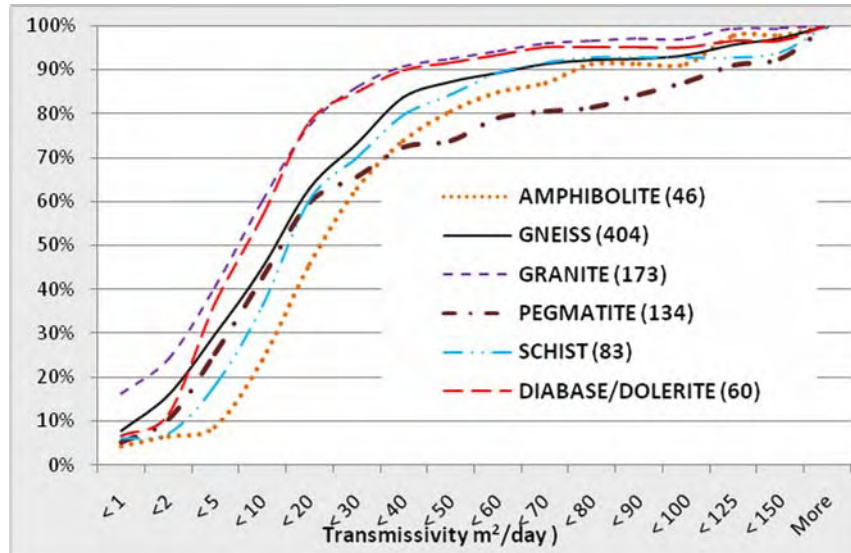


Figure 5.43. Spatial distribution of transmissivity obtained from the GRIP dataset.



### 5.5.1. Geological setting

The first analysis is based on the lithological information (driller’s geological note) captured in the GRIP dataset. Unfortunately 90 percent of the lithology captured pertains to the Letaba Lowveld. Nevertheless the cumulative frequency graph of the major lithologies in the area clearly indicates the relative poor productivity of granites and diabase/dolerite associated with dykes in comparison to pegmatite (Figure 5.44).



**Figure 5.44. Cumulative frequency distributions showing the influence of various rock types on borehole productivity (number of boreholes in brackets).**

Pegmatite is clearly more productive especially in the latter ranges of the frequency plot. Eighty percent of boreholes drilled in pegmatite attained transmissivities of 60 m<sup>2</sup>/d with a mean value of 44 m<sup>2</sup>/d (Table 5.19). Another rock type that supports productive boreholes is amphibolite with a mean transmissivity of 35 m<sup>2</sup>/d. These mylonitic rocks are associated with the crushing and intense shearing coupled with the Limpopo Mobile Belt orogeny. As a result the regional amphibolite-grade metamorphism within the Hout River Shear Zone is a favourable groundwater target. Specific rock type clearly plays an important role in the selection of drilling targets in the Limpopo Province, however, rocks such as pegmatite often occurs as veins, forming features of restricted extent rather than a regional groundwater exploratory feature (Cook, 2003).

**Table 5.19. Determined hydrogeological parameter based on the geology observed during drilling.**

Lithology	Nr. of BH's	Transmissivity m <sup>2</sup> /d	Rec. Yield L/s per day
<b>ALL</b>	<b>827</b>	<b>29.6</b>	<b>0.85</b>
Amphibolites	33	35	1.29
Diabase/dolerite	36	20	0.82
Gneiss	426	31	0.97
Granite	140	21	0.74
Pegmatite	117	44	1.13
Schist	75	29	0.94

For the second analysis, the boreholes were grouped according to the geological or lithological setting and the corresponding mean values along were calculated and compared (one-sample Student t-test, see section 3.5.1) to the total population Table 5.20.

**Table 5.20. Determined hydrogeological parameter based on the geological setting of boreholes.**

Parameter	Transmissivity m <sup>2</sup> /d		Rec. Yield ℓ/s per day	
	Nr. of BH's	Values	Nr. of BH's	Values
<i>All data</i>	<u>2 484</u>	<u>30</u>	<u>3 032</u>	<u>1.04</u>
<i>Alluvium</i>	200	<b>44</b>	245	<b>1.63</b>
<i>Significance</i>		100 %		100 %
<i>Aureole</i>	60	<b>42</b>	68	<b>1.64</b>
<i>Significance</i>		95%		99 %
<i>Bandelierkop Complex</i>	47	<b>34</b>	51	<b>0.89</b>
<i>Significance</i>		69 %		81 %
<i>Goudplaats-Hout River Gneiss</i>	1 400	<b>33</b>	1 650	<b>1.14</b>
<i>Significance</i>		96 %		100 %
<i>Letaba Gneiss</i>	195	<b>24</b>	281	<b>0.79</b>
<i>Significance</i>		97 %		100 %
<i>Major Batholith's</i>	84	<b>16</b>	102	<b>0.72</b>
<i>Significance</i>		100 %		100 %
<i>Greenstone Belts</i>	123	<b>31</b>	175	<b>0.90</b>
<i>Significance</i>		62 %		93 %
<i>Rooiwater Complex</i>	40	<b>29</b>	48	<b>1</b>
<i>Significance</i>		53 %		83 %
<i>Alkaline Complex</i>	50	<b>35</b>	41	<b>1.1</b>
<i>Significance</i>		93 %		86 %
<i>Leucogranites</i>	230	<b>7</b>	299	<b>0.35</b>
<i>Significance</i>		100 %		100 %
<i>Waterberg Group</i>	55	<b>12</b>	72	<b>0.73</b>
<i>Significance</i>		100 %		100 %

There is a distinct variability in the transmissivities between the lithologies and geological settings of the The highest borehole productivity is - as expected - observed in the primary alluvial aquifers, whilst the least productive boreholes are associated with the elongated granites and leucogranites straddling the escarpment between the Limpopo Plateau and Letaba Lowveld. Similarly low productivities with average transmissivities of 16 m<sup>2</sup>/d and average yields of 0.7 ℓ/s are observed in boreholes targeting the granitic batholiths (inselbergs). However, boreholes located along the contact zones of these batholiths provide the highest productivities of the crystalline bedrock. These granitic intrusives can displace the host rocks during intrusion in order to create space for the ascending magma. A number of physical changes occur in the host rock i.e. tension jointing, peripheral cleavage and ductile deformation, enhancing the water bearing characteristics of the host rock (Du Toit, 2001).The younger, large elongated leucogranites together with the main batholiths bodies itself and the sedimentary rocks of the Waterberg group have the lowest transmissivities. The Letaba gneisses which lie to the south of the leucogranites have a slightly lower productivity compared to the Goudplaats-Hout River Gneiss, which may be related to other factors such as fracture density and susceptibility to weathering (Figure 5.43). The Greenstone belts and other igneous complexes have productivities similar to the population mean.

### 5.5.2. Weathered layer (regolith) and erosion surfaces

To establish the influence of the weathered layer on the productivity of a borehole, the depth of weathering was related to borehole productivity. The scatter diagrams (Figure 5.45) show no correlation between transmissivity and weathering or between yield and weathering.

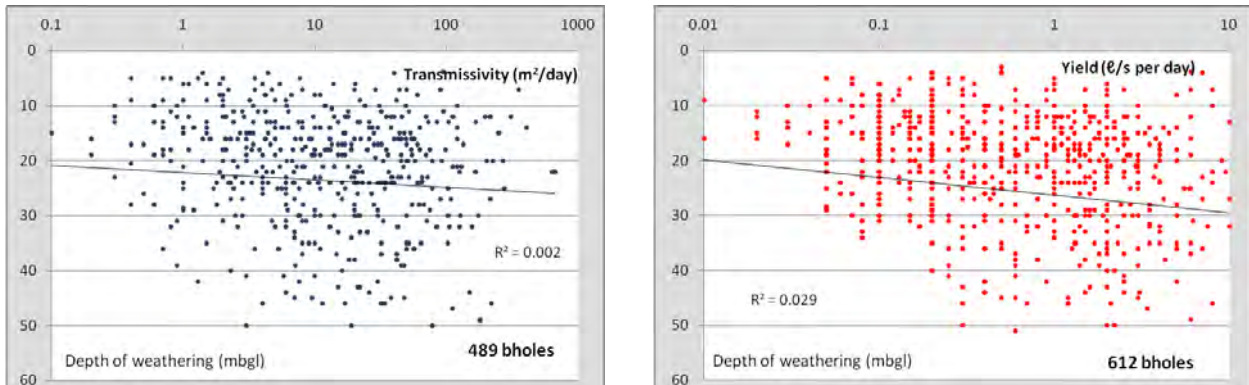


**Figure 5.45. Graphs showing the correlation between transmissivity and depth of weathering and between yield and depth of weathering.**

Chilton and Foster (1995) highlighted the fact that very few authors if any could obtain significant correlations between regolith thickness and borehole yield from statistical approaches. The authors attributed these poor correlations to the subjectivity of the yield value itself and to the overriding local factors such as well construction and efficiency. The common viewpoint in crystalline hydrogeology is therefore that a deeper weathering profile would be a major controlling factor on the borehole productivity due to the enhanced permeability and storage of this zone. However, in this case the semi-arid environment is characterised by a thin regolith (with less important water strikes) overlying the fractured aquifer where the main water bearing fractures is encountered.

The relationship between borehole productivity and the Post-African, and African erosion surfaces is illustrated in Figure 5.46. The data was compiled through a mutual Water Research Commission and British Geological Survey project known as the Grey Data Project. The results of available case histories from four individual Sub-Saharan countries (Uganda, Zimbabwe, Malawi and South Africa) were used to compare borehole productivities between the African and Post African erosion surface. The distinct high borehole productivity associated with the South African erosion surfaces are related to the high yielding nature of this basement aquifer system, while the post African erosion surface is slightly more comparable with the Malawi results. However, it is difficult to conclude that African (older) do indeed offer a more productive aquifer, due to the complexity and interplay of local factors controlling borehole yields (Figure 5.46).



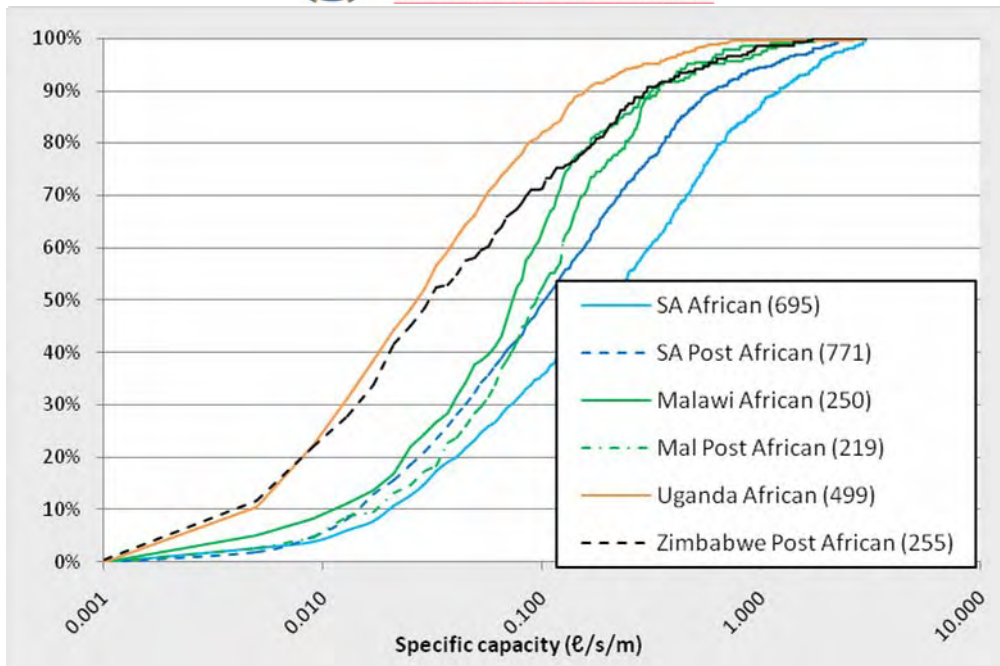


Figure 5.46. Cumulative frequency distributions showing the influence of erosion surfaces on borehole productivity (number of boreholes in brackets).

### 5.5.3. Topographic setting and drainages

The transmissivity and borehole yield data were filtered according to the topographic setting of the boreholes (as recorded by the driller) (Table 5.21) (Figure 5.47). As expected the boreholes located along rivers (alluvial aquifers) have above average transmissivities and yields, i.e. they represent the most favourable borehole locations from a topographic point of view. Boreholes in mountainous areas are on the other hand the least favourable locations.

Table 5.21. Determined hydrogeological parameter based on the topographic setting of boreholes.

Parameter	Transmissivity m <sup>2</sup> /d		Rec. Yield ℓ/s per day	
	Nr. of BH's	Values	Nr. of BH's	Values
<i>All data</i>	<u>1 449</u>	<u>30</u>	<u>1 837</u>	<u>1.04</u>
<i>Along River</i>	424	<b>33</b>	245	<b>1.35</b>
<i>Significance</i>		53 %		100 %
<i>Mountain</i>	23	<b>7</b>	35	<b>0.32</b>
<i>Significance</i>		100 %		100 %
<i>Slope</i>	300	26	392	0.84
<i>Significance</i>		100 %		100 %
<i>Valley</i>	82	31	98	0.91
<i>Significance</i>		66 %		98 %
<i>Flat Surface</i>	620	<b>38</b>	789	1.15
<i>Significance</i>		96 %		78 %



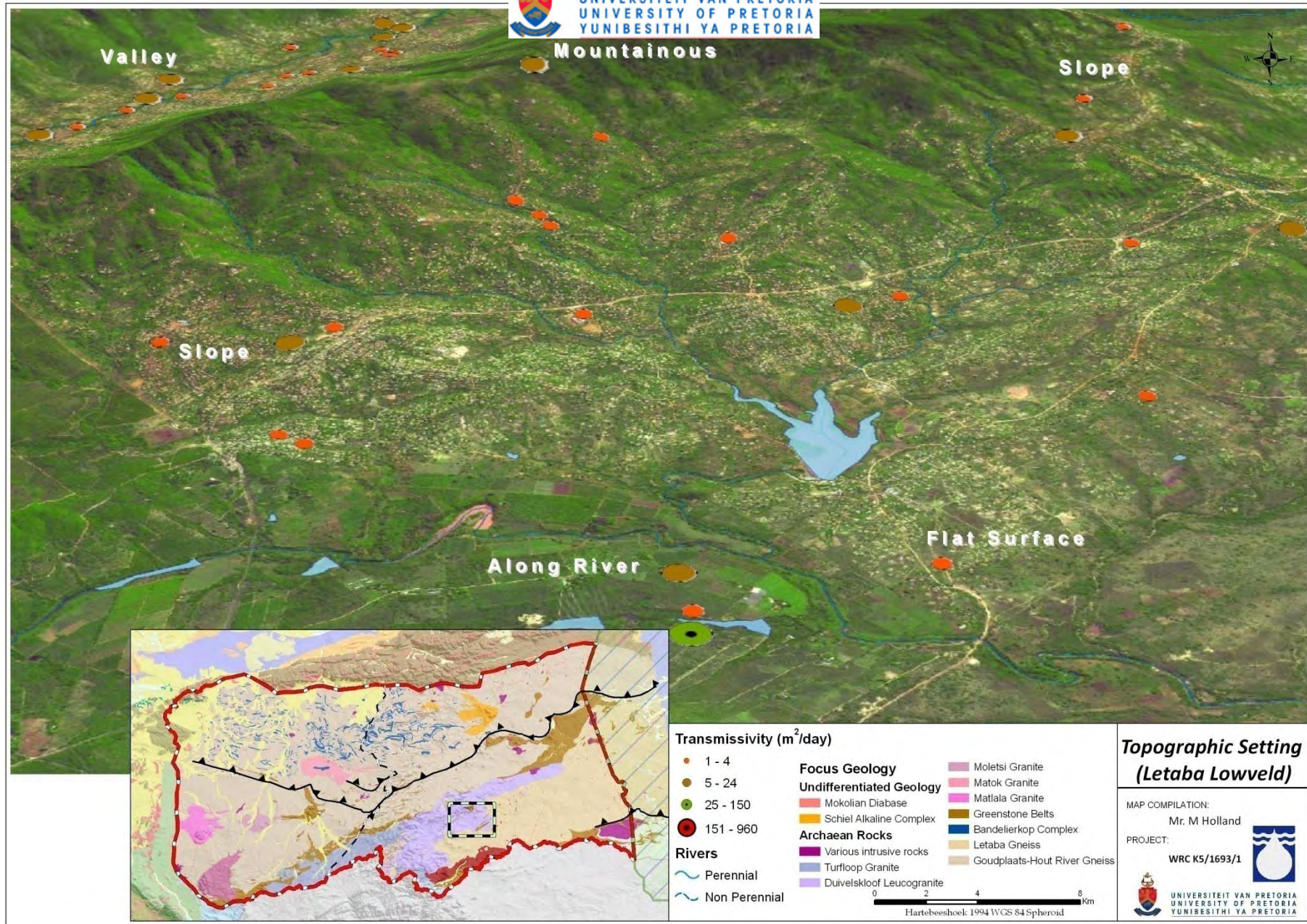


Figure 5.47. Typical setting of boreholes in relation to rivers and topography.

### Proximity to rivers

To determine the influence of drainage channels on the borehole productivity, a spatial assessment of proximity was conducted (Table 5.22). 55% of all boreholes in the dataset are drilled within 150 m to streams or rivers as mapped on the 1:50 000 topographic map sheets of South Africa. Furthermore, 19 % of these boreholes are along the major perennial drainage channels. Boreholes close to both minor and major surface drainages have above average transmissivity and yields indicate the strong influence of surface water bodies on borehole productivity.

**Table 5.22. Influence of proximity to rivers and streams on borehole productivity.**

Area	Parameter	Transmissivity m <sup>2</sup> /d			Rec. Yield ℓ/s per day		
		Nr. of BH's	Mean	Median	Nr. of BH's	Mean	Median
Limpopo	<i>All data</i>	<b>967</b>	<b>38</b>	<b>15</b>	<b>1137</b>	<b>1.45</b>	<b>0.8</b>
	<i>Within 150 m (River)</i>	177	<b>51</b>	26	206	<b>2.11</b>	1.6
	<i>Within 150 m (Stream)</i>	250	36	14	290	1.36	0.8
	<i>Further than 150 m</i>	540	<b>35</b>	12	641	1.28	0.7
Letaba	<i>All data</i>	<b>1542</b>	<b>24</b>	<b>10</b>	<b>1925</b>	<b>0.80</b>	<b>0.4</b>
	<i>Within 150 m (River)</i>	325	<b>32</b>	14	389	<b>1.03</b>	0.6
	<i>Within 150 m (Stream)</i>	742	23	9.1	918	0.79	0.3
	<i>Further than 150 m</i>	475	<b>21</b>	7.7	618	<b>0.66</b>	0.4

It can be concluded that both topography and proximity to rivers has a significant influence on borehole productivity. Drainage channels tend to follow zones of structural weaknesses (i.e. lineaments) in the near surface; therefore rocks in the vicinity of rivers might be more intensely fractured, jointed and/or weathered. From a hydraulic point of view, water levels are generally shallower at topographic lows and present discharge zones, providing more available drawdown and a larger capture zone compared to boreholes in mountainous areas drilled to approximately the same depth below ground surface.

#### 5.5.4. Relationship to dykes

As dykes occur extensively in the study area, it is important to establish their role in the occurrence of groundwater. Based on the geological logs, boreholes which encountered dykes (diabase or dolerite) have generally lower productivity than boreholes devoid of diabase/dolerite (Figure 5.48). Another useful assessment of the role of dykes on borehole productivity is proximity to the mapped (published) dykes and regional aeromagnetic data (inferred dykes). Data from 1000 boreholes shows that drilling in the Limpopo Plateau within 25 m of dykes is more productive compared to wells further away. It is evident that although boreholes intersecting dykes are poor targets, drilling along dykes seems to be promising.



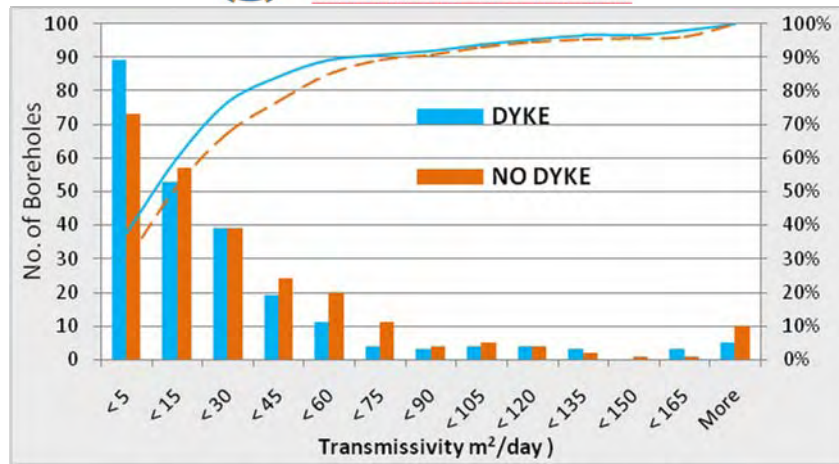


**Figure 5.48. Frequency histograms and cumulative distribution showing the influence of dykes encountered on transmissivity estimates.**

Due to the generally high transmissivity of the gneisses in the Limpopo Plateau (Figure 5.44), the cross cutting of less permeable dykes may act as flow barriers and, in conjunction with the greater fissuring commonly associated with dykes may enhance the accumulation of water. In contrast, drilling in close proximity to dykes in the Letaba Lowveld neither enhances nor reduces borehole productivity appreciably. Based on 1500 boreholes no significant relationship between transmissivity and distance to dykes exists (Table 5.23). It can be argued the permeability of these closely spaced dykes is not very different from the host rocks, the gneisses or granites, in which they occur. In this regard, their water bearing potential is as variable as the host rock, as they do not act as flow barriers or conduits.

**Table 5.23. Transmissivity (m<sup>2</sup>/d) of boreholes according to distance to inferred dykes.**

	Distance to Dyke	< 25 m	25 – 50 m	50 -150 m	≥ 150 m	Total
<b>Limpopo</b>	N	25	34	96	812	967
	Mean T (m <sup>2</sup> /d)	<b>51.4</b>	39.4	<b>27.6</b>	38.7	38.0
	Median T (m <sup>2</sup> /d)	<b>26.0</b>	19.5	<b>13.9</b>	15.0	15.0
<b>Letaba</b>	N	65	50	200	1227	1542
	Mean T (m <sup>2</sup> /d)	22.6	24.0	21.5	<b>25.1</b>	24.5
	Median T (m <sup>2</sup> /d)	10.0	<b>8.8</b>	9.2	10.0	10.0

To evaluate the correlation between borehole productivity and the trend of dykes (azimuth), boreholes occurring within 150 m of dykes were examined more closely within each region (Figure 5.49). Within the Limpopo Plateau NW to NNE (315° to 30°) striking dykes offer evidently poorer water bearing characteristics compared to dykes striking NE (30 to 45°) or ENE (75 to 90°) with median transmissivities above 25 m<sup>2</sup>/d. However, the box plots show similar transmissivity ranges (i.e. lower and upper quartiles) for WNW (270-315°) NE to ENE (30 to 90°) trending dykes (Figure 5.49). On the one hand high transmissivity along WNW dyke trends supports the assumption that structures striking parallel to the maximum horizontal stress are open. On the other hand, despite the fact that the effects of the neo-tectonic regime suggest

closure of conduits striking NE, these NE to ENE trending dykes have remained open throughout geological history. These older structures can be regarded as extensional features. The results clearly show the variability in targeting dykes based on their strike, but if any conclusion can be made, it is to reconsider drilling along dykes trending NW to NNE (315-30°). This is also observed in the Letaba Lowveld where dykes trending NW to NNE (315-30°) are associated with lowest median transmissivity and also the lowest lower range (Figure 5.49). However, apart from a slightly larger range of transmissivities observed along lineaments with a W to WNW (275-315°) trend, no obvious orientations with significantly increased lower or upper quartiles are evident from the results in the Letaba Lowveld (Figure 5.49). As shown in the previous discussion the significance of drilling within the proximity of a dyke in the Letaba Lowveld is neither positive nor negative and this is supported by the dyke orientation analysis.

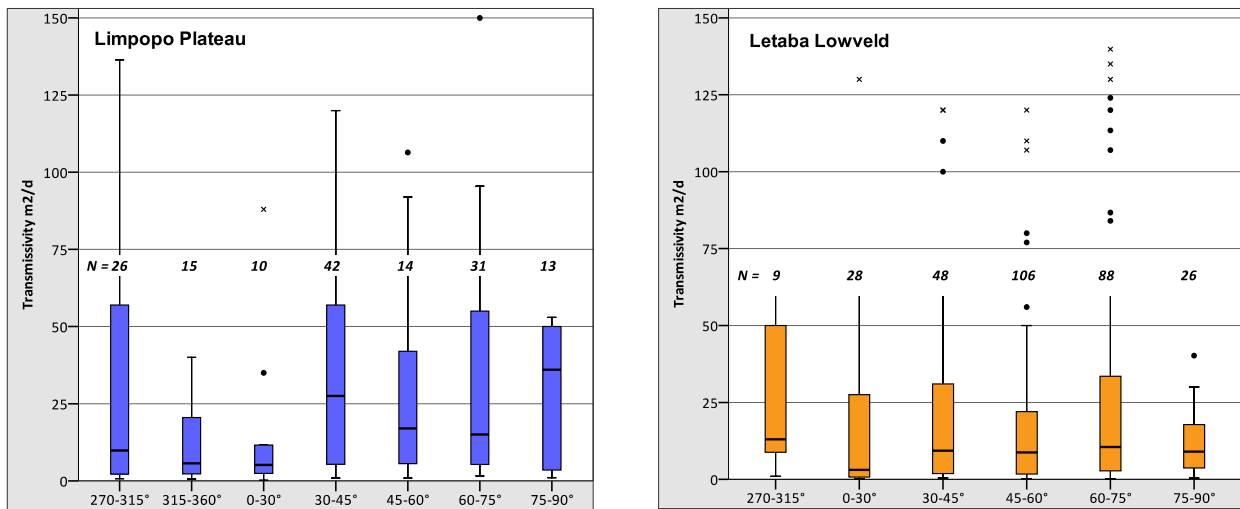


**Figure 5.49.** Box plot of transmissivity and dyke azimuth for both the Limpopo and Letaba regions. The box represents the 25 and 75 % quartiles, while the median is represented by the *horizontal line within the box*. Outliers are marked by circles and by crosses. The vertical lines (*whiskers*) connect the smallest and largest non-outliers.

### 5.5.5. Relationship to lineaments

The most significant correlation between transmissivity and proximity to lineaments is found in the north-western domain where both mean and median transmissivities within 50 m of a lineament exceed the population average (Table 5.24). Results vary slightly for the south-western domain with regards to the arbitrary distance ranges chosen, however, average transmissivities within 150 m of a lineament do show slightly higher borehole productivities compared to further away. Boreholes within 25 m of mapped lineaments in the north-eastern domain have higher median transmissivities compared to boreholes further than 150 m, although mean transmissivities are similar for all distance classes (Table 5.24). In the south-eastern domain notably higher borehole productivities are observed within the 50 – 150 m range compared to boreholes further than 150 m. Based on the results, it can be generally accepted that lineaments have a positive influence on borehole productivity and should be considered for future drilling programs.



**Table 5.24. Productivity of boreholes according to distance to inferred lineaments.**

Domain	Distance to lineaments	< 25 m	25 – 50 m	50 -150 m	≥ 150 m	Total
NW Domain	N	6	13	33	294	346
	Mean T (m <sup>2</sup> /d)	<b>93.3</b>	69.8	<b>32.7</b>	44.6	45.2
	Median T (m <sup>2</sup> /d)	<b>64</b>	36	18.4	<b>15.5</b>	17
	N	6	13	33	328	380
	Mean Rec. yield ℓ/s	<b>2.8</b>	1.43	1.6	1.64	1.65
SW Domain	N	16	9	61	459	545
	Mean T (m <sup>2</sup> /d)	<b>38.9</b>	<b>27.9</b>	36.6	37.1	37
	Median T (m <sup>2</sup> /d)	<b>25.5</b>	22	20	<b>16</b>	17
	N	16	9	61	495	581
	Mean Rec. yield ℓ/s	<b>2.1</b>	1.5	1.55	<b>1.44</b>	1.47
NE Domain	N	30	28	80	628	766
	Mean T (m <sup>2</sup> /d)	21.8	25.1	<b>19.6</b>	<b>28.4</b>	27.1
	Median T (m <sup>2</sup> /d)	<b>15.6</b>	9.4	11	12	12
	N	30	28	80	682	820
	Mean Rec. yield ℓ/s	<b>0.69</b>	0.93	<b>0.94</b>	0.94	0.93
SE Domain	N	23	21	63	668	775
	Mean T (m <sup>2</sup> /d)	<b>21.5</b>	19.8	<b>28.3</b>	22.6	23
	Median T (m <sup>2</sup> /d)	<b>6</b>	9.5	<b>12</b>	8	8
	N	23	21	63	840	947
	Mean Rec. yield ℓ/s	0.86	<b>0.41</b>	<b>0.94</b>	0.81	0.81

*North-western and South-western domain (Limpopo Plateau)*

The NW structural domain has a complex tectonic history and intense shearing and fracturing of the crystalline rocks has created highly productive fractured aquifers (Figure 5.42). The most common lineament strike direction is ENE (70° to 80°), based on the rose diagram developed for each domain (Figure 5.50). This trend is almost parallel with the dominant dyke trend of 66° and oblique to the average azimuth of joints (23°) observed from field measurements (see Figure 4.10). Productive boreholes are not associated with only one lineament trend direction, but the least favourable lineament trend appears to be ENE (60-75°) with below average transmissivities observed (Table 5.25). However, the results are in some cases based on a small borehole population.



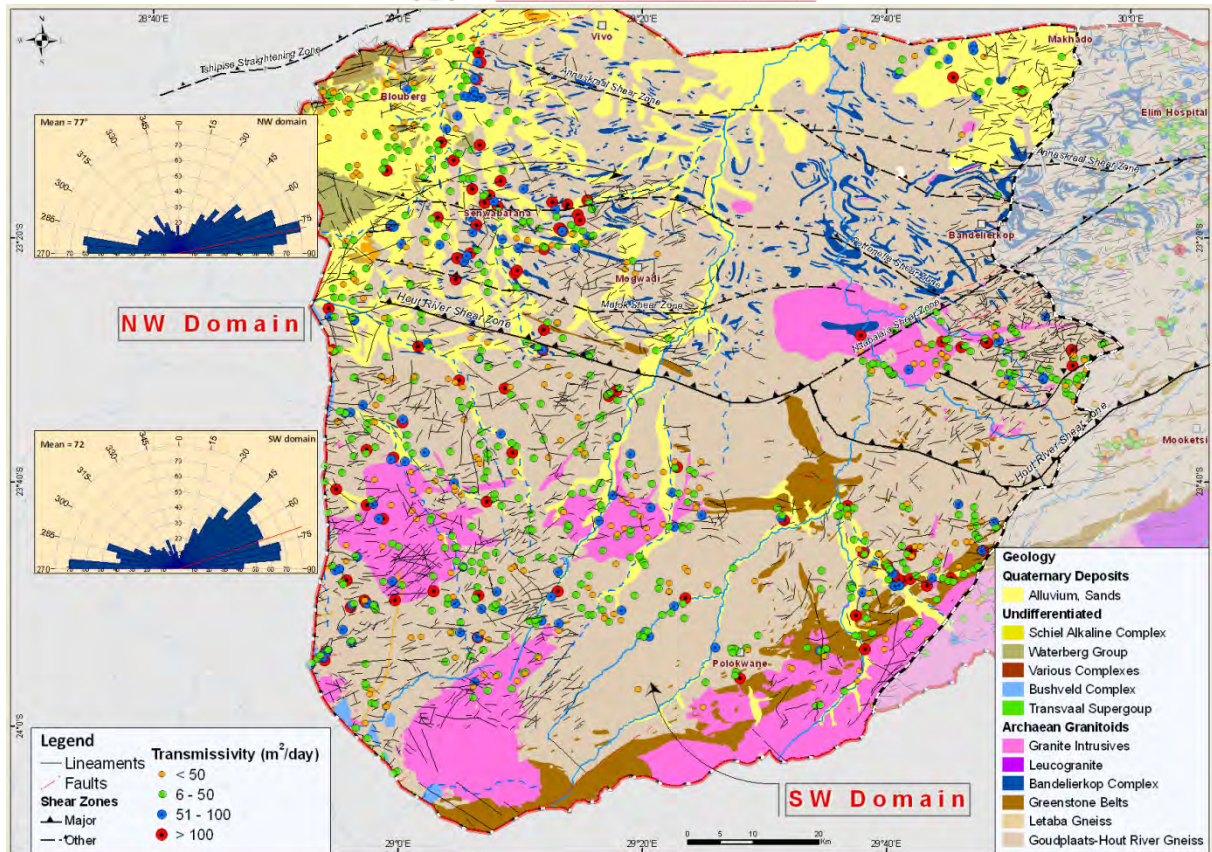


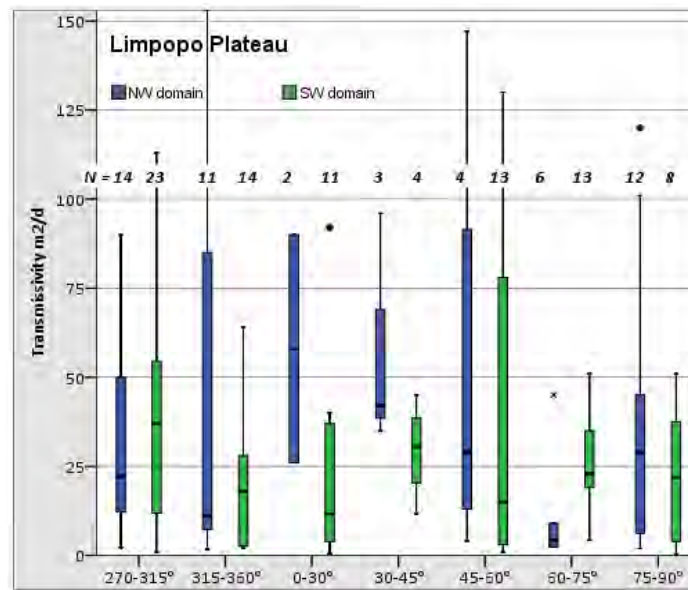
Figure 5.50. Distribution of shear zones, faults and lineaments in the Limpopo Plateau, with the lineament frequency rose diagram showing main structural trends.

Table 5.25. Transmissivity (m<sup>2</sup>/d) of boreholes according to distance to inferred lineaments within the Limpopo Plateau.

Domain	Lineament azimuth	270-315°	315-360°	0-30°	30-45°	45-60°	60-75°	75-90°
NW domain	N	14	11	2	3	4	6	12
	Mean T (m <sup>2</sup> /d)	50.5	49.5	58.0	<b>57.7</b>	52.3	11.2	36.3
	Median T (m <sup>2</sup> /d)	22.2	11.0	58.0	<b>42.0</b>	29.0	4.3	29.0
SW domain	N	23	14	11	4	13	13	8
	Mean T (m <sup>2</sup> /d)	41.4	21.1	28.4	29.4	<b>48.6</b>	39.0	36.6
	Median T (m <sup>2</sup> /d)	<b>37.0</b>	18.0	11.6	30.5	15.0	23.0	22.0

Considering the borehole populations, median transmissivity and range of transmissivity it is interpreted that the most productive boreholes may be associated with ENE to E trends (75-90°) (Figure 5.51) which is almost perpendicular to the current NW maximum horizontal stress regime. Lineaments striking W to WNW (270-315°) are associated with higher average and median borehole productivities compared to NNW to N (315-360°) (Table 5.25). These trends are slightly oblique to the current horizontal stress regime and it may be interpreted that the W to WNW trends are more favourable targets compared to the latter and may have opened due to this acting stress regime. This is even more apparent in the south-western domain where above average and

median transmissivity are associated with lineament trends striking W to WNW (270-315°) and offer potentially the most productive lineament target. Other high borehole productivities was observed along lineaments striking ENE to E (60-90°) with the least favourable lineaments associated with N to NNE (0-30°) trends (Figure 5.51).



**Figure 5.51.** Box plot of borehole transmissivity in relation to the lineament azimuth in the Limpopo Plateau.

*North-eastern and South-eastern domain (Letaba Lowveld)*

The prominent ENE (60-75°) lineament strike direction in the NE structural domain is almost parallel to the observed dyke trend and joint orientations based on field measurements (Figure 5.52). Although no single preferred lineament orientation is distinctly clear, based on the observed average and median transmissivity 45 to 60° provide the least favourable groundwater potential, while it is clear the N to NE (0-45°) and ENE to E (60-90°) is by far superior compared to lineaments striking W to N (270-360°) (Table 5.26) (Figure 5.53). This is in contrast to what is expected under current stress conditions, with lineaments striking perpendicular to the current stress regime providing higher transmissivity.

**Table 5.26.** Transmissivity (m<sup>2</sup>/d) of boreholes according to distance to inferred lineaments within the Letaba Lowveld.

Domain	Lineament azimuth	270-315°	315-360°	0-30°	30-45°	45-60°	60-75°	75-90°
NE domain	N	26	14	11	9	13	35	30
	Mean T (m <sup>2</sup> /d)	17.4	12.9	<b>36.2</b>	35.7	6.7	25.2	20.4
	Median T (m <sup>2</sup> /d)	11.8	10.6	12.4	12.9	4.0	12.0	<b>16.7</b>
SE domain	N	21	8	15	27	4	15	17
	Mean T (m <sup>2</sup> /d)	15.4	15.3	<b>25.4</b>	14.5	13.0	21.5	23.0
	Median T (m <sup>2</sup> /d)	8.0	13.5	12.0	7.7	10.0	<b>19.0</b>	14.0



Similar results is observed in the SE structural domain where preferred lineament orientations are associated with lineament trending ENE to E (60 to 90°), while lineaments striking NE (30 to 60°), which is along the strong main NE lineament trend (Figure 5.53), provide evidently the least favourable groundwater potential.

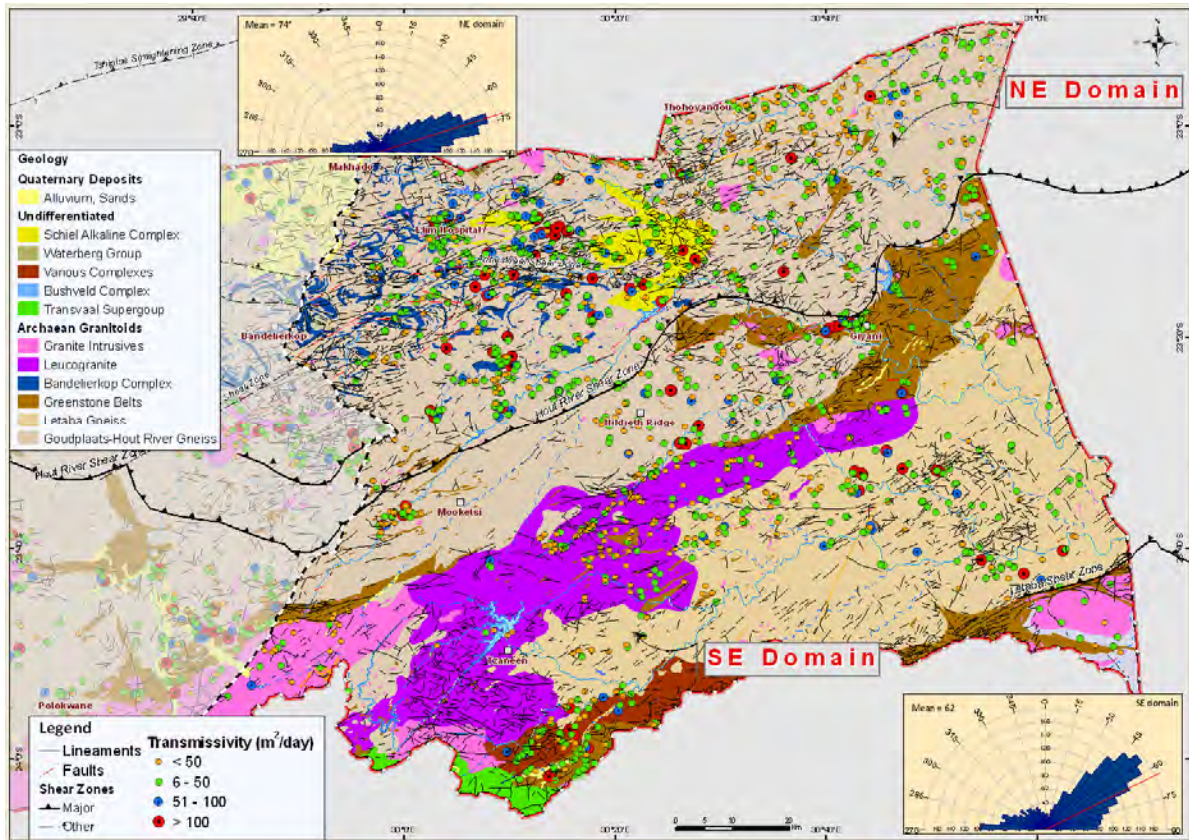


**Figure 5.52.** Distribution of shear zones dykes, faults and lineaments in the Letaba Lowveld, with the lineament frequency rose diagram showing main structural trends (squares indicate field studies).

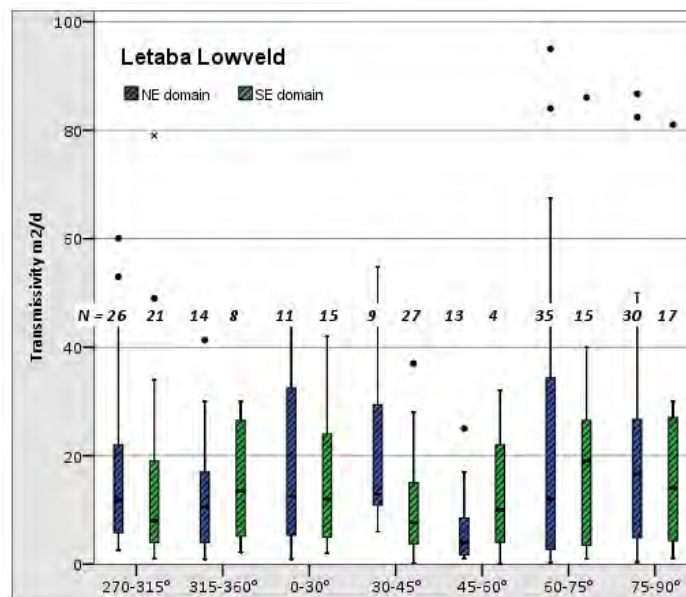


**Figure 5.53.** Box plot of borehole transmissivity in relation to the lineament azimuth in the Letaba Lowveld.



### 5.5.6. Field observation (testing the results)

Field verification of the lineament borehole productivity relationship were tested as part of the GRIP programme for the augmentation of a surface water supply scheme in the Great Letaba catchment (SE Domain, see Figure 5.52).

#### *Dzumeri*

A 5000 m geophysical profile striking NNE to SSW was conducted to pin-point drilling targets and to verify regional ASTER lineaments and aeromagnetic dykes (Figure 5.54). A number of anomalies from the geophysical profile correspond with the regional lineaments Five out of the 7 boreholes drilled along the profile were successful with an airlift yield of more than 0.1 l/s.

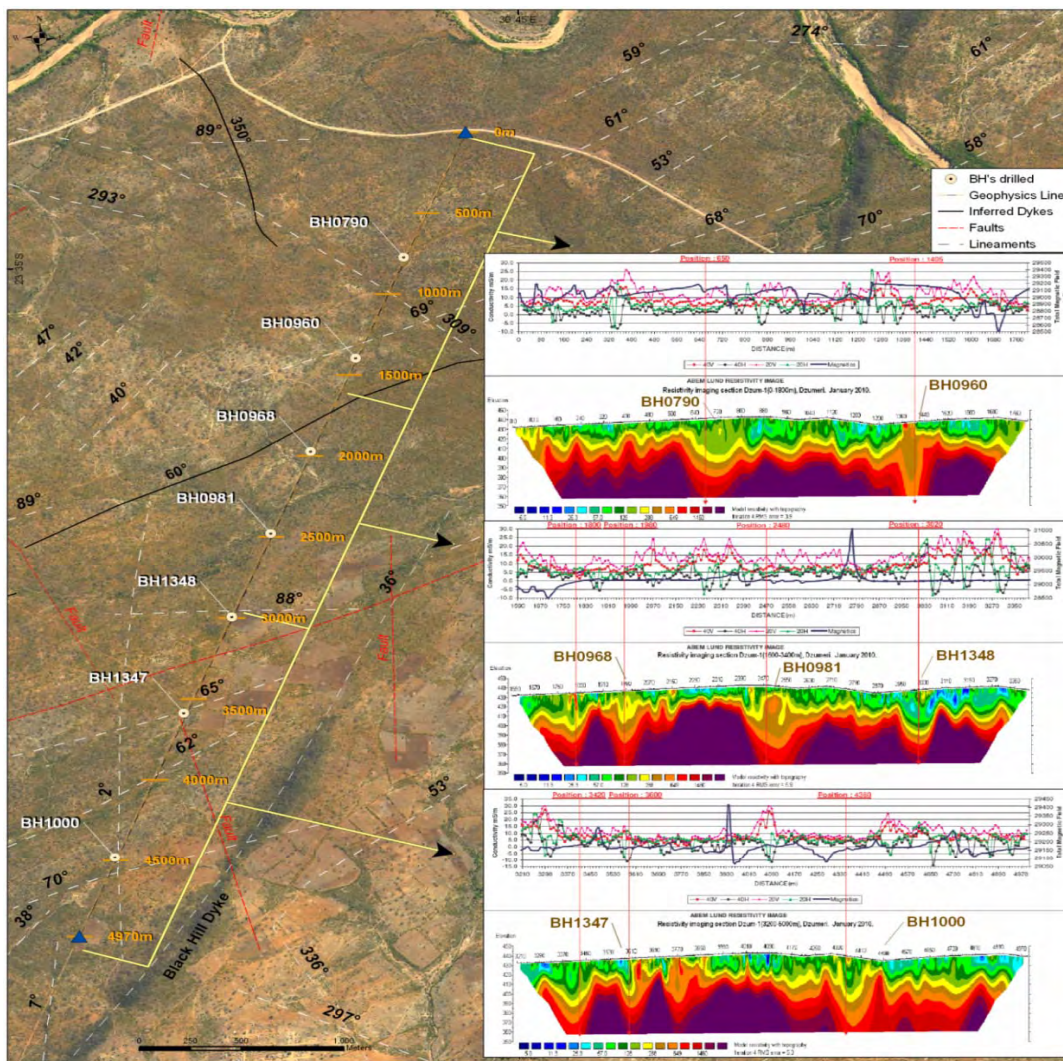
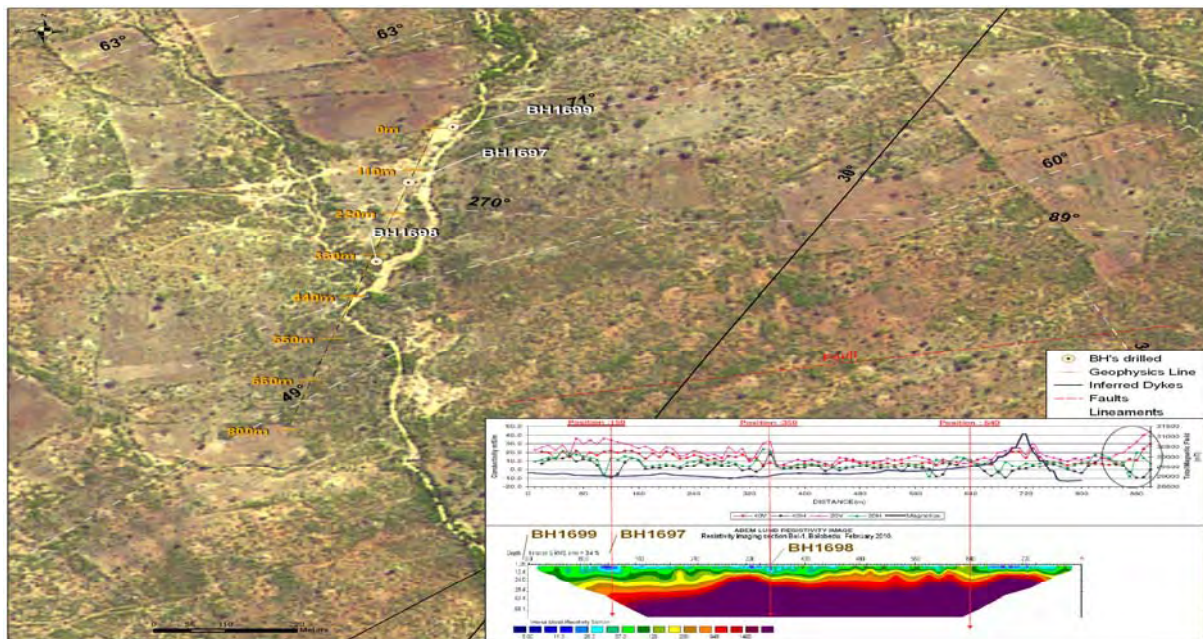


Figure 5.54. Field study location and the 5 km geophysical profile near Dzumeri village.

Throughout the length of the resistivity profile a number of deeper weathering zones ( $< 100 \Omega\text{m}$ ) are observed which relates to the lineaments observed in the field. Although boreholes targeting these weathered zones were successful, the yields were relatively low (Table 5.27). In most cases water was encountered below the regolith which highlights the fact that the relatively thin regolith ( $< 25 \text{ m}$ ) alone does not produce significant yields for water supply purposes. Fissure zones could be identified from the anomalies detected on the conductivity profile especially from 3 000 m to 3 300 m where borehole BH1348 was drilled. Boreholes targeting these anomalies were not all high yielding (i.e. BH1347 and BH 1000) and this could be related to the fact that some of these fractures are closed to groundwater flow. Two boreholes with an airlift yield of 1  $\ell/\text{s}$  (BH0790) and 7  $\ell/\text{s}$  (BH1348) were drilled on anomalies striking predominantly N305°W and N88°E respectively. The highest yielding borehole (BH1348) is also associated with a deeply weathered and fracture zone evidently to a depth of 30 m.

### *Bolubedo*

An 800 m geophysical profile striking NNE to SSW near Bolobedu highlights three distinct anomalies which correspond spatially reasonably well with the regional ASTER image lineaments (Figure 5.55).



**Figure 5.55. Field study location and the 800 m geophysical profile near Bolobedu.**



Borehole BH1699 was drilled based on field observations while BH1697 and BH1698 targeted geophysical anomalies at positions 150 and 350 m respectively (Figure 5.55). The highest yielding borehole is associated with a distinct E-W trending lineament while the noisy conductivity profile may suggest a fissured zone. BH1698 lies seemingly on a N60°E trending lineament and produced the lowest yield of the three sites, corresponding to the theory that ENE to E (N60°E to N90°E) striking structures offer potentially higher yields compared to lineaments striking NNE to NE (N30°E to N45°E).

**Table 5.27. A summary of drilling results in the Great Letaba Catchment.**

Site	BH Nr.	Lineament/dyke		Water Strike (m.b.g.l)	BH Depth (m.b.g.l)	Airlift Yield (ℓ/s)	Regolith Depth (m.b.g.l)	Rec. Yield ℓ/s per day	T-value m <sup>2</sup> /d
		Dist (m)	Azimuth						
Dzumeri	BH0790	180	305°	66	120	1	22	0.8	9
	BH0960	90	69°	131	156	0.2	32	-	-
	BH0968	204	60°	Dry	144	Dry	16	-	-
	BH0981	475	60°	123	148	0.3	26	-	-
	BH1348	18	88°	35	210	7	43	1.7	3
	BH1347	23	65°	Dry	120	Dry	20	-	-
	BH1000	88	2°	45	114	0.3	30	-	-
Bolobedu	BH1699	30	71°	21	72	2	20	1	5.5
	BH1697	60	270°	23	72	5.2	24	-	-
	BH1698	73	60°	21	72	0.5	18	0.2	2

\*- meters below ground level.

### 5.5.7. Discussion of results

Historical groundwater exploration within the area has successfully targeted structural features and geological contacts at depth within the unweathered bedrock instead of in the rather thin regolith. Regionally, the influence of the weathering layer on borehole productivity is therefore considered poor. However, an ideal borehole or well would still intercept long or interconnected fractures in the solid rock which are in contact with a large volume of overlying, low permeability material that provides a consistent source of water. While the geological analysis of the data set indicates the obvious, that the rock type and lithology influences borehole productivity, the four structural domains identified within the study area show distinct differences in groundwater potential suggesting that the factors involved in controlling borehole productivity vary with each geological setting. Although dykes are poor groundwater targets drilling along these features may prove to be more successful in the Limpopo Plateau, where these dykes may act as barriers to flow. In the Letaba Lowveld dykes can be regarded as part of the host rock with no difference in permeability. These magnetic anomalies may present poor drilling targets with often disappointing results unless their strike direction is considered.

In general, the proximity of lineaments plays a role in borehole productivity and based on the transmissivity results it is assumed that the intensity of fracturing decreases with increasing distance away from the lineament.



Although highly variable, a number of specific lineament orientations provide above average transmissivities. It is generally expected that boreholes influenced by lineaments striking NW-SE (presumed to be under dilation and shear stress caused by the NW-SE maximum horizontal stress direction) should have higher productivities than boreholes associated with lineaments striking perpendicular to that direction. However, based on the results it seems that higher borehole productivities are in fact associated with lineaments and dykes perpendicular to the current stress regime, more specifically ENE to E and WNW to W. A possible explanation for this may be a localised compressive stress regime which is inconsistent with the regional maximum horizontal stress regime of NW-SE as determined by Bird et al. (2006). The ENE-WSW trending Tshipise-Bosbokpoort fault system immediately north of the area under investigation was for example notably reactivated in post-Tertiary times (Brandl 1995). The cause of the rejuvenation of these structures may be related to the southerly propagation of the East African Rift system (Figure 5.56). This would suggest that the Limpopo Plateau and the Letaba Lowveld might be considered to be under N-S extension, which is more pronounced towards the east. The higher transmissivities observed along lineaments trending ENE to E in the Letaba Lowveld support this assumption. In the Limpopo Plateau this model is not as distinct, with higher borehole productivities associated with lineaments trending both NE and WNW.

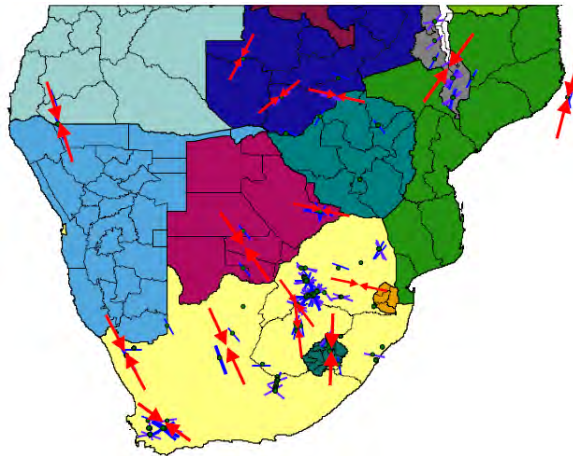


**Figure 5.56. Stress orientations of southern Africa (Stacey and Wesseloo, 1998).**

Geology has been identified as the main influence on borehole productivity while topography and proximity to surface water drainages have an obvious influence on the groundwater potential. However, since the topographic setting is directly related to the underlying geology, it is not an independent factor. The influence of topography on well yield in fractured rocks has also been shown by Mabee et al. (1994), Henriksen, (1995) and Fernandes and Rudolph, (2001). In all cases the authors found higher well yields in low topographic settings (i.e. valleys). Valleys are often associated with regional fracture features. From a hydraulic point of view, water levels are generally shallower at topographic lows and present discharge zones, providing more available drawdown and a larger capture zone compared to boreholes in mountainous areas drilled to approximately the same depth below ground surface. This may also explain in part the high observed borehole productivities in proximity of surface water drainages. In most cases these high productive boreholes are associated with elongated primary alluvial aquifers. In addition drainage

channels tend to follow zones of structural weaknesses (i.e. lineaments) in the near surface; therefore rocks in the vicinity of rivers might be more intensely fractured, jointed and/or weathered.

A conceptual understanding of the most significant features controlling groundwater occurrence in the Limpopo Basement aquifers is illustrated in Figure 5.57. A summary of the potential groundwater targets based on the knowledge obtained during this investigation is listed in Table 5.28 and presented spatially in Figure 5.58. The occurrence of alluvium aquifers was discussed in previous sections and while this remains a prime target for groundwater exploration it was excluded from the list in Table 5.28.

**Table 5.28. Recommended drilling targets per structural domain.**

Feature	Limpopo Plateau	Letaba Lowveld
<i>Dykes (proximity)</i>	High borehole productivity within 50 m of dyke	Little influence on the borehole productivity
<i>Dyke (orientation)</i>	NW to NNE (315° to 30°) striking dykes offer evidently poorer water bearing characteristics compared to dykes striking NE (30 to 45°) or ENE (75 to 90°)	No preferred orientation, although W to NNE (315-30°) seem less favourable
Feature	NW Domain	NE Domain
<i>Lineaments (proximity)</i>	High borehole productivity within 25 m and 50 m of lineament	Slight influence on the borehole productivity (within 25 m of lineament)
<i>Lineaments (orientation)</i>	W to WNW (270-315°) and ENE to E trends (75-90°) are associated with higher borehole productivities compared to NNW to N (315-360°)	N to NE (0-45°) and ENE to E (60-90°) are associated with higher borehole productivities compared to W to N (270-360°)
<i>Neo-tectonics</i>	High borehole productivities observed parallel, perpendicular and oblique to the current NW maximum horizontal stress regime	High borehole productivities observed oblique and perpendicular to the current NW maximum horizontal stress regime
Feature	SW Domain	SE Domain
<i>Lineaments (proximity)</i>	High borehole productivity within 25 m of lineament	Slight influence on the borehole productivity (within 150 m of lineament)
<i>Lineaments (orientation)</i>	W to WNW (270-315°) and ENE to E (60-90°) with the least favourable lineaments associated with N to NNE trends (0-30°)	ENE to E (60 to 90°) are associated with higher borehole productivities compared to W to NW (270-315°) and NE (30 to 60°)
<i>Neo-tectonics</i>	High borehole productivities observed perpendicular and slightly oblique to the current NW maximum horizontal stress regime	High borehole productivities observed oblique and perpendicular to the current NW maximum horizontal stress regime

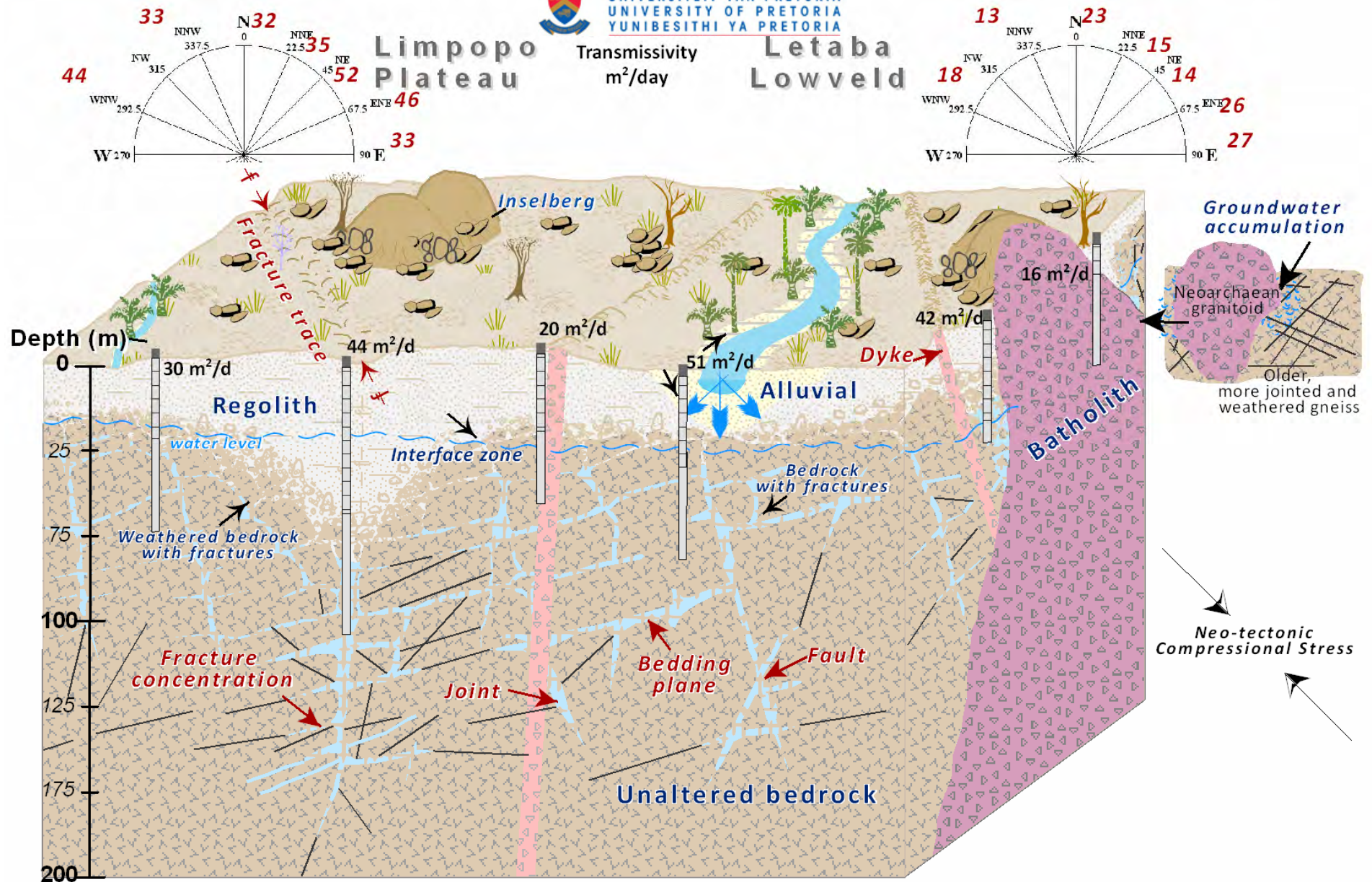


Figure 5.57. Conceptualisation of transmissivity values obtained from various borehole settings in the Limpopo basement aquifers (rose diagram indicating mean transmissivities for selected lineament azimuths based on Table 5.25).



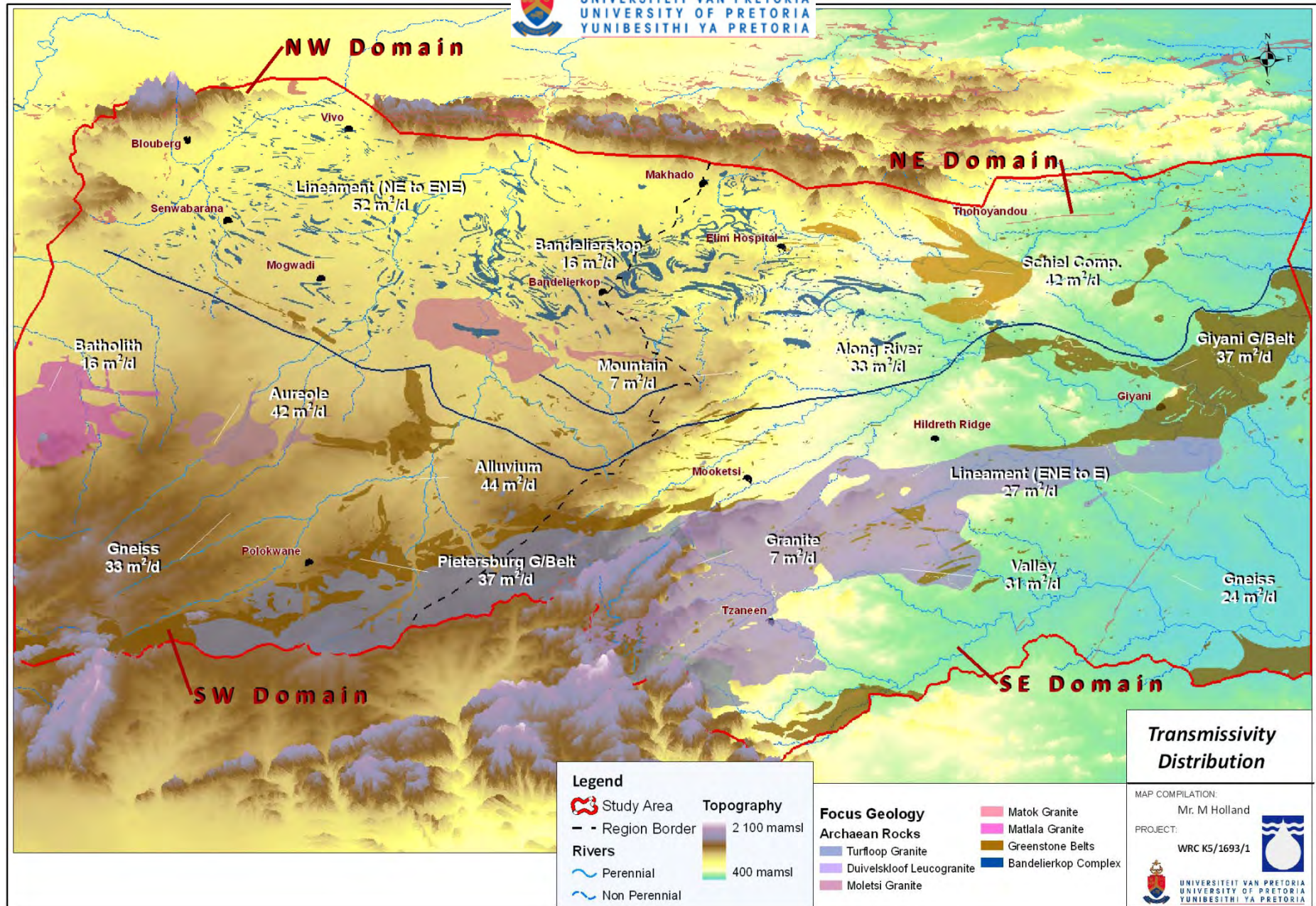


Figure 5.58. Regional distribution of transmissivity to illustrate the potential productive groundwater areas.

## 6. CONCLUSION

### 6.1. Synthesis

The regional hydraulic characterisation study in combination with the recharge investigation together with the isotope and hydrochemical analysis formed the basis of the conceptual hydrogeological model. The Limpopo basement rocks can be characterised by a generally thin regolith ( $\approx 20$  m) and groundwater aquifers are primarily structurally controlled. Although the weathered zone is capable of storing water and transmitting it to the fractured bedrock, the general lack of recharge ( $\approx 2$  % of MAP) implies an important circulation in the underlying fractured zone of the bedrock which is recharged along vertical to sub-vertical fractures with lateral flow along horizontal to sub-horizontal fracture systems. The groundwater table reflects topography showing an overall gradient towards the catchment (basin) outlet. Locally, however, groundwater flow directions are controlled by fracture orientation. On a regional scale the aquifer can be regarded as (semi-)confined and capable of receiving diffuse recharge, but its water supply potential is primarily dependent on groundwater flow in discrete fractures in the weathered-fractured bedrock which are hydraulically connected. Due to the irregular groundwater flow pattern which is determined by the fracture system, groundwater is mostly a mixture of waters with different ages.

These composite weathered-fractured aquifer systems do not satisfy the underlying assumptions for porous media, and the inherent heterogeneity needs to be considered in groundwater investigations. A commonly encountered problem in crystalline aquifers is how to conceptualize their hydrogeological behaviour in order to determine long term abstraction rates and estimate aquifer properties. Advances in hydrogeological well test interpretation software over the last few years, such as derivative plots, flow regime tools and automatic curve fitting of a range of analytical solutions, have made the interpretation of pumping test data easier. But the applicability of a certain model (i.e. leaky, double porosity) to an observed dataset especially in fractured bedrock aquifers still requires a clear understanding of the fundamental principles and assumptions governing the analytical solution. This thesis proposes modern methods for the analysis of pumping test data in crystalline basement aquifers and highlights the importance of diagnostic plots, especially derivatives, for the detection of flow regimes and the choice of the correct 'theoretical' model. The analysis of drawdown responses showed that all typical conceptual models can occur in the weather-fractured basement rocks and can be related to the physical parameters that control them at the specific scale of interest (i.e. fractured aquifer behaves in some instances identically to an unconsolidated medium).

Several geological and geomorphologic factors including structural features have been identified as most suitable targets for further groundwater exploration and an improved conceptual understanding for groundwater occurrence in the basement aquifers of the Limpopo Province was developed. The most obvious variation in borehole yield and transmissivity can be related to different lithologies and rock types. Although it is expected that a thicker regolith should enhance borehole productivity, the poor correlation between borehole yield and weathering thickness suggests that high yields are predominantly related to a geological structure at depth as reflected



by the average waters strike depth of 30 m. While the metamorphic aureoles of the granite batholiths present good conditions regarding groundwater supply, the granitic body itself can be considered as a poor target. Alluvial deposits, mainly composed of permeable material have high groundwater supply potential but may be limited in extent and are vulnerable to pollution. Favourable drilling targets are also along major rivers and topographic lows (i.e. valleys). Dykes are generally considered barriers to groundwater flow and in some instances can be regarded as part of the host rock with no difference in permeability. These magnetic anomalies may present overrated targets for groundwater exploration with often disappointing results unless their strike direction and geological setting is considered.

Specific lineament orientations have been identified which may provide above average yields and transmissivities. However, further intrusive investigations are needed to confirm whether these identified lineament orientations do indeed offer higher groundwater potential. Due to the complex geological history of the area, it is difficult to link these open discontinuities to a distinct recent or past tectonic event. The regional stress field data, as in this case, may not account for local, possibly highly significant, stress field variations.

It can be concluded, as in so many other basement aquifer investigations (i.e. Wright, 1992), that despite the apparent influence of regional factors on groundwater occurrence, the complexity of the weathered-fractured aquifer system suggests an over-riding influence of local features, which results in significant variations in yield and response to abstraction.

## **6.2. Recommendations and suggestions for future investigations**

It has been shown that the recommended ‘sustainable’ borehole yields can exceed the annual recharge, which emphasises the fact that simply recommending a borehole yield without considering the cumulative influence it may have on the environment can be to the long-term detriment of the system (i.e. decrease discharges). In this regard there is also a need to accurately identify and quantify potential groundwater discharge zones. A recommended long term basin yield should be based on recharge (including rainfall variability) and baseflow studies, pumping test interpretation, and numerical models.

In terms of pumping tests, proper planning and execution of a test will yield reliable data and enable the user to estimate realistic parameter values along with ‘sustainable’ yields. Observation boreholes are often monitored haphazardly by contractors without understanding the importance of the observed results. The following procedure is recommended: A step drawdown test (minimum 4 steps of 1 hour each) to locate the depth of the main water strike as well as to determine a suitable abstraction rate for the constant discharge test and to determine well loss.

- The constant discharge rate should ideally reach 80-90% of the available drawdown after one or two days and maintain it for another day if the drawdown stabilises in order to stress the aquifer sufficiently. Otherwise the test should continue until failure of the borehole.



- At least one observation borehole at a distance of 20 to 50 m from the abstraction borehole should be installed and monitored at regular intervals to determine the spatial extent of drawdown. The confidence of determined hydraulic parameters increases significantly as the monitoring borehole allows the direct determination of storativity values.
- A sound conceptual model for the aquifer including locations and distances to potential flow boundaries needs to be developed and applied for the interpretation of the test. The model will determine the choice of analytical solution employed for the interpretation of the test.

Despite a number of site-specific studies within this thesis, the focus was mainly on a regional scale. It is hoped that in future more site specific studies will be undertaken to enhance the understanding of both aquifer behaviour and the occurrence of groundwater. This relates mostly to:

- A better understanding of the hydraulic connection between the regolith and the underlying fractured bedrock,
- the origins of (high) nitrates in the Limpopo basement aquifers, with special reference to nitrogen isotopes,
- expand on the knowledge of groundwater ages and mixing by using common isotopes as well as recent tracers such as CFCs and  $^3\text{H}/^3\text{He}$ ,
- with this in mind the occurrence of deep-seated groundwater should be investigated with the purpose of proving or disproving the presence of deep, more regional groundwater flow systems,
- delineation of aquifer system and resource units,
- in order to better identify the structural controls on groundwater more intensive site-specific studies be conducted with a comprehensive drilling program, and
- the following questions should also be addressed in future research: how much water is available and exploitable?, and what are the needs for water (i.e. development and ecological Reserve)?

#### 6.2.1. Groundwater management

Water management issues differ from place to place, depending on various factors but generally upon the overall availability of water and water demand. In South Africa, despite the new national water Act (1998) which includes excellent general protection measures, the challenge lies in the implementation of the available approaches and instruments. Perhaps one of the biggest weights lies on water service providers to convey the value of groundwater to the communities. Groundwater resource management has to deal with balancing the exploitation of a complex resource (in terms of quantity and quality) with the increasing demands of water and land users (who can pose a threat to the resource availability and quality).

## 7. REFERENCES

- Acworth, R.I. (1987). The development of crystalline basement aquifers in a tropical environment. *Q. J. Eng. Geol.*, 20: 265-272.
- Adams, S., Titus, R. and Xu, Y. (2004). Groundwater recharge assessment of the Basement aquifers of Central Namaqualand. WRC Report no. 1093/1/04. Water Research Commission, Pretoria.
- Agarwal, R.G. (1980). A new method to account for producing time effects when drawdown type curves are used to analyze pressure build-up and other test data, SPE Paper 9289 presented at the 55th SPE Annual Technical Conference and Exhibition, Dallas, TX, Sept. 21-24, 1980.
- Alley, W.M., and Leake, S.A. (2004). The Journey from Safe Yield to Sustainability. *Ground Water*, 42(1): 12-16.
- Alley, W.M., Reilly, T.E. and Franke, O.L. (1999). Sustainability of ground-water resources. U.S. Geological Survey Circular 1186.
- Anhaeusser, C.R. (1992). Structures in granitoid gneisses and associated migmatites close to the boundary of the Limpopo Belt, South Africa. *Precambrian Res.*, 55: 81-92.
- Banks, D. and Robins N.S (2002). *An introduction to groundwater in crystalline bedrock*. Geological Survey of Norway, Trondheim.
- Banks, E.W., Simmons, C.T., Love, A.J., Cranswick, R., Werner, A.D., Bestland, E.A., Wood, M. and Wilson, T. (2009). Fractured bedrock and saprolite hydrogeologic controls on groundwater/surface-water interaction: a conceptual model (Australia). *Hydrogeol. J*, 17(8), 1969-1989.
- Barenblatt, G.I., Zheltov, Yu.P. and Kochina, I.N. (1960). Basic Concepts in the Theory of Seepage of Homogeneous Liquids in Fissured Rocks. *In: Well Testing in Heterogeneous Formations*. An Exxon Monograph. T.D. Streltsova. John Wiley & Sons, New York, 413p.
- Barker, J.A. (1988). A Generalized Radial Flow Model for Hydraulic Tests in Fractured Rock. *Water Resources Res.*, 24(10): 1796-1804.
- Barker, R.D., White, C.C. and Houston, J.F.T. (1992). Borehole siting in an African accelerated drought relief project. *In: Wright, E.P. and Burgess, W.G. (eds.) Hydrogeology of Crystalline Basement Aquifers in Africa*. Geological Society Special Publication No 66. Geological Society, London.
- Batu, V., (1998). *Aquifer Hydraulics: A Comprehensive Guide to Hydrogeologic Data Analysis*, John Wiley & Sons, Inc., New York, 727p.
- Bäumle, R. (2003). Geohydraulic Charactersisation of Fractured Flow Regimes: Regional Studies in Granite (Linday, Black Forest, Germany) and Dolomite (Tsumed Aquifers, Northern Namibia). *Unpublished PhD Thesis*. Universität Karlsruhe. Germany, 149p.
- Bean, J.A. (2003). A critical review of recharge estimation methods used in South Africa. *Unpublished PhD Thesis*. Institute for Groundwater Studies. University of the Free State, Bloemfontein.
- Bird, P., Ben-Avraham, Z., Schubert, G., Andreoli, M. and Viola, G. (2006). Patterns of Stress and Strain Rate in Southern Africa. *K.Geophys. Res.*, 111(B8). B08402.
- Black, J.H. (1994). Hydrogeology of fractured rocks – a question of uncertainty about geometry. *Applied Hydrogeology.*, 2(3): 56-70.
- Bockgård, N., Rodhe, A., Olsson, K.A., (2004). Accuracy of CFC groundwater dating in a crystalline bedrock aquifer: data from a site in southern Sweden. *Hydrogeol. J.*, 12, 171-183.
- Böhlke, J.K., (2006). TRACERMODEL1. Excel workbook for calculation and presentation of environmental tracer data for simple groundwater mixtures. *In: IAEA, (2006). Use of Chlorofluorocarbons in Hydrology. A Guidebook*. International Atomic Energy Agency, Vienna. [http://water.usgs.gov/lab/software/tracer\\_model/](http://water.usgs.gov/lab/software/tracer_model/)
- Boonstra, J. and Boehmer, W.K. (1986). Analysis of Data from aquifer and Well Tests in Intrusive Dykes. *Journal of Hydrology*, 88: 301-317.
- Boshoff, R., Van Reenen, D.D., Smit, C.A., Perchuk, L.L., Kramers, J.D. and Armstrong, R. (2006). Geologic History of the Central Zone of the Limpopo Complex: The West Alldays Area. *The Journal of Geology*, 114: 699–716.

- Botha, F.S. (2005). A proposed method to implement a groundwater resource information project (GRIP) in rural communities, South Africa. Unpublished PhD. Thesis Department of Geohydrology. University of Free State, Bloemfontein.
- Boulton, N.S. (1954). The drawdown of the water table under non steady conditions near a pumped well in an unconfined aquifer. *Proc Institution Civil Eng.*, 3: 564-579.
- Bourdet, D., Whittle, T.M., Douglas, A.A. and Pirard, Y.M. (1983). A new set of type curves simplifies well test analysis. *World Oil*, 95-106.
- Braathen, A. and Gabrielsen, R. (1998). Lineament architecture and fracture distribution in metamorphic and sedimentary rocks, with application to Norway. *Geol Surv Norway Rep.*, 98.043.
- Brandl, G. and Kröner, A. (1993). Preliminary results of single zircon studies from various Archaean rocks of the north-eastern Transvaal. *Abstr. 16<sup>th</sup> Coll. African Geology, Mbabane, Swaziland*, (1): 54-56.
- Brandl, G. (1995). Reactivation of certain faults in the Limpopo Belt during the Quaternary, in Extended Abstracts of the Centennial Geocongress, vol. 1, J. M. Barton and Y. E. Copperthwaite, *Geol. Soc. Of S. Africa*, 442-444.
- Brandl, G., Cloete, M. and Anhaeusser, C. R. (2006). Archaean Greenstone Belts. In: Johnson, M.R., Anhaeusser, C.R., and Thomas, R.J. (Eds.), *The geology of South Africa*. Geological society of South Africa, Johannesburg/Council for Geoscience, Pretoria, 209-236.
- Bredenhoeft, J.D. (2002). The water budget myth revisited: why hydrogeologists model. *Ground Water* 40 (4): 340-345.
- Bredenkamp, D.B., Botha, L.J., Van Tonder, G.J. and Van Rensburg, H.J. (1995). Manual on quantitative estimation of groundwater recharge and aquifer storativity WRC Report No. TT 73/95. Water Research Commission, Pretoria.
- Busenberg, E., Plummer, L.N., (2000). Dating young groundwater with sulphur hexafluoride: natural and anthropogenic sources of sulfur hexafluoride. *Water Resour. Res.*, 36: 3011-3030.
- Bush, R.A. (1988). An assessment of the groundwater resources potential of the defence force camp at Soekmeaar. GH 3582. Directorate Geohydrology, Department of Water Affairs and Forestry, Pretoria.
- Butler, J.J. Jr. (2008). Pumping Tests for Aquifer Evaluation—Time for a Change? *Ground Water*, 47(5): 615-617.
- Chilton, P.J. and Smith-Carington, A.K. (1984). Characteristics of the weathered basement aquifer in Malawi in relation to rural water supplies. In: Proc. Challenges in African hydrology and water resources Symp. *IAH Series Publ.*, 144: 15-23.
- Chilton, P.J. and Foster, S.S.D. (1995). Hydrological characterization and water-supply potential of basement aquifers in tropical Africa. *Hydrogeol J.*, 3: 36-49.
- Cinco-Ley H. (1996). Well-test analysis for naturally fractured reservoirs. *Journal of Petroleum Technology*, 51–54.
- Cinco-Ley, H. and Samaniego, F. (1981). Transient pressure analysis for fractured wells. *Jl Petroleum Technology*, September 1981.
- Clark, L. (1985). Groundwater abstraction from Basement Complex areas of Africa. *Quarterly Journal of Engineering Geology*, 18: 25-34.
- Clark, I. and Fritz, P. (1997). *Environmental isotopes in hydrogeology*. Lewis Publishers, New York, 328p.
- Craig, H. (1961). Isotopic variation in meteoric water. *Science*, 133: 1702-1703.
- Cook, P.G. and Böhlke, J.K. (2000). Determining timescales for groundwater flow and solute transport. In: Cook, P. and Herczeg, A. (Eds.), *Environmental Tracers in Subsurface Hydrology*.
- Cook, P.G. (2003). *A guide to regional groundwater flow in fractured rock aquifers*. Seaview Press, Adelaide, Australia.
- Cooper, H.H. and Jacob, C.E. (1946). A generalized graphical method for evaluating formation constants and summarizing well field history. *American Geophysical Union Transactions*, 27: 526-534.
- Department of Water Affairs and Forestry. (1996). South African Water Quality Guidelines, Second edition, Pretoria.
- Department of Water Affairs and Forestry. (2004). Internal Strategy Perspective (ISP) of the Luvuvhu/Letaba Water Management Area. Report No. PWMA 02/000/00/0304.
- Department of Water Affairs and Forestry. (2006). Groundwater Resource Assessment II – Task 3 Recharge. Department of Water Affairs and Forestry. Pretoria.



- Department of Water Affairs and Forestry. (2009). Community water supply backlog database. Department of Water Affairs and Forestry. Pretoria.
- Devlin, J.F. and Sophocleous, M. (2005). The persistence of the water budget myth and its relationship to sustainability. *Hydrogeol J.*, 13: 549-554.
- Dewandel, B., Lachassagne, P., Wyns, R. Maréchal, J. C. and Krishnamurthy, N. S. (2003). A Generalized 3-D Geological and Hydrogeological Conceptual Model of Granite Aquifers controlled by Single or Multiphase Weathering. *Journal of Hydrology*, 330: 260-284.
- Doe, T.W. (1991). Fractional dimension analysis of constant-pressure well tests. *SPE paper 22702*: 461-467.
- Du Toit, W.H. (1986). Die aanwys en kontrolering van boorwerk en pomptoetse van boorgate in die Pietersburgse dorpsgebied vir die gebruik deur die munisipaliteit. GH 3448. Directorate Geohydrology, Department of Water Affairs and Forestry, Pretoria.
- Du Toit, W.H. (2001). An investigation into the occurrence of groundwater in the contact aureole of large granite intrusions (batholiths) located west and northwest of Pietersburg. Report GH 3923. Directorate Geohydrology, Department of Water Affairs and Forestry, Pretoria.
- Dutta, S., Krishnamurthy, N.S., Arora, T. Rao, V.A., Ahmed, S. and Baltassat, J.M. (2006). Localization of water bearing fractured zones in a hard rock area using integrated geophysical techniques in Andhra Pradesh, India. *Hydrogeol. J.*, 14: 760-766.
- Dziembowski, Z.M. (1976). Die geohydrologie van die Dendrongebied, distrik Pietersburg. Report GH 2878. Directorate Geohydrology, Department of Water Affairs and Forestry, Pretoria.
- Ehlig-Economides, C.A., Hegeman, P. and Vik, S. (1994). Guidelines simplify well test analysis. *Oil Gas J.*, 92: 33-40.
- Eriksson, E. and Khunakasem, V. (1969). Chloride concentrations in groundwater recharge rate and rate of deposition of chloride in the Israel coastal plain. *Journal of Hydrology*, 7: 178-197.
- Fernandes, A.J. and Rudolph, D.L. (2001). The influence of Cenozoic tectonics on the groundwater production capacity of fractured zones: a case study in São Paulo, Brazil. *Hydrogeol J.*, 9: 151-167.
- Freeze, R.A. and Cherry, J.A. (1979). *Groundwater*. Prentice-Hall, Englewood Cliffs, NJ, 604p.
- Galanos, I. and Rokos, D. (2006). A statistical approach in investigating the hydrogeological significance of remotely sensed lineaments in the crystalline mountainous terrain of the island of Naxos, Greece. *Hydrogeol. J.*, 14: 1569-1581.
- Gernand, J.D and Heidtman, J.P. (1997). Detailed pumping test to characterise a fractured bedrock aquifer. *Ground Water*, 35 (4): 632-637.
- Glynn, P.D and Plummer, L.N. (2005). Geochemistry and the understanding of ground-water systems. *Hydrogeol. J.*, 13: 263-287.
- Gonthier, G.J. (2009). Conceptual model of groundwater flow in fractured crystalline rock – A case study based on constant discharge tests at U.S. Air force plant 6, Marietta, Georgia. Proceedings of the 2009 Georgia Water Resources Conference, held April 27–29, 2009, at The University of Georgia.
- Goody D.C., Darling W.G. Abesser, C and Lapworth D.J. (2006). Using chlorofluorocarbons (CFCs) and sulphur hexafluoride (SF<sub>6</sub>) to characterise groundwater movement and residence time in a lowland Chalk catchment. *Journal of Hydrology*, 330: 44-52.
- Greenbaum, D. (1992). Structural influence on the occurrence of groundwater in SE Zimbabwe. In: Wright, E.P. and Burgess, W.G. (eds.) *Hydrogeology of Crystalline Basement Aquifers in Africa*. Geological Society Special Publication No 66. Geological Society, London.
- Gringarten, A. C., H.R. Ramey, and Raghavan, R. (1974). Unsteady-state pressure distributions created by a well with a single infinite-conductivity vertical fracture. *Society of Petroleum Engrs JI*, 347-360.
- Gringarten, A.C. and Ramey, H.J. (1974). Unsteady-state pressure distribution created by a well with a single horizontal fracture, partially penetrating or restricted entry. *Trans. Am. Inst. Min. Eng.*, 257: 413-426.
- Gringarten, A.C. (1982). Flow-test evaluation of fractured reservoirs. In: Narasimhan, T. N., (ed.), *Recent trends in hydrogeology*. *Geological Society of America*, 189: 237-263.
- Gringarten, A.C. and Ramey, H.R. (1973). The Use of Source and Green's Functions in Solving Unsteady-Flow Problems in Reservoirs. SPE 3818. *SPE Journal*, 255:285 – 296.



- Güler C, Thyne, G.D, McCray, J.E, and Turner, A.K. (2002). Evaluation of graphical and multivariate statistical methods classification of water chemistry data. *Hydrogeol. J.*, 10: 455-474
- Gustafson, G. and Krásný, J. (1994). Crystalline rock aquifers: Their occurrence, use and importance. *Applied Hydrogeology*, 2: 64-75.
- Hantush, M.S and Jacob, C.E. (1955). Nonsteady radial flow in an infinite leaky aquifer. *Trans Am Geophys Union*, 36: 95-100.
- Hantush, M.S. (1961). Drawdown around a partially penetrating well, Jour. of the Hyd. Div., Proc. of the Am. Soc. of Civil Eng., 87(4): 83-98.
- Harte, P.T. and Winter, T.C., (1996). Factors affecting recharge to crystalline rock in the Mirror Lake Area, Grafton County, New Hampshire. In: U.S.G.S. Toxic Substances Hydrology Program – Proceedings of the Technical Meeting, Colorado Springs, Colorado, September 20–24, 1993, Water-Resources Investigations Report 94-4015.
- Healy, R.W. and Cook, P.G., 2002. Using groundwater levels to estimate recharge. *Hydrogeol. J.*, 10(1): 91-109.
- Heath, R. (1983). Basic groundwater hydrology. United States Geological Survey. Water-supply paper 2220.
- Heidbach, O., Tingay, M., Barth, A., Reinecker, J., Kurfes, D. and Müller, B. (2008). The World Stress Map database release 2008 doi:10.1594/GFZ.WSM.Rel2008.
- Henriksen, H. (1995). Relation between topography and well yield in boreholes in crystalline rocks, Sogn og Fjordane, Norway. *Ground Water*, 33: 635-643.
- Henriksen, H (2003). The role of some regional factors in the assessment of well yields from hard-rock aquifers of Fennoscandia. *Hydrogeol J.*, 11:628–645.
- Henriksen, H and Braathen, A. (2003). Effects of fracture lineaments and in-situ rock stresses on groundwater flow in hard rocks: a case study from Sunnfjord, western Norway. *Hydrogeol J.*, 14:444-461.
- Hiscock, K.M. (2005). *Hydrogeology: Principles and Practices*. Blackwell Science, UK. 388p.
- Hoeksema, R.J. and Kitanidis, P.K. (1985). Analysis of the spatial structure of properties of selected aquifers, *Water Resour. Res.*, 21(4): 563-572.
- Holland, M and Witthüser, K.T (2009). Factors that control sustainable yields in the Achaean basement rock aquifers of the Limpopo province. In: Titus, R.A., Adams S. and Strachan, L. (eds.) The basement aquifers of Southern Africa. WRC Report Nr. TT 428/09. Water Research Commission, Pretoria.
- Horst, A., Mahlknecht, J., Merkel, B.J., Aravena, R. and Ramos-Arroyo, Y.R. (2008). Evaluation of the recharge processes and impacts of irrigation on groundwater using CFCs and radiogenic isotopes in the Silao-Romita basin, Mexico. *Hydrogeol. J.*, 16(8): 1601-1614.
- Houston, J.F.T. and Lewis, R.T. (1988). The Victoria Province drought relief project, II. Borehole yield relationships. *Ground Water*, 26(4): 418-426.
- Houston, J.F.T. (1992). Rural water supplies: comparative case histories from Nigeria and Zimbabwe. In: Wright, E.P. and Burgess, W.G. (eds.) Hydrogeology of Crystalline Basement Aquifers in Africa. Geological Society Special Publication No 66. Geological Society, London.
- Howard, W.F and Karandu, J. (1992). Constraints on the exploitation of basement aquifers in East Africa-water balance implications and the role of the regolith. *Journal of Hydrology*, 139: 183-196.
- IAEA, (2006). *Use of Chlorofluorocarbons in Hydrology*. A Guidebook. International Atomic Energy Agency, Vienna.
- Jacob, C.E., (1947). Drawdown Test to Determine Effective Radium of Artesian Well. American Society of Civil Engineers, Transactions, Paper N. 2321.
- Jayasena, H.A.H., Chandrajith, R. and Dissanayake, C.B. (2007). Hydrogeochemistry of the groundwater flow system in a crystalline terrain: a study from the Kurunegala district, Sri Lanka 2007. *Env. Geology* 55: 723-730.
- Jolly, J.L. (1986). Borehole/irrigation survey and groundwater evaluation of the Doringlaagte drainage basin, Dendron (N.Tvl.). Report GH 3495. Directorate Geohydrology, Department of Water Affairs and Forestry, Pretoria.

- Jones, M.J. (1985): The weathering zone aquifers of the basement complex areas of Africa. *Quarterly Journal of Engineering Geology*, 18: 35-46.
- Kalf, F.R.P., and Woolley, D.R. (2005). Applicability and methodology of determining sustainable yield in groundwater systems. *Journal of Hydrogeology*, 13: 295-312.
- Kazemi, H. (1969). Pressure Transient Analysis of Naturally Fractured Reservoirs with Uniform Fracture Distribution. SPE 2156A. Society of Petroleum Engineers. Paper Presented at the 43rd Annual Fall Meeting held in Houston, Texas, 29 September – 2 October 1969.
- King, L.C. (1975). Geomorphology: A basic study for civil engineers. Proceedings of the Sixth Regional Conference for Africa on Soil Mechanics and Foundation Engineering, Durban, Volume 2: 259 - 263.
- Kinzelbach, W., Aeschbach, W., Alberich, C., Goni, I.B., Beyerle, U., Brunner P., Chiang, W.H., Rueedi J., and Zoellmann K. (2002). A Survey of Methods for Groundwater Recharge in Arid 109 and Semi-arid regions. Early Warning and Assessment Report Series, UNEP/DEWA/RS.02-2. United Nations Environment Programme, Nairobi, Kenya.
- Kramers, P., McCourt, S., and van Reenen, D.D. (2006). The Limpopo belt. *In: Johnson, M.R., Anhaeusser, C.R., and Thomas, R.J. (Eds.), The geology of South Africa*. Geological society of South Africa, Johannesburg/Council for Geoscience, Pretoria, 209-236
- Kröhn, K.P. and Zielke, W. (1990): Modelling Transport in Discrete Fracture Systems with a Finite Element Scheme of Increased Consistency. , *In: Gambolati et al. (eds.): Computational Methods in Subsurface Hydrology*. Computational Mechanics Publications, Boston, 1990.
- Kruger, G.P. (1983). Terrain morphological map of southern Africa. Published Map. Soil and Irrigation Research Unit, Department of Agriculture, Pretoria.
- Kruseman, G.P. and De Ridder, N.A. (1990). *Analysis and Evaluation of Pumping Test Data* (2nd ed.) International Institute for Land Reclamation and Improvement. Wageningen, Netherlands.
- Lambrakis, N., Antonakos, A. and Panagopoulos, G. (2004). The use of multicomponent statistical analysis in hydrogeological environmental research. *Water Research*, 38, 1862-1872.
- Lerner, D.N. Issar, A.S. and Simmers, I. (1990). Groundwater recharge. IAH, International contributions to Hydrogeology, 8. Verlag Heinz Heise, Hanover.
- Leveinen, J. (2001). Conceptual and analytical modeling of fracture zone aquifers in hard rock – Implications of pumping tests in the Pohjukansalo well field, east-central Finland. Report YST-105.
- Mabee, S.B., Hardcastle, K.C and Wise, D.U. (1994). A method of collecting and analyzing lineaments for regional-scale fractured-bedrock aquifer studies, *Ground Water*, 32: 884-894.
- Mabee, S.B. (1999). Factors influencing well productivities in glaciated metamorphic rocks, *Ground Water*, 37: 88-97.
- Mabee, S.B., Curry, P.J. and Hardcastle, K.C. (2002). Correlation of lineaments to ground water inflows in a bedrock tunnel, *Ground Water*, 40: 37-43.
- MacDonald, A., Davies, J., Calow, R., and Chilton, J. (2005). *Developing Groundwater: A Guide for Rural Water Supply*. British Geological Survey, ITDG Publishing. 358p.
- Maimone, M. (2004). Defining and Managing Sustainable yield. *Ground Water*, 6: 809-814
- Marais, S. 1999. Dependency of communities on groundwater for water supply and associated nitrate and fluoride problems. Paper presented at Water Research Commission workshop on fluorides and nitrates in rural water supplies. Mafikeng, South Africa.
- Maréchal, J.C., Dewandel, B. and Subrahmanyam, K. (2004). Contribution of hydraulic tests at different scales to characterize fracture network properties in the weathered-fissured layer of a hard-rock aquifer. *Water Resources Research*. 40: W11508.
- Maréchal, J.C., Dewandel, B. and Subrahmanyam, K. (2007). Characterization of Fracture Properties in Hard Rock Aquifer System *In: Groundwater, Resource Evaluation, Augmentation, Contamination, Restoration, Modeling and Management* (Ed. M. Thangarajan). Springer, New York, USA.
- Masiyandima, M (2009). Groundwater management in southern Africa. *In: Titus, R.A., Adams S. and Strachan, L. (eds.) The basement aquifers of Southern Africa*. WRC Report Nr. TT 428/09. Water Research commission, Pretoria.





- McFarlane, M.J., Chilton, P.J. and Lewis, M.A. (1992). Geomorphological controls on borehole yields: a statistical study in an area of basement rocks in central Malawi. In: Wright, E.P. and Burgess, W.G. (eds.) *Hydrogeology of Crystalline Basement Aquifers in Africa*. Geological Society Special Publication No 66. Geological Society, London.
- McNeil, V.H., Malcolm, E.C. and Preda, M. (2005). Assessment of chemical water types and their spatial variation using multi-stage cluster analysis, Queensland, Australia. *Journal of Hydrogeology*, 310: 181-200.
- Meyer, R. (2005). Analysis of groundwater level time series and the relation to rainfall and recharge. WRC Report No. 1323/1/05. Water Research Commission, Pretoria.
- Misstear B, Banks D and Clark, L. (2006). *Water Wells and Boreholes*. John Wiley & Sons, Ltd. West Sussex, England.
- Moench, A.F. (1984). Double-porosity models for a fissured groundwater reservoir with fracture skin. *Water Resour. Res.*, 20(7): 831-846.
- Moench, A.F. (1985). Transient flow to a large-diameter well in an aquifer with storative semi-confining layers. *Water Resour. Res.*, 21(8): 1121-1131.
- Moench, A.F. (1997). Flow to a well of finite diameter in a homogeneous, anisotropic water-table aquifer. *Water Resour. Res.*, 33(6): 1397-1407.
- Mook, W.G. and de Vries, J.J., 2001, *Environmental Isotopes in the Hydrological Cycle: Principles and Application*, Volume I: Introduction, Theory, Methods, Review (Mook, W.G, ed.), UNESCO/IAEA, Vienna, Austria and Paris France, 280p.
- Moon, S., Woo, N.C. and Lee, K.S (2004). Statistical analysis of hydrographs and water-table fluctuation to estimate groundwater recharge. *Journal of Hydrology*, 292: 198-209.
- Moore, R. B., G. E. Schwarz, S. F. Clark, Jr., G. J. Walsh, and Degnan, J.R. (2002). Factors related to well yield in the fractured-bedrock aquifer of New Hampshire U.S. *Geological Survey Professional Paper*, 1660: 51p.
- National Water Act (Act No. 36 of 1998). Government Printer, Pretoria.
- Nel, M. (2000). Geohidrologiese evaluering van 'n gedeelte van die Sand Rivier opvanggebied Pietersburg distrik, Noord Provinsie. GH 3947. Directorate Geohydrology, Department of Water Affairs and Forestry, Pretoria.
- Neuman, S.P. (1972). Theory of flow in unconfined aquifers considering delayed response of the water table. *Water Resour. Res.*, 8(4): 1031-1045.
- Neuman, S.P., 1974. Effect of partial penetration on flow in unconfined aquifers considering delayed gravity response, *Water Resour. Res.*, 10(2): 303-312.
- Neves, M.A. and Morales, N. (2007). Well productivity controlling factors in crystalline terrains of southeastern Brazil. *Hydrogeol. J.*, 15: 471-482.
- Nkotagu, H. (1996). Application of environmental isotopes to groundwater recharge studies in a semi-arid fractured crystalline basement area of Dodoma, Tanzania. *Journal of African Earth Science*. 22(4): 443-457.
- Orpen, W.R.G. (1986). A preliminary evaluation of the possible groundwater resources within a radius of 30 km of Pietersburg for use by the municipality. Report GH 3465. Directorate Geohydrology, Department of Water Affairs and Forestry, Pretoria.
- Owen, R., Maziti, A, and Dahlin, T. (2007). The relationship between regional stress field, fracture orientation and depth of weathering and implications for groundwater prospecting in crystalline rocks. *Hydrogeol J*, 15: 1231-1238.
- Pannatier, E.G., Broers, H.P., Venema, P. and Van Beusekom, G. (2000). *A new process-based hydro-geochemical classification of groundwater*. Netherlands institute for applied science.
- Papadopoulos, I.S. and Cooper, H.H. (1967). Drawdown in a well of large diameter. *Water Resour. Res.*, 3(1): 241-244
- Partridge, T.C. and Maud, R.R. (1987). Geomorphic evolution of southern Africa since the Mesozoic. *South African Journal of Geology*, 90(2): 179-208.
- Partridge, T.C. (1998). Of diamonds, dinosaurs and diastrophism: 150 million years of landscape evolution in southern Africa. *S. Afr. J. Geol.*, 101(3): 167-184.
- Pearson, A.V. and Hartley, H.O. (1970) *Biometrical tables for statisticians*, vol 1. Cambridge University, Cambridge.

- Petzer, K.J. (2009). Structural geological controls on the flow and occurrence of groundwater in the basement lithologies of the Limpopo Province, South Africa. *Unpublished M.Sc Dissertation*, University of Pretoria, South Africa.
- Plummer, L.N., and Sprinkle, C.L. (2001). Radiocarbon dating of dissolved inorganic carbon in groundwater from confined parts of the Upper Floridan Aquifer, Florida, USA: *Hydrogeol. J.*, 9 (2): 127-150.
- Praamsma, T., Novakowski, K., Kyser, K. and Hall, K. (2009). Using stable isotopes and hydraulic head data to investigate groundwater recharge and discharge in a fractured rock aquifer. *Journal of Hydrology*, 366: 35-45.
- Ranganai, R.T. and Ebinger, C.J. (2008). Aeromagnetic and Landsat TM structural interpretation for identifying regional groundwater exploration targets, south-central Zimbabwe Craton. *Journal of Applied Geophysics*, 65: 73-83
- Razack, M. and Lasm, T. (2006). Geostatistical estimation of the transmissivity in a highly fractured metamorphic and crystalline aquifer (Man-Danane Region, Western Ivory Coast). *Journal of Hydrology*, 325, 164–178.
- Renard, P. (2005a). The future of hydraulic tests. *Hydrogeol. J.*, 13: 259-262.
- Renard, P. (2005b). Hydraulics of well and well testing. In: Anderson MG (ed) Encyclopedia of hydrological sciences. Wiley, New York. pp. 2323–2340.
- Renard, P., Glenz, D. And Mejias, M. (2009). Understanding diagnostic plots for well-test interpretation. *Hydrogeol. J.*, 17: 589-600.
- Robb, L. J., Brandl, G., Anhaeusser, C. R. and Poujol, M. (2006). Archaean Granitoid Intrusions. In: Johnson, M.R., Anhaeusser, C.R., and Thomas, R.J. (Eds.), *The geology of South Africa*. Geological society of South Africa, Johannesburg/Council for Geoscience, Pretoria, pp. 209-236.
- Robins, N.S. Davies, J. Farr, J.L. and Calow, R.C. (2006). The changing role of hydrogeology in semi-arid southern and eastern Africa. *Hydrogeol. J.*, 14: 1483-1492.
- Rodhe, A. and Bockgård, N. (2006). Groundwater recharge in a hard rock aquifer: A conceptual model including surface-loading effects. *Journal of Hydrology* 330: 389-401.
- Roering, C. Van Reenen, D.D., Smit, C.A., Barton, J.M. Jr., De Beer, J.H., De Wit, M.J., Stettler, E.H. Van Schalwyk, J.F. Stevens, G. and Pretorius, S.J. (1992). Tectonic model for the evolution of the Limpopo Belt. *Precambrian Research*, 55: 539-552.
- Rossouw, T.G. (2010). Geochemical Characterization of Basement Aquifers within the Limpopo Province, South Africa. *Unpublished M.Sc Dissertation*, University of Pretoria, South Africa.
- Rushton, K.R. and Weller, J. (1985). Response to pumping of a weathered-fractured granite aquifer. *Journal of Hydrology*, 80: 299-309
- Samani, N., Pasandi, M. And Barry, D.A. (2006). Characterizing a heterogeneous aquifer by derivative analysis of pumping and recovery test data. *Journal of Geological Society of Iran*, 1: 29-41
- Sami, K. (2009). Groundwater exploration and development. In: Titus, R.A., Adams S. and Strachan, L. (eds.) *The basement aquifers of Southern Africa*. WRC Report Nr. TT 428/09. Water Research commission, Pretoria.
- Sander, P. (2007). Lineaments in groundwater exploration: a review of applications and limitations. *Hydrogeol J.*, 15: 71–74.
- SANS (2006). South African National Standard (241) Drinking Water (Edition. 6). South Africa, Pretoria.
- Sekhar, M., Mohan Kumar, M.S. and Sridbaran, K. (1994). A leaky aquifer model for hard rock aquifers. *Applied Hydrogeology*, 3: 32-39.
- Seward, P., Xu. Y. and Brendonck L. (2006). Sustainable groundwater use, the capture principle, and adaptive management. *Water SA*, 32(4): 473-482.
- Solomon, S., and F. Quiel (2006), Groundwater study using remote sensing and geographic information systems (GIS) in the central highlands of Eritrea, *Hydrogeol. J.*, 14, 729-741.
- Solomon, S and Ghebreab, W. (2008). Hard-rock hydrotectonics using geographic information systems in the central highlands of Eritrea: Implications for groundwater exploration. *Journal of Hydrology*, 349: 147–155.
- Sophocleous, M. (1997). Managing Water Resources System: Why “Safe Yield” is not Sustainable, *Ground Water*, 35(4): 561.

- Sophocleous, M. (2005). Groundwater recharge and sustainability in the high plains aquifer in Kansas, USA. *Hydrogeol. J.*, 13, 351-365.
- Stacey T.R. and Wesseloo J. (1998). Evaluation and Upgrading of Records of Stress Measurement Data in the Mining Industry. SRK consulting. Safety in Mines Research Advisory Committee, South Africa.
- Stettler, E.H., de Beer, J.H. and Blom, M.P. (1989). Crustal domains in the northern Kaapvaal as defined by magnetic lineaments. *Precambrian Res.*, 45: 263-276.
- Sukhija, B.S., Reddy, D.V., Nagabhushanam, P., Bhattacharya, S.K., Jani, A. and Kumar, D. (2006). Characterisation of recharge processes and groundwater flow mechanisms in weathered-fractured granites of Hyderabad (India) using isotopes. *Hydrogeol. J.*, 14: 663-674.
- Talma, A.S. and Weaver, J.M.C. (2003). Evaluation of groundwater flow patterns in fractured rock aquifers using CFC's and Isotopes. WRC Report No. 1009/1/03. Water Research Commission, Pretoria.
- Taylor, R.G and Howard, K.W.F. (1999). Lithological evidence for the evolution of weathered mantles in Uganda by tectonically controlled cycles of deep weathering and stripping. *Catena*, 35, 65-94.
- Taylor, R. and Howard, K. (2000). A tectono-geomorphic model of the hydrogeology of deeply weathered crystalline rock: Evidence from Uganda. *Hydrogeol. J.*, 8(3): 279-294.
- Theis, C.V. (1935). The Relation between the Lowering of the Piezometric Surface and the Rate and Duration of Discharge of a well using Ground-water Storage. American Geophysical Union *Transactions*, 14, 519-524.
- Thomas, J.M. and Rose T.P. (2003). Environmental isotopes in hydrogeology. *Environmental Geology*, 43: 523.
- Timmerman, K.M.G., Timmerman, L.R.A. and Orpen, W.R.G. (1983). Geohydrological investigation for the proposed military base near Louis Trichardt. Report GH 3286. Directorate Geohydrology, Department of Water Affairs and Forestry, Pretoria.
- Titus, R.A., Adams S. and Strachan, L. (eds.) (2009) The basement aquifers of Southern Africa. WRC Report Nr. TT 428/09. Water Research Commission, Pretoria.
- Tóth, J. (1963). A theoretical analysis of groundwater flow in small drainage basins. *J. Geophys. Res.*, 68: 4795-4812.
- Tredoux, G. and Talma, A.S. (2006). Nitrate pollution of groundwater in southern Africa. In: Xu Y and Usher B (Eds.) *Groundwater pollution in Africa*. Taylor & Francis Group. London, UK.
- Uken, R. and Watkeys, M.K. (1997). An interpretation of mafic dyke swarms and their relationship with major mafic magmatic events on the kaapvaal Craton and Limpopo Belt. *S. Afr. J. Geol.*, 100(4): 341-348.
- USGS (2009). Atmospheric mixing ratios of CFC-11, CFC-12, CFC-13, CFC-113 and SF<sub>6</sub> in the Southern Hemisphere. U.S. Geological Survey Chlorofluorocarbon Laboratory. [http://water.usgs.gov/lab/software/air\\_curve/](http://water.usgs.gov/lab/software/air_curve/)
- Van Tonder, G. Bardenhagen, I., Riemann, K. Van Bosch, J., Dzanga, P and Xu, Y. (2002). Manual on pumping test analysis in fractured rock aquifers. WRC Report No. 1116/1/02. Water Research Commission. Pretoria.
- Van Tonder, G.J., J.F. Botha, W-H. Chiang, H. Kunstmann, and Y. Xu, (2001). Estimation of the sustainable yields of boreholes in fractured rock formations. *Journal of Hydrology*. 241: 70-90.
- Van Tonder G.J. and Steyl, G. (2010). Estimation of representative transmissivities in heterogeneous aquifers. (In Press.).
- Vegter, J.R. (1995). An explanation of a set of national groundwater maps; WRC Report No. TT 74/95. Water Research Commission, Pretoria.
- Vegter, J.R. (2003a) Hydrogeology of groundwater regions, Region 7, Polokwane/Pietersburg Plateau. WRC Report No. TT 209/03. Water Research Commission, Pretoria.
- Vegter J.R. (2003b). Hydrogeology of groundwater regions. Region 19 Lowveld. WRC Report No. TT208/03. Water Research Commission, Pretoria.
- Verbovšek, T. and Veselič, M. (2008). Factors influencing the hydraulic properties of wells in dolomite aquifers of Slovenia. *Hydrogeol J.*, 16: 779-795.

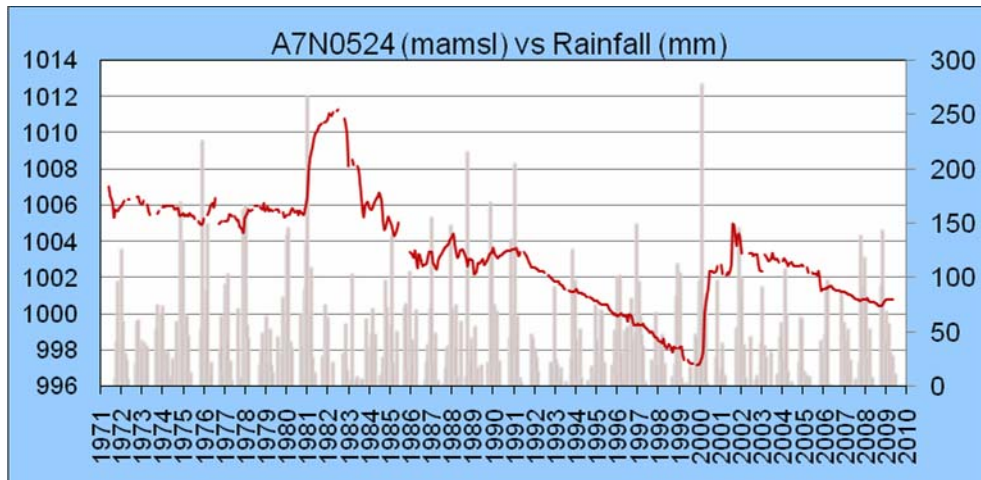


- Verhagen, B. Th., Geyh, M.A., Fröhlich, K. and Wirth, K. (1991). *Isotope hydrological methods for the quantitative evaluation of groundwater resources in arid and semi-arid areas*. Research Report, Fed. Ministry for Econ. Coop. Of the Fed, Republic of Germany.
- Verhagen, B.T. (2000). *Environmental isotope hydrology: Principles and application to the geohydrology of the Karoo Basin*. In Woodford, A and Chevallier, L. (eds.) Karoo Aquifer Handbook, WRC Report No. TT179/02. Water Research Commission. Pretoria.
- Verhagen, B.T., Butler, M.J., Van Wyk, E and Mutheiwana, S (2009). A multi-tracer study of the origins, systematic and hydrological linkages of high concentrations in ground water in the Bochum District, Limpopo Province. WRC Report No. 1328/1/09. Water Research commission, Pretoria.
- Vogel, J.C. (1970). *Carbon-14 dating of groundwater*. Isotope hydrology 1970, Proc. Symp. IAEA, 9-13 March 1970, 225-237.
- Walton, W.C. (1962). Selected analytical methods for well and aquifer evaluation. Illinois State Water Survey, Bull. 49, 81pp.
- Warren, J.E. and Root, P.J. (1963). The behaviour of naturally fractured reservoirs. *Society of Petroleum Engineers Journal*, 3: 245-255.
- Weaver, J.M.C., Talma, A.S. and Cavé, L.S. (1999). Geochemistry and Isotopes for resource evaluation in the fractured rock aquifers of the Table Mountain Group. WRC Report No. 1009/1/03. Water Research Commission, Pretoria.
- Wood, W.W. (1999). Use and misuse of the chloride-mass balance method in estimating ground water recharge. *Ground Water*, 37(1): 2-3.
- Wright, E.P. (1992). The hydrogeology of crystalline basement aquifers in Africa. In: Wright, E.P. and Burgess, W.G. (eds.) *Hydrogeology of Crystalline Basement Aquifers in Africa*. Geological Society Special Publication No 66. Geological Society, London.
- Wright, E.P. and Burgess, W.G (eds.). (1992). *Hydrogeology of Crystalline Basement Aquifers in Africa*. Geological Society Special Publication No 66. Geological Society, London.
- Wu, C., Yeh, T.J., Zhu, J., Lee, T.H., Hsu, N., Chen, C. and Sancho, A.F. (2005). Traditional analysis of aquifer tests: Comparing apples to oranges? *Water Resour. Res.*, 41: W09402.
- Xu, Y. and Van Tonder, G. (2000). Recharge excel spreadsheet. The Institute of Groundwater Studies. Bloemfontein.
- Xu, Y. and Van Tonder, G.J. (2001). Estimation of recharge using a revised CRD method. *Water SA*, 27(3): 341-343.
- Xu, Y. and Beekman, E. (Eds.) (2003). *Groundwater recharge estimation in South Africa*. UNESCO Paris, Cape Town.
- Yeh, T.-C.J., and Lee, C.-H. (2007). Time to change the way we collect and analyze data for aquifer characterization. *Ground Water*, 45(2): 116-118.
- Zhou, Y. (2009). A critical review of groundwater budget myth, safe yield and sustainability. *Journal of Hydrology*, 370: 207-213.
- Zoback, M.L. (1992). First and second-order patterns of stress in the lithosphere: The World Stress Map Project. *J. Geophys. Res.*, 97(B8): 11703-11728.

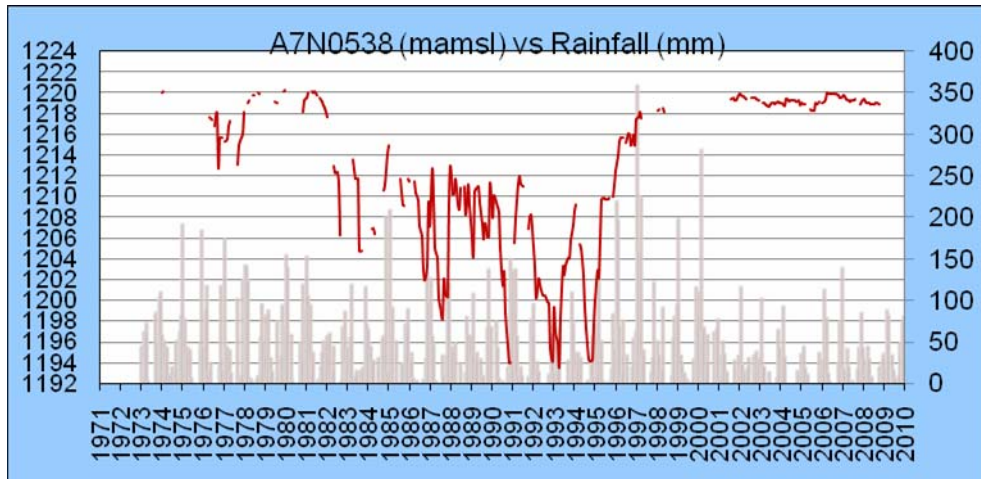


## 8. APPENDIXES

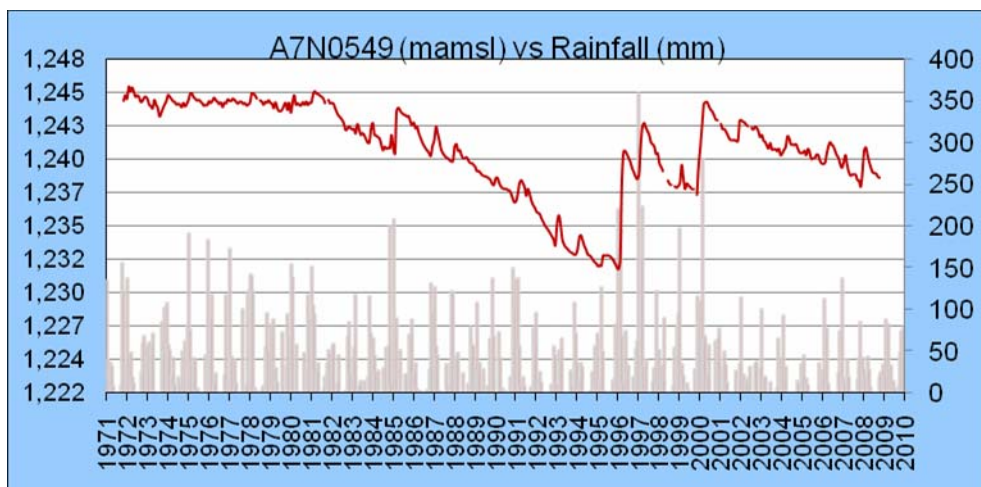
### Appendix A - Borehole hydrographs



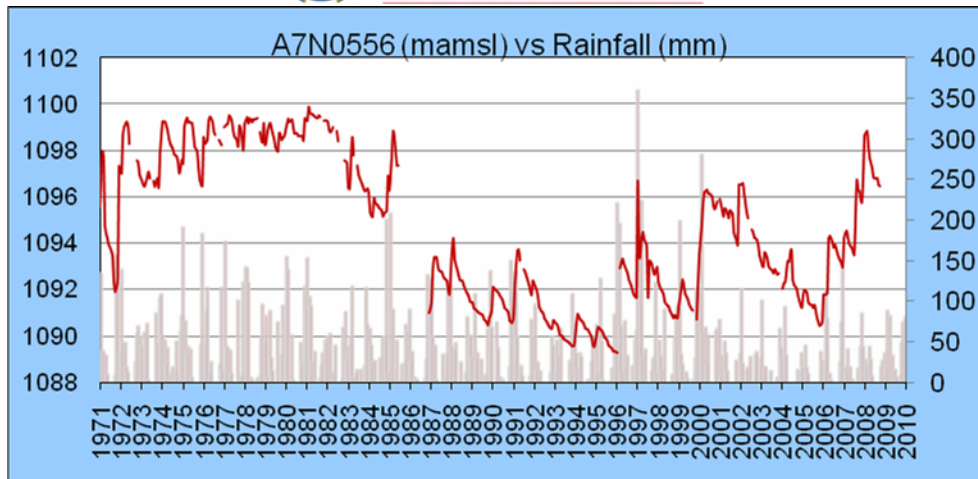
Borehole hydrograph of station A7N0524.



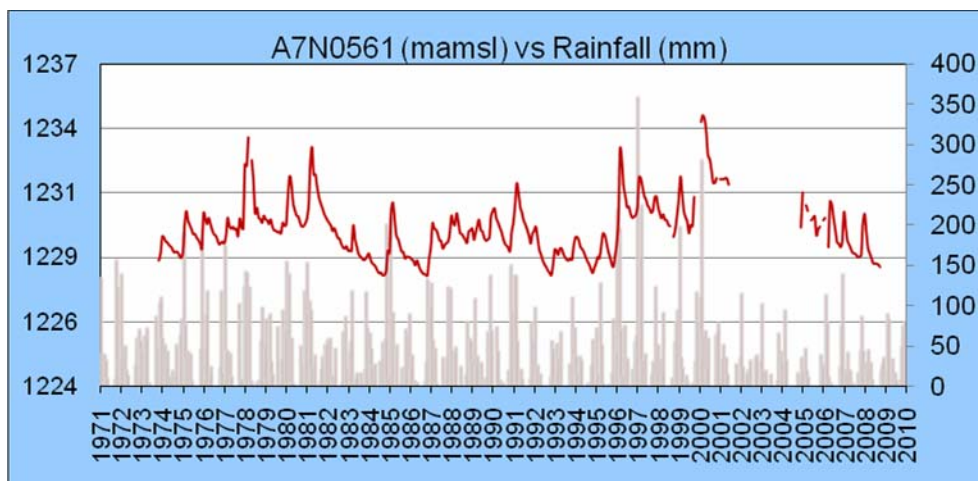
Borehole hydrograph of station A7N0538.



Borehole hydrograph of station A7N0549.

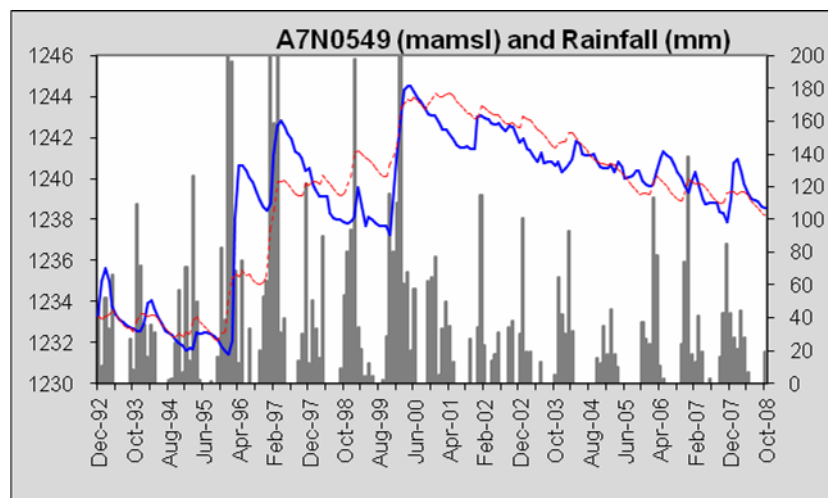


Borehole hydrograph of station A7N0556.



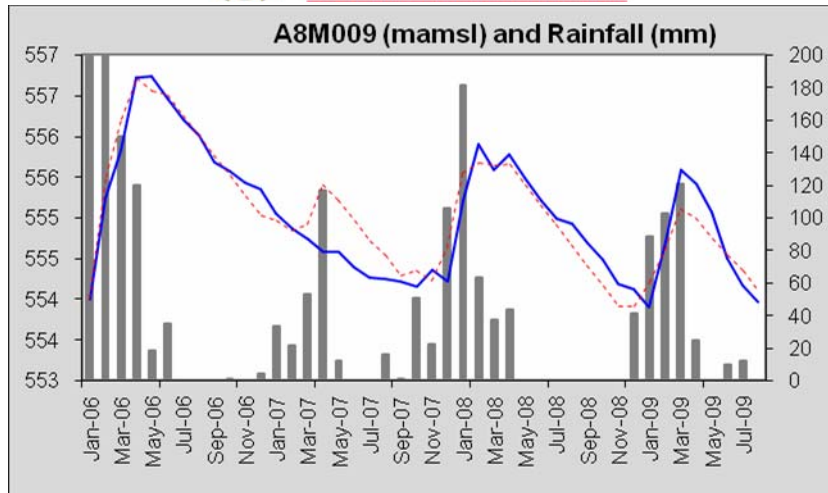
Borehole hydrograph of station A7N0561.

### Appendix B - CRD simulations

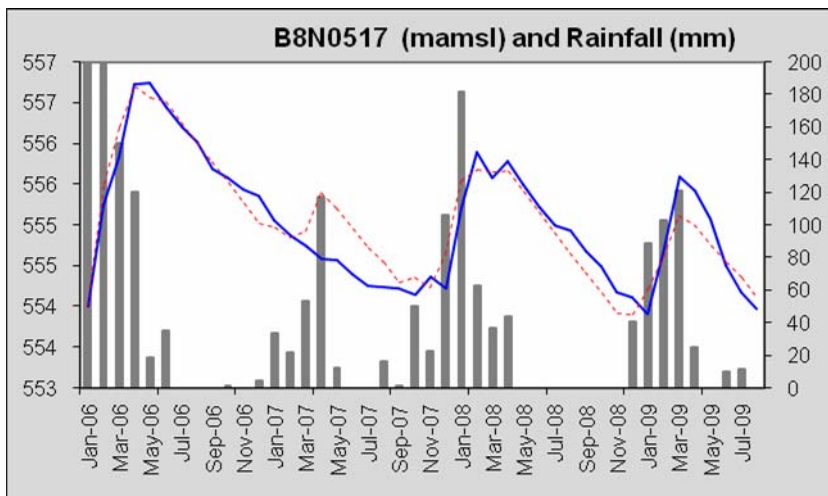


Observed and simulated CRD graph for station A7N0549.

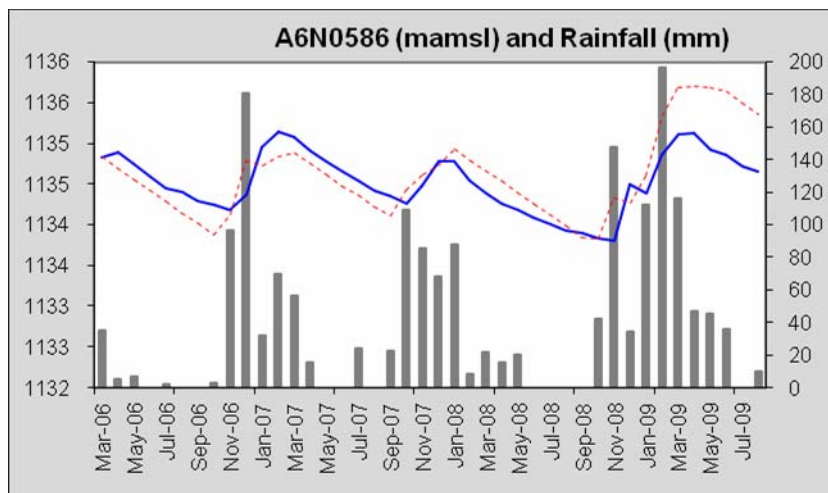




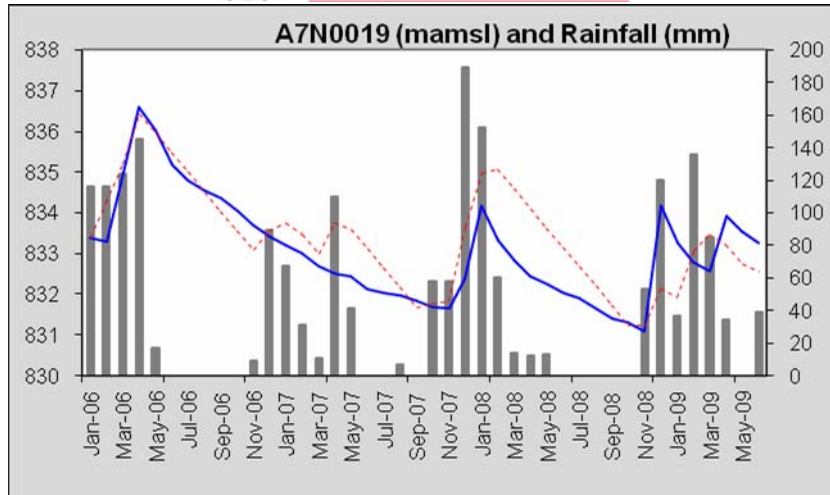
Observed and simulated CRD graph for station A8M009.



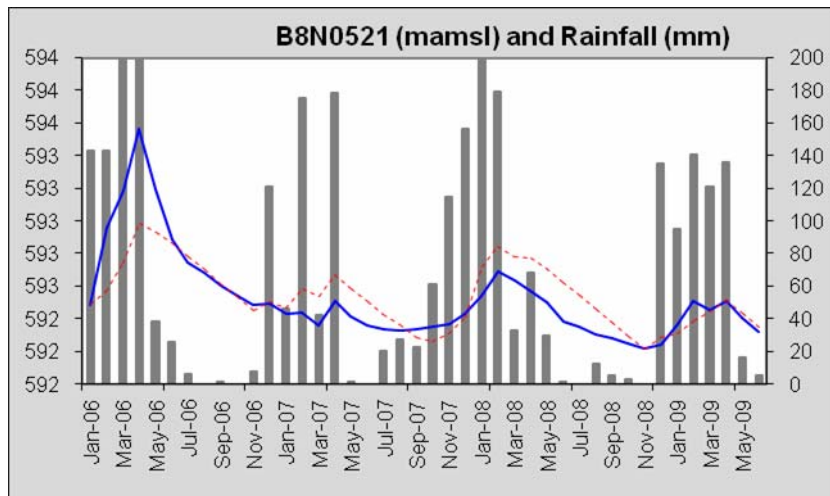
Observed and simulated CRD graph for station B8N0517.



Observed and simulated CRD graph for station A6N0586.

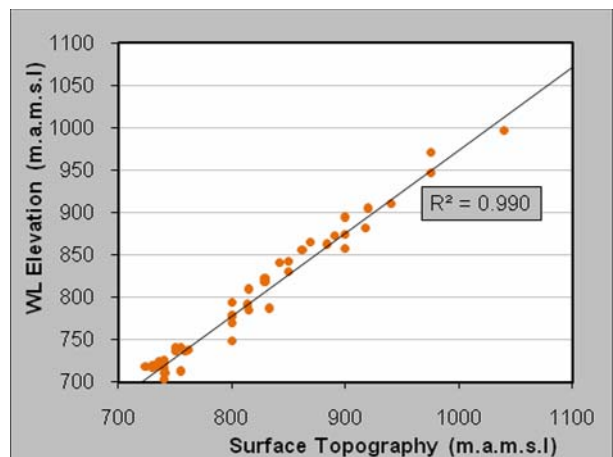
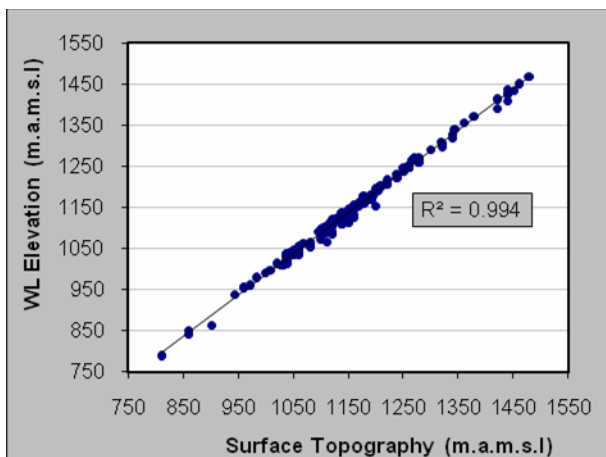


Observed and simulated CRD graph for station A7N0019.



Observed and simulated CRD graph for station B8N0521.

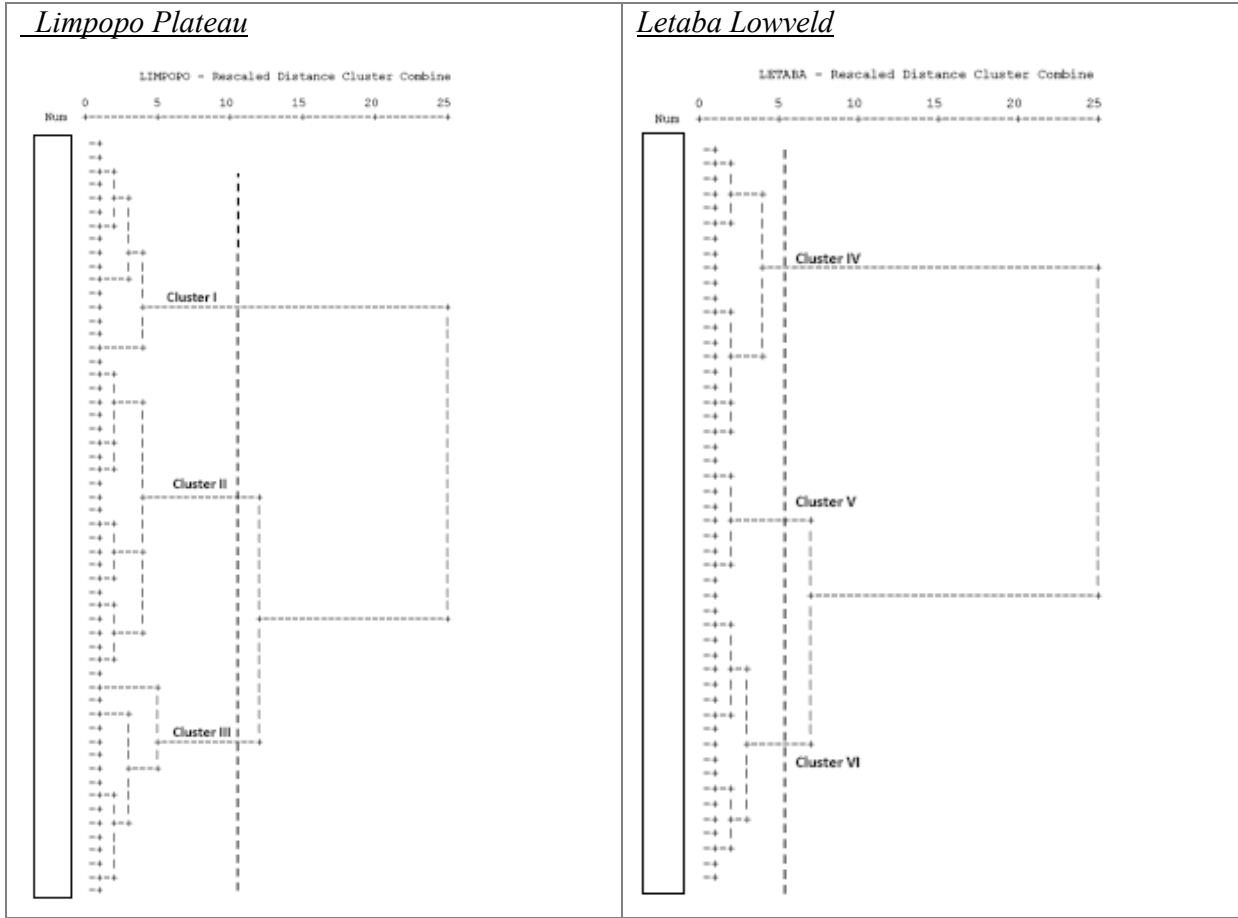
### Appendix C - Surface topography vs. groundwater level correlation



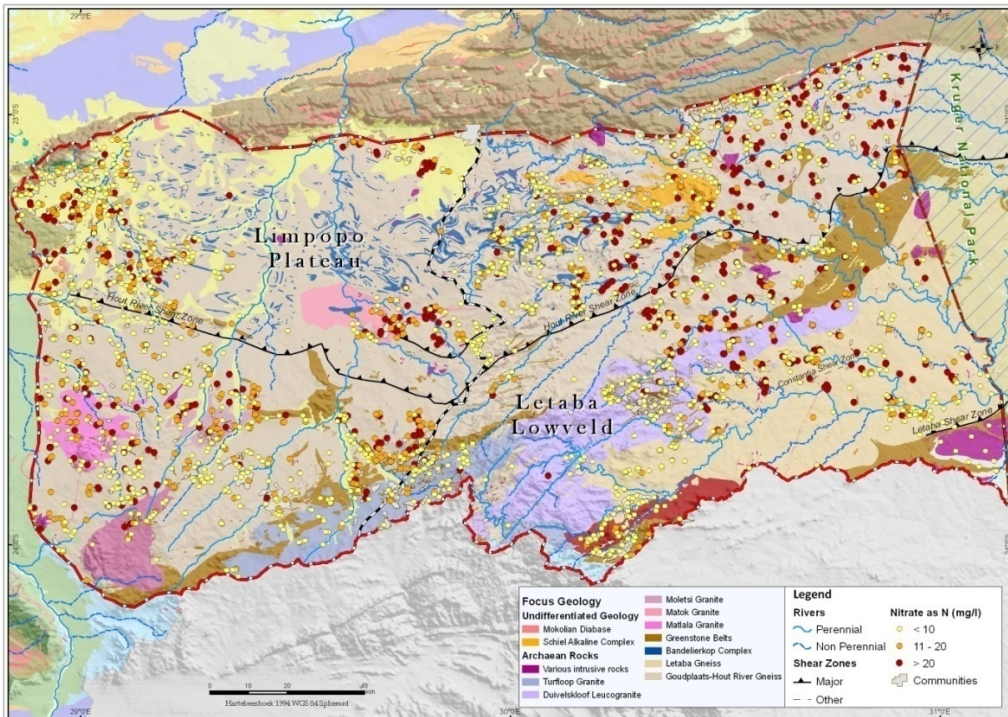
Correlation between surface topography and water level elevations for Limpopo Plateau (left) and Letaba Lowveld (right).



### Appendix D - Hierarchical cluster analysis (dendrogram)



### Appendix E - Nitrate distribution map



Map showing distribution of nitrate in groundwater in the Limpopo Plateau and Letaba Lowveld.





## Appendix F - Details of pumping tests

Area	BH Nr.	Date	BH Depth (m.b.g.l)	Water Level (m.b.g.l)	Constant Yield (ℓ/s)	Duration (hrs)	Drawdown	Well Efficiency @ constant rate	Well loss (C)
Limpopo Plateau	H11-1650	Aug-08	64	21.44	31	72	5.6	65%	978
	H11-1653	Sep-08	79	22.23	33	24	4.6	60%	1543
	H11-2110	Sep-08	67	22.52	22	24	11.4	50%	1860
	H11-1782	Aug-08	101	36.38	11	24	16.0	20%	> 3800
	11-1763	May-08	150	34.64	1.4	24	11.0	30%	> 3800

Area	BH Nr.	Date	BH Depth (m.b.g.l)	Water Level (m.b.g.l)	Constant Yield (ℓ/s)	Duration (hrs)	Drawdown	Well Efficiency @ constant rate	Well loss (C)
Letaba Lowveld	H10-0818	May-08	51	12.48	2	24	7.3	-	-
	H10-0796	Apr-08	80	23.16	0.9	24	7.9	> 3800	41%
	H10-0191	Apr-08	83	30.09	5	24	19.0	> 3800	50%
	H14-0277	Aug-09	60	6.36	5.4	48	10.2	> 3800	15%
	H14-0279	Aug-09	85	7.61	6.3	48	20.9	> 3800	10%
	H14-0453	Aug-09	47	7.86	7.5	48	18.0	-	-
	H17-0359	Dec-07	113	24.80	1.2	24	18.0	> 3800	20%
	H17-0724	Dec-07	72	22.56	1.1	24	23.4	> 3800	40%
	H17-0774	Nov-07	52	12.53	1.2	24	8.0	> 3800	46%
	H14-0454	Aug-09	37	11.24	5	48	12.7	> 3800	45%
	H14-0275	Aug-09	59	28.55	5	48	11.9	-	-